Chemical Proteomic Methods to Study Bacterial Cell Wall Biosynthesis

A DISSERTATION

SUBMITTED TO THE FACULTY OF THE

UNIVERSITY OF MINNESOTA

BY

Shabnam Sharifzadeh

IN PARTIAL FULFILLMENTOF THE REQUIREMENTS

FOR THE DEGREE OF

DOCTOR OF PHILOSOPHY

Advisor: Prof. Erin Carlson

November 2019

ACKNOWLEDGEMENTS

This amazing adventure of mine was made possible by my phenomenal advisor, loving family and dear friends, and I would like to dedicate my doctoral dissertation to you all. To my advisor, Prof. Erin Carlson; *Erin*, thank you for being a tremendous mentor and guiding me through every stage of my PhD life. To my *mom*, *dad* and sisters, *Shiler*, *Shermin* and *Shideh*, I cannot imagine getting through this journey without your constant emotional support and unconditional love. You always believed in me and gave me the confidence to never stop trying.

ABSTRACT

Bacterial cells are surrounded by an external layer called the cell wall that defines cellular shape and protects them from osmolysis. A major component of this protective coating, which is unique to prokaryotes, is the peptidoglycan (PG), a heteropolymeric structure composed of saccharide backbones that are cross-linked by peptide subunits. This exclusive presence in bacteria makes the cell wall an ideal antimicrobial target due to the elimination of side effects in humans and other eukaryotes. Indeed, the largest class of clinically-utilized antibiotics, β-lactams such as the penicillins, target the final stages of PG biosynthesis. Penicillin-binding proteins (PBPs) are membrane-associated proteins that are involved in the final stages of bacterial cell wall synthesis and assembly. Discovered as the target of β-lactam antibiotics, PBPs have received much attention for many decades as crucial antibacterial targets and for their role in antibiotic resistance. However, specific roles of individual family members in each bacterial strain, as well as their protein-protein interactions, are yet to be understood. Besides their therapeutic applications, β-lactams have long been used as chemical probes to study the PBPs. Bocillin-FL, for example is a commercially available fluorescent analog of penicillin V with global affinity for all PBPs. Our group is interested in developing PBP-selective activity-based probes to explore these proteins. This dissertation expands on my efforts in developing such probes to specifically target individual PBPs, based on selected β-lactam antibiotics, as well as a β-lactone scaffold that we designed and showed that specifically targets PBPs. Using our probe toolbox, we visualized the activity of specific PBPs in *Bacillus subtilis* and *S. pneumoniae.* With the established potency of these probes, we intend to study PBP-associated proteins via pulldown assays. Ultimately, these studies will shed light on bacterial cell wall construction and division, which would potentially lead to discovery of novel key players involved in these processes that could be harnessed as novel antibacterial targets.

Table of Contents

List of Figures

List of Schemes

List of Tables

CHAPTER 1

INVESTIGATION OF PENICILLIN-BINDING PROTEINS: CURRENT STATE OF THE FIELD

1. Investigation of Penicillin-Binding Proteins: Current State of the Field

Infectious diseases are the leading cause of death in low-income countries and the death toll resulting from infection is projected to outpace cancer in the US by 2050. To overcome this crisis, novel approaches to antibacterial therapy development are urgently needed. Among the main bacterial targets, cell wall biosynthesis stands out with many favorable features. However, there are significant gaps in our knowledge about this complex process, especially the function, regulation, and interactions of key protein players. The overarching goal of my thesis research was to address this challenge by uniting tools and insights from chemistry and biology and explore bacterial growth and division to fill in some of these knowledge gaps, hoping that our efforts will pave the road toward discovery of new potential antimicrobial targets.

1.1. Bacterial Cell Wall as an Antibacterial Target

The bacterial cell wall was first described as a region of specific staining behavior that surrounds the bacterial cell body.(1) However, it was soon demonstrated to be involved with essential processes such as cell growth and division.(2) Moreover, upon the advancement of microscopy and purification techniques, it was shown that purified cell wall material can maintain cellular shape and size. Indeed, the cell wall is commonly known as *sacculus* (Latin word for small bag), referring to its bag-like macromolecular structure (**Fig. 1.1**).(3, 4) Perhaps the most important function of the cell wall is protection against turgor pressure due to the high osmolarity of cytoplasm.(5-7) A major component of this protective coating, which is unique to prokaryotes, is the peptidoglycan (PG), a heteropolymeric structure composed of a saccharide backbone that is crosslinked by peptide subunits.(6, 8, 9) This exclusive presence in bacteria makes the cell wall an ideal antimicrobial target as the probability of interfering with mammalian targets is low.(9)

Indeed, the largest class of clinically-utilized antibiotics, β-lactams such as the penicillins, as well as glycopeptide antibiotics such as vancomycin, inhibit the synthesis of the bacterial cell wall as their mechanism of action.(10) Although most bacteria have PG, there are variations in the thickness of PG layer, the amino acid composition of their stem peptides, structural modification and the length of the glycan chains, as well as the level of PG crosslinking between different organisms.(6, 7, 11) Regarding the amino acid composition of PG, while it is highly conserved among most bacterial species, the highest variation is observed in the third residue in the chain. This residue is typically *meso*-diaminopimelic acid in Gram-negative bacteria and L-lysine in Gram-positive bacteria.(6, 7)

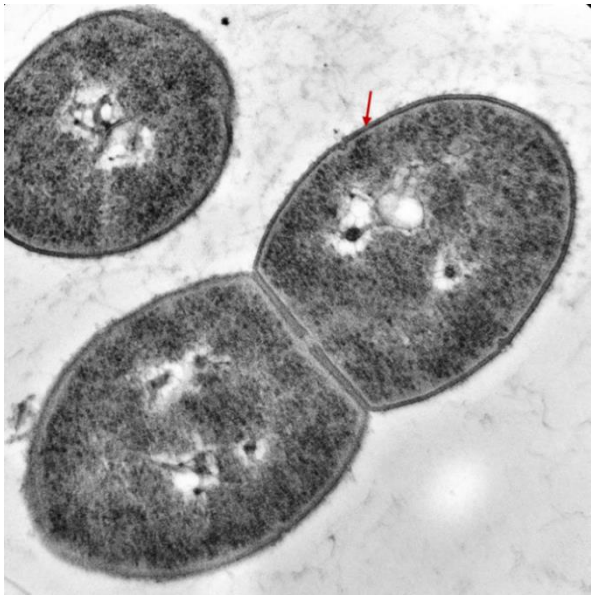

Figure 1.1. Transmission electron microscopy (TEM) image of exponentially growing Streptococcus pneumoniae IU1945. Cells at late-divisional stage and a newly divided cell are represented here at 66k magnification. The red arrow demonstrates cell wall component, which has shown up as a dense layer surrounding the cells. Pneumococcal cells were statically grown in Brain Heart Infusion media at 37 °C in an atmosphere of 5% CO_2 until an OD_{620} of ~0.2 was reached. Exponentially growing cells were captured and fixed with 2.5% glutaraldehyde followed by 1% osmium tetroxide and stained in 2% uranyl acetate solution. Stained cells were embedded in propylene oxide / Epon resin and cross-sections at ~20 nm thickness were prepared and imaged. *TEM sample preparation and imaging was performed under the direct supervision of Dr. Gail Celio at the UMN Imaging Center.*

1.1.2. Peptidoglycan Biosynthesis

The biosynthesis of the bacterial cell wall has been targeted as one of the most promising antibacterial targets.(12) PG synthesis begins in the cytoplasm where the building block of PG, a lipid-modified precursor known as lipid II, is synthesized by the Mur enzyme family.(12-14) The lipid II molecule is then transported across the cytoplasmic

membrane into the periplasmic space, where it is inserted into the growing PG layer through two processes; i) transglycosylation (TG) which refers to polymerization of lipid II and formation of the glycan backbone and ii) transpeptidation (TP) that crosslinks the stem peptides from adjacent PG chains. The crosslink is mainly formed between the 3rd amino acid from the acceptor chain and the 4th D-Ala moiety of the donor chain, (3 → 4 crosslink). Other forms of linkage, such as 3 → 3 are common in specific species such as *Mycobacteria* or penta-glycine bridges that are found in *Staphylococcus aureus*.(6) The PG polymerization and assembly processes are mainly mediated by enzymes known as the penicillin-binding proteins (PBPs).(8) A variety of tailoring reactions may subsequently occur, such as attachment of wall teichoic acids and modifications on the glycan backbone, to further diversify PG in different species.(6, 9)

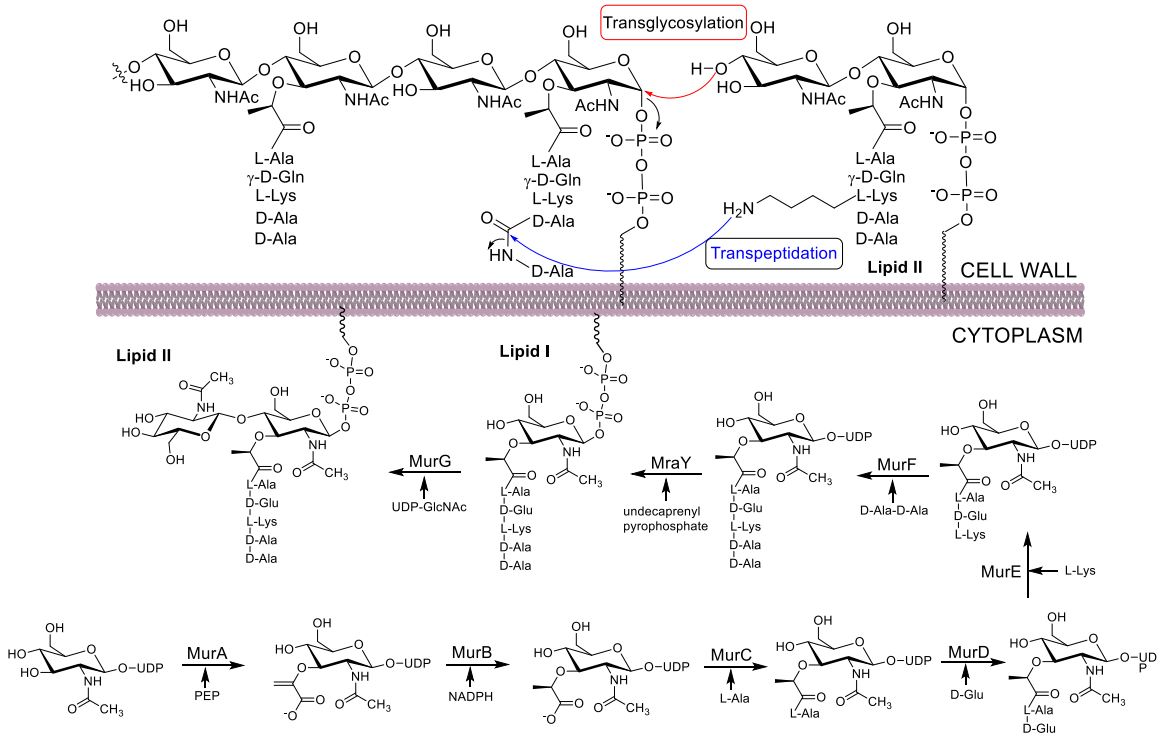

Figure 1.2. Biosynthesis of peptidoglycan (PG). PG precursors are synthesized in the cytoplasm and are linked to a membrane-associated undecaprenyl pyrophosphate group to generate lipid I. Subsequently, lipid I is converted to lipid II by addition of a UDP-GlcNAc, which is then transferred across the membrane. Once in the periplasmic space, lipid II units are added to growing PG chains (transglycosylation). PG chains are crosslinked through a process called transpeptidation to form mature PG. Both the transglycosylation and 3 → 4 transpeptidation that are shown here are mediated by PBP enzymes.

1.2. Focus on Penicillin-Binding Proteins (PBPs)

As the name suggests, PBPs are PG synthase enzymes that were discovered as the targets of the β-lactam antibiotic penicillin. Different bacterial strains have a total of 4-15 PBPs, most of which perform seemingly identical functions. As the targets of β-lactams, PBPs have been studied for decades. However, the discrete functions of individual PBP homologs have remained unknown, largely due to this apparent functional redundancy, making investigation of individual PBPs challenging.

Although resistance has decreased the efficacy of β-lactam antibiotics, there are potential opportunities for the identification of novel antibacterial targets involved with this process. However, a more comprehensive understanding of the macromolecular machineries involved with cell wall construction, especially PBP-associated proteins, is necessary.

1.2.1. PBPs Classification and Roles

PBPs are classified based on their molecular weight and conserved amino acid motifs. PBPs are divided into two main subclasses based on their molecular mass; high molecular mass (HMM) and low molecular mass (LMM). HMM PBPs are composed of multiple domains and are involved in polymerization and crosslinking of the PG chains. Based on the number of reactions that each enzyme can catalyze, HMM PBPs are further classified. While class A proteins are bifunctional and catalyze both polymerization and crosslinking processes, class B PBPs only catalyze the latter. LMM PBPs, which are also referred to as class C, catalyze a different process called D,D-carboxypeptidation, during which the stem pentapeptide is hydrolyzed to a tripeptide.(8, 15) PBPs are known as the main PG synthases that catalyze these reactions despite other enzymes possessing the same or similar functions, such as the L,D-transpeptidases (Ldts) and the SEDS (Shape, Elongation, Division and Sporulation) protein families.(16) All three classes of PBPs

contain a penicillin-binding domain at their C-terminus, which performs the peptidase activity. There is a conserved catalytic serine in this peptidase domain, which is required for substrate turnover and is the site for covalent modification by the β-lactam antibiotics. These molecules occupy the active site for extended periods as hydrolysis of the β-lactam complex is slow, preventing further catalysis and often leading to cell lysis (**Fig. 1.3**).

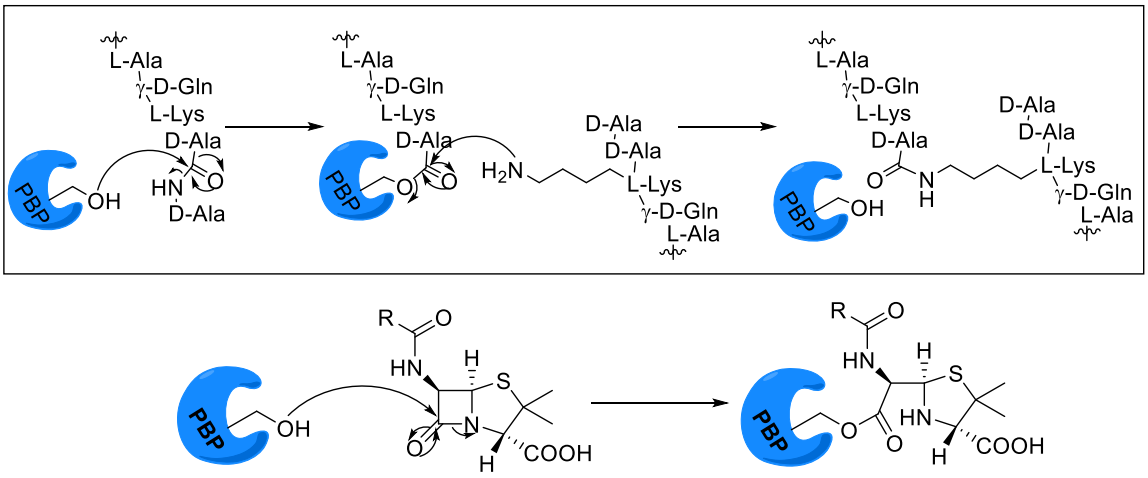

Figure 1.3. Mechanism of transpeptidation reaction by PBPs. *Top:* PG transpeptidation reaction as mediated by PBPs. A catalytic serine residue from the peptidase domain reacts with the terminal D-Ala-D-Ala of the stem peptide of a PG chain. The resulting complex, containing an activated ester group, is then attacked by the third amino acid (L-lysine here) from another stem peptide and the two PG chains are crosslinked. *Bottom*: Penicillins can react with the catalytic serine residue in a similar way to stem peptide and form a covalent complex that inactivates the enzyme.

1.3. Methods of Studying PBPs

1.3.1. Radioactive Penicillins

Historically, the earliest strategy for detection of PBP activity was tagging of these proteins with radiolabeled penicillin followed by separation by sodium dodecylsulfate polyacrylamide gel electrophoresis (SDS-PAGE). As suicide inhibitors of the PBPs, radioactive penicillins can provide information about the catalytic state of the PBPs, and as such, they have been used in kinetic and inhibitor binding assays.(17-19) Although a longstanding and established method for studying PBPs, radioactive compounds impose several inherent limitations. First, radioactive materials are hazardous and require special

operational and disposal procedures. Second, the procedure is time-consuming and may take up to several days in order to collect enough signal. Lastly, radioactive probes cannot be used for *in vivo* visualization. Moreover, penicillin V-based compounds label all PBPs, preventing discrete characterization of each homolog. Therefore, fluorescent labeling methods have been commonly employed over the past few decades, enabling spatiotemporal exploration of biomolecules in their native environments.

1.3.2. Genetically Encoded Tags

Fluorescent protein (FP) tags and immunofluorescence labeling have enabled visualization of bacterial proteins and components. Such studies have been performed for the PBPs and have provided invaluable information about protein localization dynamics during different stages of cell growth cycle.(20-23) Genetically encoded FP tags, such as green fluorescent protein (GFP), have been widely employed in localization studies. While the use of FPs has led to major advances, they too suffer from limitations such as relatively low brightness and photo-stability, making the detection of low-abundant proteins very challenging. Most importantly, such tags are bulky, 27 kDa in the case of GFP, and can affect the localization, abundance and function of the proteins.(24) Indeed, a study looking at the localization of ClpP and five other foci-forming proteins revealed that the foci concentration was caused by the fluorescent tag that had induced oligomerization.(25)

Epitope tagging is another valuable technique that can be applied to localization studies. In this technique, an oligonucleotide sequence coding a particular epitope is inserted next to the gene that encodes a protein of interest (PoI), resulting in the production of the PoI affixed to a specific peptide sequence, such as FLAG, HA, or c-myc, which are immunoreactive with a known antibody. This methodology is particularly of interest for newly discovered proteins and proteins of low immunogenicity. Genetically encoded tags are continuously being developed and have expanded the toolbox that protein tags

provide. Currently, epitope tags are applied to protein purification, localization, quantification or degradation, as well as protein complex analysis and proximity labeling.(26) However, when applied to localization studies, this method requires fixation of cells, which can affect the localization of the PoI.(27, 28)

1.3.3. Antibiotic-Fluorophore Conjugates

Inspired by the success of radioactive penicillins in detecting the activity of the PBPs, fluorescent β-lactams such as BODIPY-conjugated penicillin-V (**Fig. 1.4;** BOCILLIN FL and BOCILLIN 650/665) were developed more recently and have been used in gel-based and live cell studies to explore the global PBP activity in different bacterial species.(29, 30) Commonly known as activity-based probes (ABPs), such small molecule probes only react with the active enzymes, and not the inactive or inhibited forms. As will be discussed in CHAPTER 2, ABPs have been developed for different enzyme classes in both eukaryotic and prokaryotic systems.(31) The ABPs specifically developed to examine PBP activity will also be discussed in CHAPTER 2.

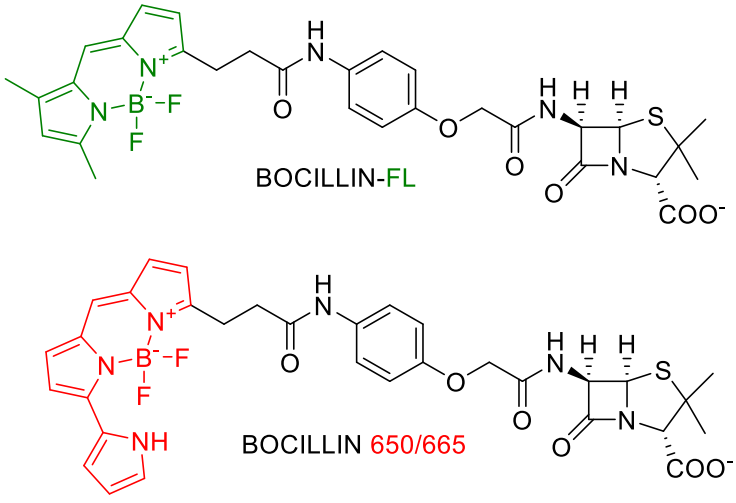

Figure 1.4. Fluorescent Bocillin probes.

Aside from the fluorescent β-lactams, fluorophore-conjugated vancomycin and ramoplanin have been generated and used to label PG biosynthetic precursors in various Gram-positive bacteria to reveal the sites of new PG synthesis in these organisms.(32, 33) Ramoplanin binds to the reducing end of the nascent glycan chains, which is found at the initiation sites of PG synthesis and lipid II.(12, 33) Vancomycin is a clinically important antibiotic that binds to the terminal D-Ala-D-Ala of the PG. Since this portion of the stem peptide is rapidly processed either through crosslinking to another PG chain or hydrolysis by carboxypeptidases, vancomycin-based probes are proposed to bind to nascent PG chains and lipid II only and as such, report on the synthesis of new cell wall material.(12, 32) However, D-Ala-D-Ala is also present in the mature PG of some organisms, such as *Staphylococcus aureus*.(34)

1.3.4. Production of PG Intermediates

One major obstacle that hindered the investigation of PG synthase enzymes for decades was limited access to the PG precursor, lipid II. The total synthesis of lipid I and lipid II (**Fig. 1.2**), the natural substrates of PG synthases, has been described by a number of research groups.(13, 35-37) However, due to its complex structure, presence of an undecaprenyl pyrophosphate group and the structural variations among different bacterial species, obtaining sufficient amount of this substrate has long been a bottleneck in the field. More recently, the Walker research group demonstrated that accumulation of lipid II material could be induced through inhibition of PG polymerization and crosslinking reactions. Using a labeling reaction that enables detection of the lipid II molecule, it was shown that incubation with cell wall acting antibiotics such as moenomycin A and vancomycin or inhibition of lipid II transfer into the periplasmic space through blocking the flippase enzymes, leads to accumulation of substantial amounts of lipid II that can be isolated *via* a facile two-step extraction method.(38-41) Such ready access to the lipid II

substrate has enabled the identification of several non-PBP enzymes that function in concert with the PBPs to synthesize PG.(42, 43)

1.3.5. Metabolic Labeling of PG

Metabolic stem peptide remodeling through synthetic PG mimetics has paved the way for a novel class of PBP chemical probes. D-amino acids are essential components of PG. It has been shown that the terminal D-amino acids of the stem peptide undergo exchange reactions with free D-amino acids, a process that is mediated by D,D-transpeptidases. This process is inherently promiscuous with respect to the substrate structure and allows insertion of a wide variety of D-amino acids.(44, 45) Interestingly, L-amino acids are not tolerated by this enzymatic machinery.(45, 46) Inspired by this phenomenon, unnatural D-amino acids (UNDAA) have been devised to track PG production.(47-49) For example, the presence of PG in *Chlamydia trachomatis*, which was the subject of intense debate for many decades, was proved using D-amino acid dipeptide probes and click chemistry.(49, 50) Similarly, a number of fluorescent D-amino acid (FDAA) have been developed as *in situ* probes to detect active peptidoglycan synthesis and/or remodeling in cells.(51-53) Currently, a full color palette of FDAAs exists, with emission wavelengths that span the entire visible spectrum, which have been employed to live-time tracking of PG synthesis in different bacteria (**Fig. 1.5**).(53, 54) Moreover, a more recent group of fluorogenic FDAAs are in development that only become fluorescent upon their incorporation into PG.(55) One of the limitations of FDAAs is their restricted outer-membrane permeability in Gram-negative bacteria, which could be particularly problematic with more bulky fluorophore groups. Additionally, since this is a relatively new strategy, our understanding regarding the selectivity of different transpeptidases toward individual UNDAAs and FDAAs is still limited.(45, 52) A more comprehensive knowledge

of the substrate selectivity of different PBPs will ultimately provide an alternative strategy for the selective examination of PG transpeptidases.

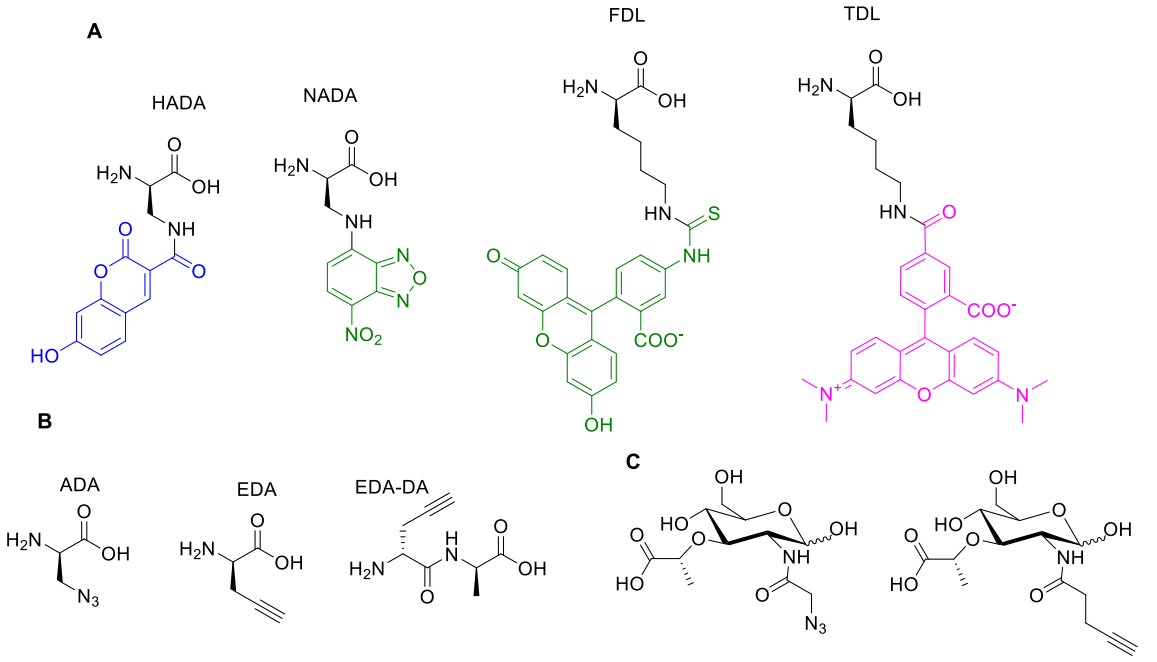

Figure 1.5. Unnatural D-amino acid probes and sugar-based probes for metabolic labeling of PG; fluorescent D-amino acids (A); unnatural D-amino acids with click groups (B) and MurNAc derivatives (C).

In addition to stem peptide modifications, strategies to label the sugar backbone of the PG have been explored over the past few years. Relying on the many advantages provided by click chemistry, MurNAc derivatives containing bioorthogonal groups such as azide and alkyne have been introduced into the PG, followed by labeling with appropriate fluorophores (**Fig. 1.5**).(56, 57) The results of such studies have provided insights into PG synthesis and architecture in different bacteria.

1.4. Summary and Conclusion

Despite being a subject of intense research for decades, many aspects of the bacterial cell wall and its biogenesis remain a mystery. Although the primary catalytic roles of different enzymes involved in the cell wall machinery such as PBPs have been uncovered, many questions such as the regulation and coordination of the activity of

individual components are unanswered. With the main focus on PBPs, this chapter summarized the current molecular and chemical biology tools that have been developed and utilized to examine PG synthases. CHAPTER 2 further elaborates on the ABPP technique and its application to studying PBP, as the main methodology of this dissertation.

CHAPTER 2

PENICILLIN-BINDING PROTEIN ACTIVITY-BASED PROTEIN PROFILING

Portions of this chapter have been published in:

Sharifzadeh, S., Shirley, J. D., Carlson, E. E. Activity-Based Protein Profiling Methods to Study Bacteria: The Power of Small Molecule Electrophiles. Curr. Top. Microbiol. Immunol. 2018, 420, 23-48. doi:10.1007/82_2018_135

2. PBP Activity-Based Probes

Activity-based protein profiling (ABPP) methods have been utilized for the last two decades as a means to investigate complex proteomes in all three domains of life. Extensive use in eukaryotes has provided a more fundamental understanding of the biological processes involved in numerous diseases, which has massively benefited drug discovery campaigns. However, the use of ABPP in prokaryotes has lagged behind and has only gained more attention over the last decade, in order to better understand bacterial physiology and pathogenicity at a foundational level driven by the alarming rise in antibiotic resistance. ABPP provides a means for which new, clinically relevant drug targets may be identified through gaining insight into biological processes. In this chapter, ABPP strategies that have been commonly applied to study biological systems are discussed, with a particular focus on the penicillin-binding protein class of bacterial enzymes. Moreover, the methodology employed to design and apply these novel PBP activity-based probes will be discussed as an introduction to the proceeding chapters.

2.1. Activity-Based Protein Profiling

Advancement of genomic and proteomic methods has enabled rapid characterization and functional assignment of poorly annotated genes and proteins. While proteomics has tremendously accelerated such assignments through the development of analytical methods for large mixtures of proteins, cellular proteins are constantly generated, modified and degraded. Many enzymes are produced as inactive zymogens requiring specific post-translational modifications (PTMs) for activation. Therefore, comparative profiling techniques which enable assessment of these dynamic changes in proteome abundance, modification, intracellular location and functional state are employed.(58) ABPP has emerged as a powerful complimentary approach to monitor the activity of proteins in complex proteomes. Taking advantage of active site-directed

chemical probes, called activity-based probes (ABPs), this strategy enables visualization of the active form of enzymes. ABPs are mechanism-based irreversible inhibitors, consisting of an *active warhead*, which reacts with components of the active site, a binding or *spacer group* that provides spacing between the active warhead and the *reporter*, while also modulating the reactivity and/or specificity of the probe and a reporter tag for identification and purification purposes (**Fig. 2.1.a**). The active warhead is typically an electrophile, which reacts with an active site nucleophile and is retained on-site due to the formation of a covalent bond. Since only catalytically competent proteins can undergo this reaction, active isoforms are visualized in this way. The permanent covalent nature of the ABPs' bond with their targets has made them amenable for diverse applications including live-cell imaging, target enrichment and direct biochemical analysis of the targeted proteins (**Fig. 2.1.b**). Moreover, assessment of the selectivity of enzyme inhibitors is another potential application for activity-based proteomics. In bacterial systems, ABPs have been applied for various applications such as target discovery, the study of microbial pathogenesis and host-pathogen interactions, live cell imaging, and inhibitor discovery.(59, 60) Bottcher, 2008 #26;Heal, 2012 #84;Willems, 2014 #85;Sharifzadeh, 2017 #123}

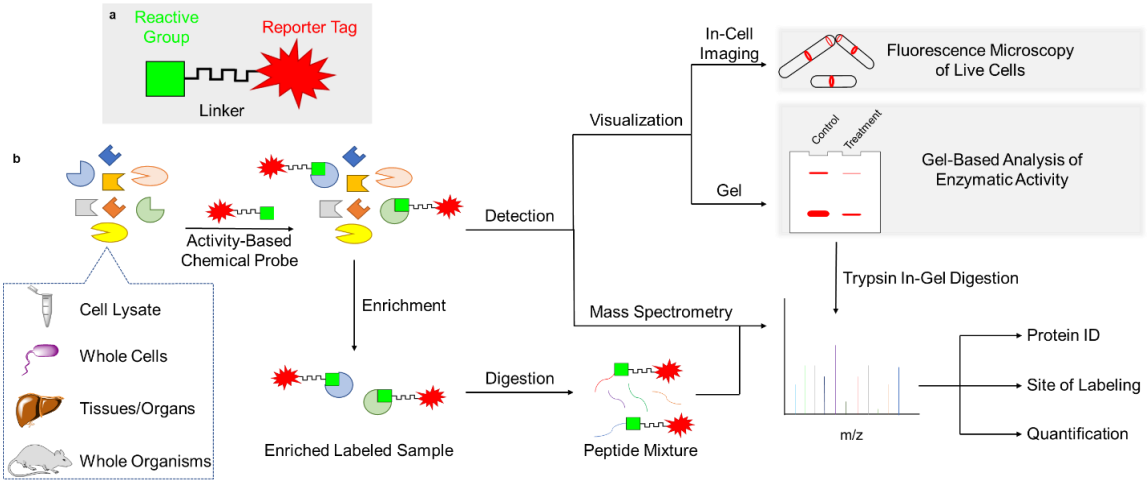

Figure 2.1. a) General structure of an ABP. Reactive warhead, usually an electrophilic group, is linked to a reporter tag such as a fluorophore or biotin via an inert linker. b) General workflow of ABPP. A sample is treated with an ABP, followed by the detection of the interaction between enzyme and ABP. Additional steps may be carried out in between, including washes or enrichment. Labeled proteome can be detected through either visualization or mass spectrometry methods.

2.1.1. Activity-Based Probes: What They Are and How They Work

Since ABPP has been applied to a broad range of probes with various modes of action, one must be aware of the technical differences. By definition, ABPs represent any active-site-directed chemical probe that reacts with the enzyme in a mechanism-based manner, covalently attaching to a catalytic residue and is retained in the active site. Other groups of covalent protein modifiers, which could potentially be mistaken for ABPs include substrate-based probes and affinity probes. Substrate-based probes are fluorogenic molecules that depend on reactivity of the enzyme to become fluorescent. This group of probes consists of a recognition element that binds within the active site, usually designed based on the enzyme's natural substrate, and a reporter group that generates a signal once processed by the enzyme. The enzymatic cleavage leads to either increase or quenching of fluorescence.(61)

Proteases are perhaps the best example for which both classes of probes have been established and applied. Protease enzymes constitute an extensive family of enzymes in both prokaryotes and eukaryotes, comprising almost 2% of the human

genome. Their primary function to cleave peptide bonds, is critical for maintaining normal physiology of cells and any dysregulation of their expression levels and activity could lead to serious pathologies such as inflammatory diseases and cancer. Accordingly, direct assessment of the proteolytic activity and regulation under normal and pathologic conditions is critical. Based on their mechanism of action, proteases are classified into seven subfamilies, three of which, cysteine, serine, and threonine proteases, use nucleophilic amino acids to perform catalysis. Protease enzymes are often highly selective and only perform limited cleavage of specific sites. The primary amino acid sequence surrounding the scissile amide bond is one of the important factors that determines the selectivity of proteases. Accordingly, substrate- and activity-based probes have been devised based on the structural preferences of individual enzymes. In the former group of probes, the proteolytic function of the enzyme leads to a shift in fluorescent properties of the probe. In the latter group, as mentioned earlier, covalent modification of the enzyme occurs in an activity-dependent manner. While substrate-based probes are processed by the enzyme, ABPs act as an irreversible covalent inhibitor of the enzyme. Moreover, ABPs can be modified to carry different groups such as fluorophores, biotin, and clickable functionalities. Due to irreversible modification of targets by ABPs, labeled proteins can be identified, enriched, and quantified if needed. The activity of proteases has been visualized by fluorescent ABPs, as a non-invasive imaging technique under various pathologic conditions such as inflammatory diseases and cancer.(62)

Finally, affinity-based probes are compounds that are recognized by enzymes, but do not rely explicitly on enzymatic activity. Photoactivatable groups such as benzophenone or diazirine are often installed on affinity probes in order to covalently tag their targets. Similarly, chemically reactive groups such as alkyl halides and succinimidyl esters can be incorporated to enable covalent tagging of nucleophilic residues in the proximity of the binding site.(63) Although this latter strategy has been exploited in the

same applications as ABPs, such as target discovery and binding site identification, it must be noted that this class of probes functions regardless of the activity state of their target.(64)

2.1.2. Probe Design Strategies:

2.1.2.1. Reactive Warhead and Recognition Elements

Ideal warheads must possess proper reactivity with proteins as well as biocompatibility. Multiple small molecule electrophilic probes have been developed that show class-specific reactivity toward nucleophilic active site residues of certain enzyme classes. Such electrophiles are designed to exhibit mechanism-based reactivity toward enzyme family members, while remaining inert to physiologically abundant nucleophiles such as hydroxyls, thiols, and amines. Therefore, these small molecule probes can be exploited to irreversibly label enzymes within their native environment. Available design strategies take advantage of the unique intrinsic reactivity of each enzyme class, as well as the structural features required for substrate recognition. The selectivity of reactive residues toward specific electrophiles could be explained by the Hard and Soft, Acids and Bases (HSAB) theory.(65) According to HSAB theory, reacting species are classified into “hard” or “soft” based on the polarizability; i.e. the inherent property of an atom or functional group that describes how easily the electron density can be delocalized to form covalent bonds, and electrophiles react with nucleophiles of similar hardness or softness. The sulfhydryl group of cysteine residues is highly polarizable and “soft”, due to the large atomic radius of the sulfur atom. In contrast, the hydroxyl group of serine residue is considered to be “hard”. Therefore, the serine hydrolase family of enzymes are targeted by hard electrophiles such as fluorophosphonates, while the cysteine hydrolase family is targeted by softer electrophiles such as α,β-unsaturated ketone. (63) However, some

electrophiles such as sulfonyl fluoride, show promiscuity toward diverse nucleophiles, demonstrating the complexities associated with probe design.(66)

The active warhead of several successful activity-based probes has been designed based on known covalent, mechanism-based inhibitors of that class of enzymes. In this regard, serine and cysteine hydrolases were the first enzyme classes that were successfully targeted upon the introduction of the ABPP strategy. In the absence of such cognate inhibitors, de novo probes have been designed inspired by structural features found in natural products. In the event of broad applications, such as profiling the activity of a class of enzymes rather than a single isoform, fine tuning the selectivity of ABPs is of utmost importance. In those instances, off-target labeling can be an issue, and appropriate controls and statistical measures must be devised in order to limit false discoveries. While concentration-dependent selectivity can be achieved through adjusting the amount of probe applied in some cases, additional controls such as competitive inhibition and no probe added samples are essential in most cases.

2.1.2.2. Linker

The linker group, which connects the active warhead to the reporter group or the click handle, is a crucial component and affects target identification. Ideally, the linker must be inert and does not form any interactions with the target, while distancing the reporter group from the active site. Hydrophobic linkers, such as alkyl chains, have been reported. However, the use of hydrophobic linkers presents the challenge of non-specific binding of proteins through hydrophobic interactions. This non-specificity, along with solubility issues, presents unfavorable aspects of using hydrophobic linkers. A hydrophilic linker group, such as polyethyleneglycol, PEG, is the linker of choice in most cases.

Cleavable linkers, such as a TEV cleavable linker, allow for selective peptide elution upon enrichment and avoid background signals resulting from non-specific binding. TEV cleavable linkers have been incorporated in isoTOP-MS analysis strategies for the characterization and quantification of ABP labeling (see Detection Methods). Moreover, cleavable linkers enable determination of the site of labeling using MS-MS technique, since the reactive portion of the probe remains attached to the target protein after cleavage. Additional cleavable linkers that have been employed in ABPP are trypsin-cleavable linkers, diazobenzenes capable of cleavage with sodium dithionite, vicinal diols cleaved with sodium periodate, and light-sensitive linkers capable of being cleaved with UV-light.(67)(67-71). An intrinsic drawback of these types of linkers, however, is incomplete cleavage, which can result in low signal.

2.1.2.3. Reporter

Upon enzyme binding, ABPs must possess a feature that facilitates the detection of labeling. The reporter tag of ABPs enables this to happen through direct visualization of the probe (gel-based or imaging) or through enrichment and protein identification (mass

spectrometry).(72) Initial ABPP studies took advantage of direct radiochemical detection, through incorporation of ^{125}I.(73) Radiochemical detection is not applicable in large scale analysis, due to limitations imposed by radioactive material. More recently, fluorescent and affinity tags were developed and have been utilized to detect enzymatic labeling of ABPs for several decades.(74) Biotinylated ABPs have also been developed to enable target enrichment, a more time-consuming detection strategy. Fluorescent ABPs are the most direct method for in-gel detection of activity with high sensitivity and throughput.

Tags can either be directly conjugated to probes, in a one-step labeling process, or can be attached post-labeling, in a two-step labeling strategy. The latter carries a significant advantage in allowing the probe to retain more native properties, as a bulky tag can disrupt protein-probe interactions and/or decreases probe cell permeability. Installation of a bioorthogonal handle on the probe can replace the fluorescent or affinity tag used in the one-step process. Following an incubation period and binding to the enzyme, a bioorthogonal reaction can be utilized to add on a tag, in a two-step labeling process. This method enables the probe to interact with the protein targets without the potential interference of the bulky read-out tag.

2.1.3. Bioorthogonal Ligation Reactions

In order to preform two-step labeling, conjugation strategies must be employed in which reactions are fast, highly selective, and can be carried out under physiological conditions.(75) The key component of the two-step labeling strategy is the incorporation of a bioorthogonal handle onto the probe. Bioorthogonal handles are unique functional groups that are unreactive to native biological functionalities, such as water and other abundant nucleophilesThis property, along with their relatively small size, allows bioorthogonal handles to be attached to activity-based probes without disrupting the desired interactions between probe and protein.(76, 77) A number of different strategies

have been developed in the field of bioorthogonal chemistry over the last two decades.(78) The copper-catalyzed Hüisgen [3 + 2] azide-alkyne cycloaddition (CuAAC), an example of click chemistry optimized for biological applications by Sharpless et al, has been used widely to ligate reporter tags and probes. (79-82) The CuAAC reaction has superiority over the Staudinger ligation, which utilizes phosphines and azides as highly selective reactants, but has poor reaction kinetics. However, the CuAAC strategy also has a key limitation in the use of copper, which is cytotoxic in nature. The strain-promoted [3 + 2] cycloaddition between an azide and a strained alkyne eliminates the need for copper, while retaining superior reaction kinetics (**Fig. 2.2**).(78, 83, 84) However, it has also been noted that strained alkynes can undergo reactions with nucleophilic groups.(75, 85-87)

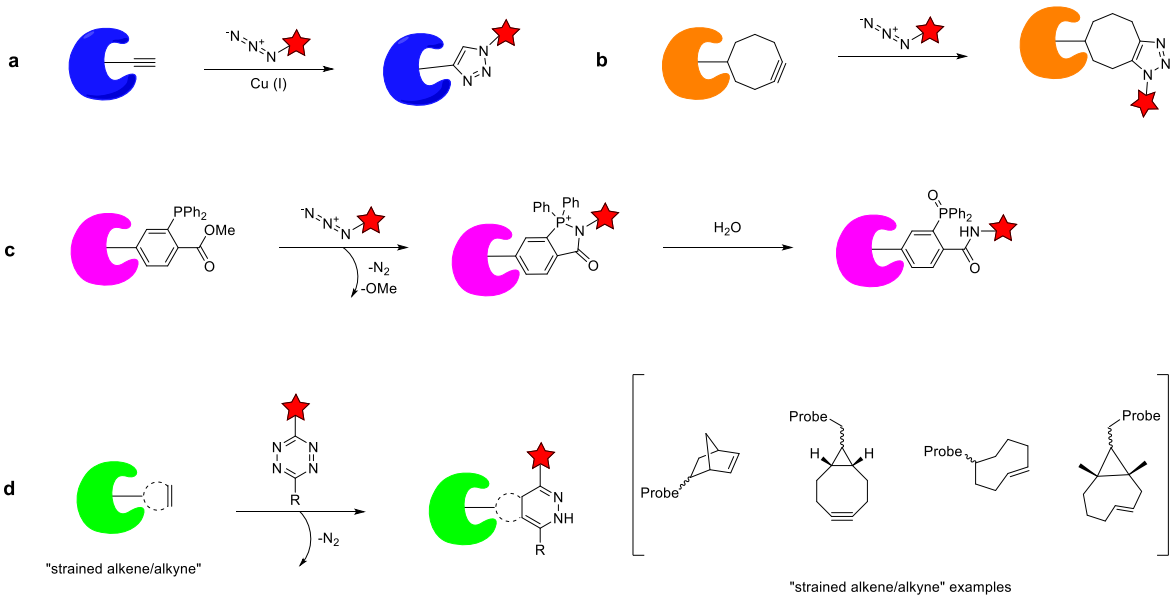

Figure. 2.2. Common bioorthogonal reactions. Colored semi-circles represent probe-labeled enzymes and red stars indicate fluorescent or affinity tags. a) Copper(I)-catalyzed alkyne-azide cycloaddition (CuAAc), b) strain-promoted alkyne-azide cycloaddition, c) Staudinger ligation, d) Inverse electron-demand Diels-Alder reaction.

An alternative strategy that reigns superior when considering reactions kinetics is inverse electron-demand Diels-Alder reaction between strained alkenes or alkynes and tetrazines. These reactions are highly selective, in addition to incredibly fast, and releases

nitrogen gas as a byproduct and dihydropyridazines or pyridazines as products.(78) Significant advancements in the use of this reaction have been developed in the last few years and the use of unnatural amino acids containing these functional groups have been reported for improving the specificity of labeling. Additionally, development of quenched tetrazine-fluorophore conjugate probes that upon reaction with a bioorthogonal partner yield high fluorescence that does not require a washing step to remove unreacted probe has been reported. This has provided a useful tool for in-cell and in-animal imaging.(88)

2.1.4. Detection Methods

2.1.4.1. Gel-Based Detection

One of the first detection strategies employed for the analysis of ABPP was gel electrophoresis. Following a labeling step with the ABPs, proteomes can be separated and analyzed by either one-dimensional (1D) or two-dimensional (2D) gel electrophoresis. 1D-gel electrophoresis, most often sodium dodecyl sulfate polyacrylamide gel electrophoresis (SDS-PAGE), is utilized to separate proteins based on their molecular weight. 2D-gel electrophoresis separates proteins based on isoelectric point (1^{st} dimension), followed by separation based on size (2^{nd} dimension).These strategies can be applied for ABPs possessing both affinity and fluorescent tags. Upon separation of the proteome, labeled proteins can be visualized via fluorescence gel-imaging or blotting strategies. Gel-based detection is heavily relied upon, as it is robust, simple, high-throughout, and requires relatively little material. Upwards of hundreds of proteome samples can be analyzed by gel electrophoresis per day, however, this strategy has its limitations. The number of proteins that can be resolved is often a limitation of gel-based strategies, as well as the inability to determine the molecular targeting of a probe (i.e., the identity of most labeled proteins and which amino acid is being labeled). As a result of

these limitations, strategies were developed to increase the resolving power of ABPP and to determine specific interactions between a probe and its targets.

2.1.4.2. Live Cell Imaging

Gel-based fluorescence detection has been the most utilized application of fluorescent probes, however, cell imaging strategies have also been employed. For example, the Carlson group has utilized both strategies to study the penicillin-binding proteins (PBPs) in bacteria. In an initial effort to study individual PBPs in *Bacillus subtilis* and *Streptococcus pneumoniae*, fluorophore-containing cephalosporin derivatives were synthesized and assessed for their ability to bind PBPs. *In vivo* labeling of the PBPs was observed through fluorescence microscopy and gel-based analyses and it was determined that these cephalosporin-analogues are more selective than Bocillin-FL, a commercially available analogue of penicillin V that labels all PBPs (Fig. 1.3). Furthermore, dual labeling experiments suggested that subpopulations of PBPs are localized separately during cell growth and division (89). β-lactone-based probes, developed to extend the PBP-targeting toolbox, enabled selective tagging of PBP2x and PBP2b in *S. pneumoniae*. Super resolution fluorescence microscopy of pneumococcal cells treated with two lactone analogs, labeling PBPs 2x and PBP2b, respectively, demonstrated that PBP2b activity is restricted to a ring around the division site. PBP2x activity, on the other hand, was detected in both the surrounding ring and the septum at the division center.(90) This was the first time that individual PBP activity was detected with high spatial and temporal resolution, demonstrating the prowess of ABPs.

2.1.4.3 Mass Spectrometry

Gel-based strategies enable visualization of tagged proteins, however, they do not provide insight about the identity of the labeled proteins. In order to address this issue,

liquid chromatography-mass spectrometry (LC-MS) strategies have been developed in which labeled proteins can be enriched from complex mixtures, using proper affinity tags, and subsequently characterized. A typical target identification experiment includes treatment of cells with ABPs, followed by enrichment of target-probe complexes via affinity purification. Biotin tags enable facile enrichment of probe-protein complexes by avidin beads and hence, are the most common reporter used in ABPP target identification studies. Given that biotin affects cell permeability, a click group is often appended to the probe, which can subsequently be ligated to a biotin or fluorescent reporter. Following enrichment of labeled proteins, proteomics can be carried out using LC-MS to characterize the proteome. Additionally, the sensitivity of MS instruments enables detection of very low-abundant proteins, which is not possible using gel-based methodologies.

Quantitative methods for chemical proteomics have been developed to more accurately quantify probe targets. It should be noted that these methods rely on relative quantification to compare a non-treated sample to a probe-treated sample and not an exact quantification, in the sense of a number of moles of protein being labeled. Activity-based protein profiling and multidimensional protein identification technologies (ABPP-MudPIT) enable comparing enzymes activities between different proteome samples.(91, 92) However, ABPP-MudPIT does not provide site-specific labeling information, in addition to being low throughput, which are key limitations of this platform. This issue was overcome with the development of tandem orthogonal proteolysis (TOP). TOP introduces a TEV-biotin tag onto probe-labeled proteins in complex mixtures. Upon streptavidin enrichment, proteins are first cleaved with trypsin and the resulting peptides eluted. Next, the remaining resin-bound peptides are incubated with TEV protease to selectively release probe-labeled species, which are analyzed via LC-MS/MS. Site-specific labeling of the probe can be elucidated via algorithms such as SEQUEST (93). SEQUEST is one example of peptide analysis software, but there are numerous programs that can be

utilized.(94) Further advancement of this methodology has led to isotopic-TOP (iso-TOP)-ABPP, in which an isotopically tagged probe can be utilized to differentiate the extent of protein labeling in multiple proteomes.(95)

LC-MS/MS is commonly utilized in ABPP, often with “label free” methods and spectral counting to quantify relative amounts of labeled peptides. This is due to the fact that enrichment steps utilizing an affinity tag, such as biotin, remove a large amount of excess proteins from the proteome that have not been labeled by an ABP. On the other hand, “labeled” methods have been used less often. In this case, isotopically labeled amino acids are utilized in ABP treated and untreated samples to quantify the peak areas associated with peptides from each sample. Such methods include SILAC, SILAM, iTRAQ, and iCAT. These methods are used more often in systems where the entire proteome is to be analyzed, as opposed to an enriched sub-population of the proteome. However, this is not always the case and both “labeled” methods and enrichment have been used. An in-depth discussion of these methods is outside the scope of this chapter and readers should referrer to more comprehensive reviews.(96-99)

2.2. ABPP of PBPs

Small molecule chemical probes enable spatiotemporal assessment of biochemical processes of interest. As such ABPP methods have been developed and applied to study bacterial systems to understand the molecular mechanisms of bacterial pathogenesis and virulence. We reviewed the ABPP of prokaryotic systems recently, which summarizes the work done in the field and recently published a book chapter.(100) Here, we will focus on the ABPP applied to PBPs specifically.

2.2.1. Previous Work

β-lactams comprise the largest class of antibiotics in clinical use and have shown great success in combating Gram-positive and Gram-negative bacteria. β-lactams prevent cell growth and division through inhibition of a class of bacterial enzymes known as the penicillin-binding proteins (PBPs). PBPs catalyze the polymerization (transglycosylation) and cross-linking (transpeptidation) of bacterial cell wall, also known as the peptidoglycan (PG). β-lactams structurally resemble the terminal D-Ala-D-Ala group of PG stem peptides, and hence the transpeptidation (TP) domain of PBPs recognize them as their natural substrate (**Fig. 1.2**). Although the PBPs were discovered as targets of the β-lactam antibiotics multiple decades ago, the specific roles of individual PBP homologs remain enigmatic.

During the TP step, a conserved serine residue from the active site attacks the β-lactam ring in a mechanism-based manner, leading to formation of an inert acyl-enzyme complex that inhibits biosynthesis of the cell wall (**Fig. 1.2**) .Given the chemical stability of this acyl-PBP intermediate, β-lactams have long been used as chemical probes to study the PBPs. While radioactive penicillins were commonly applied in this regard for several decades (reviewed in Chapter 1), fluorescent analogues were more recently produced and quickly replaced their radioactive counterparts in profiling the activity of PBPs. Bocillin-FL (Boc-FL), comprised of penicillin-V and BODIPY FL as a reporter group, is commercially available. Showing global affinity for the entire PBP content in a given microorganism, Boc-FL has been exploited to monitor TP activity in pure protein samples, as well as cell lysates and whole cells in multiple microbes (**Fig. 2.3a**). In order to obtain selectivity for individual or a subset of PBPs, cephalosporin C molecules tagged with different fluorophores were developed which targeted a subset of PBPs in *B. subtilis* and *S. pneumoniae* (**Fig. 2.3b**).(89) Staub and Sieber produced ABPs using natural product-based antibiotics, ampicillin, cephalosporin C, or aztreonam, that were functionalized with

an alkyne handle to target penicillin-binding proteins (PBPs; **Fig. 2.3c**).(101) These antibiotic probes were tested in multiple organisms including *Pseudomonas putida*, *Listeria welshimeri* and *Bacillus licheniformis*, and were shown to target PBPs specifically. In the same study, synthetic β-lactams were also developed, which were shown to target a diverse set of resistance- and virulence-associated proteins in addition to the PBPs. Among the targeted non-PBP proteins, caseinolytic protein protease (ClpP) stood out, which is a highly conserved serine protease with established crucial roles in virulence of pathogenic bacteria such as *Staphylococcus aureus* and MRSA strains (101).

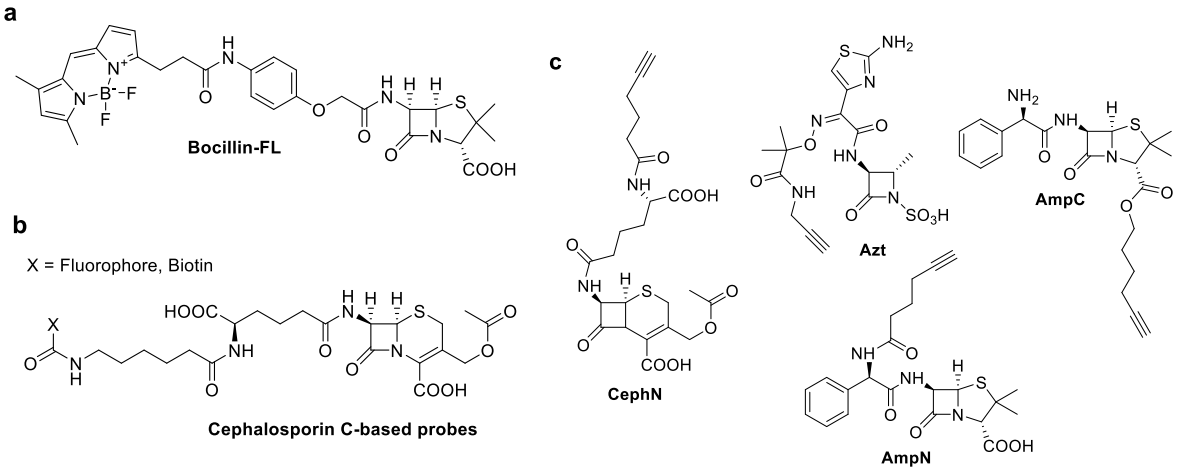

Figure 2.3. Antibiotic-based probes containing an electrophilic β-lactam ring.

2.3. Thesis Work

As mentioned earlier, the β-lactam scaffold has acted as inspiration in designing chemical probes for various bacterial enzymes, including the PBPs.(89) In this work, we developed meropenem-based probes for selective targeting and visualization of the activity of certain PBPs in a number of bacteria. in *Bacillus subtilis* DK654, fluorescent (MEM-BODIPY) and alkyne-functionalized meropenem (Click-MEM) analogs were used to target PBP3, a transpeptidase with generally low affinity for β-lactams. These probes enabled the selective visualization of PBP3 activity using high resolution fluorescent

microscopy (CHAPTER 3). In *Streptococcus pneumoniae* IU1945, an unencapsulated strain of D39, Click-MEM was used to enrich PBP2x, one of the essential transpeptidases in this microorganism (CHAPTER 5).

In order to expand our PBP chemical toolbox, we devised a library of fluorescent probes containing a β-lactone scaffold. Our results indicated that the β-lactone probes are specific for the PBPs in different bacterial species, including *S. pneumoniae*, *B. subtilis*, *Escherichia coli* and *Staphylococcus aureus*. We used two of the β-lactone probes, **7FL** and **8T**, to visualize the activity of two essential transpeptidases, PBP2x and PBP2b, in *S. pneumoniae* E193, an IU1945 mutant in which *pbp1b* is knocked out. This work was the very first time that the activity of individual PBPs was monitored in live bacterial cells (CHAPTER 4).(90)

2.4.1. Probe Design Rationale

Fluorophore-functionalized β-lactams have been successfully applied to monitor the transpeptidation activity of PBPs in bacteria.(23, 29, 89, 102) We envisioned that selective activity-based probes for our PBPs of interest could be obtained by derivatization of β-lactam antibiotics known to target the desired PBPs. Accordingly, we evaluated 21 commercially available β-lactams from different structural subclasses for their selective PBP binding in *B. subtilis* PY79, by applying an established whole-cell assay using Bocillin-FL as the read-out probe (**Fig. 2.4**). Such titration assays produce a comprehensive PBP selectivity profile dataset, which can be used for different purposes. In general, the pencillins and cephalosporins were co-selective for all or different combinations of PBP1, 2a, 2b and 4. On the other hand, the two carbapenems that were examined, doripenem and meropenem, were co-selective for PBP3 and PBP5 (**Table 3.1**). We were seeking β-lactams that selectively bind to one or a small number of PBPs, which also carry functional groups that enable future derivatization and installation of reporter

groups. Accordingly, meropenem was chosen to produce an ABP, given its selectivity profile and the presence of a secondary amine group on the pyrrolidine ring, enabling further functionalization via an amidation reaction (**Fig. 3.7**). Mecillinam was another compound that stood out amongst the tested library, due to its specificity for the only essential transpeptidase in *B. subtilis*, PBP2b. Since there were no functional groups for derivatization, probes were designed in which a homopiperazine ring replaced the azepane ring (**Fig. 3.14**).

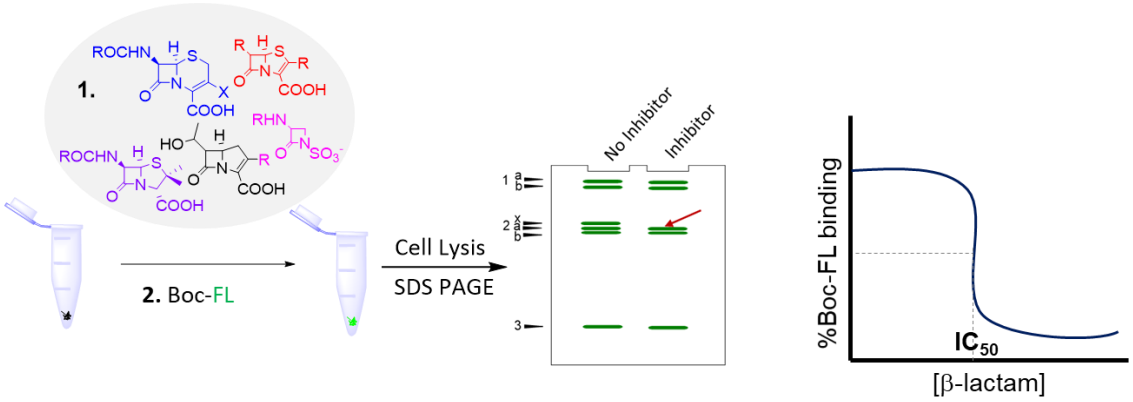

Figure 2.4. Schematic representation of fluorescent-based PBP binding assay used in this thesis. Whole bacterial cells were treated with increasing 10-fold concentrations of different β-lactams chosen from various structural subclasses, followed by addition of Bocillin-FL probe. SDS PAGE analysis of cell lysates and subsequent integration of fluorescence signal yielded % PBP labeling at each β-lactam concentration. IC_{50} values were obtained using the % labeling values (further discussion and full experimental details in CHAPTER 3).

The design rationale for the β-lactone probes is extensively discussed in CHAPTER 4. Briefly, the β-lactone scaffold was inspired by its presence in a number of natural products showing antibacterial activity, as well structural mimicry of the D-Ala-D-Ala portion of the stem peptide, which is indeed the natural substrate for transpeptidastion (**Fig. 2.5**). Structural diversity was produced through insertion of different amino acids. Three fluorophores, fluorescein, BODIPY FL and tetramethylrodamine (TAMRA) were introduced as reporter groups.

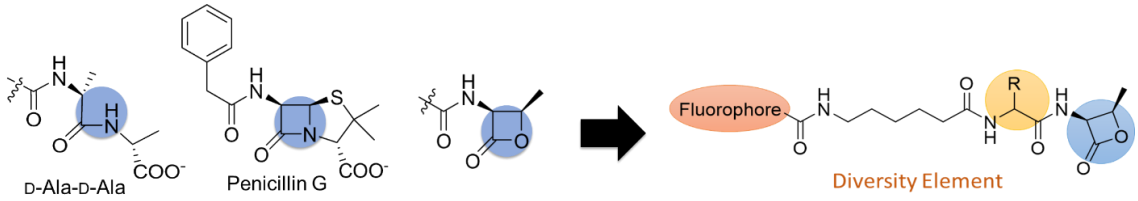

Figure 2.5. Library of probes based on β-lactone scaffold, inspired by the structural similarity of β-lactam antibiotics and the natural substrate of PBPs.

2.4.2. Application to a Proteome Workflow

Specific PBP targeting in each case was tested by evaluation of the probes in knock-out strains where single PBPs were removed (**Fig. 3.9**, **Fig. 4.10**). In the case of essential PBPs, such as pneumococcal PBP2x, which are indispensable for bacterial growth and viability, competition assays with cognate inhibitors of PBPs, such as methicillin, were performed (**Fig. 4.12**). Such competition treatments were also applied to live cell imaging experiments (**Fig. 4.12**). For *click-mem*, further assessment of PBP specificity was achieved through introduction of a biotin affinity tag and enrichment of the tagged proteins. Mass spectrometry analysis of the tryptic digest of the captured proteins confirmed the identity of targeted PBPs (CHAPTER 3).

Once the PBP targeting profile of the probes were confirmed, they were exploited to track the transpeptidation activity of specific PBPs in live cells, using super resolution fluorescence microscopy. On occasions where PBP selectivity was achieved at PBP subset level, mutant strains where one of the PBPs was removed were acquired and used in imaging experiments. (**Fig. 4.10-13**, **Fig. 3.10**)

2.5. Summary of Methodology

ABPP strategies for the study of different bacterial enzyme classes have been receiving more attention over the past decade. This dissertation describes the development of PBP-selective activity-based probes using cognate inhibitors of PBPs, β-

lactams, and *de novo* design of a β-lactone scaffold. The specificity of both groups of probes for the PBPs was evaluated in a number of microorganisms using a combination of knock-out strains, competition assays and chemical proteomic techniques. Upon validation, selected probes were used to monitor the transpeptidation activity of PBPs in *B. subtilis* (CHAPTER 3) and *S. pneumoniae* (CHAPTER 4) via super resolution fluorescent microscopy of live cells.

CHAPTER 3

DEVELOPMENT OF β-LACTAM PROBES FOR SELECTIVE TARGETING OF PBPS IN *BACILLUS SUBTILIS*

Portions of this work will be published in:

Sharifzadeh S, Dempwolff , Kearn DB, Carlson EE. 2019. Harnessing β-lactam Antibiotics for Illumination of the Activity of Penicillin-Binding Proteins in *Bacillus subtilis*. *Manuscript in Preparation*

* Fluorescent microscopy experiments were performed by Dr. Felix Dempwolff in the laboratory of Professor Dan Kearns at Indiana University.

3. Development of β-lactam Probes for Selective Targeting of PBPs in *Bacillus subtilis*

3.1. Significance

Bacterial cell shape is dictated by the rigid external layer that surrounds the cell, known as the cell wall or peptidoglycan (PG) layer. Peptidoglycan is unique to bacterial cells and has a conserved structure, often unique to a particular species. It is composed of glycan chains with peptide side chains that are crosslinked.(6) The final stages of PG polymerization and assembly are mediated by enzymes known as the penicillin-binding proteins (PBPs).(8) PBPs are divided into two main subclasses based on their molecular mass; high molecular mass (HMM) and low molecular mass (LMM). HMM PBPs are composed of multiple domains and are involved in polymerization and crosslinking of the PG chains. Based on the number of reactions that each enzyme can catalyze, HMM PBPs are further classified. While class A proteins are bifunctional and catalyze both polymerization and crosslinking processes, class B PBPs only catalyze the latter.(8, 15) PG crosslinking occurs through a mechanism known as transpeptidation (TP) during which two stem peptides are covalently linked. LMM PBPs, on the other hand, are D,D-carboxypeptidases or D,D-endopeptidases that regulate the level of PG reticulation.(15) Selective targeting of the PBPs enables individual investigation of these critical antibacterial targets and complements genetic-based models by providing critical information about their enzymatic activity with spatial and temporal resolution. β-Lactams comprise the largest class of antibiotics, which inhibit the TP activity of the PBPs through formation of covalent complexes. As such, β-lactams are excellent tools to probe PG biosynthesis.

B. subtilis is a sporulating Gram-positive organism with a large number of PBPs. Sixteen genes are known to encode PBPs in this microorganism, which include four class

A, six class B and six LMM or class C PBPs.(20, 90, 103, 104) Some of these PBPs play roles in cell growth and division,(20, 103, 105) while others are involved in synthesis of the spore PG.(106-110) However, as described previously, the specific tasks of individual members have been difficult to assign due to functional redundancy of these enzymes.(20, 21, 103, 109) The PBPs in *B. subtilis* have long been studied as the targets of β-lactam antibiotics. The covalent nature of the complex formed between β-lactams and PBPs has made them invaluable tools, aside from their therapeutic utility, for both isolation(111) and analysis of this family of enzymes.(29, 89, 102, 112-116) Studies of β-lactam selectivity in *B. subtilis* and other microorganisms have been conducted for two main purposes: 1) β-lactam binding studies to identify those PBPs directly related to measured MICs, which reveals that those PBPs are potentially essential for the growth of microorganism; and 2) studies on strains resistant to specific β-lactams to identify which PBPs show a change in sensitivity for that antibiotic and if those PBPs play a role in resistance.(117)

B. subtilis possesses four class A PBPs in total that polymerize PG, PBP1, 4, 2c and 2d, which are encoded by genes *ponA*, *pbpD*, *pbpF* and *pbpG*, respectively.(109, 118-120) Construction of mutant strains lacking one or multiple class A PBP-encoding genes revealed that only the loss of PBP1 results in a significant phenotypic and PG structure changes(105, 121, 122) and concomitant deletion of PBP1 and 4 accentuates this, along with a profound decrease in growth rate.(121) PBP2c and 2d are known to mainly play roles in spore PG synthesis.(109)

PBP2a has long been believed to participate in maintaining rod shape in *B. subtilis* and its mutation results in twisted cells.(103, 123, 124) PBP2b, encoded by *pbpB*, is the only PBP found to be essential for growth in *B. subtilis*, which is attributed to its major role in septum formation.(21, 124, 125) PBPH, encoded by *pbpH*, is a class B transpeptidase with high structural similarity to PBP2a, encoded by *pbpA*.(103) Deletion of *pbpH* does not cause phenotype changes. However, Δ*pbpA* Δ*pbpH* double mutants are not viable.(103)

PBP3, encoded by *pbpC* gene, is another class B HMW transpeptidase that is largely expressed during the vegetative phase. The activity of PBP3 is indispensable in wild-type cells. Mutations in *pbpC* were shown to cause helical cells, with no significant effect on PG composition and increased susceptibility to β-lactams.(21, 123) More recently, it was discovered that the catalytic role of PBP3 becomes essential in the absence of PBP2b activity.(21, 126) Analysis of the primary sequence of PBP3 revealed significant similarity to *Enterococcus faecium* PBP5, *S. aureus* PBP2a and *Escherichia coli* PBP2.(127) All this suggests a potential role for this PBP in resistance to the β-lactams.

Among the class C PBPs present in *B. subtilis*, PBP5 is the major carboxypeptidase and PBP4a is the equivalent of *E. coli* PBP4. Two other carboxypeptidases similar to PBP5 are present in *B. subtilis*, PBP5* and dacF, which are involved with proper spore cortex synthesis and regulation of PG crosslinking during the sporulation stage, respectively.(128, 129)

The PBP inhibition profiles of various β-lactams have traditionally been investigated in membrane lysates using radioactive penicillins.(130) Such classic surveys exist for *B. subtilis* (111, 114, 117). In spite of the invaluable information that such *in vitro* studies have provided about the ability of the β-lactams to inhibit the PBPs, it must be noted that membrane preparation could affect protein activity.(131) More recently, fluorescent β-lactams have been exploited in PBP studies on whole cells.(29, 89, 102) Following this advancement, we developed a fluorescence-based assay for profiling PBP inhibition using Boc-FL as the readout probe.(115, 116)

In order to facilitate the development of chemical tools to study cell growth and division in *B. subtilis*, we assessed the PBP inhibition profile of a library of commercially available β-lactam antibiotics in the PY79 strain. *B. subtilis* PY79 is a prototrophic laboratory strain and has been commonly exploited for studying different cellular pathways.(132, 133) β-Lactam compounds were selected from different subclasses

including the penicillins, cephalosporins, carbapenems, penems and monobactams. Herein, we report the inhibition profiles that we observed in comparison with results obtained *in vitro*. A total of 21 β-lactam antibiotics from different subclasses (penicillin, cephalosporin, carbapenem, penem and monobactam) were tested in *B. subtilis PY79* strain. This is the first example of a comprehensive *in vivo* profiling of PBP activity in this model microorganism. As expected, several targeting profiles were observed for each structural subclass, including substantial inhibition of PBP3 by the carbapenems, a transpeptidase known for low sensitivity to β-lactams, and specific inhibition of PBP2b (and 2a) by mecillinam. Given the significance of PBP2b and 3, as the main transpeptidase and a potential resistance factor respectively, we designed probes using the selective inhibitors discovered in our titration assay. Fluorescent and alkyne analogs of meropenem were generated and applied to whole cells. Fluorescent microscopy studies revealed that the activity of PBP3 mostly concentrates to the septal region and moves toward the division site at later stages of growth. Moreover, we achieved an optimized condition for click chemistry *in vivo*, through which we showed that the alkyne-containing meropenem probe could also be used for imaging the activity of PBP3. Regarding the mecillinam-based probe, we made structural modifications to the antibiotic core to enable insertion of reporter groups. An analog carrying an alkyne group was generate, which retained its selective binding to PBP2b and 2a. Efforts are currently underway to install reporter groups through click chemistry.

3.2. Selectivity Profile of β-Lactam Library in *B. subtilis*

The results of β-lactam titration assays are presented as gel images and graphs in **Table 3.1** and **Figure 3.2**. We measured the IC_{50} values of individual PBPs for each compound (**Table 3.1**). Selectivity criteria were the same as described in our previous work.(115, 116) Briefly, a compound was considered selective for a specific PBP if the

measured IC_{50} was at least 4-fold lower than that of the next most inhibited PBP (smaller IC_{50}). When a second, third or fourth PBP fell below this threshold, that compound was considered co-selective for all of the most inhibited PBPs.

Five of the tested β-lactams, including aztreonam, faropenem, piperacillin, cefuroxime and cefsulodin, were selective for PBP1 (class A). 6-aminopenicillanic acid (6-APA) selectively inhibited PBP5, the only LMM PBP that is active in the vegetative state of *B. subtilis*. This is in contrast with our previous work that indicated low affinity of this compound for any PBPs in *Streptococcus pneumoniae* and *E. coli*.(115, 116) The remainder of the β-lactams were co-selective for multiple PBPs (**Table 3.1**).

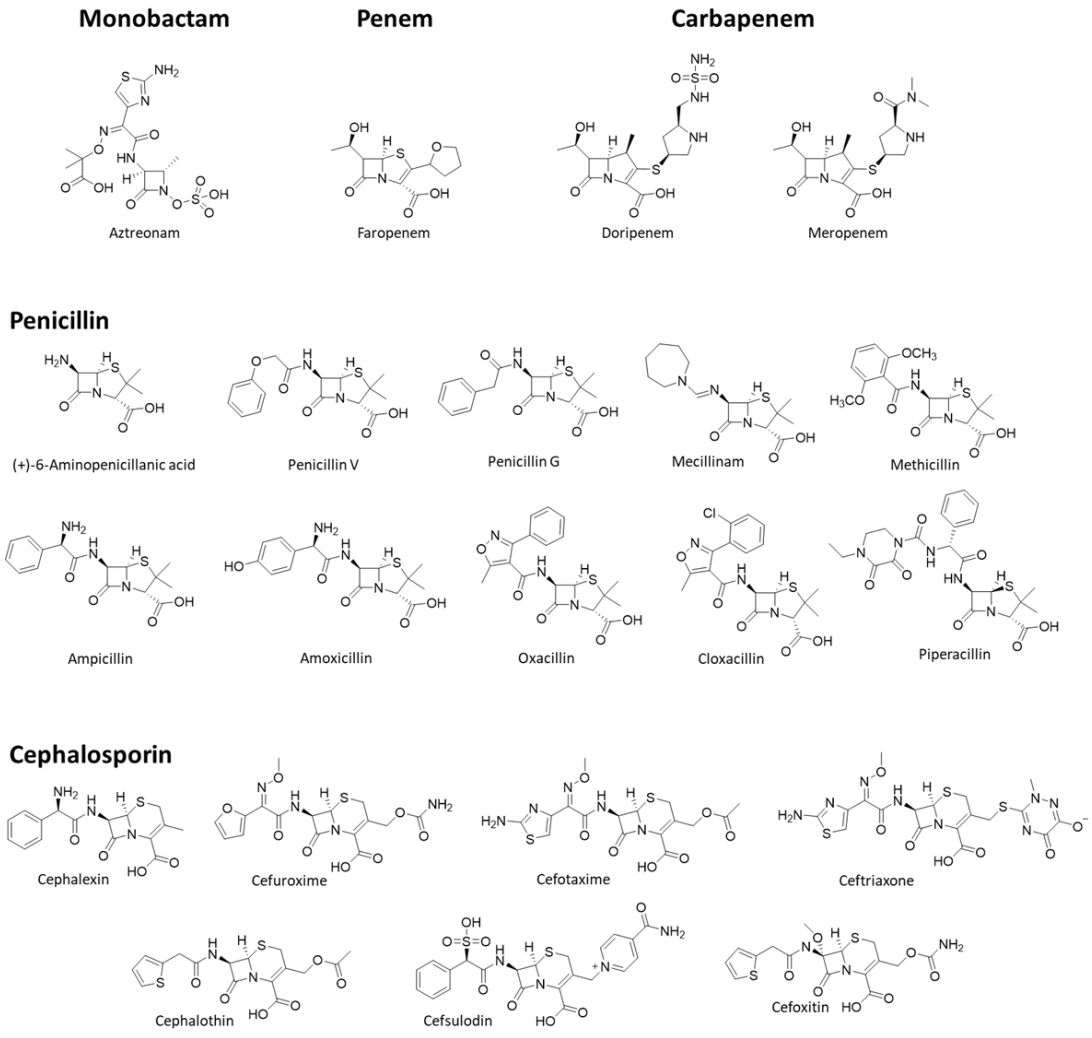

Figure 3.1. Structures of the β-lactam antibiotics used in this study.

Table 3.1. IC_{50} values of β-lactams in *B. subtilis* PY79.

		IC_{50}(s) (μg/ml)						
β-Lactam	MIC (μg/ml)	PBP1a/1b	PBP2a	PBP2b/H	PBP3	PBP4	PBP5	PBP selectivity
Aztreonam	16	<0.01	>1000	26.13	192.7	5.8	>1000	1
Faropenem	0.125	0.00059	0.011	0.0051	0.94	0.009	0.20	1
Doripenem	0.125	>1000	<1000	<1000	0.12	>1000	0.23	3, 5
Meropenem	0.125	>1000	<1000	<1000	0.26	≥1000	0.22	3, 5
Amdinocillin	16	>1000	6.72	1.07	89.6	>1000	>1000	2a, 2b
Penicillin V	32	<0.01	0.00042	<0.01	2.04	<0.01	0.62	2a, 2b, 4
Penicillin G	16	> 1000	0.0043	0.019	1.4	0.0090	0.62	2a, 2b, 4
Ampicillin	8	<0.01	0.0036	0.0094	0.042	0.0037	0.12	2a, 2b, 4
Amoxicillin	4	0.0010	0.074	0.088	0.1±0.04	0.076	1.11	2a, 2b, 4
Piperacillin	64	0.0012	0.16	< 1.0	1.9	0.030	11.3	1
Methicillin	0.25	>1000	< 0.01	< 0.1	9.0	0.11	148.8	2a, 2b
Oxacillin	0.25	>1000	0.056	0.061	66.8	<0.1	>1000	2a, 2b, 4
Cloxacillin	0.125	>1000	0.09	0.13	ND	0.022	>1000	2a, 2b, 4
6-APA	8-256	>1000	110.6	>1000	>1000	>1000	4.1	5
Cephalexin	0.5	>1000	<0.1	<0.1	24.1	254.4	>1000	2a, 2b
Cefuroxime	0.125	0.0018	27.9	0.08	22.2	0.015	>1000	1
Cefotaxime	0.0625	0.0013	<100	<0.1	0.99	<0.1	>1000	1, 2b, 4
Ceftriaxone	0.25	0.0075	16.3	0.066	2.6	0.020	>1000	1,4
Cephalothin	0.03125	0.0026	0.0065	0.0076	11.8	0.006	108.1	1, 2a, 2b, 4
Cefsulodin	8	0.0098	38.0	0.66	138.6	0.12	>1000	1
Cefoxitin	1	0.014	0.72	0.19	1.04	0.014	0.19	1, 4

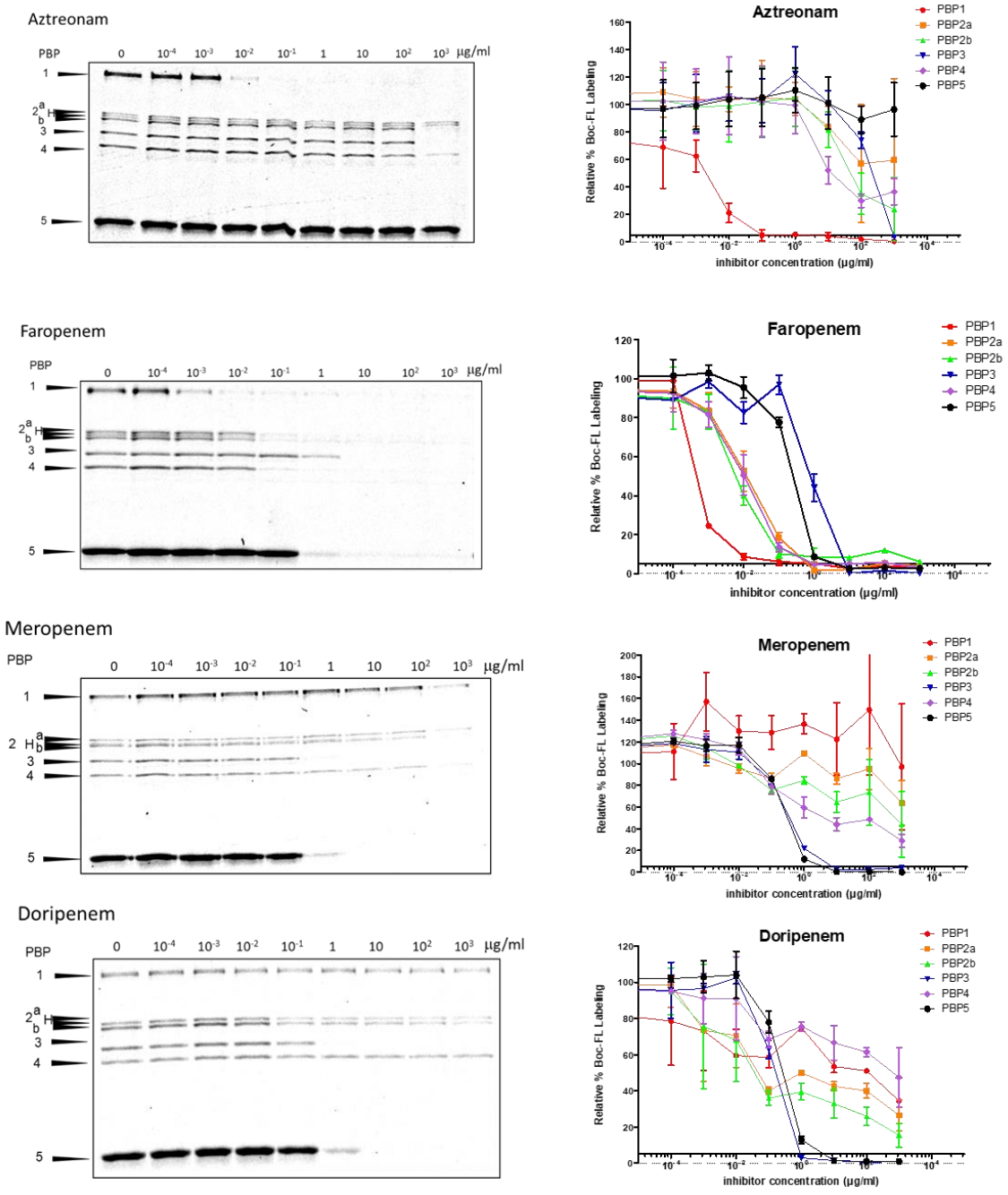

Figure 3.2. Continued on next page

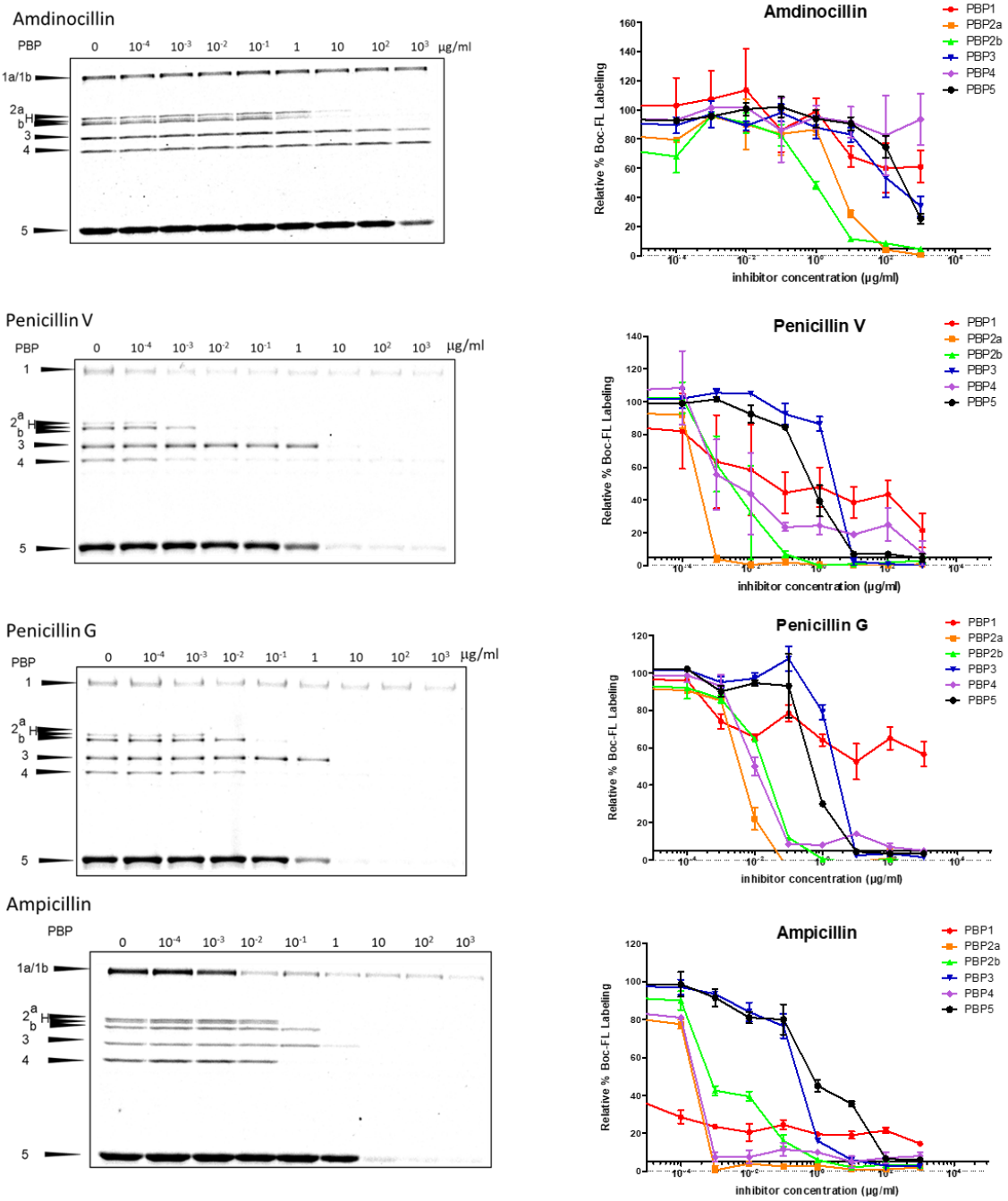

Figure 3.2. Continued on next page

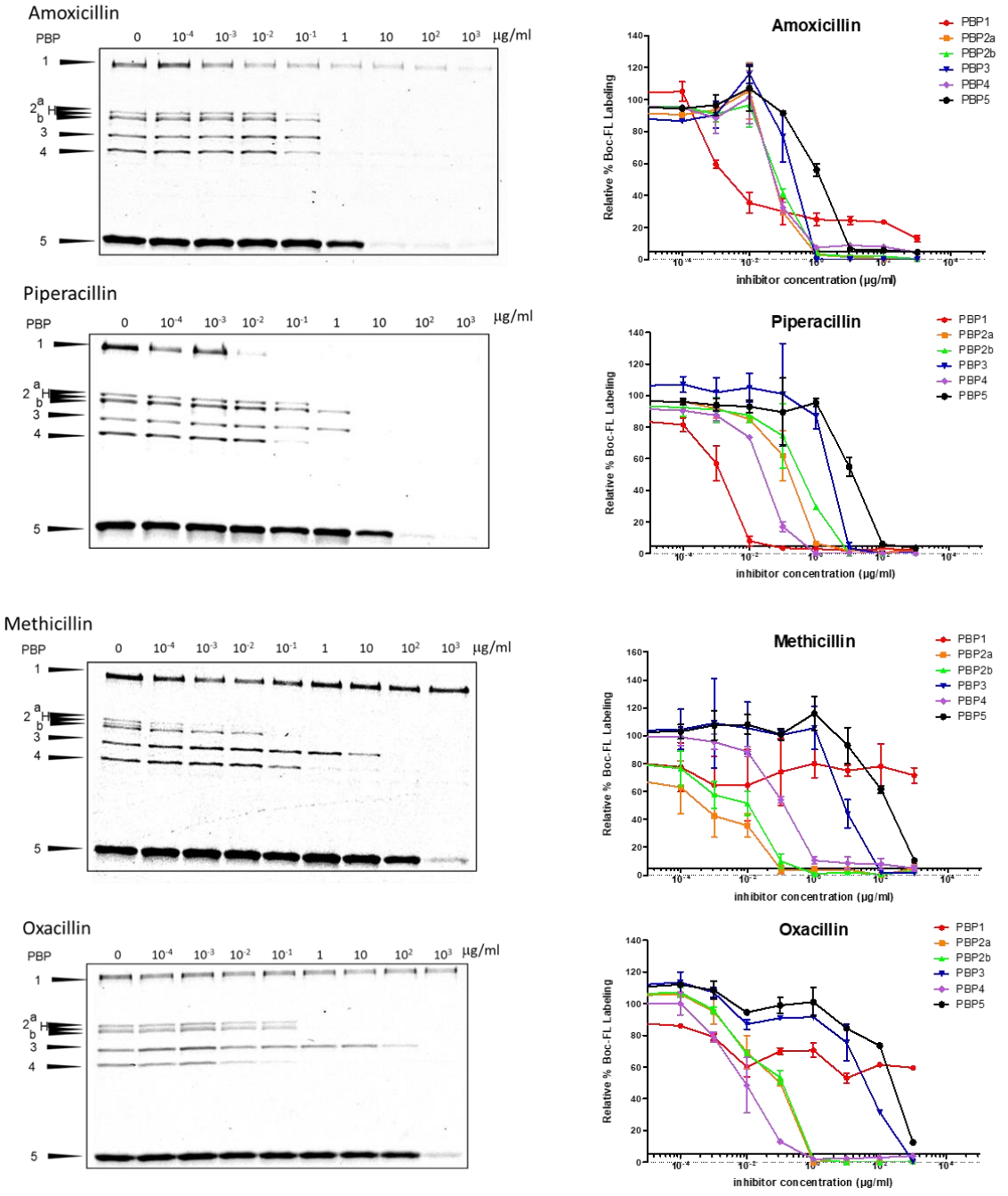

Figure 3.2. Continued on next page

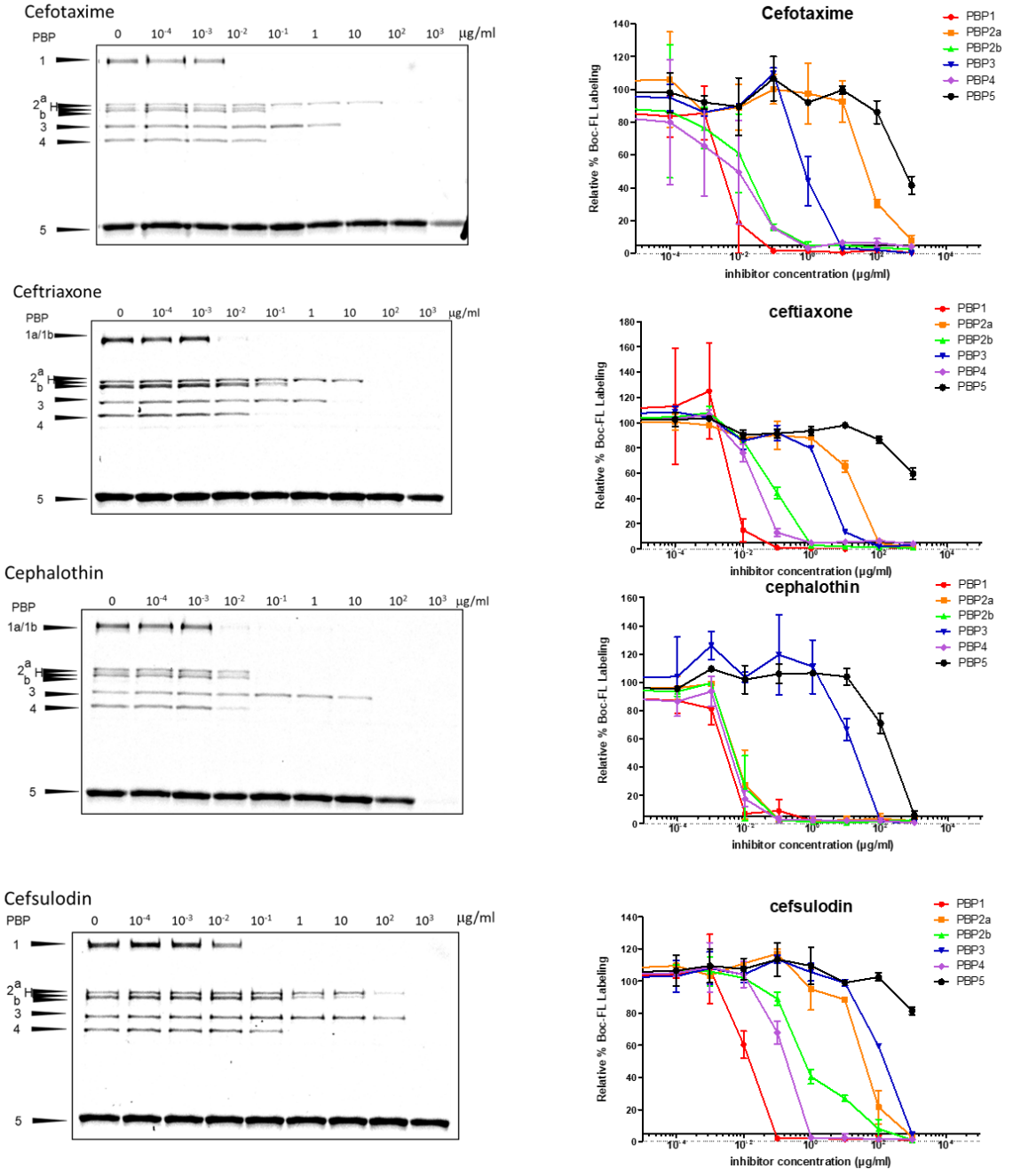

Figure 3.2. Continued on next page

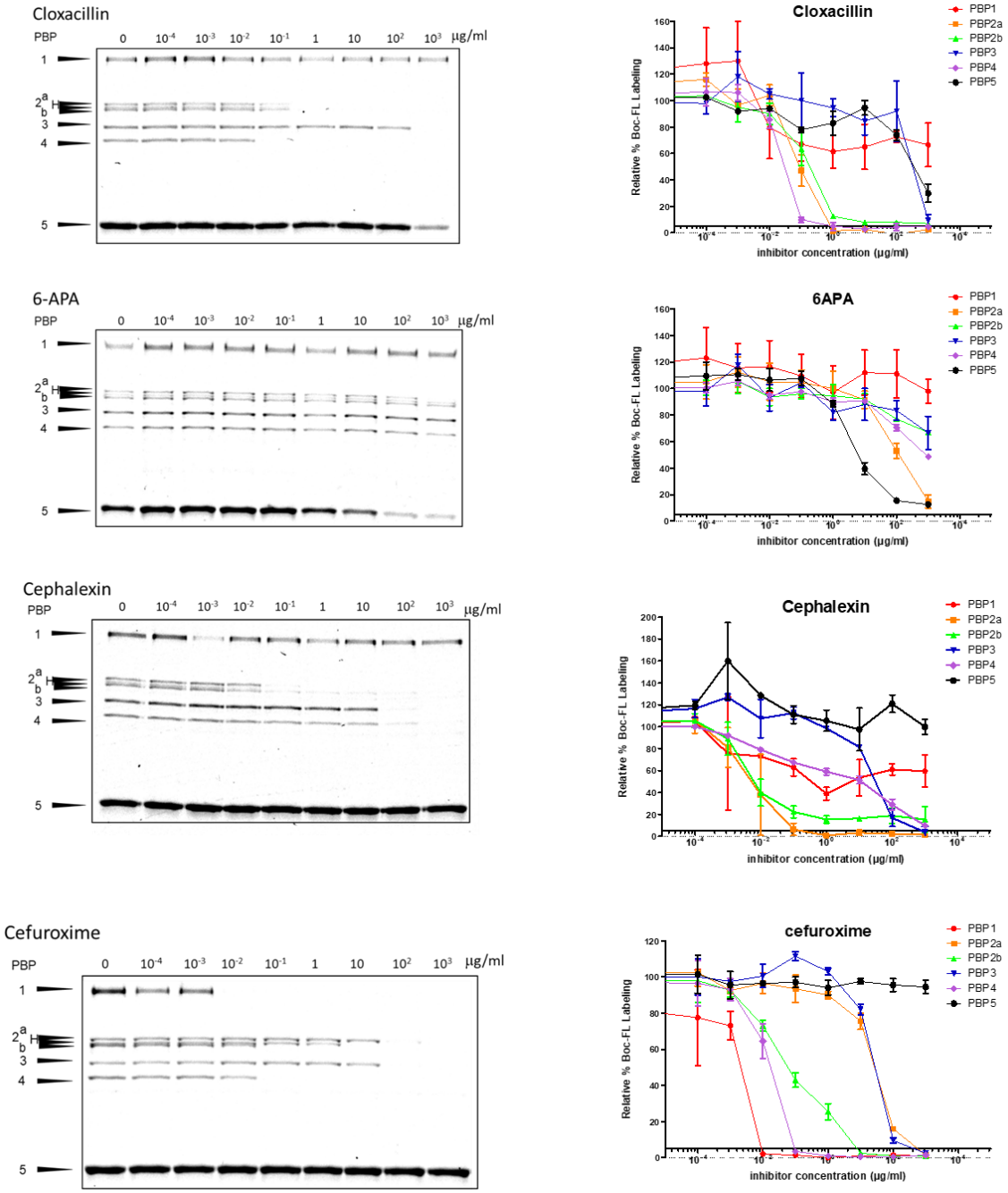

Figure 3.2. Continued on next page

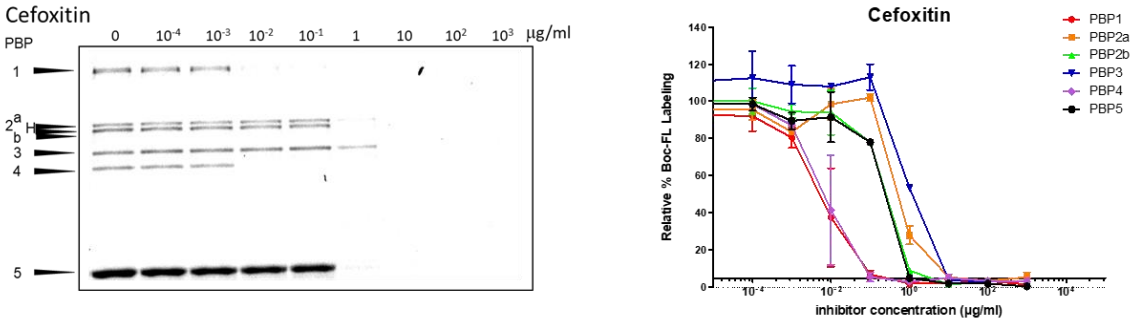

Figure 3.2. Representative SDS-PAGE gels (one of two independent experiments) and the representative graphs for β-lactam titration of the PBPs in *B. subtilis* PY79. Whole cells were treated with various concentrations of antibiotics and subsequently labeled with 5 μg/ml BOCILLIN FL (Boc-FL). Gel bands were integrated and relative fluorescence intensity was calculated in comparison with the control. The average relative intensity from two independent assays is plotted against β-lactam concentration.

3.2.1. PBPH Co-migration with PBP2b

Before performing further analysis of the titration results, it must be noted that what is reported as PBP2b labeling throughout this chapter is in fact a sum of PBP2b and PBPH labeling. Based on the molecular weight and labeling experiments with different PBP knock out strains, we demonstrated that PBPH is co-migrating with PBP2a and PBP2b under our assay conditions (**Figure 3.3**).

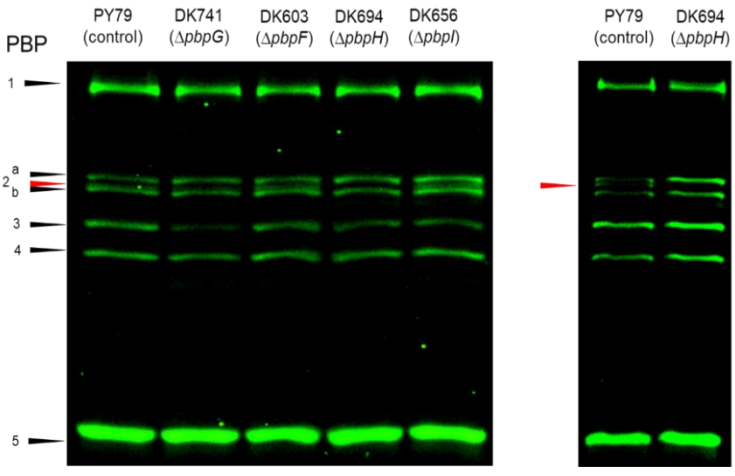

Figure 3.3. Left: PBP activity profile of *B. subtilis* PY79 (wild type) and mutant strains. Cells were treated with 5 μg/mL Bocillin-FL for 10 minutes at RT. *pbpG*, *pbpF*, *pbpH* and *pbpI* encode PBPs 2d, 2c, H and 4b, respectively. All strains, except Δ*pbpH*, display an additional faint band between PBP2a and 2b (pointed out by a red arrow). Lysate protein concentration was adjusted at 5.0 mg/mL.
Right: PBP activity profile of *B. subtilis* PY79 (wild type) and DK694 (Δ*pbpH*) compared. Lysate protein concentration was adjusted at 3.0 mg/mL to better resolve bands in the PBP2 region.

PBPH, encoded by *pbpH*, is a class B transpeptidase with high structural similarity to PBP2a, encoded by *pbpA*.(103) Deletion of *pbpH* does not cause phenotype changes. However, Δ*pbpA* Δ*pbpH* double mutants are not viable.(103) At the time that this study was run, this was the first report of PBPH detection through labeling by a chemical probe. Sassine *et al,* reported the same finding later on.(21) Comparison of the fluorescence intensity between wild-type and the Δ*pbpH* strain labeled by Boc-FL, which is a measure of TP activity, revealed no significant difference in relative activity for most of the PBPs (**Table 3.2**).(52)

Table 3.2. Relative peptidase activity of different PBPs in B. subtilis PY79 (wild type) vs DK694 (ΔpbpH).(1) We assumed that in the absence of PBPH, a class B transpeptidase, the activity of PBP5, the only D,D-carboxypeptidase in B. subtilis, would be least affected. Thus, the activity of the individual PBPs was compared to the total activity, as well as PBP5, in wild type and mutant strain.

% Activity of Total

PBP	PY79	DK694
1a/1b	21.8	18.8
2a	5.2	9.8
2b	7.6	11.0
3	8.7	4.7
4	8.9	8.8
5	47.9	46.9

% Activity compared to PBP5

PBP	PY79	DK694
1a/1b	45.4	40.0
2a	10.9	20.8
2b	15.8	23.5
3	18.2	10.0
4	18.6	18.8
5	100.0	100.0

To further investigate the impact of PBPH labeling on the IC_{50} value of the co-migrating bands, titrations with ampicillin (PBPs 2a, 2b and 4 inhibitor) and methicillin (PBPs 2a and 2b inhibitor), were performed with DK694 (Δ*pbpH*) cells (**Figure 3.4**) and gel bands for all the PBPs were quantitated. IC_{50} values for individual PBPs were comparable, and within 2-fold in all cases for PBP2 region bands and in most cases overall, with the main

exceptions being PBP3 and 5 in ampicillin titrations(**Table 3.3**). These results are consistent with the fact that PBPH activity is minimal in early log phase and becomes prominent only in late exponential phase. Given the minimal contribution of PBPH activity to fluorescent labeling observed in the PBP2 region, PBP2b and PBPH were integrated together and the resulting value used as a measure of PBP2b activity.

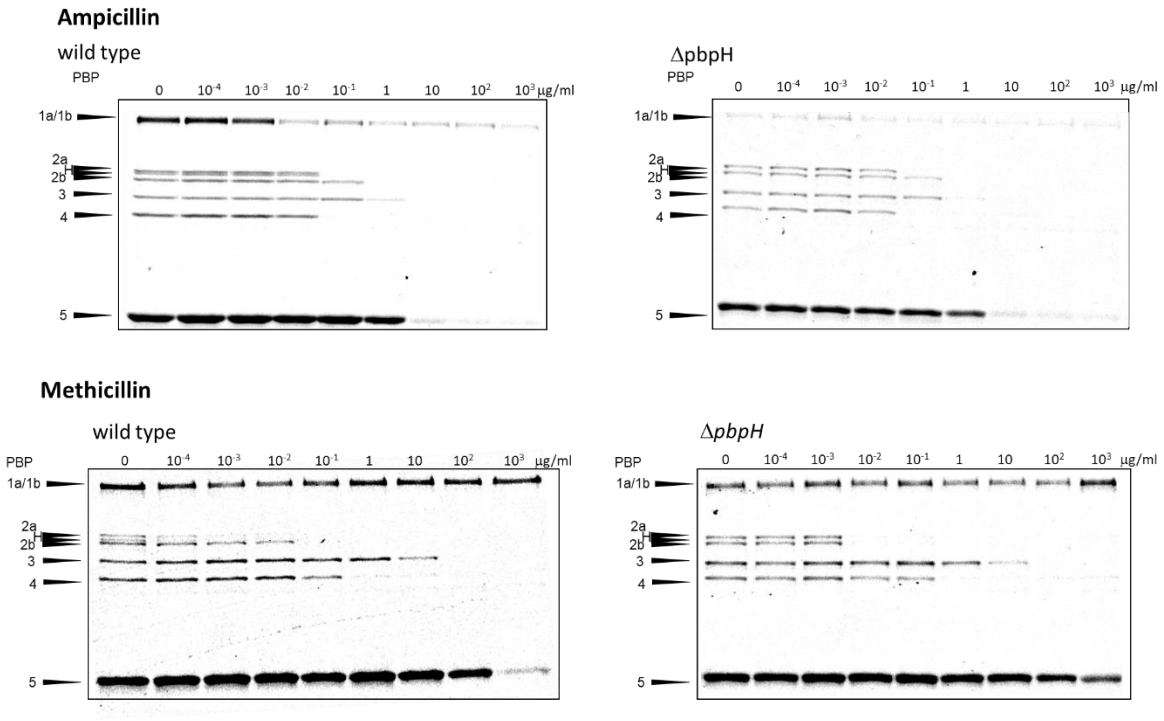

Figure 3.4. Representative SDS-PAGE gels (one of two independent experiments) for ampicillin (top) and methicillin (bottom) titration of PBPs in *B. subtilis* DK694 (Δ*pbpH*) compared with wild-type. Whole cells were treated with various concentrations of antibiotics and subsequently labeled with 5 µg/mL BOCILLIN FL (Boc-FL)

	Ampicillin		Methicillin	
	PY79	DK694	PY79	DK694
PBP1a/1b	<0.01	<0.01	>1000	>1000
PBP2a	0.0036	0.0061	<0.01	0.028
PBP2b/H	0.0094	0.02	<0.1	0.049
PBP3	0.042	0.19	9	12.1
PBP4	0.0037	0.0068	0.11	0.35
PBP5	0.12	0.76	148.8	127.2

Table 3.3 IC_{50} values (μg/mL) for individual PBPs from wild-type (PY79) and Δ*pbpH* (DK694) strains of *Bacillus subtilis* are compared. Average of two individual experiments are provided. An IC_{50} of >1,000 was assigned when GraphPad Prism reported an ambiguous number and significant inhibition was not seen at 1,000 μg/mL. In cases where GraphPad Prism resulted in ambiguous values, the IC_{50} was reported as lower than the concentration that caused >50% inhibition of that PBP.

3.2.2. Class A PBPs as the Most Targeted Transpeptidases

All tested cephalosporins, except cephalexin, were selective or co-selective inhibitors of PBP1 (class A; **Table 3.1**). Aztreonam and faropenem, a monobactam and a penem, also showed potent inhibition of this PBP. On the other hand, piperacillin was the only compound from the penicillin subclass that resulted in complete inhibition of this PBP within the tested concentrations (**Fig. 3.2**). This result is in contrast with a previous report on the titration of *B. subtilis* membrane lysates by [^{14}C]penicillin G followed by SDS PAGE and fluorography, which revealed that PBP1a, 1b and 2a saturate at very low concentrations, followed by PBP2c and 4.(134) Moreover, another report suggested penicillins such as methicillin and ampicillin as strong inhibitors of both PBP1 and 2 from *B. subtilis* membrane lysates.(114) In another study on *B. megaterium*, which is similar to *B. subtilis*, whole cells were treated with [^{14}C]penicillin G and PBP1 was suggested as the main target for this β-lactam.(135) Aside from the many selective inhibitors for PBP1, several penicillins and a small number of cephalosporin compounds including ceftriaxone, cephalothin and cefoxitin, resulted in very low IC_{50} values for PBP4. Overall, all tested compounds except the carbapenems, amdinocillin, cephalexin, and 6-aminopenicillanic acid, favored PBP1, 4 or both, as their main target in *B. subtilis*. This is in contrast with

our preceding results with other microorganisms, in which the LMM PBPs were favored. In our previous work on *S. pneumoniae*, another Gram-positive model microorganism, the most inhibited PBPs were 3, followed by 2x, which are LMM and class B HMM PBPs, respectively.(116) Similarly in *E. coli*, a rod shape model organism, we found that PBP3, a class B transpeptidase, as well as PBPs 4, 7 and 8, all LMM PBPs, were targeted more frequently compared with the class A HMM PBPs.(115)

3.2.3. Penicillins as Potent Inhibitors of PBP2a and PBP2b

In this study, all tested penicillins with the exception of piperacillin, were potent inhibitors of PBP2a and/or 2b, with calculated IC_{50} values in submicromolar range for most compounds. PBP2a has long been believed to play roles in maintaining rod shape in *B. subtilis* and mutation in PBP2a has been found to cause twisted cells.(103, 123, 124) PBP2b, encoded by *pbpB*, is the only PBP found to be essential for growth in *B. subtilis*, which is attributed to its major role in septum formation.(21, 124, 125) Methicillin and mecillinam, the latter is also known as amdinocillin, selectively inhibited PBP2a and 2b. Interestingly, mecillinam showed 3-10 fold higher affinity for PBP2b and therefore, it is a good candidate molecule that could be used as a chemical probe to further investigate the activity of this essential transpeptidase in *B. subtilis*.

3.2.4. Distinct Inhibition Pattern of Carbapenems

All tested compounds showed the highest affinity for class A HMW PBPs, except for 6-APA (PBP5 inhibitor) and the two tested carbapenems; doripenem and meropenem, which selectively inhibited PBP3 and PBP5, a transpeptidase and a D,D-carboxypeptidase, respectively. Interestingly, these two carbapenems yielded very low MIC values, 0.125 µg/ml, under which no PBP is inhibited to a detectable extent. Among the currently available β-lactam antibiotics, carbapenems have gained a unique status due

to their broad spectrum antibacterial activity and resistance to hydrolysis by different classes of β-lactamases or even inhibition of these enzymes in some cases.(136, 137) Previous *in vitro* studies have shown that carbapenems induce morphological changes in *Pseudomonas aeruginosa* strains in a time- and concentration-dependent manner.(138, 139) Meropenem and doripenem are potent inhibitors of PBP2 and 3 in *P. aeruginosa* and PBP2 in *E. coli*, both rod-shaped Gram-negative organisms.(140) Morphological studies in *P. aeruginosa* revealed that both meropenem and doripenem cause filamentation, with central oval swelling, and no significant cell wall breakage and lysis.(139, 141, 142) Our PBP binding results suggest potential interactions between meropenem and other components involved in the cell elongation and division processes in *B. subtilis*.

3.3. Investigation of Lethal Targets of β-Lactam Antibiotics in *B. subtilis*

Early gel-based studies on *B. subtilis*, performed prior to resolution of PBP2a and 2b, identified PBP2 as the main killing target of the β-lactams in this microorganism.(113, 123, 143) Two main strategies have been employed to investigate lethal targets of β-lactams in different microorganisms. One method is to identify the PBPs that are inhibited the most at concentrations leading to growth inhibition.(114) An alternative method is to determine which PBPs show altered activity in mutant strains, assuming that decreased affinity of certain PBPs for the lactams has caused resistance.(113) β-Lactam PBP binding profiles in *B. subtilis* strains with different susceptibilities to β-lactams have suggested PBP2 as the main lethal target in this microorganism.(113, 114) PBP2 was identified as the main killing target of cloxacillin in *B. subtilis* strain Porton and carbenicillin-resistant mutants.(113, 143) However, the penicillin inhibition of PBP2 in mutant strains did not change in this study, which raises the possibility of distinct modes of interaction for different β-lactam molecules with the active site of the enzyme.(113) Upon resolving the PBP2 bands into 2a and 2b, the former was suggested as the lethal target(143), although

PBP2b was never completely eliminated as a potential option.(117) PBP2a and 2b are believed to be involved in vegetative cell elongation and septum formation, respectively.(144) Moreover, *B. subtilis* strains lacking PBP2a or 3 have been shown to become more sensitive to the β-lactams.(21)

Relying on our titration and growth inhibition results, we sought to determine the main killing target(s) for the tested β-lactams. Minimum inhibitory concentration (MIC) values were plotted against IC_{50} values for each PBP separately (**Fig. 3.5**).

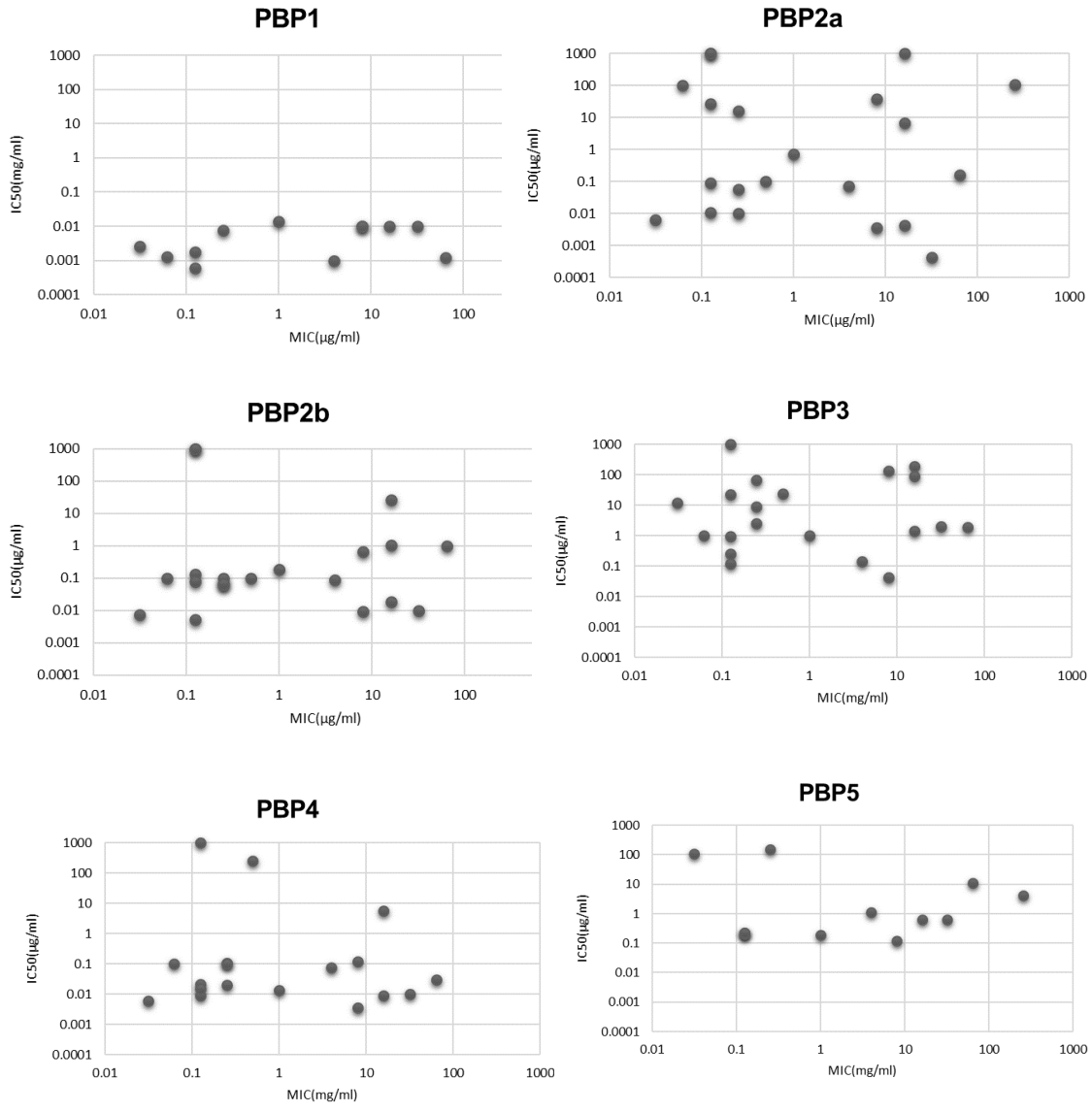

Figure 3.5. Graphs of MIC vs IC_{50} for PBPs in *B. subtilis*.

No conclusive relationship could be drawn between inhibition of any specific PBP and cell growth (*i.e.*, there is not a linear relationship between the IC_{50} values for any single PBP and the MIC values). However, a closer look at the profile of the PBPs targeted at the inhibitory concentrations of individual compounds reveals some interesting trends within different β-lactams subclasses. Most penicillins completely blocked PBP2a and PBP2b, in addition to one or more other PBPs at sub-MIC levels (**Fig. 3.6**). All cephalosporins, excluding cephalexin, targeted PBP1 under sub-MIC concentrations. The same result was observed with aztreonam and faropenem, a monobactam and a penem, respectively (**Fig. 3.6**). While this cumulative data might implicate all of these PBPs as potential lethal targets in *B. subtilis*, we found that meropenem, doripenem, and 6-APA failed to significantly inhibit any PBPs at sub-MIC concentrations, immediately contradicting this hypothesis. Overall, our data suggests the PBPs as potential lethal targets of β-lactam antibiotics, while raising the possibility of additional intracellular targets for different β-lactams.

	PBP1a/1b	PBP2a	PBPH/2b	PBP3	PBP4	PBP5	MIC
Aztreonam	4	84	82	100	52	100	16
Faropenem	6	19	10	97	14	78	0.125
Doripenem	59	40	36	63	69	78	0.0625
Meropenem	100	86	75	84	79	86	0.0625
Amdinocillin	68	28	12	83	92	91	16
Penicillin V	38	0	1	2	19	7	32
Penicillin G	52	0	0	3	14	5	16
Ampicillin	19	1	2	6	5	36	8
Amoxicillin	25	3	3	0	8	56	4
Piperacillin	3	1	0	0	0	6	64
Methicillin	74	4	10	100	54	100	0.25
Oxacillin	70	50	54	91	13	99	0.25
Cloxacillin	67	47	63	100	10	78	0.125
6-APA	100	53	77	84	71	16	128
Cephalexin	39	1	15	98	52	100	0.5
Cefuroxime	1	94	43	100	3	97	0.125
Cefotaxime	1	100	16	100	10	100	0.0625
Ceftriaxone	1	90	45	92	13	92	0.25
Cephalothin	7	28	25	100	13	100	0.03125
Cefsulodin	1	89	27	99	3	99	8
Cefoxitin	2	28	9	54	3	5	1

Figure 3.6. PBP inhibition at MIC illustrated as a heat map to summarize level of PBP inhibition at growth inhibitory concentration. The numbers in each cell are the average of % Boc-FL labeling of each PBP at MIC concentration, from two separate experiments. Since titrations were done in 10-fold intervals, the Boc-FL labeling at the concentration closest to MIC was used. Low binding (red) demonstrates high inhibition of that PBP at that concentration, whereas blue cells indicate high levels of Boc-FL labeling/low PBP inhibition.

3.4. Development of Meropenem-Based Probes

As mentioned earlier, PBP3 has intrinsically low affinity for most β-lactams and has not received much attention until recently that it was shown to become catalytically essential in the absence of PBP2b transpeptidation activity.(21, 126) Given the unique affinity of the carbapenems for PBP3, we designed chemical probes based on meropenem molecule to target the activity of this protein. The secondary amine group located on the pyrolidine ring was used to attach a fluorophore to enable visualization of the TP activity. Another analog containing an alkyne side chain, **click-MEM**, was produced to enable

installment of different reporter and affinity tags through the copper(I)-catalyzed Hüisgen azide-alkyne cycloaddition (CuAAc). (**Fig. 3.7**)

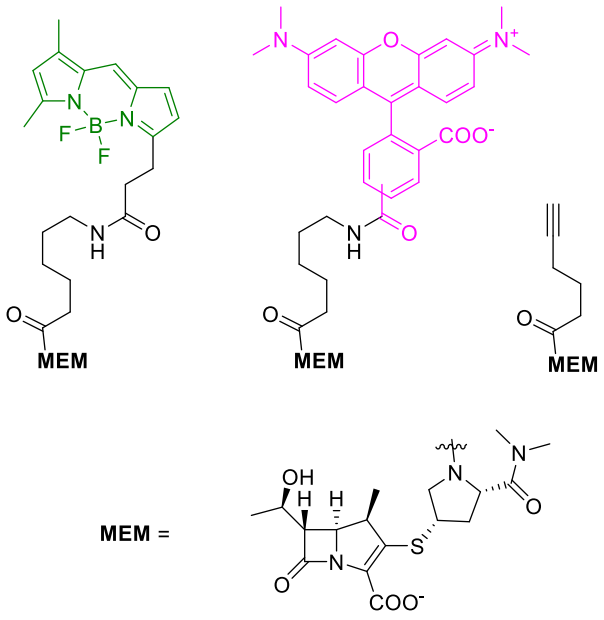

Figure 3.7. Structure of meropenem-based probes. Meropenem (MEM) was coupled to BODIPY-FL or TAMRA to generate fluorescent probes (*MEM-BODIPY FL* and *MEM-TAMRA*). 5-Hexynol group was attached to generate *mem-Click* with could be further conjugated with different azide-containing molecules.

3.4.1. Meropenem-Based Probes Retain the Expected PBP Selectivity Profile

MEM-BODIPY-FL and Click-MEM probes retained specificity for PBP 3 and 5, identical to the core meropenem molecule. With the TAMRA conjugate, MEM-TAMRA, PBP1 was also labeled in addition to PBP3 and PBP5 (**Fig. 3.8**). Assessment of PBP targeting profile in strains in which PBP3 and 5 were knocked out, DK654 and DK695, respectively, further proved these proteins as the targets of our meropenem-based probes (**Fig. 3.9**). It must be noted that at this point in the study, we had to switch from *B. subtilis PY79* to *3610*, since we had access to engineered constructs of the latter strain. These two strains show comparable morphology and growth behavior and we achieved identical PBP selectivity profile with our chemical probes.

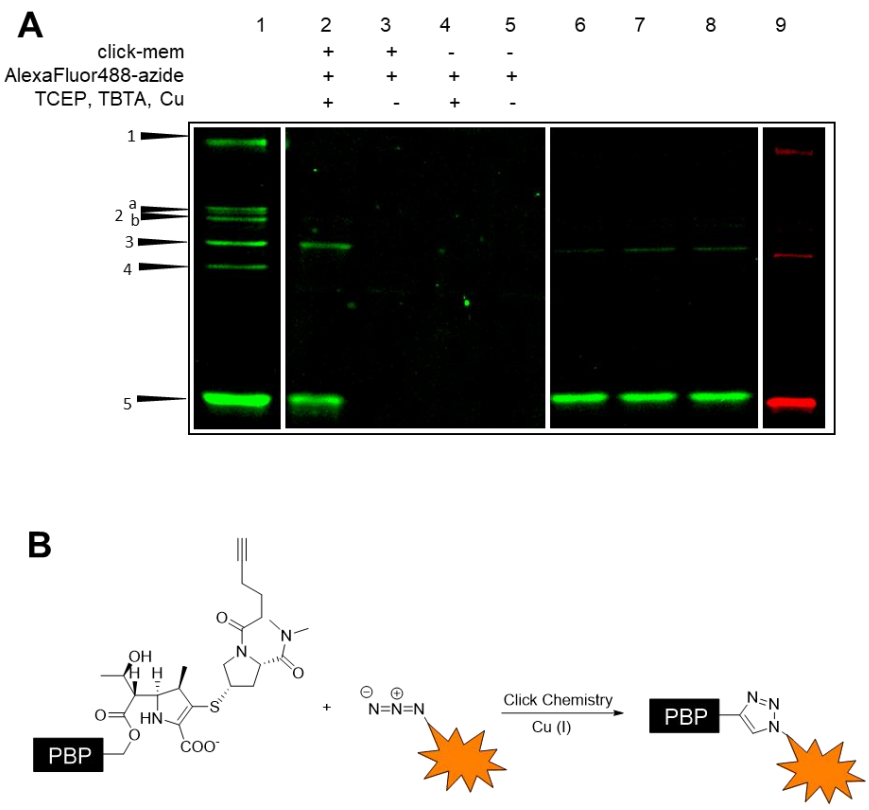

Figure 3.8. Meropenem-based probes target PBP3 and 5 in *B. subtilis*. A) PBP labeling profile of meropenem-based probes in *B. subtilis* 3610 cells assessed by SDS PAGE. 1: 10 µM Bocillin-FL (control) 2-5: treatment by 5 µM click-mem (2,3) or no probe (4,5) followed by reaction with different combinations of click reagents. Only lane 2, where cells were treated with the probe and reacted with AlexaFluor488-azide in the presence of all click reagents resulted in fluorescent labeling of PBPs. 6-8: treatment by 2 µM mem-BODIPY for 10 min (6), 20 min (7) or 30 min (8). Labeling intensity plateaus after 20 minutes. 9: treatment by 2 µM mem-TAMRA for 30 min. B) Scheme of click reaction between alkyne-tagged PBP and AlexaFluor 488-azide.

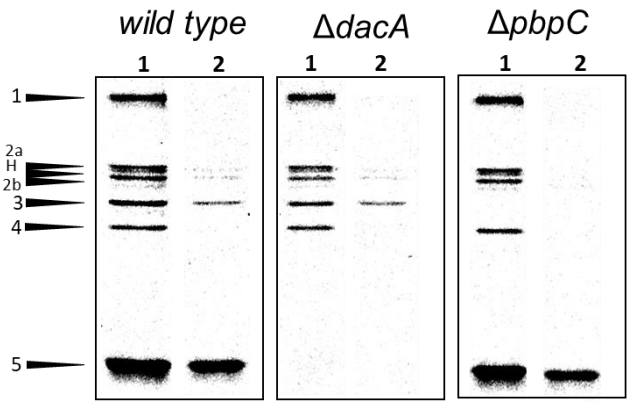

Figure 3.9. PBP labeling profile of MEM-BODIPY in *B. subtilis* 3610 (wild type), DK654 (Δ*dacA*) and DK695 (Δ*pbpC*). 1 : Boc-FL 10µM; 2 : mem-BODIPY 2µM.

3.4.2. Identification of Meropenem Targets in *B. subtilis* Using Mass Spectrometry

While comparison with saturating concentration of Boc-FL, whose protein content has been previously assigned, enabled speculation about the proteins labeled with meropenem-based probes, we employed Click-MEM to confirm their identities. *B. subtilis* PY79 cells were incubated with Click-mem probe and a biotin affinity tag was installed *via* azide-alkyne Huisgen cycloaddition. Biotinylated proteins were subsequently enriched by Neutravidin-agarose beads, subjected to proteolytic digestion by trypsin and the resulting peptide mixture was analyzed by LC-MS/MS. The obtained data were searched against the *B. subtilis* FASTA amino acid sequence database using the MaxQuant suite. The MS identification results confirmed that PBP3 and PBP5 were enriched as expected. Inspired by these results, we sought to expand this methodology to pulldown analysis of other PBPs in different bacterial systems (CHAPTER 5).

3.4.3. Visualization of PBP3 activity in *B. subtilis*

We utilized MEM-BODIPY FL probe in imaging studies to localize PBP3 activity in *B. subtilis* DK654, in which PBP5 is knocked out (**Fig. 3.10**). These images showed that PBP3 localized at the division septum as a ring in early-to-mid divisional cells and moved to the constricting ring and the separation site during late divisional stages. This is an unprecedented finding and is in contrast with a previous study that used fusion protein tags to localize PBPs in *B. subtilis* and reported that fluorescent PBP3 construct distributed around the cell periphery and was not enriched at the site of the septum.(20) In fact, we only noticed patch-like distribution of fluorescence signal in a number of single cells. Our findings were consistent with a more recent study in which *B. subtilis* PBP3 was immunolabeled and showed predominant localization at mid-cell and the cell poles.(21) The fact that we visualized the active PBP3 content in cells could be used to explain the differences observed.

Next, we sought to employ our Click-MEM probe for the same purpose, since the alkyne functionality would enable installation of different reporter groups in future. Performing the labeling and click chemistry in phosphate buffer saline led to lysis of the majority of the cells. It was discovered that performing these steps in minimal media would overcome this problem, and we were able to track the activity of PBP3 in live cells (**Fig. 3.10**).

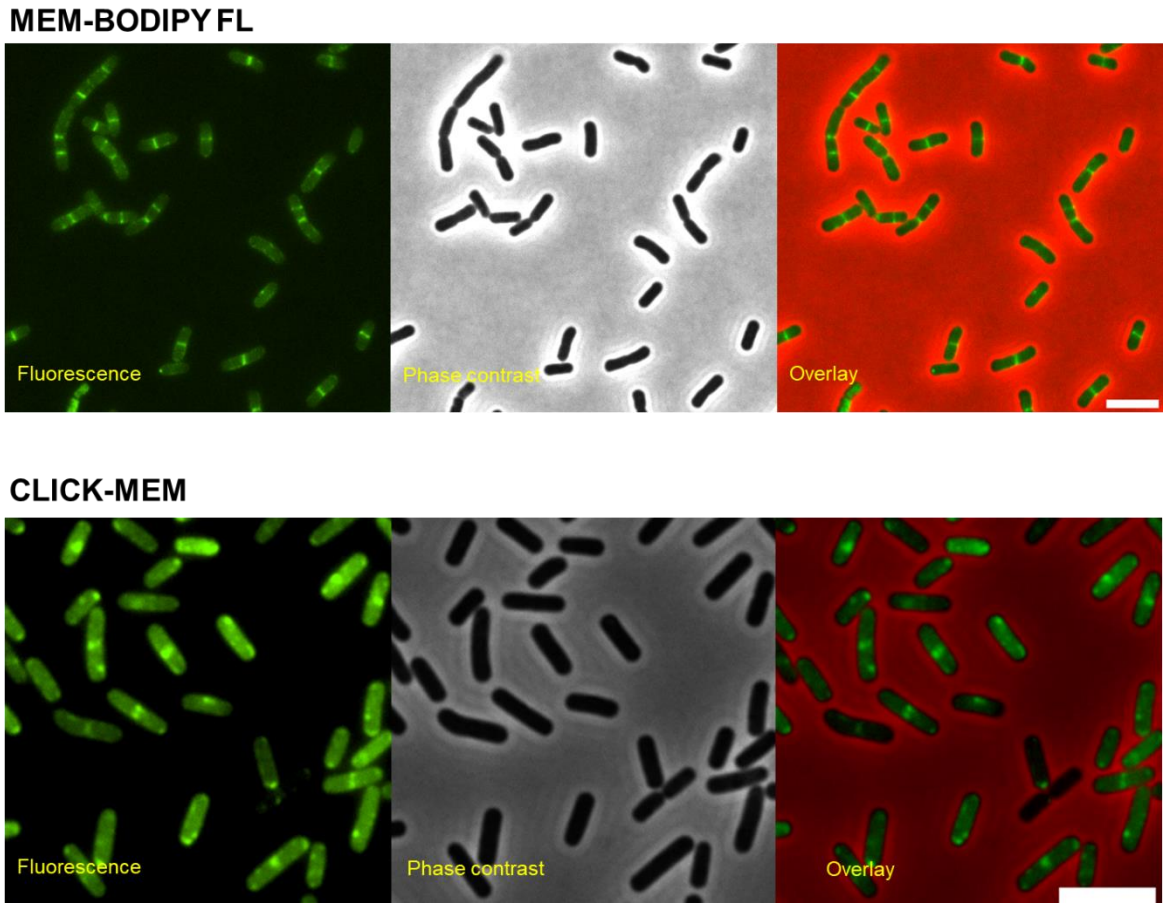

Figure 3.10. Visualization of PBP3 activity in live *B. subtilis DK654* cells. Exponentially growing *B. subtilis DK654* cells were labeled with 2 μM MEM-BODIPY FL (*top*) or 5 μM Click-MEM followed by click reaction with 50 μM AlexaFluor488-azide in the presence of 2.5 mM sodium ascorbate, 200 μM BTTAA and 100 μM copper sulfate in minimal media(*bottom*). Further experimental details are reported at the end of the chapter. Scale bar = 5 μm.

3.4.4. PBP Targeting Profile of Meropenem Probes in Other Bacteria

As previously described, meropenem and doripenem have high affinity for PBP2 and 3 in *P. aeruginosa* and PBP2 in *E. coli*, both of which are rod-shaped Gram-negative organisms.(140, 145) We tested our meropenem-based probes in *E. coli* DC2 to verify the PBP labeling profile (**Fig. 3.11**). PBP2, as well as PBP4, were selectively labeled by MEM-TAMRA at lower concentrations and saturation of all PBPs occurred at ≥ 10 µg/mL of the probe.

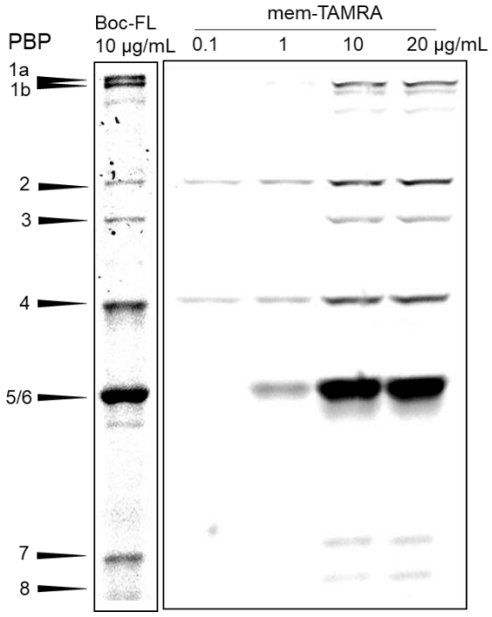

Figure 3.11. PBP labeling profile of MEM-TAMRA in *E. coli* DC2 cells. MEM-T selectively targets PBP2 and 4 at lower concentrations. Saturation of all PBPs occurs at ≥ 10 µg/mL of the probe.

In *S. pneumoniae*, which was assessed as another Gram-positive model, PBP2x followed by PBP1b and PBP3 were tagged by click-MEM (**Fig. 3.12**). This result is consistent with our previous β-lactam titration study in this microorganism.(146)

Interestingly, when MEM-TAMRA was used in *S. aureus* cells, PBP1, PBP2 and PBP4 were labeled more intensely than with Boc-FL, even at comparable concentrations(**Fig. 3.13**). PBP4 was recently shown to mediate high-level broad-spectrum resistance to β-lactams that had been otherwise believed to be mediated by PBP2a, a non-essential PBP that shows low-affinity to entire class of β-lactams.(147, 148)

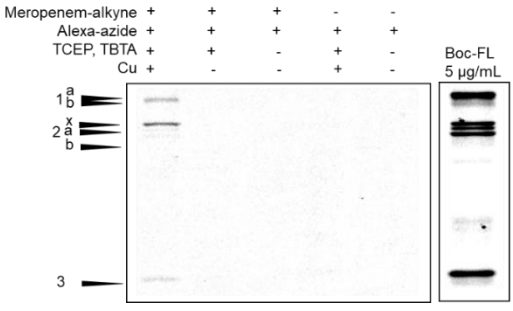

Figure 3.12. PBP labeling profile of click-mem in S. pneumoniae IU1945 cells. Mem-click was used at 5 µg/mL. PBP2x was tagged predominantly followed by PBP1b and 3.

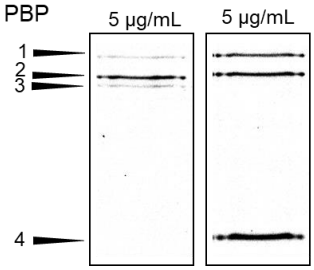

Figure 3.13. PBP labeling profile of MEM-TAMRA in *S. aureus BAA-1721* cells. MEM-T selectively targets PBP1, 2 and 4 at 5 µg/mL concentration.

3.5. Development of Mecillinam-Based Probes

Among the tested β-lactams in this study, mecillinam (amdinocillin) stood out with high selectivity for PBP2b followed by PBP2a, both of which are class B transpeptidases in *B. subtilis*. Aside from PBP3, which was inhibited at higher concentrations of mecillinam, no other PBP was targeted by this antibiotic (**Table 3.1**). Mecillinam is an extended spectrum penicillin, from the amidinopenicillin subclass, which is a specific inhibitor of PBP2 in the cell elongation machinery of *E. coli*.(115, 149-151)

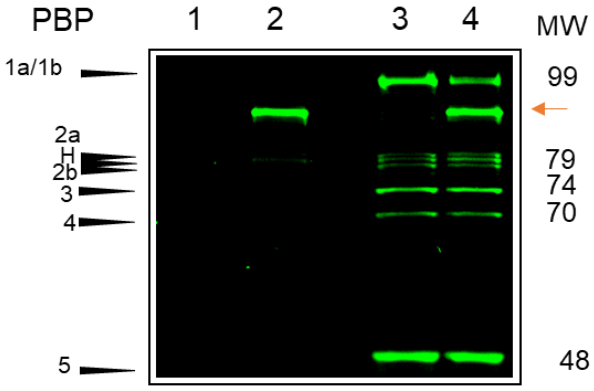

Figure 3.14. SDS-PAGE analysis of the transpeptidation activity of PBPs in *B. subtilis* cells expressing GFP-PBP2b (DK4224). The yellow arrow shows the GFP-PBP2b construct on the gel. 1. DK4224 membrane lysates, heated at 95 °C for 5 mins prior to loading. 2. DK4224 membrane lysates. 3. DK4224 membrane lysates labeled by 10 µg/mL Boc-FL for 10 mins, and heated at 95 °C for 5 minutes prior to loading. 4. DK4224 membrane lysates labeled by 10 µg/mL Boc-FL for 10 mins, and loaded without heating. The GFP-PBP2b band disappeared upon heating. More experimental details are discussed at the end of this chapter.

PBP2b is the only essential PBP in *B. subtilis* and its presence has been shown to be essential for septum formation.(103, 125, 152) Preceding studies using GFP constructs of PBP2b indicate that it localizes to the septum, suggesting an essential catalytic role during cell division.(20, 21) However, when we labeled *B. subtilis* cells expressing *gfp-pbpB*, (DK4224) with Bocillin-FL, which is a measure of transpeptidation

activity of PBPs, we discovered that the GFP construct is inactive. This was concluded from the observation that the GFP-PBP2b fluorescent signal in Boc-FL labeled cells is lost upon heating, which can be explained by the thermal instability of GFP, which decreases at higher temperatures.(153, 154) Conversely, heat does not affect the covalent interaction between Boc-FL and the PBP active site. Thus, the loss of signal is due to the degradation of chromophore group in GPF (**Fig. 3.14**). Based upon this result, we decided to develop activity-based probes using the mecillinam core in order to assess the essential catalytic activity and localization of PBP2b during cell growth in *B. subtilis*.

3.5.1. Design and Synthesis of MEC Probe

Mecillinam (MEC) is a 6-β-amidinopenicillanic acid derivative containing a hexahydro-1H-azepin-1-yl side chain *via* an amidine linker group. The amidine linker group is presumably responsible for the specifically high affinity of amidinopenicillins for PBP2 in *E. coli*.(151) As the mecillinam core does not possess any functional group that could be readily appended to a reporter group, an alternative scaffold was proposed by introduction of a homopiperazine ring into the structure (**Fig. 3.15**).

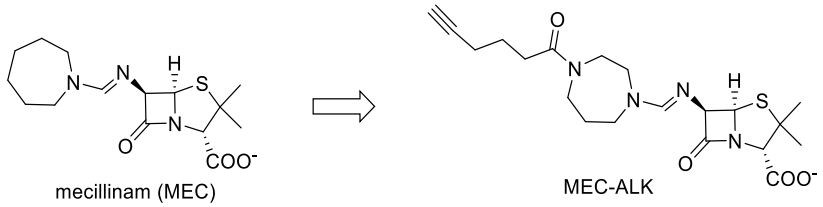

Figure 3.15. Design of MEC-ALK probe, inspired by the mecillinam structure.

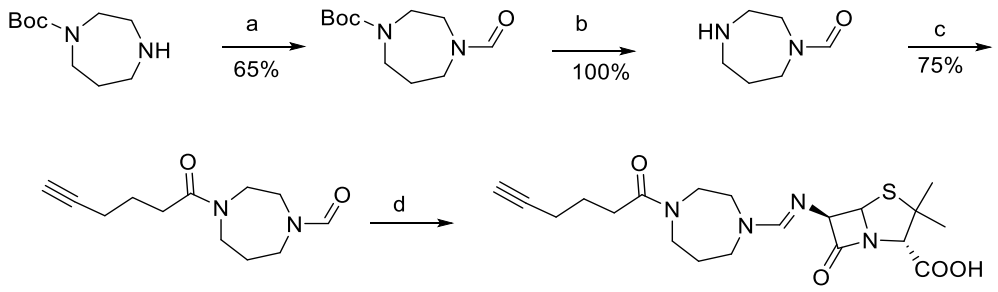

Scheme 3.1. Synthesis of MEC-ALK. a) Ammonium formate, acetonitrile, 4h reflux; b) 50% TFA/DCM, 0 °C-R.T., 30 min; c) i) 5-hexynoic acid, EDC, HOBt, TEA, 0 °C-R.T., 1h. ii) TEA, R.T. overnight; d) i) $(COCl)_2/CHCl_3$, -10 °C, 1 h, ii) 6-APA, TEA/$CHCl_3$, -65 °C → -15 °C (1h) → R.T. (overnight).

The synthetic route for MEC-AZ was inspired by a previous method for the synthesis of mecillinam derivatives(155) and is shown in **Scheme 3.1**. Experimental details and characterization data are reported at the end of chapter. Titration of *B. subtilis* PY79 cells by MEC-ALK revealed that the probe has retained specificity for PBP2b and PBP2a (**Fig. 3.15**). Our attempts to install fluorescent reporting groups on the tagged PBPs has been unsuccessful so far. Further optimization of the click chemistry condition is currently underway.

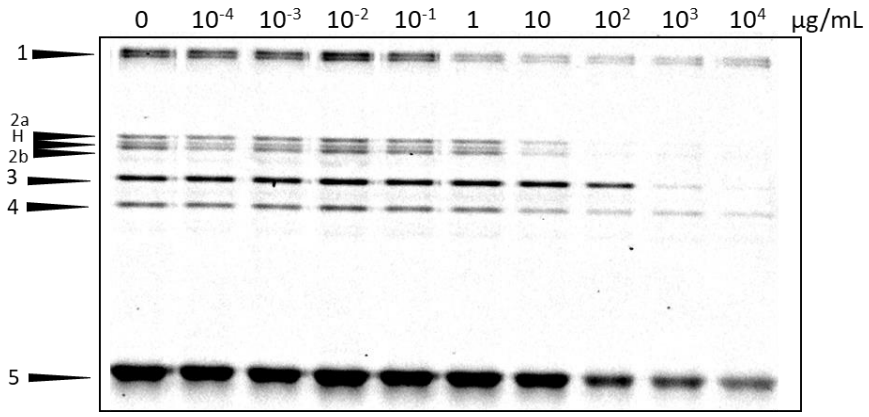

Figure 3.15. SDS PAGE analysis of PBP labeling with MEC-ALK probe in *B. subtilis* PY79 cells. Cells were treated with increasing concentrations of MEC-ALK for 30 min followed by 10 µg/mL Boc-FL for 10 min.

3.6. Conclusions and Future Applications of Data

This is the first extensive analysis of PBP inhibition profiles by the β-lactam antibiotics in *B. subtilis*. Seven compounds showed dose-dependent selectivity for a single PBP, while the remainder of the molecules inhibited multiple PBPs. In general, most cephalosporins were most potent against HMW PBP1 and 4, with minimal inhibition of D,D-carboxypeptidase, PBP5. On the other hand, most penicillins failed to fully inhibit PBP1 even at millimolar concentrations, while PBP5 was completely inhibited by most. Penicillins were strong inhibitors of PBP2a, 2b and 4. Mecillinam stood out as a specific inhibitor of PBP2b and PBP2a. Meropenem and doripenem resulted in a distinct selectivity profile by exclusively inhibiting PBP3 and 5. Based on these results, chemical probes were designed and synthesized using meropenem and mecillinam core, to target PBP3 and PBP2b, respectively. Meropenem-based probes enabled us to examine PBP3 in live *B. subtilis* cells, which localized mainly as a ring during early divisional stages and moves to the central septal region and the division site at later stages. This finding is unprecedented and suggests a potential role for PBP3 during the division process in *B. subtilis*. Moreover, biotin-mediated enrichment of meropenem-tagged proteins from whole cells enabled the isolation of PBP3 and PBP5, highlighting the significance of our chemical tools for investigation of PBPs and proteins associated with them. Overall, this work highlights the significance of the development of PBP-selective chemical tools to complement the existing molecular and cell biology tools, in order to augment our understanding of bacterial growth and division processes.

3.7. Materials, Methods and Characterization Data

3.7.1. Bacterial Strains, Growth Conditions, Antibiotics and Chemicals

B. subtilis PY79, *3610*, PBP knock-out strains and *DK4224* were generously provided by our collaborator, Prof. Dan Kearns, at Indiana University, Bloomington. *E. coli*

DC2 was received from the same source. *S. pneumoniae IU1945* was generously provided by our other collaborator at Indiana University, Prof. Malcolm Winkler. *B. subtilis PY79*, *3610* and PBP knockout strains (52) were cultured in Luria-Bertani (LB) broth at 30 °C with shaking at 220 rpm to reach the desired optical density at 600 nm (OD_{600}). *B. subtilis DK4224*, which expresses GFP-tagged PBP2b was cultured in LB broth containing 100 μg/ml spectinomycin (hydrochloride salt, Sigma) antibiotic and 1 mM Isopropyl β-D-1-thiogalactopyranoside (IPTG; Amresco). *E. coli DC2* was cultured in LB broth as 37 °C with shaking at 220 rpm to reach OD_{600} ~0.4. *S. aureus BAA-1721* (a methicillin-sensitive strain) was purchased from ATCC and grown in Tryptic Soy Broth at 37 °C with shaking at 220 rpm to an OD_{600} ~0.5. *S. pneumoniae IU1945* was cultured in Brain Heart Infusion (BHI) broth at 37 °C statically in an atmosphere of 5% CO_2 to an OD_{620} of ~0.15-0.2.

Faropenem, doripenem, meropenem, (+)-6-aminopenicillanic acid (6-APA), ampicillin, methicillin, oxacillin, cloxacillin, piperacillin, cephalexin, cefsulodin, cefoxitin, cephalothin, cefuroxime, ceftriaxone and cefotaxime were purchased from Sigma-Aldrich (St. Louis, MO). Penicillin V and penicillin G were from USP. Amdinocillin was purchased from Fluka. Aztreonam and amoxicillin were obtained from MP Biomedicals (Solon, OH). Bocillin-FL was purchased from Life Technologies (Grand Island, NY). All antibiotics were stored as solids at 4 °C (except for meropenem, doripenem, aztreonam and faropenem stored at -20 °C) and were dissolved in Milli-Q purified water (unless noted otherwise) at 10 mg/mL immediately before each experiment. 6-APA, amoxicillin, and cefuroxime were not soluble in water. Thus, they were dissolved in phosphate-buffered saline (PBS), pH 7.4, at a 1 mg/mL concentration. All stock solutions were serially diluted (10-fold) in PBS to make 0.0001- to 1,000 μg/mL working solutions. For MIC determination studies, antibiotics were dissolved and serially diluted in LB broth.

All reactions were carried out in anhydrous solvents under Ar atmosphere. Hydroxybenzotriazole (HOBt) was purchased from Chem-Impex International, N-(3-Dimethylaminopropyl)-N-ethylcarbodiimide HCl (EDC.HCl) and ammonium formate were purchased from Fluka. BODIPY- and TAMRA-succinimidyl esters were purchased from ThermoFischer Company. Meropenem (anhydrous) was purchased from ChemCruz. Oxalyl chloride was purchased from Acros. All other reagents were purchased from Sigma-Aldrich and used without further purification.

AFDye 488 azide (equivalent of Alexa Fluor ® 488 azide), biotin-PEG3-azide, tris-hydroxypropyltriazolylmethylamine (THPTA) and (4-{[bis-(1-tert-butyl-1H-[1,2,3]triazol-4-ylmethyl)-amino]-methyl}-[1,2,3]triazol-1-yl)-acetic acid (BTTAA) were purchased from Click Chemistry tools. Tris(2-carboxyethyl)phosphine (TCEP), Tris[(1-benzyl-1H-1,2,3-triazol-4-yl)methyl]amine (TBTA), sodium ascorbate and copper sulfate were purchased from Sigma-Aldrich. All click reagents were kept at -20 °C as powder, except TCEP (stored at 4 °C) and copper sulfate and sodium ascorbate which were stored at room temperature. Five mM stock solutions of azide cargo was prepared in DMSO and stored at -20 °C. All the other solutions were prepared by dissolving the required amounts in miliQ water every time.

^{1}H and ^{13}C NMR spectra were recorded on Varian VI- 400, and VI-500 spectrometers and are reported in parts per million (δ). The following abbreviations were used to explain the multiplicities: s = singlet, d = doublet, t = triplet, q = quartet, quin = quintet, m = multiplet, b = broad, app. = apparent. BioTof II electrospray ionization-time-of-flight mass spectrometer with internal standard (Methanolic solution of PEG), UPLC-ESI-TOF MS instrumentation (Agilent, 6220) were used to obtain accurate mass spectral data. HPLC purification was performed using an Agilent 1200 HPLC using a reverse phase

column and detected by diode array detector (200–600 nm). Gradients consisted of 5–95% B (A: H_2O, 0.1% formic acid (FA); B: CH_3CN, 0.1% FA) over 20-30 minutes.

3.7.2. β-Lactam Titration and Detection of PBPs

B. subtilis cells from 1.0 mL of an exponential culture at an OD_{600} of 0.4 were harvested by centrifugation (16,000 × *g* for 2 min at room temperature). The cell pellets were washed in 1 mL of PBS (pH 7.4) by gently pipetting up and down a few times, and the cells were again pelleted. The same centrifugation settings were used throughout the assay, unless otherwise noted. Cells were resuspended in 50 µL PBS containing 0.0001 to 1,000 µg/mL β-lactam antibiotics, and a reference sample was resuspended in 50 µL PBS without antibiotic (blank). After 30 min of incubation at room temperature, the cells were pelleted, washed with 1 mL PBS, and resuspended in 50 µL PBS containing 5 µg/mL Boc-FL (0.1% DMSO). After 10 min of incubation at room temperature, the cells were pelleted and washed in 1 mL PBS. Next, the cells were resuspended in 100 µL PBS containing 10 mg/mL lysozyme (chicken egg white, Fluka) and statically incubated at 37 °C for 30 min, after which samples were sonicated using a Hielscher vial tweeter UP200St (70% C, 95% A, 5% adjustment snap and 1s SD Interval / 10s for 6 x 1 min intervals with 1 min cooling time in between) on ice. The membrane proteome was isolated by centrifugation at 21,000 × *g* for 15 min at 4 °C, as previously reported.(115, 116) The supernatant was discarded, the membrane was resuspended in 100 µL PBS and protein concentration adjusted to 5.0 mg/mL by dilution with PBS. The protein concentration was measured by NanoPhotometer P330 (IMPLEN). Thirty microliters of proteome sample was dispensed into a clean 1.5-mL microcentrifuge tube and 10 µL of 4 × SDS-PAGE loading buffer was added to each sample. The samples were heated for 5 min at 90-95 °C to denature the proteins then cooled to RT. Twelve microliters of sample were loaded onto a 10% SDS-PAGE gel (acrylamide:bis-acrylamide = 29:1). The protein bands were

separated by gel electrophoresis for 1.5 h at 180 V, 400 mA, 60 W. The gel was rinsed with distilled water three times before fluorescence scanning using a Typhoon 9210 gel scanner (Amersham Biosciences, Pittsburgh, PA) with a 526-nm wavelength short-pass filter at 50-µm resolution. The gel images were analyzed using ImageJ software (National Institutes of Health, Bethesda, MD). The background signal of the gel images was subtracted, and the brightness and contrast were adjusted to optimize the signal-to-noise ratio (all operations were uniformly performed over the entire gel). Integrated density values were measured for gel band quantitation, and Boc-FL labeling of each PBP in antibiotic-treated samples was shown relative to the blank. Integrated density values were inserted into GraphPad Prism (GraphPad Software, La Jolla, CA) to create graphs showing relative percentiles of Boc-FL labeling versus inhibitory concentrations (ICs). Determinations of 50% IC values (IC_{50}s) were performed using the same software. For all dose-response curves, data were fitted to a four-parameter logistic equation. The average of IC_{50} values calculated from two independent assays was reported for individual PBPs for each β-lactam.

3.7.3. Antimicrobial Susceptibility Assay

B. subtilis strain PY79 was streaked from the glycerol stock to LB-Agar plates and incubated at 37 °C for 14 to 16 h. Four colonies were inoculated into 5 mL of LB broth and grown to an OD_{600} of 0.08-0.13. Cultures were then diluted 100-fold (2.8×10^5 CFU/mL). 0.125 – 64 µg/mL solutions of antibiotics in LB broth as two-fold dilutions was prepared. *Lower or higher concentrations were prepared as needed, in case growth inhibition could not be assessed within the mentioned range.* In 96-well plates, 100 □L diluted culture was added to 100 □L of serially diluted antibiotic in each well. Each compound was run in duplicate. After incubation at 37°C for 18 to 20 h, plates were examined by eye. The lowest concentration that inhibited cell growth was recorded as the MIC.

3.7.4. PBP Labeling Profile by Meropenem-Based Probes

3.7.4.1. Mem-BODIPY Probe Concentration Determination

All probes were stored as DMSO solutions at -80 °C. Concentration of MEM-BODIPY was determined by measuring UV-Vis absorption of its solution at λ_{max} of its corresponding fluorophore. 10× and 100× dilutions of probe was made in methanol and absorbance was read at 504 nm using NanoPhotometer P330 (IMPLEN). The average of 3 reads of the concentration that was in 0.1-0.9 range was used to calculate concentration. (ε = 85,000 $M^{-1}.cm^{-1}$).

3.7.4.2. Probe Labeling.

B. subtilis cells from 1.0 mL of an exponential culture at an OD_{600} of 0.4 were harvested by centrifugation (16,000 × *g* for 2 min at room temperature).

E. coli cells from 1.0 mL of an exponential culture at OD600 ~0.4 were harvested by centrifugation (8,000 × g for 2 min at room temperature).

S. aureus cells from 1.0 mL of an exponential culture at an OD_{600} of 0.5 were harvested by centrifugation (16,000 × *g* for 2 min at room temperature).

S. pneumonaie cells from 1.5 mL of an exponential culture at an OD_{620} of ~0.18 were harvested by centrifugation (16,000 × *g* for 2 min at room temperature).

The cell pellets were washed in 1 mL of PBS (pH 7.4) by pipetting up and down a few times, and the cells were again pelleted using the same setting. Cells were subsequently suspended in 50 µL PBS containing 0.5-2 µM mem-BODIPY, 1-10 µM click-mem or 50 µM-1 mM Click-MEC. After 30 min of incubation at room temperature, cells were pelleted, washed with 1 mL PBS, and pelleted again.

****For imaging experiments, cells were kept in S750 minimal media throughout the preparation.*

3.7.4.3. Click Reaction

B. subtilis cell pellets labeled by click-MEM (as described above) were suspended in 50 µL of click reaction cocktail consisting of PBS containing 20-50 µM AF488 azide, 1 mM TCEP, 0.5 mM TBTA and 1 mM $CuSO_4$. The resulting suspension was incubated at room temperature for an hour. For SDS PAGE analysis, cells were subsequently pelleted and washed with 1 mL PBS. Membrane proteome collection and analysis was performed as described in section 3.7.2 for β-lactam titration.

For fluorescent imaging experiments, cell pellets were suspended in 50 µL of click reaction cocktail consisting of S750 minimal media containing 50 µM AF488 azide, 2.5 mM sodium ascorbate, 0.2 mM BTTAA and 0.1 mM $CuSO_4$ and the incubation time was dropped to 30 min.

3.7.5. Proteomic Analysis of Meropenem Targets

3.7.5.1. Protein Enrichment and Digestion

B. subtilis membrane lysates labeled by click-MEM (as described above) were suspended in 50 µl of click reaction cocktail consisting of PBS containing 50 µM biotin-PEG3-azide (or Alexa488-Fluor azide as control for click reaction/binding), 1 mM TCEP, 0.5 mM TBTA and 1 mM $CuSO_4$. The resulting suspension was incubated at room temperature for one hour. (Fluorescent samples were run on 10% SDS PAGE gels to detect the tagged PBPs as described above) To remove excess biotin and click reagents, protein precipitation was performed using ProteoExtract ® protein extraction kit following the manufacturer's protocol. The resulting pellet was resuspended in 1ml of 1.2% SDS/PBS and sonicated for 3–4 s to obtain a homogenized solution. After heating it at 80–90 °C for 5 min, it was cooled on ice. The sample was transferred to a 15-ml conical tube and diluted to 0.2% SDS with 5 ml of PBS. 100 µl streptavidin-agarose beads (pre-equilibrated with 3 × 200 µl PBS) were aliquoted into a 1.2-ml Bio-Spin column and washed

three times with PBS. Washed beads were suspended in 200 µl of PBS and added to the sample in the conical tube. The sample was rotated for 3 h at RT, and then centrifuged for 3 min at 1,400 × g. The beads were transferred into a Bio-Spin column, and the beads were washed with 10 ml of 0.2% SDS/PBS and then with 10 ml of PBS. The dried beads were transferred into a 1.7-ml eppendorf tube, to which 500 µl of a 6 M urea/PBS solution was added. In order to reduce the proteins, 25 µl of 200 mM Tris (2-carboxyethyl) phosphine (TCEP) was added to the sample, and it was heated at 65 °C for 15 min and then cooled to 37 °C. Alkylation of reduced proteins was accomplished by addition of 25 µl of 400 mM iodoacetamide (IAA) and incubation of the sample for 30 min at 37 °C with agitation in dark. The sample was diluted with 950 µl of PBS, and then centrifuged at 1,400 × g for 2 min. The supernatant was discarded, and the beads were suspended in a premixed solution of 200 µl of 2 M urea/PBS, 2 µl of 100 mM $CaCl_2$ and 4 µl of 0.5 µg/ml trypsin. The reaction was allowed to proceed overnight at 37 °C with agitation, and then it was transferred to a 1.2-ml Bio-Spin column. After eluting the tryptic peptides into a low adhesion tube by centrifugation at 1,000 × g for 5 s, the beads were washed with 50 µl of water twice, and the eluent and water washings were combined in the same tube. Following the addition of 2 µl of formic acid (FA), the peptide sample was desalted using ZipTip C_{18}.

3.7.5.2. Preparation of Samples for Mass Spectrometry Analysis

Ziptip ® C18 pipette tips (Millipore Sigma) were used to remove salts using the protocol from the manufacturer. MS grade water, acetonitrile (ACN) and trifluoroacetic acid (TFA) were used. Briefly, the dried samples were reconstituted with 13 µL of reconstitution solution (R; 5:95, ACN:water, 0.1% TFA), vortexed and centrifuged (sample pH must be acidic at this point; TFA was added as necessary). ZipTip was placed on a P10 pipettor set to 10 µL. The ZipTip was hydrated by aspirating solution 1 (50:50 ACN:water, 0.1%

TFA) followed by solution 2 (0.1% TFA in water). Next, 10 µL of the sample was loaded by pipetting up and down 5-6 times. Next, the salts were removed by aspirating 10 µL of solution 2 (0.1% TFA in water) for a total of 4-5 washes (expel the wash into waste each time). Finally, the peptides were eluted by aspirating and expelling 10-20 µL of elution solution (60:40 ACN:water, 0.1% TFA) on ice 10 times (sample expelled into the same solution each time). Samples were stored at –20 °C until LC-MS/MS analysis.

3.7.5.3. LC-MS/MS Analysis of Tryptic Digest

Peptides from three biological replicates were analyzed using an UltiMate 3000 Nano HPLC system (Thermo Scientific) coupled to an Orbitrap Elite Hybrid Ion Trap (Thermo Scientific). One-5 µl of tryptic peptides was loaded onto a 15 mm × 0.1 mm trapping column which was washed with solvent A (0.1% formic acid in water) to remove any salts and the retained peptides were separated on a column (75 µm inner diameter, 35 cm) manufactured in-house and eluted at 300 nl/min using a 120-min gradient with 0.1% formic acid in water and 0.1% formic acid in acetonitrile.

MS raw files were processed using MaxQuant software (version 1.6.2; Max Planck Institute of Biochemistry). MS/MS-based peptide identification was carried out using the Andromeda search engine against the *B. subtilis* 168 UniProt database. For label-free protein quantification, the MaxLFQ algorithm was used as part of the MaxQuant package. The ‘match between runs’ option was enabled to maximize the number of quantification events across all replicates. Statistical analysis was performed in Perseus (version 1.6.1.1). Proteins identified only by site modification, reverse hits or contaminants were removed. Volcano plots were generated by performing a two-sample t-test with permutation-based statistics (FDR 0.01, S0 = 2).

3.7.6. Fluorescence Microscopy

Microscopy experiments were performed by Dr. Felix Dempwolff at Indiana University, Bloomington. Briefly, cells were grown in S750 minimal medium. Cells were labeled with MEM-BODIPY and Click-MEM as described in 3.7.3.2, except that PBS was substituted with S750 minimal media to avoid lysis. Microscopy was performed with a Nikon eclipse 80i microscope, equipped with a Plan Apo 100X Ph 3 objective (NA 1.4). Cells were mounted on 1% (wt/vol) agarose pads containing $S7_{50}$ minimal medium on object slides. Images were acquired with a Cool snap HQ2 camera (Photometrix) and were processed with Metamorph 7.7.9 software (Universal Imaging Corp.).

3.7.7. Probe Synthesis and Characterization

3.7.7.1. Meropenem-TAMRA

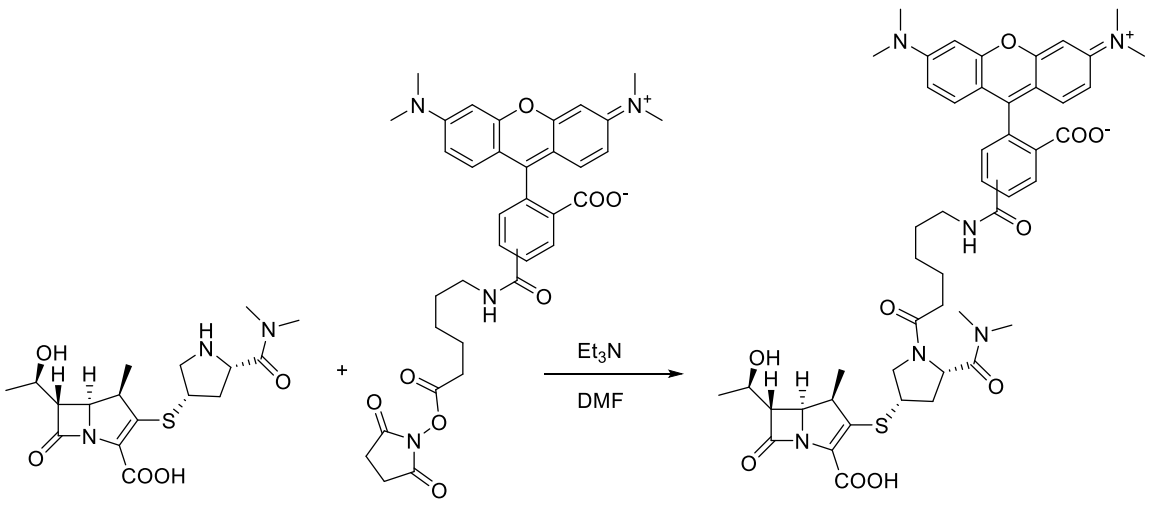

To a solution of TAMRA-X, SE (1.0 mg, 0.0015 mmol, 1.0 equiv) in anhydrous DMF (0.1 mL) at room temperature was added meropenem (0.66 mg, 0.0017 mmol, 1.1 equiv) and TEA (0.0017 mmol, 0.24 µL, 1.1 equiv) in DMF (0.1 mL) and the mixture was stirred under Ar. Once the reaction was completed according to HPLC analysis, the solvent was evaporated and residue purified by HPLC using a linear gradient of

acetonithrile over 20 minutes on an Agilent Eclipse plus C18, 5 µm particle size, 4.6 × 150 mm at a flow rate of 2 mL/min (retention time = 8.6 min).

Reaction time of 5 days. Yield = not calculated, HRMS-ESI: calc for $C_{48}H_{57}N_6O_{10}S^+$ $(M + H)^+$ 909.3851, found 909.3912..

3.7.7.2. Meropenem-BODIPY FL

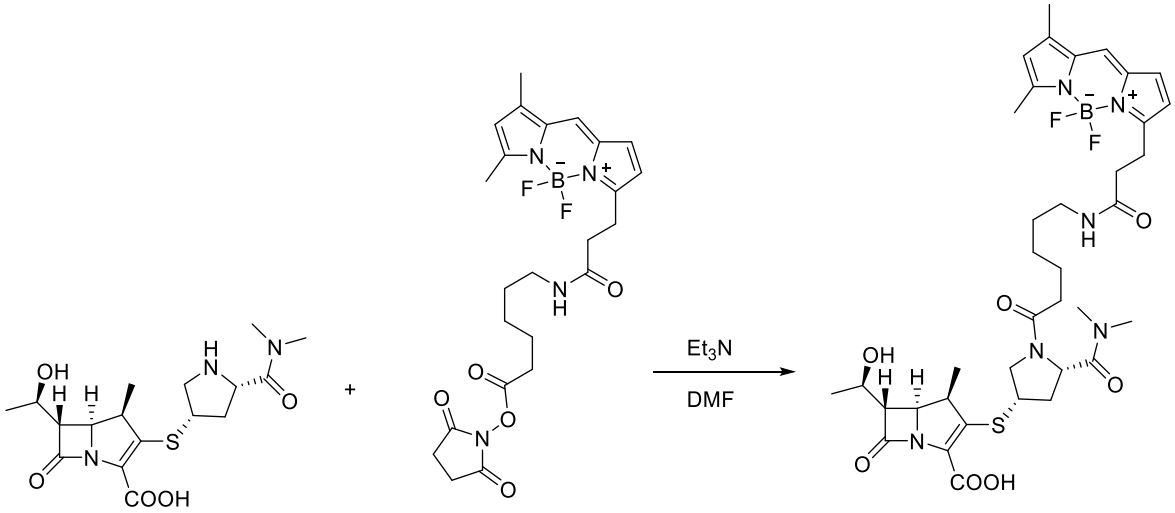

To a solution of BODIPY FL-X, SE (1.0 mg, 0.002 mmol, 1.0 equiv) in anhydrous DMF (0.1 mL) at room temperature was added meropenem (0.8 mg, 0.0022 mmol, 1.1 equiv) and TEA (0.0022 mmol, 0.3 µL, 1.1 equiv) in DMF (0.1 mL) and the mixture was stirred under Ar. Once the reaction was completed according to HPLC analysis, the solvent was evaporated and residue purified by HPLC using a linear gradient of acetonithrile over 30 minutes on an Agilent Eclipse plus C18, 5 µm particle size, 4.6 × 150 mm at a flow rate of 2 mL/min (retention time = 9.5 min).

Reaction time of 5 days. Yield = not calculated, HRMS-ESI: calc for $C_{37}H_{50}BF_2N_6O_7S^+$ $(M + H)^+$ 771.3517, found 771.3560. calc for $C_{37}H_{49}BF_2N_6NaO_7S^+$ $(M + Na)^+$ 793.3337, found 793.3367.

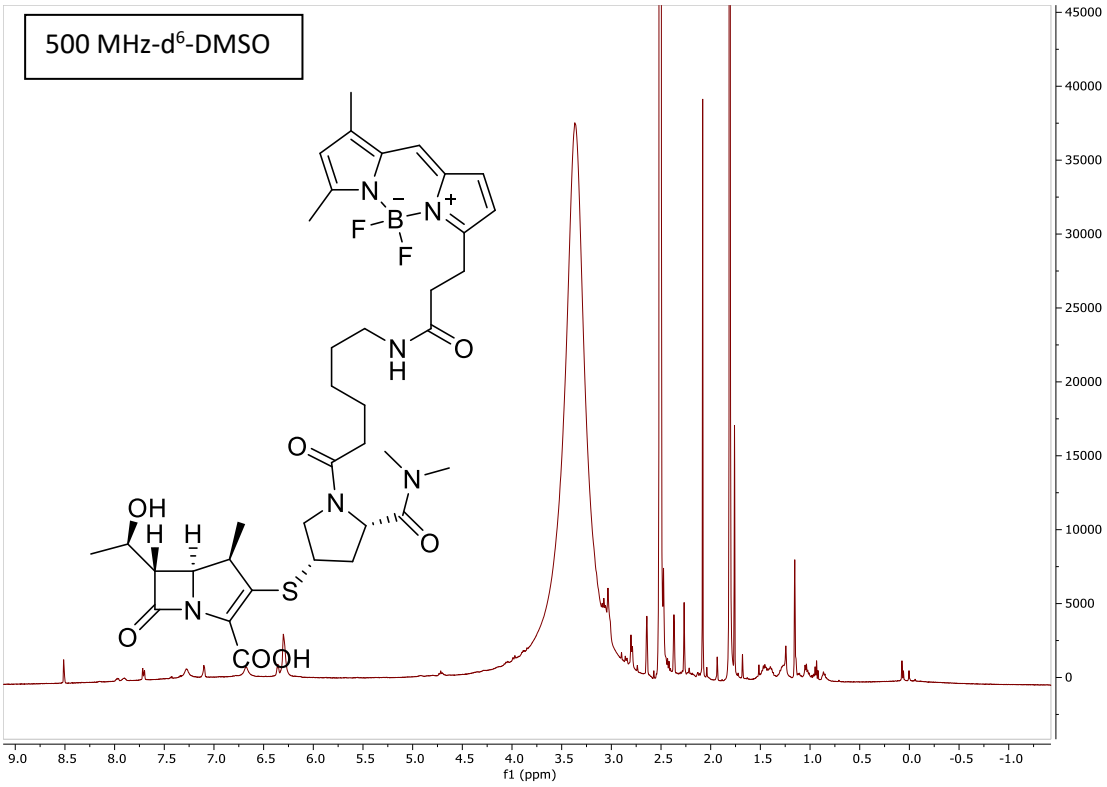

3.7.7.3. Click-MEM

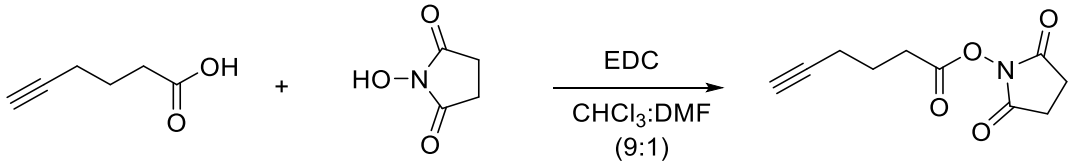

N-Succinimidyl-5-hexynoate

5-Hexynoic acid (1.0 g, 8.3 mmol, 1.0 equiv.) was dissolved in $CHCl_3$/DMF (5 mL, 9:1) and stirred. *N*-(3-dimethylaminopropyl)-*N′*-ethylcarbodiimide (EDC; 1.58 g, 8.3 mmol, 1.0 equiv.) and *N*-hydroxysuccinimide (0.96 g, 8.3 mmol, 1.0 equiv.) were added to the solution and the reaction stirred overnight under Ar. The reaction mixture was diluted to 100 mL with dichloromethane and washed with 3 × 50 mL 0.1 N HCl, followed by 3 × 50 mL saturated $NaHCO_3$ and 1 × 50 mL saturated NaCl, dried over $MgSO_4$ and concentrated under vacuum to yield 1.14 g of yellow oil, which was taken to the next step without further purification. R_f ~ 0.7 (3:7 EtOAc:CH_2Cl_2). ^{1}H NMR (500 MHz, $CDCl_3$): δ 1.93-2.01 (quin, *J*

= 7.2 Hz, 2H), 2.01 (t, *J* = 2.6 Hz, 1H), 2.32-2.36 (m, 2H), 2.75-2.78 (t, *J* = 7.2 Hz, 2H), 2.83 (br., 4H).

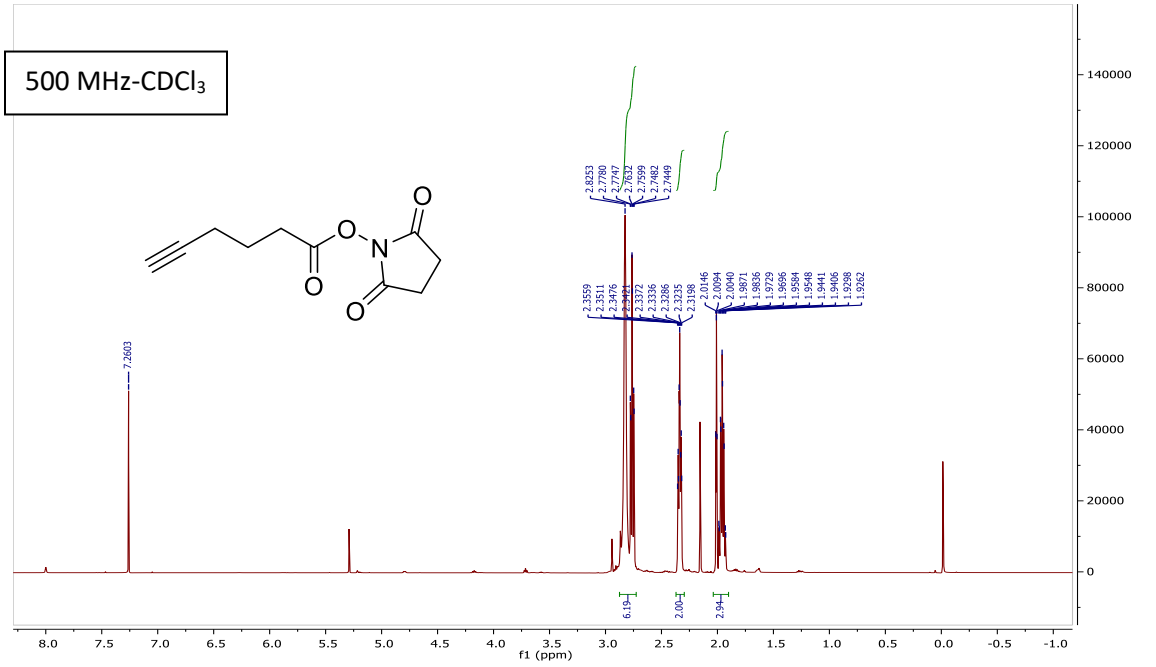

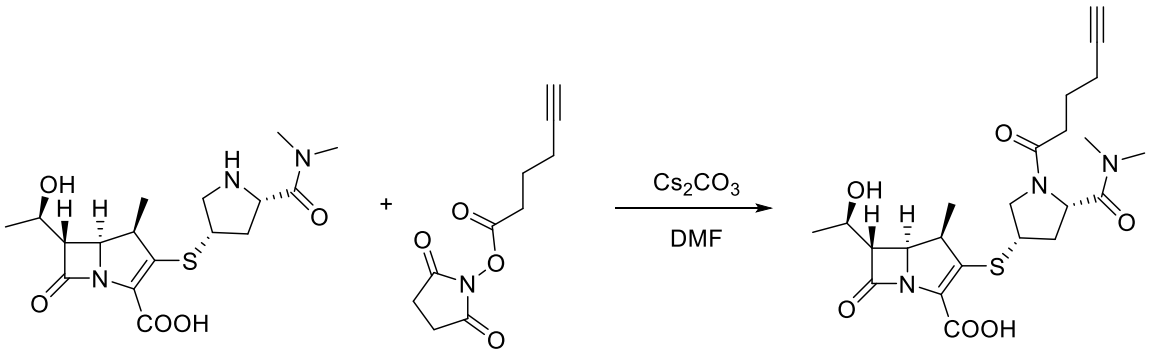

Coupling Meropenem and N-Succinimidyl-5-hexynoate

To a solution of meropenem (3.8 mg, 0.001 mmol, 1.1 equiv) and cesium carbonate (3.2 mg, 0.01 mmol, 1.1 equiv) in anhydrous DMF (0.2 mL) in an ice bath, was added *N*-succinimidyl-5-hexynoate (1.9 mg, 0.009 mmol, 1.0 equiv) in DMF (0.1 mL) and the mixture was stirred under Ar for one hour until it reached room temperature. Next, the solvent was evaporated under vacuum and the residue purified by HPLC using a 0-20%

gradient of acetonitrile over 20 minutes on an Agilent Eclipse plus C18, 5 µm particle size, 4.6 × 150 mm at a flow rate of 3 mL/min (retention time = 14.0 min). Yield = 35%, ^{1}H NMR (CD_3OD, 500 MHz): δ 1.28 (d, *J* =7.3 Hz, 3H), 1.31 (d, *J* = 6.3 Hz, 3H), 1.71-1.79 (m, 2H), 1.82 (quin, *J* = 7.0 Hz, 2H), 2.25-2.31 (m, 3H), 2.46-2.59 (m, 2H), 2.75-2.81 (m, 1H), 2.97 (s, 3H), 3.19 (s, 3H), 3.29 (dd, *J* = 6.1, 2.55 Hz, 1H), 3.47 (t, J= 10.2 Hz, 1H), 3.56 (quin, J=7.3 Hz, 1H), 3.81-3.89 (m, 1H), 4.13 (quin, J = 6.5 Hz, 1H), 4.21-4.26 (m, 1H), 4.92 (t, J = 8.5 Hz, 1H). ^{13}C NMR (D_2O, 500 MHz): δ 12.5, 17.0, 17.7, 23.0, 23.2, 25.3, 32.6, 35.9, 37.0, 39.2, 41.3, 54.5, 56.9, 59.5, 69.8, 84.9, 87.0, 112.2, 128.8, 172.4, 173.7, 176.3, 178.4. HRMS-ESI: calc for $C_{23}H_{32}N_3O_6S^+$ $(M + H)^+$ 478.2006, found 478.2031. calc for $C_{23}H_{31}N_3NaO_6S^+$ $(M + Na)^+$ 500.1826, found 500.1846.

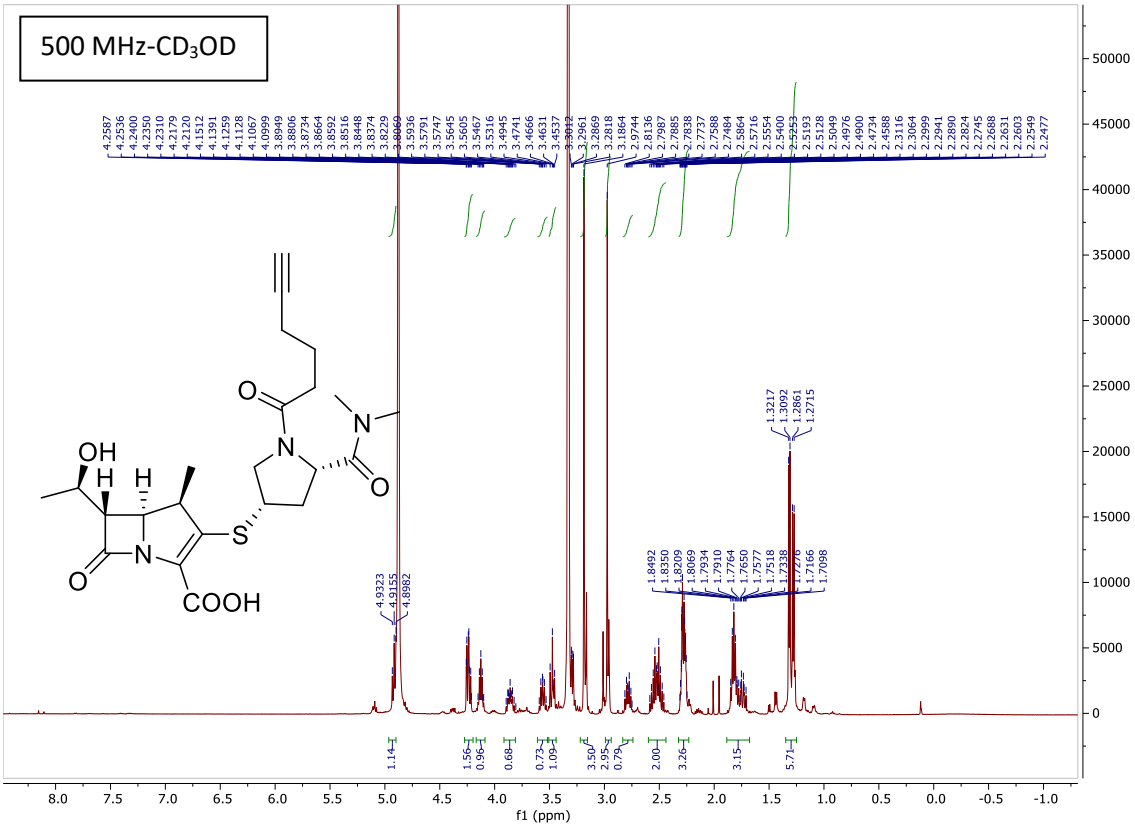

3.7.7.4. Click-MEC

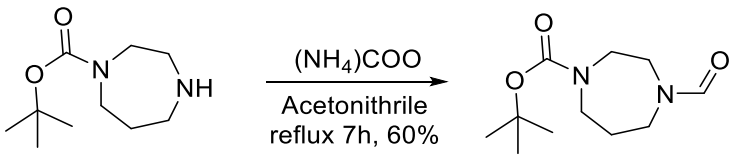

1-Boc-4-formyl-1,4,diazepane

To a solution of 1.0 g 1-Boc-1,4-diazepane (5.0 mmol, 1.0 equiv.) in 10.0 mL anhydrous acetonitrile, 480.0 mg ammonium formate (7.5 mmol, 1.5 equiv.) was added and the mixture was refluxed at 95 °C for 9 h. Acetonitrile was removed under reduced pressure. The residues were dissolved in 20.0 mL ethyl acetate and washed with 10.0 mL water twice and once with 10.0 mL brine. The organic layer was subsequently dried over anhydrous MgSO4 and concentrated under reduced pressure to yield 729.0 mg yellow oil (TLC in ethyl acetate: methanol 4:1 Rf = 0.7). Yield = 65%. ^{1}H NMR ($CDCl_3$, 500 MHz): δ 1.42 (s, 9H), 1.78-1.86 (m, 2H), 3.34-3.57 (m, 8H), 7.98-8.08 (m, 1H; *formyl proton shows up as 2 singlets*), ^{13}C NMR ($CDCl_3$, 500 MHz): δ 126.44, 28.36, 29.86, 42.41, 43.59, 45.31, 47.81, 48.37, 80.07, 154.92, 162.74. HRMS-ESI: calc for $C_{11}H_{21}N_2O_3^+$ $(M + H)^+$ 229.1, found 229.1.

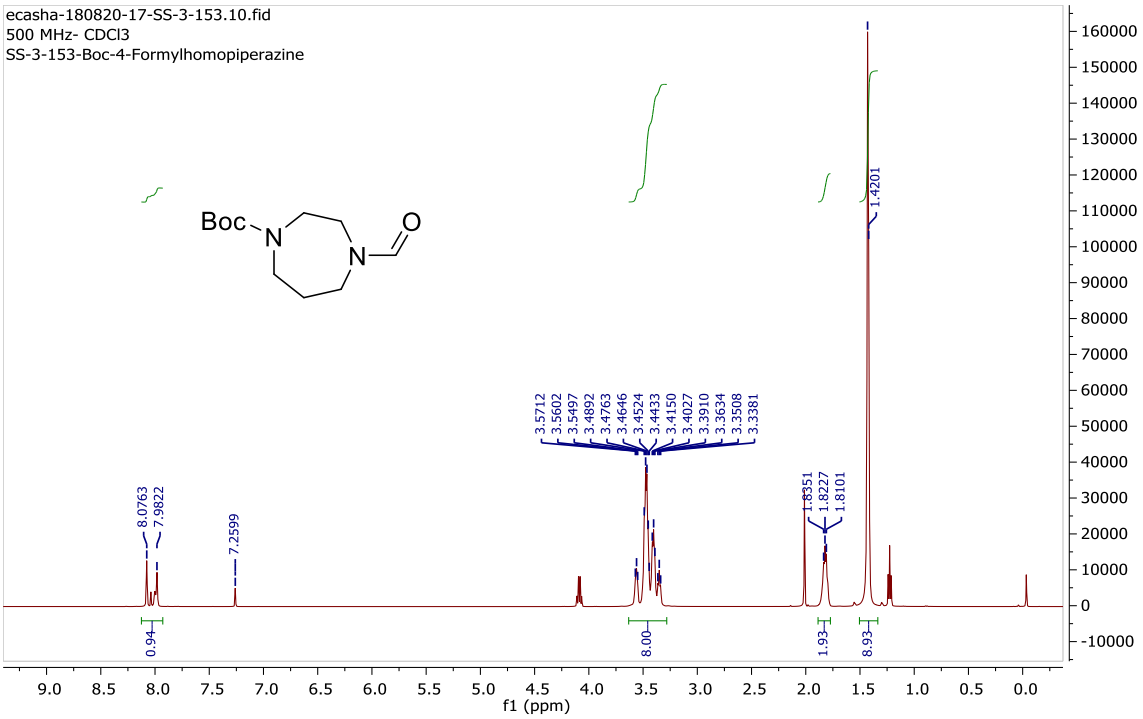
ecasha-180820-17-SS-3-153.10.fid
500 MHz- CDCl3
SS-3-153-Boc-4-Formylhomopiperazine
Boc
N
N
O
8.0763
7.9822
7.2599
3.5712
3.5602
3.5497
3.4892
3.4763
3.4646
3.4524
3.4433
3.4150
3.4027
3.3910
3.3634
3.3508
3.3381
1.8351
1.8227
1.8101
1.4201
0.94
8.00
1.93
8.93
f1 (ppm)

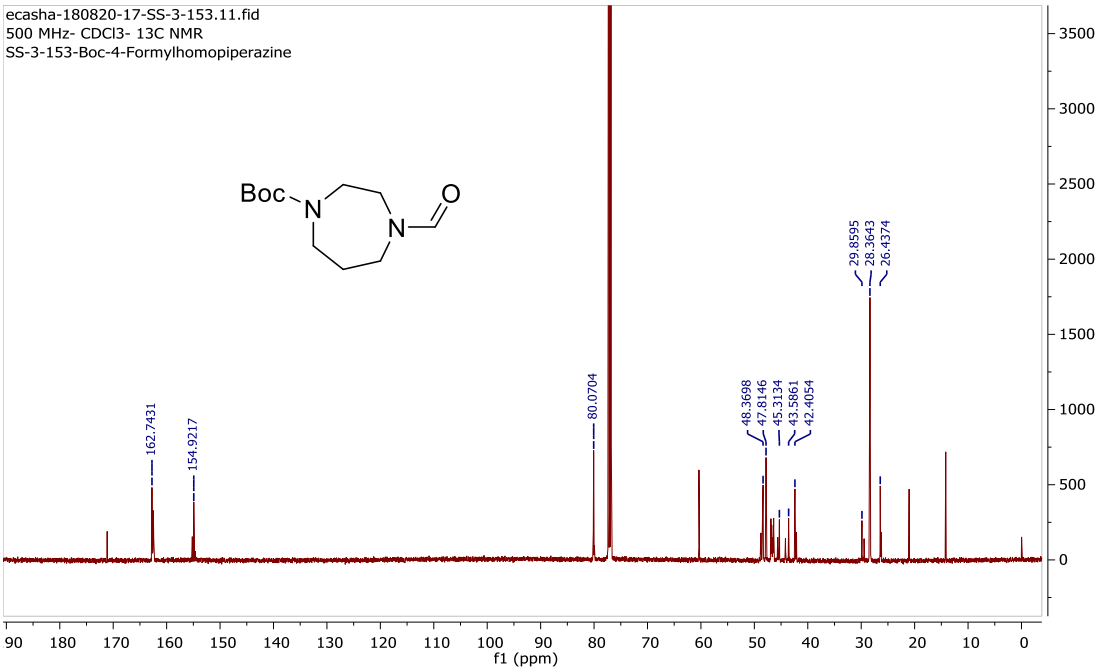
ecasha-180820-17-SS-3-153.11.fid
500 MHz- CDCl3- 13C NMR
SS-3-153-Boc-4-Formylhomopiperazine
Boc
N
N
O
162.7431
154.9217
80.0704
48.3698
47.8146
45.3134
43.5861
42.4054
29.8595
28.3643
26.4374
f1 (ppm)

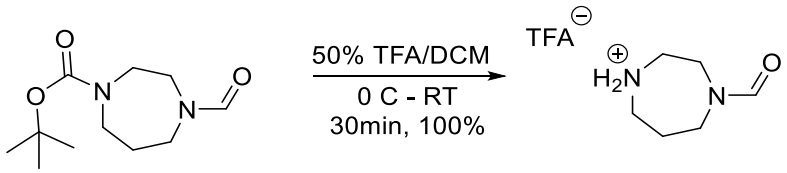

1,4-diazepane-1-carbaldehyde

1-Boc-4-formyl-1,4-diazepane (300 mg, 1.32 mmol) was dissolved in 1 mL of 50% TFA in dichloromethane. The mixture was stirred at RT for 1 hour. Reaction completion was confirmed by TLC (ethyl acetate: methanol 4:1; R_f ~0.1) using ninhydrin stain. The solvent was removed under vacuum. The residues were analyzed by HNMR and was taken to the next step without further purification. ^{1}H NMR (CD_3CN, 500 MHz): δ 2.05-2.13 (m 2H), 3.28-3.36 (m, 4H), 3.55 (t, *J* = 6.2 Hz, 2H), 3.70-3.37 (m, 2H), 7.29 (br., NH), 8.10 (d, *J* = 11.6 Hz, 1H; formyl proton).

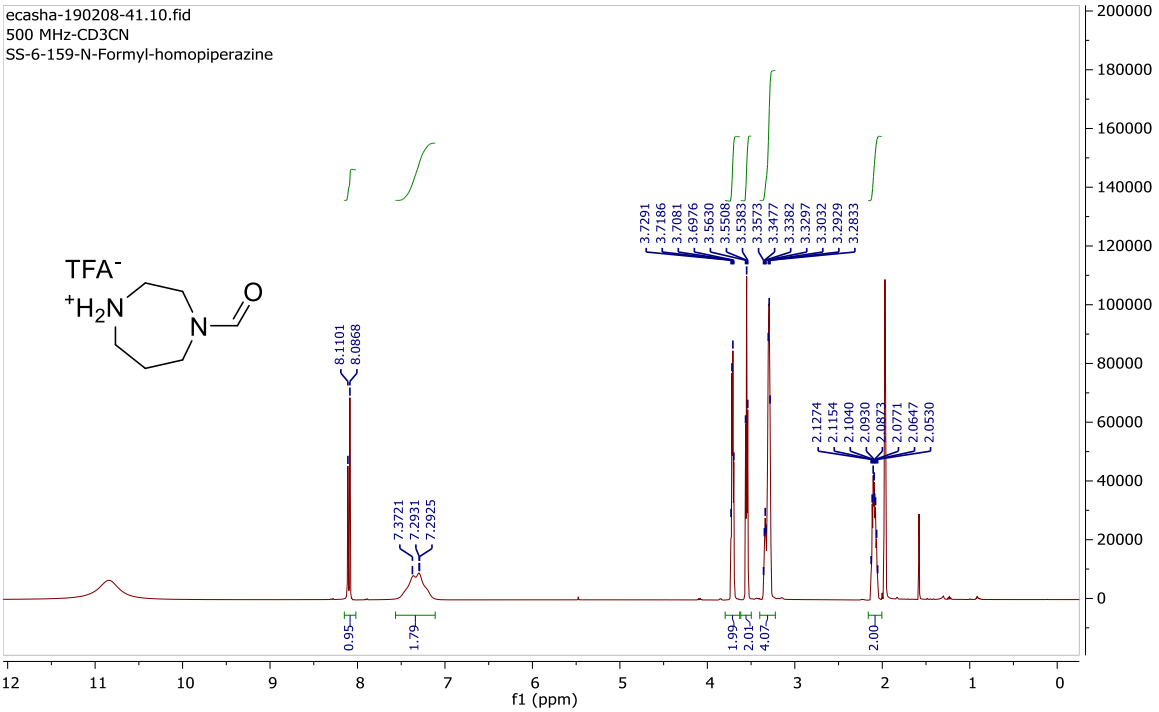

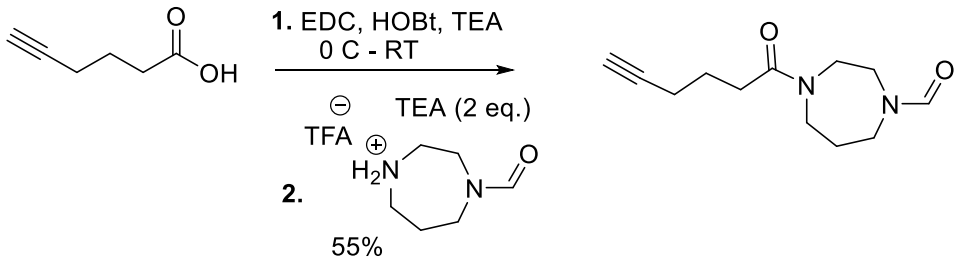

4-(hex-5-ynoyl)-1,4-diazepane-1-carbaldehyde:

5-hexynoic acid (141.0 mg, 1.26 mmol, 1.0 equiv.) was dissolved in 4 mL 9:1 mixture of DCM and DMF in an ice bath. EDC (242.0 mg, 1.26 mmol, 1.0 equiv.) and HOBt hydrate (193.0 mg, 1.26 mmol, 1.0 equiv.) and triethylamine (176 µL, 1.26 mmol, 1.0 equiv.) were added and the misture was allowed to stirfor 30 min at 0 °C. Next, N-formylhomopiperazine (1,4-diazepane-1-carbaldehyde; 182 mg, 1.32 mmol, 1.05 equiv.) and TEA (352 µL, 2.52 mmol, 2.0 equiv.)dissolved in 1 mL DCM was added dropwise at 0 °C. The reaction was allowed to reach room temperature while stirring and continued overnight. The mixture was then diluted with 20 mL DCM and washed 2× with 10 mL of 0.1 N HCl, followed by 3×20 mL of saturated $NaHCO_3$. The solution was then dried over $MgSO_4$. TLC (ethyl acetate; R_f ~0.2). Solvent was removed under low pressure to yield 200 mg of the product as a yellow oil. Yield = 75%. The residues were analyzed by HNMR and was taken to the next step without further purification. ^{1}H NMR ($CDCl_3$, 500 MHz): δ 1.83-1.97 (m, 5H), 2.27-2.32 (m, 2H), 2.45-2.49 (m, 2H), 3.42-3.71 (m, 8H), 8.01 (d, *J* = 7.05 Hz, 1H; formyl proton). HRMS-ESI: calc for $C_{12}H_{19}N_2O_2^+$ $(M + H)^+$ 223.1441, found 223.1441.

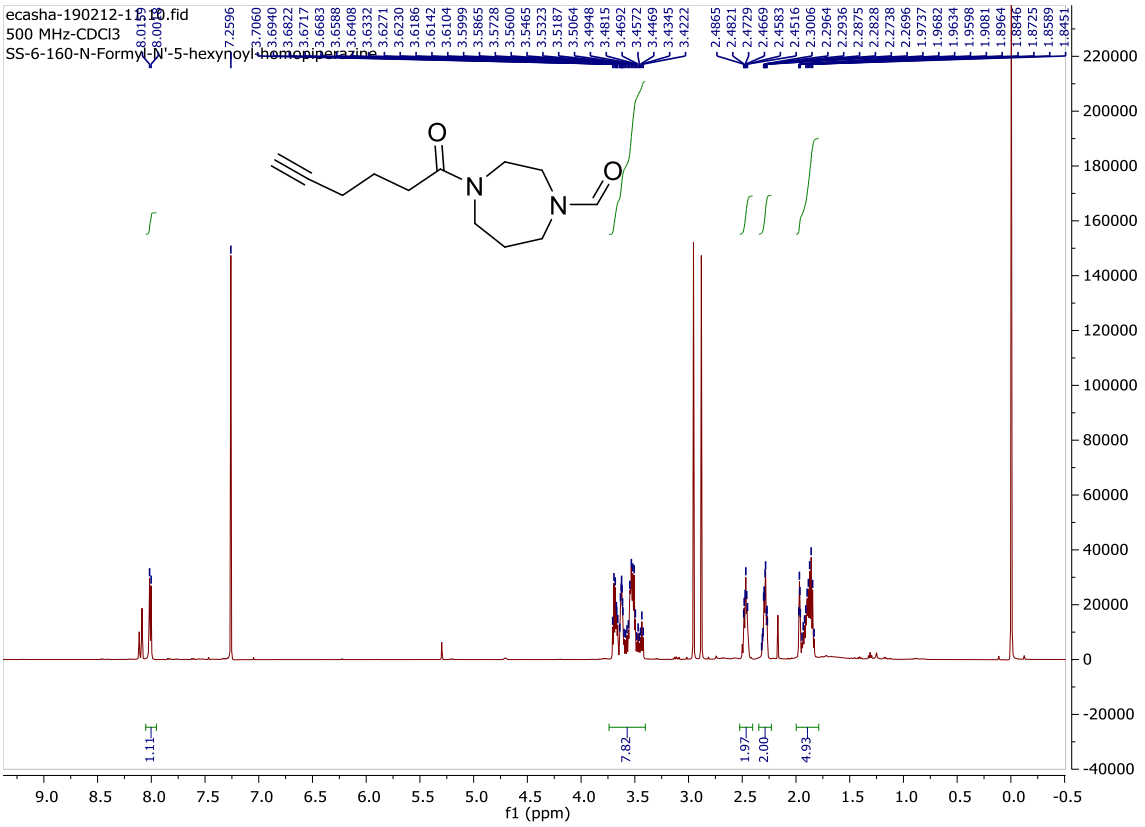

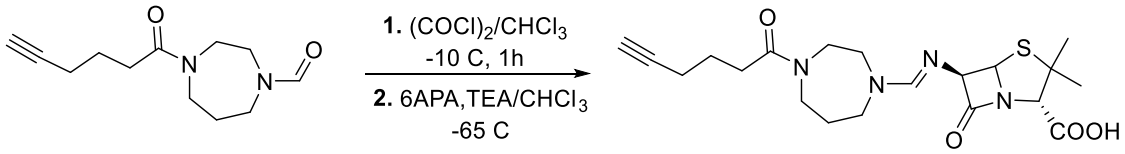

Click-MEC:

1) 6-aminopenicillanic acid (216 mg, 1 mmol, 1.0 equiv.) was dissolved in 5 mL chloroform to which 350 µL diisopropylethylamine (DIEA; 2 mmol, 2 equiv.) was added under an atmosphere of argon. Next, trimethylsilyl chloride (127 µL, 2.0 mmol, 2.0 equiv.) was added dropwise and the mixture was stirred at room temperature for 45 min.

2) A solution of 222 mg 4-(hex-5-ynoyl)-1,4-diazepane-1-carbaldehyde (1.0 mmol, 1.0 equiv.) in chloroform was cooled to -15 °C in a salt ice water bath under argon. To this solution was added dropwise 87 µL oxalyl chloride (1.0 mmol, 1.0 equiv.) and stirring was

continued for one hour at -10 °C. The mixture turned range and viscous after about 45 min.

3) The solution from step 1 was cooled down in a dry ice/acetone bath. Contents of the mixture from step 2 was added to it dropwise at -78 °C. The resulting mixture was transferred to a salt ice water bath and was stirred for one hour. After that, the salt ice water bath was removed and the stirring continued at room temperature overnight. The solvent was removed under vacuum and the residues (orange viscous oil) was stored at -20 °C until further purification was performed.

the residue purified by HPLC using a 5-95% gradient of acetonitrile over 30 minutes on an Agilent Eclipse XBD-C18, 5 μm particle size, 9.4 × 250 mm at a flow rate of 3 mL/min (retention time = 15.5 min). ^{1}H NMR (D_2O, 500 MHz): δ 1.47 (s, 3H), 1.62 (s, 3H), 1.60-1.90 (m, 2H), 2.15-2.22 (m, 3H), 2.47-2.54 (m, 2H), 3.26-3.87 (m, 8H), 4.23 (s, 1H), 5.36 (s, 1H), 5.49 (d, *J* = 3.85 Hz, 1H), 7.84-8.05 (m, 1H, N=CH-). HRMS-ESI: calc for $C_{20}H_{29}N_4O_4S^+$ $(M + H)^+$ 421.1904, found 421.1894.

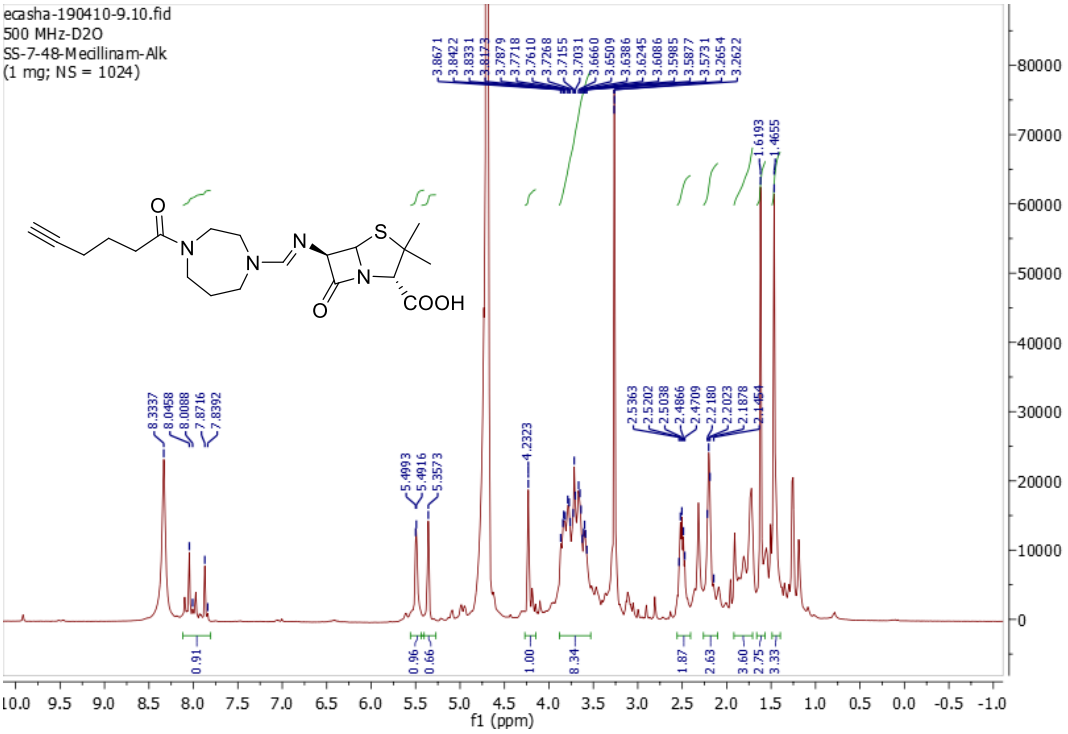

CHAPTER 4

DEVELOPMENT OF β-LACTONE PROBES

Portions of this work have been published in:

Sharifzadeh S, Boersma MJ, Kocaoglu O, Shokri A, Brown CL, Shirley JD, Winkler ME, Carlson EE. 2017. Novel Electrophilic Scaffold for Imaging of Essential Penicillin-Binding Proteins in Streptococcus pneumoniae. *ACS Chem Biol* 12:2849-2857.

* High resolution fluorescent microscopy experiments were performed by Dr. Michael Boersma in the laboratory of Professor Malcolm Winkler at Indiana University.

4. Development of β-lactone Probes

4.1. Significance

Peptidoglycan (PG) is a mesh-like heteropolymer made up of glycan chains crosslinked by short peptides. PG is the major scaffold of eubacterial cell walls, determining cell shape, size and chaining. Exclusively present in prokaryotic cells and essential for bacterial growth and survival, PG is located outside of the cytoplasmic membrane of bacterial cells making it highly accessible to antibiotics. Penicillin-binding proteins (PBPs) are essential for construction of PG through performing transglycosylation activities to generate the glycan strands and transpeptidation to crosslink the appended peptides. The β-lactam antibiotics, which comprise the biggest class of antibiotics and are among the most clinically effective antibiotics for the treatment of bacterial infections, inhibit PBP transpeptidation, ultimately leading to cell lysis. Despite this importance, the discrete functions of individual PBP homologs have been difficult to determine. These major gaps in understanding of PBP activation and macromolecular interactions largely result from a lack of tools to assess the functional state of specific PBPs in bacterial cells.

Since it was determined that penicillin V acts as a global PBP inhibitor, β-lactams have been used as probes to gain insight into bacterial physiology.(156, 157) A standard strategy is tagging with a radio- or fluorophore-labeled penicillin, followed by gel-based separation and detection(29, 130, 158) to provide information about the catalytic activity of the PBPs.(117, 159) However, penicillin-based compounds label all PBPs, preventing discrete characterization of each homolog. Single PBPs can be studied with fluorescently-labeled protein constructs; however, artificial fusions can perturb protein levels, function, or localization.(24, 160) Moreover, PBP protein localization does not provide information about the activity state. Alternatively, small molecule-conjugated fluorophores avoid the need for genetic manipulation and enable temporal resolution. For example, nascent PG

can be imaged with fluorophore-conjugated vancomycin (Van-FL) and ramoplanin, which label PG biosynthetic precursors in various Gram-positive bacteria.(33) Additionally, D-amino acid analogs that either bear a fluorophore or a bioorthogonal handle have been incorporated into the stem peptide during PG synthesis (fluorescent D-amino acids; FDAAs).(48, 52, 54, 161, 162)

To dissect the distinct roles of the enzymes responsible for PG synthesis, small molecules that selectively target individual PBPs in an activity-dependent fashion are required. β-lactam-based probes have been commonly synthesized and used for *in vitro* protein labeling, largely yielding compounds that label both PBPs and other bacterial proteins.(29, 101, 163) The Carlson group previously reported that PBP-selective imaging probes could be obtained by derivatization of an antibiotic, cephalosporin C.(89) Probes designed to target individual PBP homologs require the identification of scaffolds that selectively inhibit each enzyme. The Carlson research group reported evaluation of approximately 20 commercially available β-lactams from different subclasses of clinically utilized compounds for selective PBP inhibition in *Streptococcus pneumoniae*, *Escherichia coli* and *Bacillus subtilis*.(115, 116)[CHAPTER3] Several compounds showed concentration-dependent selectivity towards one or a few PBPs, which may provide the foundation for generation of selective probes. However, many PBPs were poorly inhibited by existing β-lactams. To address this challenge, we have identified a comparatively simple β-lactone-scaffold that we utilized to generate PBP-selective imaging reagents. We applied these probes to the examination of PBP activity in *S. pneumoniae*, with focus on the two essential homologs in this microorganism, PBP2x and PBP2b.

4.2. β-lactone Scaffold

The strained β-lactone (2-oxetanone) ring is an important pharmacophore which is present in diverse natural product and biologically active scaffolds. β-Lactone

compounds have been shown to covalently modify enzymes, including serine hydrolases.(164) As such, β-lactone drugs have application in the treatment of obesity, diabetes and cancer.(165-167) The most well-known β-lactone, tetrahydrolipstatin (THL; Orlistat®), is a long-term anti-obesity drug that functions by irreversibly inhibiting a lipase.(165) Natural products containing this moiety were first reported ~50 years ago.(168, 169) However, only a small number are known to possess antibiotic activity including Orlistat, obafluorin, SQ-26,517 and hymeglusin (168-172)(**Fig. 4.1**). Recent work has illuminated several classes of enzymes involved in β-lactone biosynthesis(173-176), but the bacterial targets of β-lactone activity remain largely undetermined. Obafluorin protects mice infected with *S. pyogenes* and causes cell elongation in *E. coli*, suggesting cell wall biosynthesis inhibition. It was also the first example of a β-lactone substrate of a β-lactamase enzyme.(177). More recently, β-lactones have been used as chemical probes to investigate their cellular targets. A study using THL-based probes revealed several lipase enzymes as potential antibacterial targets of this molecule in *Mycobacterium bovis BCG*.(172) Synthetic β-lactones have been shown to inhibit proteins involved in metabolism, antibiotic resistance, the β-lactamase PBP4* in *B. subtilis*, and a virulence-associated protein, caseinolytic protease P (ClpP).(60, 178-180) Of particular interest to us was the determination that a D,D-carboxypeptidase was one of thirteen targets of a β-lactone probe in *Mycobacterium smegmatis* (CplP inhibitor; **Fig. 4.1**).(180)

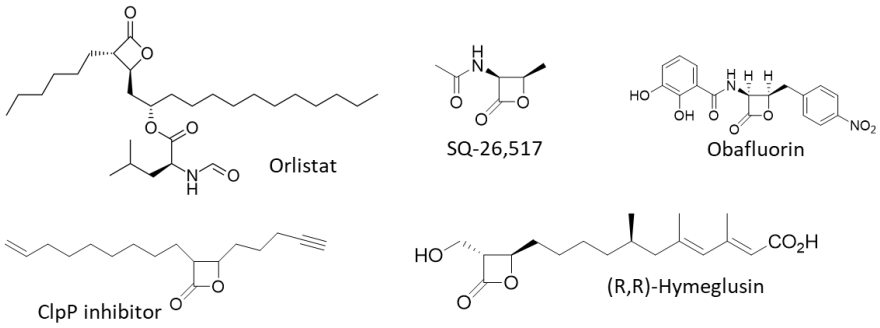

Figure 4.1. Selected biologically active β-lactone-containing compounds.

4.3. Designing a Library of β-lactones

Given the potential of the β-lactone scaffold to interact with active site serine residues, including those in β-lactamases and a carboxypeptidase,(60, 177, 179, 180) and the structural similarity of several of these compounds to the β-lactam antibiotics, we postulated that this scaffold could be optimized to create PBP-selective probes. Assessment of the natural product SQ-26,517 (**Fig 4.1**) (181) indicated that it is a weak inhibitor of PBP2a in *S.pneumoniae*. However, examination of the corresponding deacylated lactone, as well as the other *cis* isomer of this electrophilic core demonstrated no PBP inhibition (**Figure 4.2**). Given the potential for the β-lactone scaffold to bind PBPs, we decided to pursue this further.

We designed molecules with an amide group proximal to the electrophilic carbonyl and the ring substituents in the *cis* conformation to mimic SQ-26,517 and the β-lactam antibiotics (**Figure 4.3**; lactone ring numbering indicated). For diversification, we appended an amino acid moiety, such as D-Ala to mimic the natural substrate or Phe to mimic the side chain of penicillin, onto this core and a fluorophore for visualization. Probes were synthesized by adaptation of a known solution phase route (**Scheme 4.1**).(182) The library contained 24 molecules, six that display a lactone coupled directly to a fluorophore [**Fig. 4.3.C**; **2**-**4**; TAMRA (T), BODIPY-FL (B) or fluorescein (FL)], six compounds with substrate-like sidechains (**5** and **6**), eight compounds with sidechains to mimic groups found in β-lactam antibiotics (**7**-**9**), two functionalized with glycine to assess the role of the amino acid side chain in protein labeling (**10**), and two with alternative hydrophobic side chains (L-Val and L-Trp, **11** and **12**).

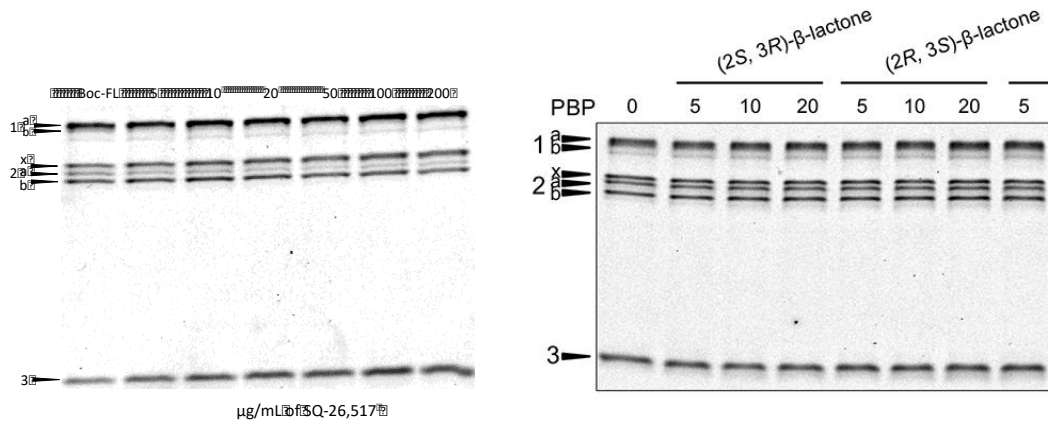

Figure 4.2. Competition experiment with β-lactones and Bocillin-FL in *Streptococcus pneumoniae*. *Left:* Titration with increasing concentrations of SQ-26,517 resulted in weak inhibition of PBP2a. *Right:* L- and D-Threonine β-lactones did not detectably inhibit any PBP.

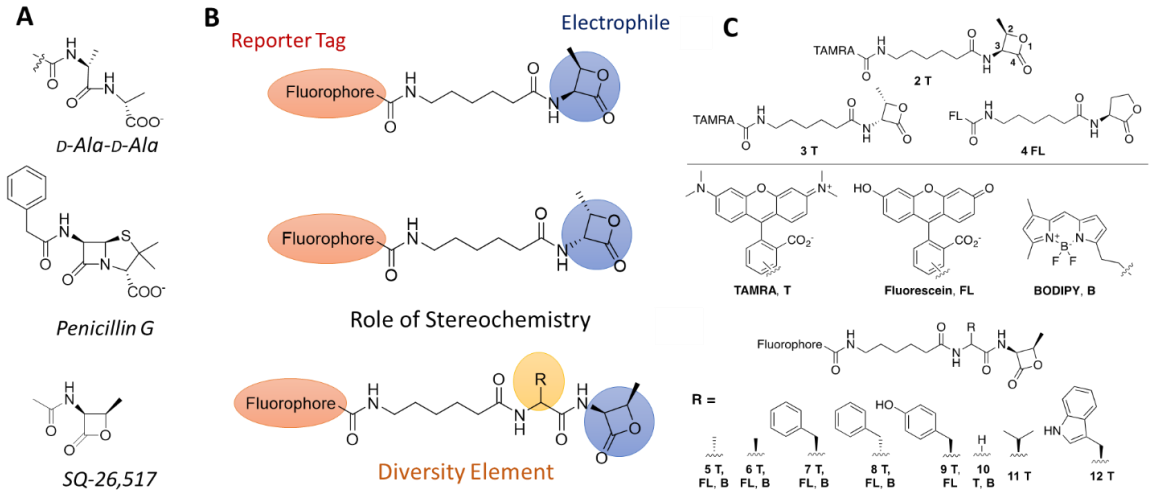

Figure 4.3. β-Lactone-based probe library. The design of the β-lactone probe library was inspired by the structural similarity between the terminal D-Ala-D-Ala moiety of PG as the natural substrate of PBPs, the β-lactam core in antibiotics and the β-lactone scaffold present in antibacterial natural products such as SQ-26,517 (A). A library of probes was designed containing the electrophilic threonine β-lactone ring as the warhead and different fluorophore groups were implemented as the reporter. Probes with altered stereochemistry of the β-lactone were included to study the importance of that feature. Different amino acids carrying a variety of side chains were introduced into the probe structure to expand the PBP binding spectrum (B). Chemical structure of the synthesized probes (C).

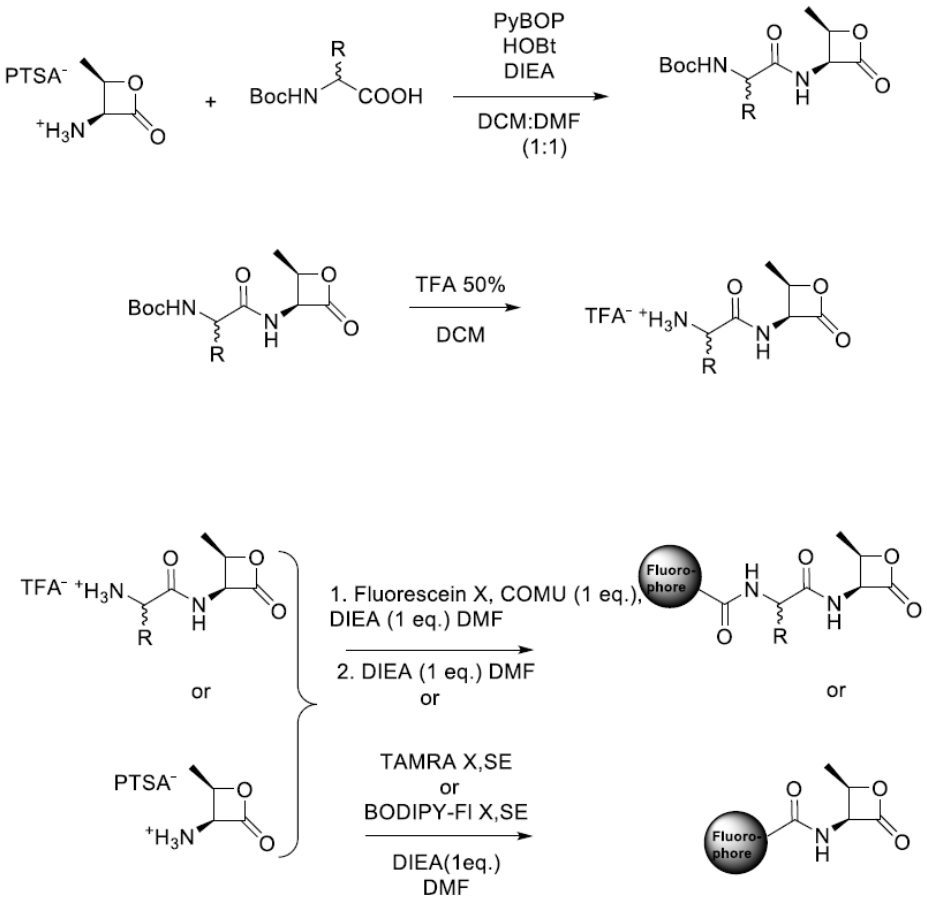

Scheme 4.1. Synthesis of β-lactone probes

4.3.1. Assessment of Structure-Activity Relationship (SAR)

Assessment of both *cis*-functionalized analogs, (2*R*, 3*S*)-β-lactone (**2**) and (2*S*, 3*R*)-β-lactone (**3**; **Fig. 4.3**), demonstrated that the stereochemistry of the substituents on the lactone ring is crucial for productive labeling. The compounds displaying these groups in the same orientation as is found in β-lactams, (2*R*, 3*S*)-β-lactone (**2FL** and **2T**), labeled most PBPs (PBP1a, PBP1b, PBP2x and PBP2a), while the opposite isomer labeled nothing ((2*S*, 3*R*)-β-lactone; **3T**; **Fig. 4.4 3T** and **3B**). Our attempts to synthesize the (2S, 3S) and (2R, 3R) stereoisomers, the diastereomers of the mother lactone scaffold, were unsuccessful. Indeed, a *syn* methyl group has been shown to significantly improve the

stability of threonine-based β-lactone ring compared with the *anti* conformation.(183) We also found that five-membered γ-lactones do not to inhibit the PBPs (**4FL Fig. 4.4** and *N*-acyl homoserine lactones;(184) **Fig. 4.5**).

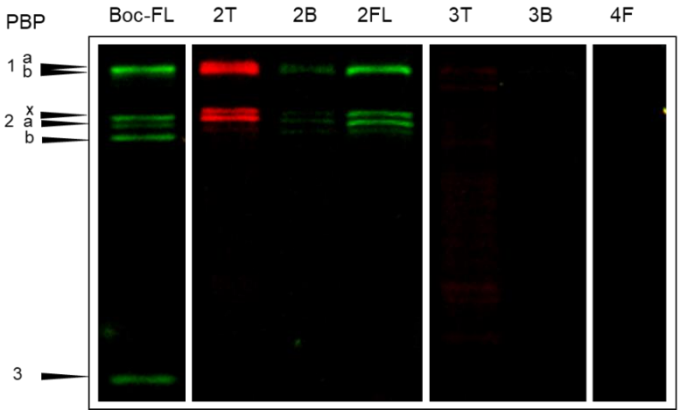

Figure 4.4. Gel-based analysis of probes to examine ring geometry (2 and 3) and ring size (4). (2*R,* 3*S*)-β-lactone (2T, 2B and 2FL) labeled a number of PBPs, whereas (2*S,* 3*R*)-β-lactone (3T and 3B) and γ-lactone (4F) probes yielded no detectable labeling, confirming the significance of ring geometry and size in targeting the PBPs.

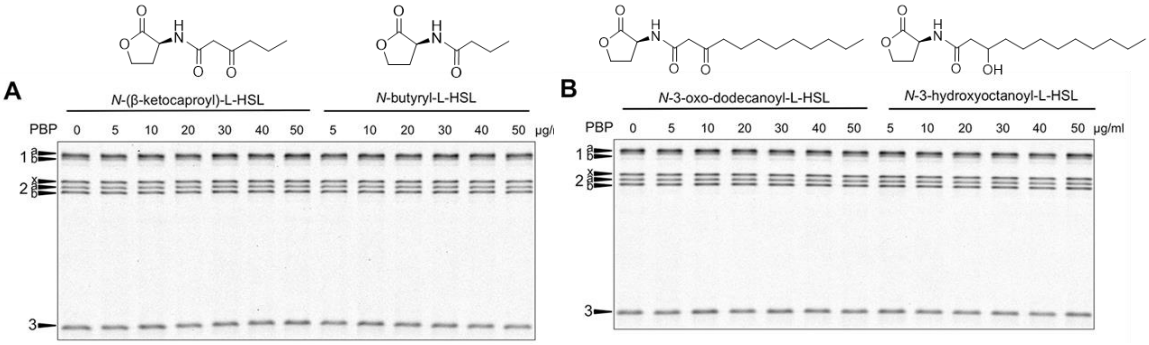

Figure 4.5. Gel-based analysis of *S. pneumoniae* PBP labeling with Boc-FL after *N*-acyl homoserine lactone treatments. (A) *N*-(β-ketocaproyl)-L-HSL and *N*-butyryl-L-HSL, (B) *N*-3-oxo-dodecanoyl-L-HSL and *N*-3-hydroxyoctanoyl-L-HSL pretreatment followed by Boc-FL labeling.

We also found that lactone labeling of the PBPs is competitive with penicillin, indicating that these molecules are active-site directed, and that the resulting acylated protein complex is stable, as it is not displaced by subsequent incubation with Boc-FL (**Fig. 4.6**). The selectivity of this simple scaffold for the PBPs is remarkable given the relatively large number of protein classes tagged in previous studies with β-lactone-containing molecules.(60, 178, 179, 182) Indeed, these results are especially intriguing

given that our probes lack an ionizable group to mimic the C-terminal D-Ala residue carboxylate in the native stem peptide, which is found in all clinically relevant β-lactam antibiotics(**Fig. 4.3.A**).(185)

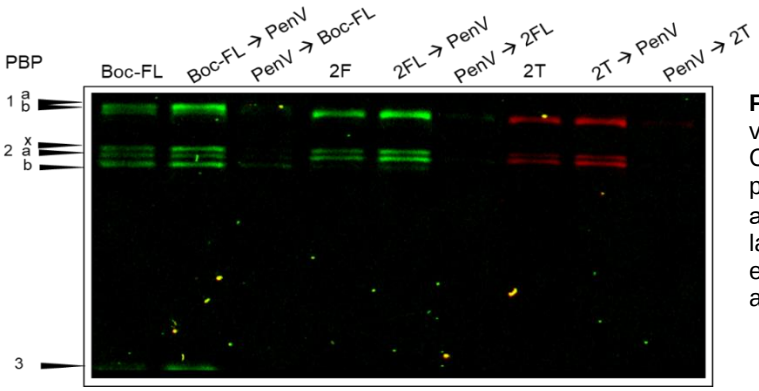

Figure 4.6. Penicillin pre-treatment versus penicillin post-treatment. Cells were treated with 5 μg/mL penicillin V for 30 minutes before or after labeling with 5 μg/mL β-lactone probes or Boc-FL. Full experimental details are discussed at the end of the chapter.

We next assessed probes designed to resemble the stem peptide. The molecule containing a D-Ala residue and TAMRA (**5T**) labeled all five HMW PBPs, making it more general than compounds without a side chain (Gly derivative, **10T**; HMW PBP2a not labeled) or those that lack an amino acid diversity element (**Fig. 4.4**; **2T**, **2B** and **2FL**; HMW PBP2b not labeled). This may indicate that a similar binding pocket is accessed by D-Ala in the probe and in the natural peptide substrate. However, the fluorescein-functionalized probe (**5FL**) labeled only PBP1b and PBP2x, suggesting that the fluorophore component can also influence protein labeling (**Fig. 4.7**). This phenomenon was most commonly observed with BODIPY-FL-functionalized molecules, which often yielded substantially different profiles, including the labeling of non-PBP targets (e.g., **Fig. 4.7 8B** versus **8FL** and **8T**).

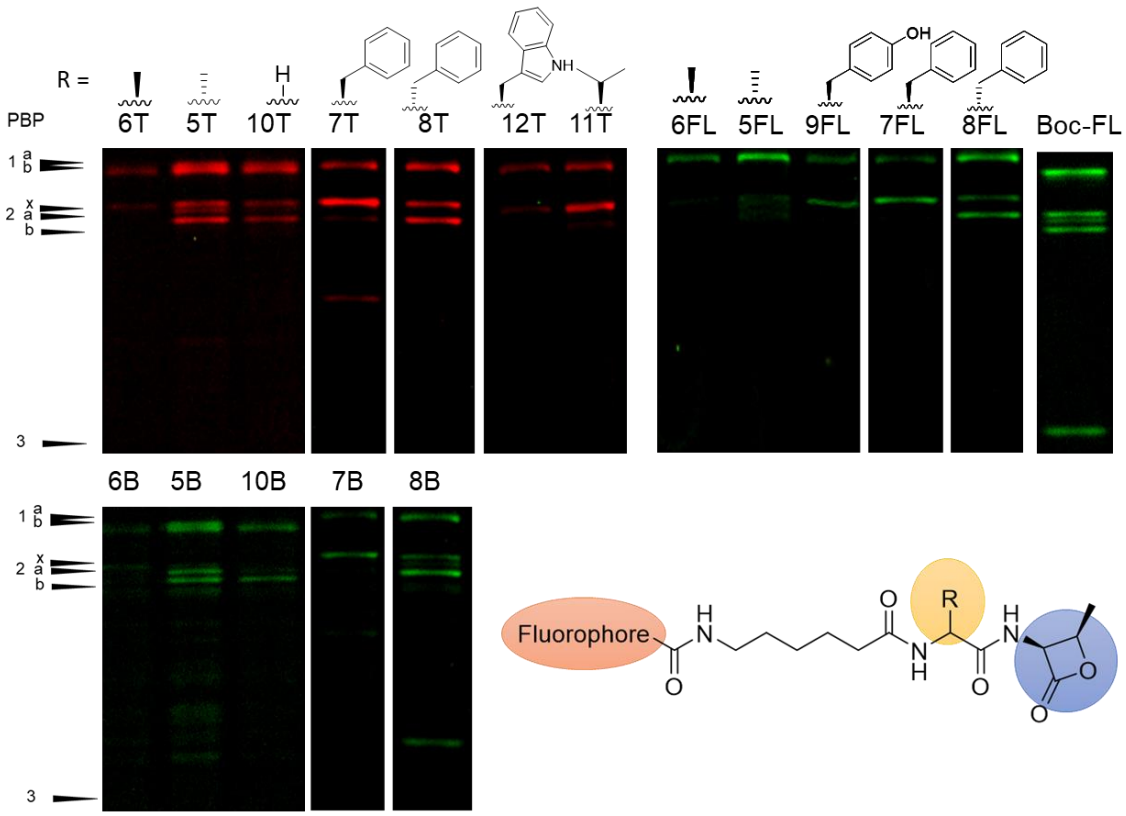

Figure 4.7. Gel-based analysis of probes to examine side chains that act as substrate mimetics (**5** and **6**), hydrogen (**10**) and bulky hydrophobic groups (**7**-**9**, **11**,**12**). The D-Ala-based probe (amino acid stereochemistry found in stem peptide; 5) labeled all HMW PBPs, while the L-Ala-functionalized molecule was more selective (**6**; PBP1b and PBP2x). The fluorescein analog of D-Ala-based probe (**5FL**; PBP1b and PBP2x) tagged fewer PBPs than the TAMRA and BODIPY FL analog (**5T** and **5B**). All probes were assessed at 5 μg/mL. Boc-FL was used as a control.

Next, we evaluated probes displaying hydrophobic side chains, several of which are found in β-lactam antibiotics, such as a phenyl group in penicillin G or the hydroxyphenyl displayed on amoxicillin. Resolution of PBP1a and PBP1b, which migrate very closely in the gels, was accomplished by utilizing Δ*pbp1a* and Δ*pbp1b* mutant strains (E177 and E193, respectively. Representative data shown for selected probes in **Fig. 4.10**). The D-Phe derivative (**8FL**) tagged PBP1b, PBP2x and PBP2b, while the L-Phe and L-Tyr FL derivatives (**7FL** and **9FL**) labeled only PBP1b and PBP2x. Indeed, a large number of probes, including those with alternative hydrophobic side chains, co-labeled

PBP1b and PBP2x (**Fig. 4.7**. L-Ala: **6T** and **6FL**, D-Ala: **5FL**, L-Phe: **7FL**, L-Tyr: **9FL**, L-Val: **11T**, L-Trp: **12T**).

4.3.2. PBP Targeting Profile of β-lactone Probes

Overall, we found that PBP1b is labeled by all of the tested β-lactone probes and several compounds co-selectively labeled PBP1b and PBP2x. This may indicate that these proteins are tolerant of side chains with diverse size and configuration. Intriguingly, PBP2x is a common target of the β-lactams and is often co-inhibited with PBP3,(116) which was not labeled by any of the β-lactone probes. In contrast, PBP1b is among the less frequently targeted PBPs by β-lactam antibiotics, indicating that our probe library may be accessing a different region of binding space within the PBP active sites. PBP2b, which is the least inhibited PBP with conventional β-lactam antibiotics, was labeled by three probe scaffolds (**5T**, **5FL 8T**, **8FL**, **10T**). PBP1a and PBP2a labeling was only observed with compounds displaying a small side chain (PBP1a: **2FL**, **2T**, **5FL**, **5T**, **5B**, **10T** and **10B**; PBP2a: **2T**, **2FL**, **5T** and **5FL**; **Table 4.1**).

Table 4.1. Summary of probe labeling of S. pneumoniae PBPs. Results are based on the PBPs labeled when 5 µg/mL of probe was used. Underlined PBPs were significantly less labeled compared to the other reported PBP(s).

	TAMRA	**BODIPY FL**	**FL**
Lactone	1a, 1b, 2x, 2a	1b, non-PBP	1a, 1b, 2x, 2a
(R,S)Lactone	no labeling	1b, non-PBP	
□-Lactone			no labeling
Gly	1a, 1b, 2x, 2b	1b, non-PBP	
(L)Ala	1b, 2x	1b, 2x	1b, 2x
(D)Ala	1a, 1b, 2x, 2a, 2b	1a, 1b, 2x, 2a, 2b	1b, 2x
(L)Phe	1b, 2x, 2b, non-PBP	1b, 2x, non-PBP	1b, 2x
(D)Phe	1b, 2x, 2b	1b, 2x, 2a, 2b, non-PBP	1b, 2x, 2b
(L)Tyr	nothing		1b, 2x
(L)Trp	1b, 2x		
(L)Val	1b, 2x		

To further examine the differences in the PBPs that may be responsible for the disparate labeling response, we compared the structures of PBP2x and PBP1a, the former being labeled by many probes and the latter tagged by only a small subset. Both proteins have been co-crystallized with tebipenem or biapenem and we overlaid these structures for comparison of their active sites (2ZC3: PBP2x-biapenem; 2ZC4: PBP2x-tebipenem; 2ZC5: PBP1a-biapenem; 2ZC6: PBP1a-tebipenem; **Fig. 4.8**).(186) In PBP1a, a bulky residue can be found near C6 of the lactam core structure (i.e., F577), a position that we anticipate may be occupied by the diversity element in our probes. The presence of this large group may explain the requirement of a small side chain on the probes for productive binding. In contrast, PBP2x has an open cleft at this position, which is consistent with the observed tagging by a diversity of probes.

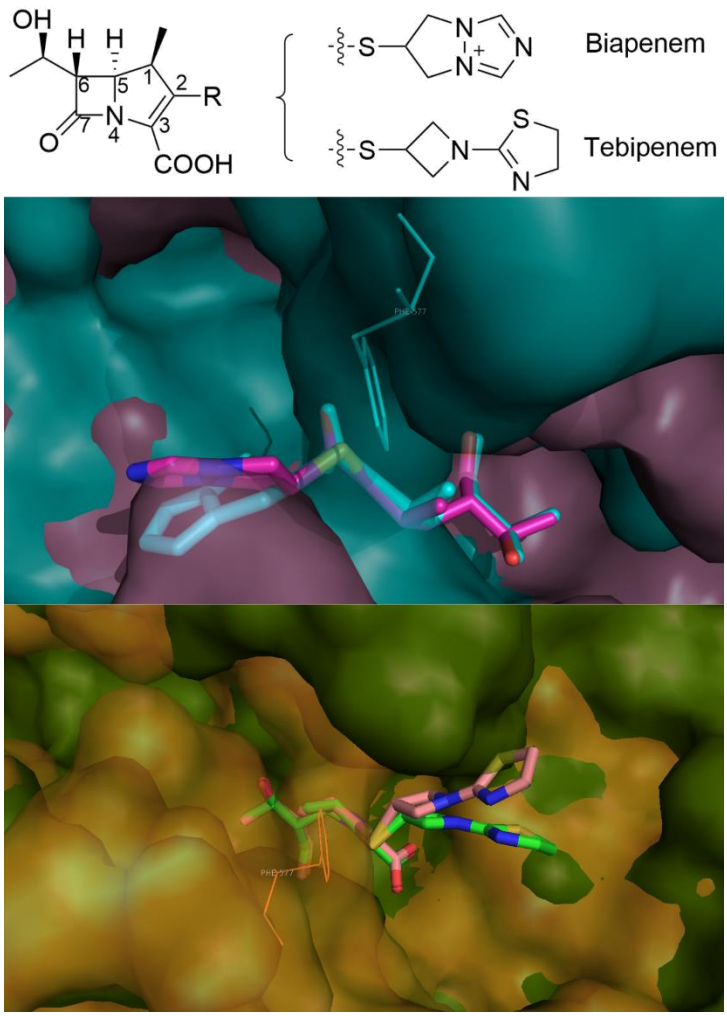

Figure 4.8. Superposition of the active site of PBP2x (magenta) and PBP1a (cyan) co-crystallized with penem drugs. Top: Chemical structures of tebipenem and biapenem; the carbapenem core is numbered. Middle: Overlaid crystal structures of PBP2x and PBP1a, each separately complexed with biapenem. Presence of bulky side chains, such as Phe577 in the active site of PBP1a, blocks the entrance. Bottom: Overlaid crystal structures of PBP2x and PBP1a, each separately complexed with tebipenem. Drugsite was used for superposition of structures. (http://drugsite.msi.umn.edu)

Our studies focused on *S. pneumoniae*, an ovoid-shaped Gram-positive bacteria that causes serious diseases such as pneumonia, bacteremia, and meningitis, and is the major cause of worldwide childhood mortality from infectious disease.(187) In addition to being clinically significant, *S. pneumoniae* is an important model of PG biosynthesis as it possesses a relatively simple PBP complement with three class A PBPs (PBP1a, PBP1b, and PBP2a), two class B PBPs (PBP2x and PBP2b), and one class C PBP (PBP3 or DacA; D,D-carboxypeptidase). Molecules based on cephalosporin C were utilized in combination with Boc-FL to separate the catalytic activity of PBP1b from that of PBP1a, PBP2x, PBP2a and PBP2b. Intriguingly, these studies indicated that different populations of PBPs may be active at discrete locations during division. Clearly, tools that facilitate deeper examination of this issue will be instrumental in teasing apart the complex biology of the PBP family.

Although the only LMW PBP in *S. pneumoniae*, PBP3, is inhibited by the vast majority β-lactam antibiotics,(116) none of the β-lactone probes labeled this protein. It has been postulated that the facile inhibition of PBP3 can be partially attributed to the high catalytic efficiency of this D,D-carboxyendopeptidase as determined by the hydrolysis of the pseudo substrate *N*-benzoyl-D-alanylmercaptoacetic acid (k_{cat}/K_M = 50,500 $M^{-1}s^{-1}$).(188) In addition, although one might anticipate rapid hydrolysis of the resulting acylated protein species in this endopeptidase, previous work has shown that the deacylation rates of PBP3 and transpeptidase PBP1b, the most commonly labeled protein in these studies, are comparable when treated with [^{3}H]benzylpenicillin (5.7×10^{-5} s^{-1} and 5.6×10^{-5} s^{-1}, respectively).(188) Thus, it is clear that neither catalytic efficiency nor hydrolysis of the resulting covalent species can explain the lack of PBP3 labeling with the β-lactone probes. Indeed, PBP3 and PBP2x are commonly inhibited to a similar extent by β-lactam antibiotics, a trend that was not observed in these studies. These data, along with the

ability of the β-lactones to achieve PBP selectivity in the absence of a negatively charged substrate mimic, suggests that our probes may be accessing different binding space than the β-lactams. Overall, we conclude that our β-lactone probes complement and extend the range of PBPs that could be targeted selectively (**Figure 4.9**).

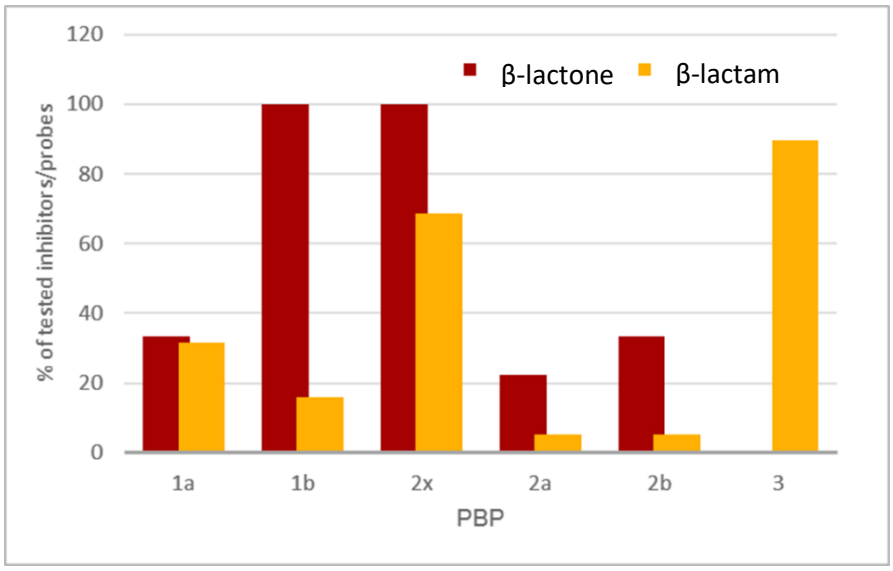

Figure 4.9. Comparison of PBP binding by tested β-lactones in this work (maroon) and β-lactam antibiotics (yellow).(146) Percentage of compounds from each class that bound to each pneumococcal PBP is shown.

4.4. Structural Analysis of β-lactone Interactions with PBPs

Activity-Based Probes (ABPs) can be utilized to identify the direct interactions between small molecules and the active site of the enzyme. The covalent nature of the bond formed between small molecule probes and the cellular targets allows for rigorous washing and enzymatic digestions, enabling subsequent mass spectrometry-based analysis of complex protein mixtures.(93, 189) Following the results of the penicillin competition assays (**Fig. 4.6**), we hypothesized that our β-lactone probes must form a covalent bond with the conserved serine residue of the transpeptidation domain. To

provide further support for this hypothesis, we generated a soluble form of PBP2x, PBP2x*, by expression of a previously reported construct in *E. coli* BL21 cells.(190) The portion of the *pbp2x* gene that encodes the transmembrane component of the protein is removed in this construct, to improve the solubility of the protein, and the resulting DNA fragment corresponds to Gly49 to Asp750 of PBP2x.(190) Recombinant PBP2x* was incubated with 7FL and subjected to tryptic digestion followed by LC-MS analysis on a MALDI-TOF instrument. Comparison of the peptide mixture with the database revealed the presence of a peptide with the exact mass corresponding to addition of a **7FL** molecule to the active site fragment (δ=32ppm) Together with the competition results, these data indicate that the (R,S)-β-lactone probes interact with the active site of the transpeptidation domain and covalently modify the fragment containing the conserved Ser residue.

4.5. Visualization of PBP2x Activity in *Streptococcus pneumoniae*

PBP2x is an essential HMW PBP in *S. pneumoniae* involved in septal PG synthesis.(22, 23, 191) Mutations in the conserved motifs of PBP2x have been associated with β-lactam resistance; therefore, it is an important target for antibacterial agents.(192-194) PBP2x has recently been shown to localize to the septa of dividing *S. pneumoniae* cells using epitope tags or optimized GFP fusion constructs,(22, 23, 195) corroborating its role in septal PG machinery. FDAA labeling of wild-type bacteria treated with methicillin to specifically inhibit PBP2x transpeptidation activity and in bacteria depleted for PBP2x also indicated that PBP2x migrates to the centers of septa in mid-to-late divisional cells.(22) A PBP2x-selective ABP is needed to directly corroborate the findings from these experiments by displaying only the active form of this PBP in live cells. Although we did not identify a probe that labels only PBP2x, we did uncover several compounds that label only PBP2x and PBP1b (**Table 4.1**), the latter of which can be deleted to yield a strain that

is phenotypically indistinguishable from the wild-type organism.(196) Thus, the Δ*pbp1b* mutant (E193) provides the ideal platform in which to image PBP2x.

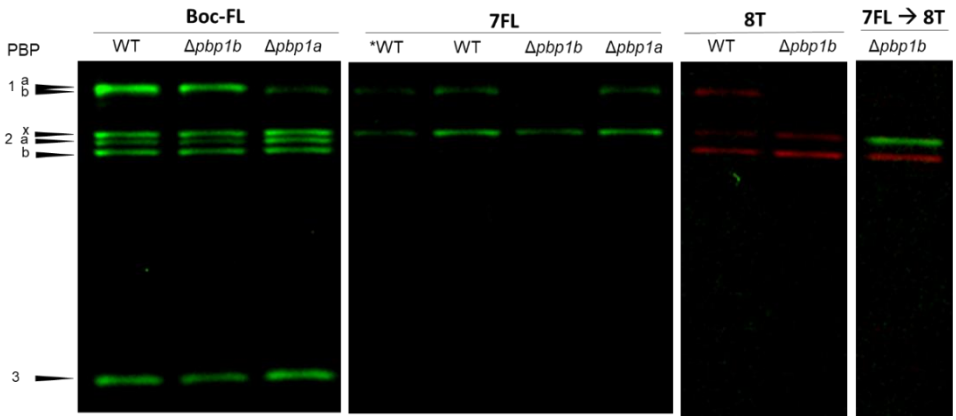

Figure 4.10. PBP profiles of *S. pneumoniae* WT (IU1945), Δ*pbp1b* (E193) and Δ*pbp1a* (E177) cells that are labeled with Boc-FL, **7FL** and **8T** probes to resolve PBP1a and PBP1b bands. All probes were used at 5 μg/mL, unless otherwise noted. (* indicates the probe was used at 1 μg/mL). Dual labeling with (*2R*,*3S*)-β-lactone-L-Phe-fluorescein (**7FL**) followed by (2*R*,3*S*)-β-lactone-D-Phe-TAMRA (**8T**) enables separate visualization of the activity of PBP2x (green) and PBP2b (red).

We utilized the **7FL** probe in imaging studies to localize PBP2x during the course of cell division (**Fig. 4-10, 4-11**). These images showed that PBP2x localized at the division septum as a ring in early-to-mid divisional cells. In mid-to-late divisional cells, PBP2x localized to both the constricting ring and to a separate site at the center of the ring, as well as the equators of daughter cells. Finally, enzyme activity was constricted down to a single point at the division site before cell separation. This indicates that subpopulations of active PBP2x demonstrate different localization patterns during a single constriction event, which correlates well with recent reports of PBP2x localization, (22, 23) as well as newly synthesized cell wall labeled by FDAA (**Fig. 4.11**). In these reports, immunolabeling showed that PBP1a remained as a larger ring at later stages of cell division, while PBP2x

concentrated to the center of the septa. Previous work using FDAAs strongly supported this finding, but could not determine if any PBP2x remained in the outer division site ring because the FDAAs are incorporated by multiple PBPs. Clarification of this question highlights a critical strength of a PBP-selective, activity-based imaging strategy, (22, 197) and emphasizes the need to understand how PBP dynamics are regulated. PBP2x has been demonstrated to interact with the serine-threonine kinase StkP, and the protein GpsB has recently been show to modulate septal closure and PBP2x migration,(198) but the exact mechanism behind PBP2x localization remains unclear. Since the **7FL** probe can specifically label PBP2x, it may be an effective way to monitor changes in PBP2x localization in future studies of PBP dynamics.

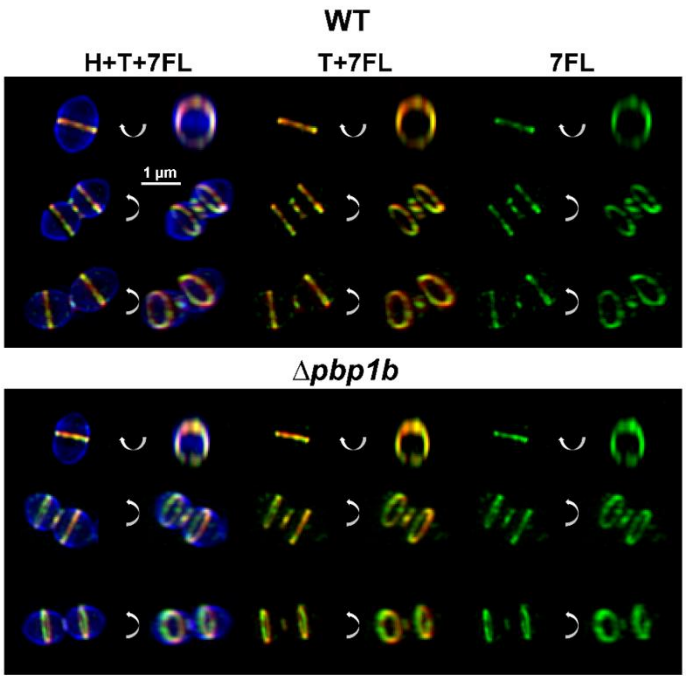

Figure 4.11. 7FL labeling co-localizes with regions of new cell wall synthesis. Wild type (IU1945) and Δ*pbp1b* (E193) cells were labeled for several generations with the FDAA HADA (H, pseudo-colored blue), then for 5 min with the FDAA TADA (T, pseudo-colored red), and finally with **7FL**, (pseudo-colored green). Each row has 6 views of the same cell, with one image in each pair rotated around the indicated axis. New cell wall synthesis and **7FL** labeling co-localize at all stages of division. These images are representative of >40 cells at all stages of division for each condition from 2 biological replicates.

To confirm that the observed patterns were due exclusively to PBP2x labeling, cells were pretreated with methicillin, which specifically inhibits PBP2x in *S. pneumoniae*.(23) Gel-based analysis confirmed that PBP2x labeling is dramatically decreased following methicillin treatment (Figure 4-12-A). 3D-SIM imaging of cells labeled with 7FL after pre-treatment with methicillin revealed elongated cells with a labeled ring at the division site, but with minimal or no constriction evident. Importantly, >98% of

methicillin-treated late division cells (≈40 cells examined) in both the wild-type and Δ*pbp1b* strains displayed empty septal rings, in contrast with untreated controls from both strains that showed central septal labeling in 85% of wild-type and 73% of Δ*pbp1b* cells (≈40 cells examined). This indicates a lack of active PBP2x due to methicillin inhibition, which aligns with previous results(199) and strongly supports the conclusion that septal 7FL labeling is due exclusively to binding of PBP2x. Any labeling at the division site after methicillin treatment is likely due to residual uninhibited PBP2x, since a small amount of PBP2x activity remains (Figure 4-12-B).

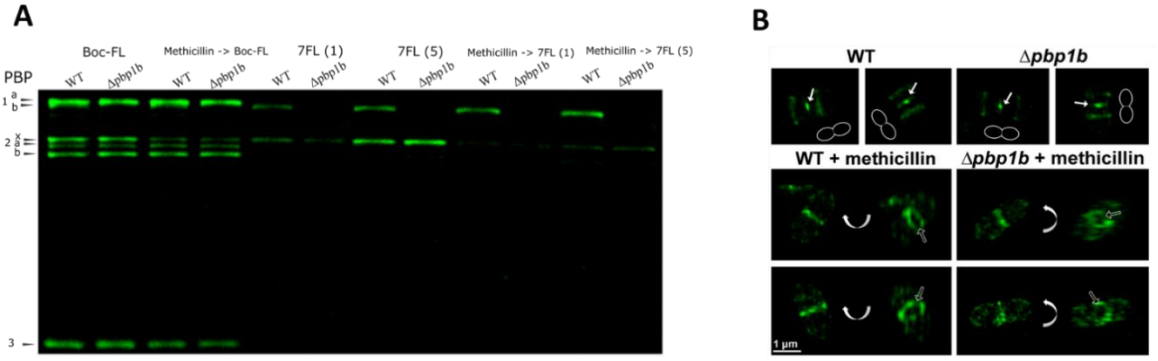

Figure 4.12. Pretreatment with methicillin blocks PBP2x activity and prevents lactone labeling. Cells were treated with 0.1 μg/mL methicillin for 30 minutes prior to labeling with Boc-FL or **7FL**. Numbers in parentheses indicate the concentration (μg/mL) at which the probe was used. Boc-FL was used at 5 μg/mL as control (A). **7FL** labeling of PBP2x with or without PBP1b and a PBP2x-inhibiting concentration of methicillin. Wild-type (IU1945) and Δ*pbp1b* (E193) were grown and pre-treated with methicillin (0.1 μg/mL) for 20 min, where indicated. Cultures were then labeled with **7FL**. Each image in the top row is a separate cell, and the outlines in each image in the top row demonstrate the orientation of the cell. The bottom two rows consist of pairs of images of the same cell, but one image has been rotated around the indicated axis. **7FL** labeling does not change in the absence of PBP1b, and methicillin-treated cells are elongated and lack septal labeling compared to the untreated controls. Solid arrows point to central septal labeling, and empty arrows highlight empty rings after methicillin pretreatment. These images are representative of ~40 mid-to-late division cells for each condition from two biological replicates.

4.6. Visualization of PBP2b Activity in *Streptococcus pneumoniae*

PBP2b is the essential peripheral transpeptidase in *S. pneumoniae*.(200) Similar to PBP2x, it is a primary penicillin-resistance determinant.(201) In previous work, we showed that PBP2b localizes differently than FtsZ, which is the primary organizer of bacterial cell division.(22) In early stages of *S. pneumoniae* division, FtsZ mediates the

recruitment of division proteins, including PBP2b, to the midcell septal ring. At later stages of division, FtsZ migrates to the equators of the new daughter cells, while PBP2b remains at the closing septum. (22) To complement this previous work, we sought to assess the activity of PBP2b throughout the bacterial cell cycle using the lactone probe **8T**, which labels PBP1b, PBP2x and PBP2b (**Fig. 4.10**). When utilized alone, this probe yields a nearly identical labeling pattern (**Fig. 4.13**) as **7FL** (**Fig. 4.12**) due to their shared targets. **8T** labels the division site as a single ring in early division, and labels the center of the division site, the constricting divisional ring, and the new equatorial rings of the future daughter cell in mid-to-late division. Finally, it constricts down to a single point at the division site just before the cells separate. Pre-treatment with methicillin produced elongated cells with **8T**-labeled divisional rings and minimal constriction. Importantly, >98% of late divisional cells treated with methicillin (≈40 cells examined) in both the wild-type and Δ*pbp1b* strains showed empty septal rings, where untreated strains showed **8T** central septal labeling in 81% (wild-type) and 76% (Δ*pbp1b*) of cells (≈40 cells examined). This mirrors our results seen for **7FL** and reinforces the idea that PBP2x alone is localized to the center of the constricting division site.

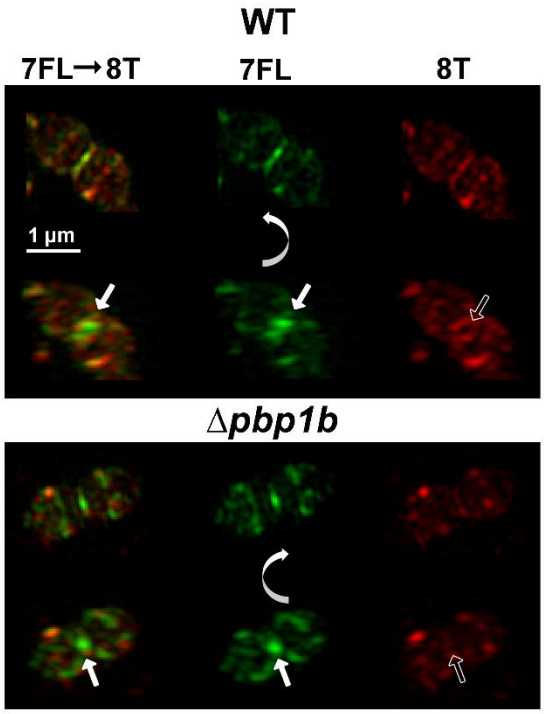

Figure 4.13. Labeling with **7FL** followed by **8T** reveals distinct PBP localization patterns. Cultures of wild-type (IU1945) and Δ*pbp1b* (E193) were grown, labeled with **7FL**, washed, labeled with **8T**, and imaged. Each set is two rows of images of the same cell, with the bottom row rotated relative to the top row around the indicated axis. In both strains, **8T** labeling is excluded from the septum and restricted to peripheral rings when the cells are labeled first with **7FL**. Solid arrows highlight central septal labeling, and empty arrows highlight the exclusion of **8T** labeling from the center of the division site. These images are representative of ~40 mid-to-late division cells for each condition from two biological replicates.

In order to target PBP2b specifically, **8T** was utilized on cells first labeled with **7FL**. Results of gel-based studies indicate that this combination tags PBP2x (green) and PBP2b (red) individually in the Δ*pbp1b* mutant (**Fig. 4.10**). 3D-SIM imaging of dual labeled cells revealed that **7FL** displayed a labeling pattern similar to the single labeling results seen in **Fig. 4.12**, as expected. However, labeling of **8T** was excluded from the center of the division site in >83% of wild-type and Δ*pbp1b* cells (≈40 cells examined). Instead, it was restricted to the outer peripheral ring around the division site and the equatorial rings of future daughter cells, which have not yet begun to constrict. These results correlate well with previous work(200) that demonstrated that PBP2b localization remained separate from and external to PBP2x during constriction, and we have now shown that active PBP2b follows this pattern as well, and ruled out the possibility that methicillin treatment disrupts PBP2b localization. Importantly, this study is the first to demonstrate co-localization of specifically labeled PBPs confirmed to be enzymatically active, and our results agree well with previous reports on PBP localization in *S. pneumoniae*,(22, 23, 191, 195, 202).

4.8. PBP Labeling with β-lactones in Other Bacteria

To demonstrate the general applicability of our novel chemical probes, we tested our β-lactone probes in other microorganisms. *Bacillus subtilis*, *Escherichia coli* and *Staphylococcus aureus* were used as model systems for rod-shape Gram-positive, rod-shape Gram-negative and cocci Gram-positive bacteria, respectively.

4.8.1. *Bacillus subtilis*

B. subtilis is a sporulating rod-shaped Gram-positive bacterium with a large number of PBPs. *B. subtilis* is a commonly studied Gram-positive model organism and thus, there is substantial knowledge about its cellular processes, including cell wall

biosynthesis.(5, 203) To date, 16 genes are known to encode PBPs in *B. subtilis*.(20, 103) Some of these PBPs have been shown to play roles in cell division and growth,(20, 103, 105) while others are involved in sporulation.(106) Among *B. subtilis* PBPs, six can be fluorescently tagged and visualized by Boc-FL: PBP1, 2a, 2b, 3, 4 and 5 in actively growing cells. The other PBPs are only expressed during sporulation. PBP2b is the only essential PBP and is a key division-specific protein, suggested to have a catalytic role in septal cell wall synthesis.(21, 125) Similar to *S. pneumoniae*, *B. subtilis* PBPs were targeted by probes containing the (R,S)-β-lactone scaffold and the probe containing the (S,R) isomer, **3B**, failed to tag any PBPs. A non-PBP protein, however, was tagged by this probe, which was observed in all of the samples tagged with a BODIPY-FL conjugate, some of which, such as **5B** and **8B**, resulted in several fluorescent bands. This could be explained by the hydrophobicity of BODIPY-FL, which could lead to non-specific protein binding (**Fig. 4.14**, top gel). Similar to *S. pneumoniae*, TAMRA and fluorescein β-lactone conjugates yielded comparable labeling profiles and are promising chemical tools to study PBP transpeptidation activity in *B. subtilis.* Interestingly, PBP5, the main D,D-carboxypeptidase during the vegetative growth phase of this microorganism, was labeled by most of the β-lactone probes. This is in contrast with the pneumococcal case, where PBP3 (the only D,D-carboxypeptidase) remained untouched by any lactone-based probe (**Table 4.1**). Moreover, the majority of these probes tagged most or all of the PBPs (**Fig. 4.14**).

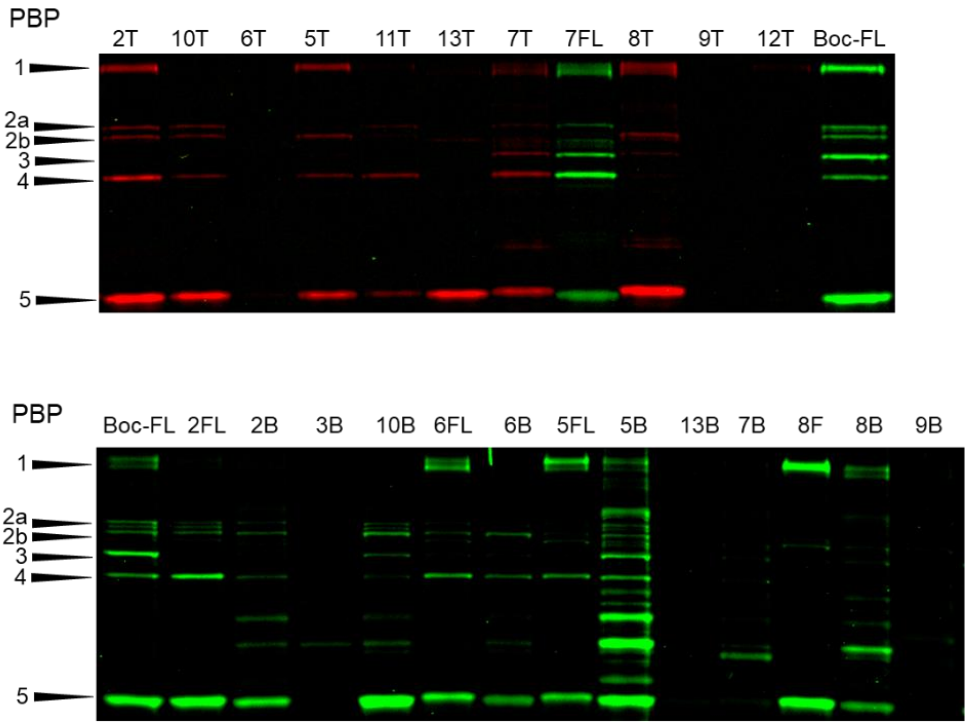

Figure 4.14. Gel-based analysis of PBP labeling profile of selected β-lactone probes in *Bacillus subtilis PY79* cells. All probes were used at a final concentration of 5 μg/mL.

4.8.2. *Escherichia coli*

Upon successful targeting of the PBPs in two Gram-positive bacteria, we examined the applicability of our β-lactone probe toolkit in *E. coli* as a Gram-negative model. Gram-negative bacteria possess a complex cell envelope consisting of a lipid-rich outer membrane (OM) as well as a plasma membrane, and a thin peptidoglycan layer sandwiched in between the two. The OM

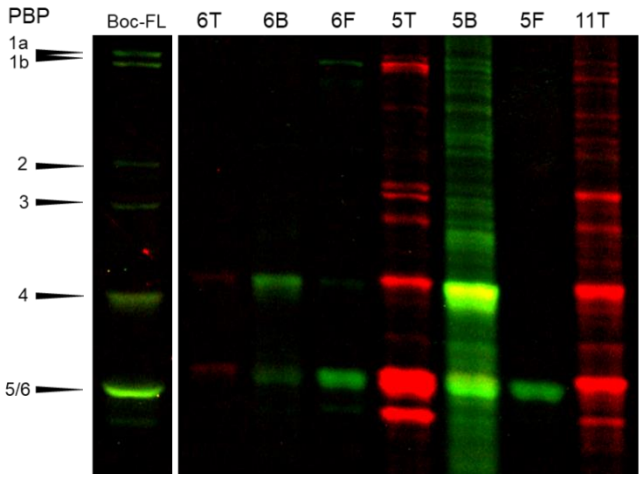

Figure 4.15. Gel-based analysis of the PBP labeling profiles of selected β-lactone probes, β-lactone-(L)Ala-fluorophore (**6T**, **6B** and **6F**) and β-lactone-(D)Ala-fluorophore (**5T**, **5B** and **5F**), in *E. coli DC2* cells. β-lactone probes were used at a final concentration of 10 μg/mL. Boc-FL was used as the positive control at a final concentration of 20 μg/mL.

is a distinct feature of Gram-negative bacteria, acting as a strong barrier to limit the diffusion of molecules across. (14) *E. coli* expresses a total of 12 PBPs, most of which play redundant catalytic roles. In order to demonstrate the applicability of the β-lactone probes in Gram-negative, we tested (D)- and (L)-Ala-containing probes, which we had shown to target the highest number of PBPs in the previous two model systems. Probe **11T**, which contains valine, was also included as an example with a bulkier side chain. Interestingly, all tested probes targeted PBP4 and PBP5, both of which are LMW carboxypeptidases and are among the most abundant PBPs. This result is consistent with the high affinity of β-lactams for these PBPs, as demonstrated by a previous titration study conducted by our group (**Fig. 4.15**).(115) Significant non-PBP labeling was detected with **5T**, **5B** and **11T**, but this experiment was not repeated to verify this result. Overall, these preliminary results in *E. coli* are promising and further testing of our β-lactone library in Gram-negative model organisms could lead to the discovery of PBP-selective probes.

4.8.3. *Staphylococcus aureus*

We aimed to test the applicability of our probes to label PBPs of *S. aureus*, given its clinical significance as a pathogenic bacterium and high level of resistance to β-lactam antibiotics. As a result, the cell envelope of *S. aureus* has received extensive attention. *S. aureus* has a unique, highly branched PG structure that displays a pentaglycine moiety that extends from the third amino acid of one stem peptide and is conjugated to the neighboring stem peptide.(14) Such branched stem peptides play various roles, such as an attachment site for PG-associated proteins and resistance to cell wall-active antibiotics such as the glycopeptides and β-lactams.(14) Indeed, relatively minimal PBP labeling was detected when we treated *S. aureus* cells with our probe toolbox. Surprisingly, the two tested β-lactone probes, **2FL** and **5T**, specifically targeted PBP1, a transpeptidase that is essential for cell septation at the end of the staphylococcal cell division.(204, 205) A non-

PBP band with a low molecular weight was also detected in proteome samples labeled by **5T** (**Fig. 4.16**).

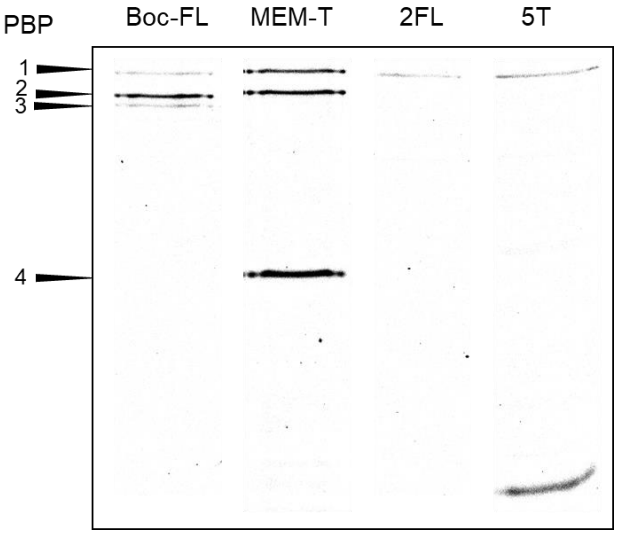

Figure 4.16. Gel-based analysis of the PBP labeling profile of 2FL and 5T in *S. aureus* cells. Boc-FL and MEM-TAMRA were used as positive controls to visualize all 4 PBPs in *S. aureus*. Live cells were incubated with the probes for 30 minutes, at a final concentration of 5 μg/mL Mem-TAMRA (meropenem attached to TAMRA fluorophore, as developed and described in CHAPTER 3) probe was used in addition to Boc-FL, to assure clear visualization of all 4 PBPs of *S. aureus*.

4.9. Summary and Conclusions

Bacterial cell wall biosynthesis remains an outstanding target for new antibiotics; however, there are significant gaps in our knowledge about this complicated process, including the mechanisms and control of PBP activity throughout this process. Continued development of tools to target and map the activities of the individual PBPs is a critical component to our understanding of bacterial growth and may lead to the identification of new therapeutic targets. Here, we report the generation of a library of compounds based upon a scaffold not previously known to target the PBPs, the β-lactones. These probes demonstrated exquisite specificity for PBPs in bacterial cells, distinct interaction patterns with the PBPs in comparison to β-lactam antibiotics and enabled us to examine the activity of two essential transpeptidases, PBP2x and PBP2b, in live *S. pneumoniae*. We found that PBP2b and PBP2x co-localize as a single ring in early division, but during mid-to-late division, PBP2x activity concentrates to the central septal site, while PBP2b activity remains at the outer division ring. This is the first demonstration of the transpeptidation activity of individual PBPs *in vivo*, which confirmed that PBP2b and PBP2x display distinct

patterns of localization during constriction. As such, this work highlights the importance of the development of PBP-selective probes. Their combination with powerful cell biology tools will be essential for examination of bacterial function by evaluating the localization and activation of the PBPs in myriad eubacteria.

4.10. Methods and Characterization Data

4.10.1. General Materials and Methods

All reactions were carried out in anhydrous solvents under Ar or N_2 atmosphere. Hydroxybenzotriazole (HOBt),(1-cyano-2-ethoxy-2-oxoethylidenaminooxy)dimethylamino-morpholino-carbenium hexafluorophosphate (COMU) and benzotriazol-1-yl-oxytripyrrolidinophosphonium hexafluorophosphate (PyBOP) were purchased from Chem-Impex international. BODIPY- and TAMRA-succinimidyl esters were purchased from ThermoFischer Company. Fluorescein was purchased from Sigma-Aldrich Company. All other reagents were purchased from Sigma-Aldrich and used without further purification, unless otherwise noted.

^{1}H and ^{13}C NMR spectra were recorded on Varian VI- 300, and VI-500 spectrometers and are reported in parts per million (δ). The following abbreviations were used to explain the multiplicities: s = singlet, d = doublet, t = triplet, q = quartet, quin = quintet, m = multiplet, b = broad, app. = apparent. NMR spectra of all the intermediates and final probes have been published.(90) BioTof II electrospray ionization-time-of-flight mass spectrometer with internal standard (Methanolic solution of PEG), UPLC-ESI-TOF MS instrumentation (Agilent, 6220) or Bruker BioTOF II ESI/TOF-MS were used to obtain accurate mass spectral data. MALDI/TOF (AB-Sciex 5800) MS instrumentation was used for MS analysis of tryptic peptides. HPLC purification was performed using an Agilent 1200 HPLC using a reverse phase column (Agilent ZORBAX C18, 5 µm, 250 × 21 mm) detected

by diode array detector (200–600 nm). Gradients consisted of 5–95% B (A: H_2O, 0.1% formic acid (FA); B: CH_3CN, 0.1% FA) over 20-30 minutes.

4.10.2. Probe Concentration Determination

Probes were stored as DMSO solutions at -80 °C. Concentrations were determined by measuring UV-Vis absorption of each solution at λ_{max} of its corresponding fluorophore. For fluorescein-containing probes, 10× and 100× dilutions of probe were made in 0.1 M Tris.HCl (pH=8) and absorbance was read at 492 nm using NanoPhotometer P330 (IMPLEN). The average of 3 reads of the concentration that was in 0.1-0.9 range was used to calculate concentration. (ε = 78,000 $M^{-1}.cm^{-1}$). TAMRA- and BODIPY FL-containing probes were diluted in methanol, and concentrations were calculated in the same way as fluorescein probes. (λ_{max} and ε value equals 543 nm, 87,000 $M^{-1}.cm^{-1}$ and 504 nm, 85,000 $M^{-1}.cm^{-1}$, respectively).

4.10.3. Bacterial Culturing and Probe Labeling

4.10.3.1. *S. pneumoniae* Culturing and Probe Labeling

Strain IU1945, an unencapsulated derivative of serotype 2 *S. pneumoniae* strain D39, was grown statically in brain heart infusion (BHI) medium in 100 x 17 mm tubes by incubation in an atmosphere of 5% CO_2 at 37 °C to an OD_{620} of ~ 0.2. For labeling experiments, overnight cultures that were still in exponential phase (OD_{620} = 0.1 – 0.4) were diluted to OD_{620} = 0.002 – 0.004 and grown as above. Samples with OD_{620} = 0.15 – 0.20 were utilized in labeling experiments conducted as previously described,(102) and summarized as follows: Cell pellets from 1.5 mL of *S. pneumoniae* cultures were harvested by centrifugation (16,100 × *g* for 2 min at RT) and washed with phosphate buffered saline (PBS x 1; pH 7.4). Cell pellets were resuspended in 50 µL of PBS containing 1–30 µg/mL of β-lactone probes and incubated at room temperature (RT) for

20 min unless noted otherwise on the figures. A reference sample was suspended in 50 µL of PBS containing 5 µg/ml Boc-FL and incubated for 10 min at RT. The cells were washed and resuspended in 100 µL of PBS containing 10 mg/mL of lysozyme and were incubated for 30 min at 37 °C. The cells were lysed by a Branson Sonifier 250 (power setting 3, 30% duty cycle for 3 × 10 s intervals) or Hielscher vial tweeter UP200St (70% C, 95% A, 5% adjustment snap and 1s SD Interval / 10s for 6 x 1 min intervals with 1 min cooling time in between), and membrane proteome was isolated by at 21,000 × *g* for 15 min at 4 °C. Membrane proteome was resuspended in 100 µL PBS, and the samples were homogenized by sonication (power setting 1, 10% duty cycle for 1 s). The protein concentration was measured by NanoDrop 1000 Spectrophotometer (Thermo Scientific) or NanoPhotometer P330 (IMPLEN). The protein concentration was adjusted to 2.5 mg/mL by diluting with PBS. Thirty microliters of proteome sample were dispensed into a clean 1.5-mL microcentrifuge tube and 10 µL of 4 × SDS-PAGE loading buffer was added to each sample. The samples were heated for 5 min at 90-95 °C to denature the proteins then cooled down to RT. Ten to twelve microliters of sample were loaded onto a 10% SDS-PAGE gel (acrylamide:bis-acrylamide = 29:1). The protein bands were separated by gel electrophoresis for 1.5 h at 180 V, 400 mA, 60 W. The gel was rinsed with distilled water three times before fluorescence scanning. The same growth and labeling procedures were utilized with mutant strains of *S. pneumoniae* E177 (Δ*pbp1a*) and E193 (Δ*pbp1b*).

4.10.3.2. *B. subtilis* Culturing

Strain PY79, a prototrophic laboratory strain that has been extensively used for studying a wide variety of cellular pathways, was grown in Luria-Bertani (LB) medium in 100 x 17 mm tubes by incubation at 30 °C while shaking at 220 rpm to an OD_{600} of ~ 0.3-0.4. For labeling experiments, overnight cultures were diluted to OD_{600} = 0.002 – 0.004

and grown as above. Samples with OD_{600} = 0.3 – 0.4 were utilized in labeling experiments conducted as previously described for S. pneumoniae. The only exception was that cell pellets from 1 mL of *B. subtilis* cultures were collected and labeled.

4.10.3.3. *E. coli* culturing

Strain DC2, an antibiotic hypersusceptible mutant, was grown in LB medium in 100 x 17 mm tubes by incubation at 37 °C while shaking at 220 rpm to an OD_{600} of ~ 0.5. For labeling experiments, overnight cultures were diluted to OD_{600} = 0.002 – 0.004 and grown as above. Samples with OD_{600} = 0.4 – 0.5 were utilized in labeling experiments. Cell pellets from 1 mL of *E. coli* cultures were collected and labeled as described above for pneumococcal cells, with slight modification in lysis step where the lysozyme digestion was skipped and labeled cells were directly taken to sonificaion.

4.10.3.4. *S. aureus* Culturing

S. aures BAA-1721 (methicillin-sensitive strain) was purchased from ATCC and was cultured in Tryptic Soy Broth (TSB) at 37 °C with shaking at 220 rpm to reach an OD_{600} of 0.5.

4.10.4. Sodium dodecyl sulfate-polyacrylamide gel electrophoresis (SDS-PAGE)

The protocol for SDS-PAGE gel preparation was previously described.(102) Briefly, polyacrylamide gels were composed of 10% resolving gel (10.5 mL of 1.5 M Tris-HCl buffer pH 8.8, 10.5 mL of acrylamide:bis-acrylamide 29:1 (40% solution), 21 mL of H_2O, 140 µL of 10% ammonium persulfate (APS), 15 µL of tetramethylethylenediamine (TEMED) and 4.5% stacking gel (2.5 mL of 0.5 M Tris-HCl buffer pH 6.8, 1.125 mL of acrylamide:bis-acrylamide 29:1 (40% solution), 6.375 mL of H_2O, 30 µL of 10% APS, 10 µL of TEMED). Running parameters were 180 V, 400 mA, and 60 W for 1.5 h. Experiments to examine competition of acyl homoserine lactones or *p*-toluenesulfonic acid salts of the β-lactones with Boc-FL were performed with acrylamide:bis-acrylamide ratio of 37.5:1.

4.10.5. In-gel Fluorescence Detection

After SDS-PAGE, labeled proteins were visualized at 50-µm resolution in gels using a Typhoon 9210 gel scanner (Amersham Biosciences) with 580-nm bandpass filter for TAMRA, 526-nm short-pass filter for fluorescein and BODIPY FL, and 670-nm bandpass filter for BODIPY 650/665. All gel images were analyzed using ImageJ software (National Institutes of Health). The background signal of the gel images was subtracted, and the brightness and contrast were adjusted to optimize the signal-to-noise ratio (all operations were performed over the entire gel uniformly).

4.10.6. Competition Assays

4.10.6.1. Competition Assays of Boc-FL and *p*-toluenesulfonic Acid Salts of the β-lactones for *S. pneumoniae* IU1945 PBPs

Cells from 1.5 mL of culture were harvested by centrifugation (16,100 × *g* for 2 min at RT) and washed with 1 mL of PBS, pH 7.4. Cell pellets were resuspended in 50 µL of PBS containing 5, 10, and 20 µg/mL of β-lactone *p*-toluenesulfonic salts and incubated for 40 min at RT. Cells were pelleted and washed in 1 mL of PBS. Next, the cells were resuspended in 50 µL of PBS containing 5 µg/mL Boc-FL and incubated for 10 min at RT. Finally, the cells were resuspended in 100 µL PBS containing 1 or 10 mg/mL lysozyme and incubated for 30 min at 37 °C. Cells were lysed and sample preparation for SDS-PAGE gel-based analysis was performed as described.

4.10.6.2. Competition Assays of Boc-FL and *N*-acylated L-homoserine Lactones for *S. pneumoniae* IU1945 PBPs

Cells from 1.5 mL of culture were harvested by centrifugation (16,100 × *g* for 2 min at RT) and washed with 1 ml of PBS, pH 7.4. Cell pellets were resuspended in 50 µL of PBS containing 5–50 µg/mL of *N*-(β-ketocaproyl)-L-HSL, *N*-butyryl-L-HSL, *N*-3-oxo-

dodecanoyl-L-HSL, and *N*-3-hydroxyoctanoyl-L-HSL (Cayman Chemical Company) and incubated for 30 min at RT. Cells were pelleted and washed in 1 mL of PBS. Next, the cells were resuspended in 50 µL of PBS containing 5 µg/mL Boc-FL and incubated for 10 min at RT. Finally, the cells were resuspended in 100 µL PBS containing 10 mg/mL lysozyme and incubated for 30 min at 37 °C. Cells were lysed and sample preparation for SDS-PAGE gel-based analysis was performed as described.

4.10.6.3. Competition Assays of Penicillin V (Pen-V) and Boc-FL, 2F, 2T Probes

Cells from 1.5 mL of culture were harvested by centrifugation (16,100 × *g* for 2 min at RT) and washed with 1 ml of PBS, pH 7.4. In Pen-V pretreatment assay, cell pellets were resuspended in 50 µL of PBS containing 5 µg/mL of Pen-V, and incubated for 30 min at RT. Cells were pelleted and washed in 1 mL of PBS. Next, the cells were resuspended in 50 µL of PBS containing 5 µg/mL Boc-FL, or 5 µg/mL 2F or 5 µg/mL 2T and incubated for 10 min (Boc-FL) or 30 min (**2F**, **2T**) at RT. In Pen-V post-treatment assay, cells were labeled with Boc-FL, 2F and 2T as just described, washed and then incubated with 5 µg/mL Pen-V. Finally, the cells were resuspended in 100 µL PBS containing 10 mg/mL lysozyme and incubated for 30 min at 37 °C. Cells were lysed and sample preparation for SDS-PAGE gel-based analysis was performed as described.

4.10.6.4. Methicillin Pre-Treatment Controls

Cells from 1.5 mL of *S. pneumoniae* IU1945 and E193 cultures at exponential phase (OD_{620} ~ 0.2) were harvested by centrifugation (16,100 × *g* for 2 min at RT) and washed with 1 mL of PBS, pH 7.4. Cell pellets were resuspended in 50 µL of PBS containing 0.1 µg/mL of methicillin and incubated for 30 min at RT. Cells were pelleted and washed in 1 mL of PBS. Next, the cells were resuspended in 50 µL of PBS containing 1 or 5 µg/mL of lactone-L-Phe-FL or 5 µg/mL Boc-FL (as control) and incubated for 20 min at RT (10 min

at RT for Boc-FL). Finally, the cells were resuspended in 100 µL PBS containing 10 mg/mL lysozyme and incubated for 30 min at 37 °C. Cells were lysed and sample preparation for SDS-PAGE gel-based analysis was performed as described.

4.10.7. Dual-Labeling Experiments.

S. pneumoniae E193 (Δ*pbp1b*) cells were grown in BHI broth at 37 °C in an atmosphere of 5% CO_2 to reach an OD_{620} of 0.2-0.25. Cells from 1.5 mL of culture were harvested by centrifugation (16,100 × *g* for 2 min at RT) and washed with 1 mL of PBS, pH 7.4. Cell pellets were resuspended in 50 µL of PBS containing 5 µg/mL lactone-L-Phe-FL and incubated at RT for 20 min. Cells were then washed with 1 mL PBS prior to suspension in 50 µL of 5 µg/mL solution of Lac-D-Phe-TAMRA in PBS. After incubation for 20 min at RT, cells were washed and resuspended in 100 µL of PBS containing 10 mg/mL of lysozyme. Cell lysis and sample preparation for SDS PAGE was followed as described earlier.

4.10.8. Antimicrobial Susceptibility Assay for *S. pneumoniae* IU1945.

S. pneumoniae strain IU1945 was streaked from the glycerol stock to plates containing Trypticase soy agar II (modified; Becton-Dickinson) and 5% (vol/vol) defibrinated sheep blood (TSAIIBA) and incubated at 37 °C in an atmosphere of 5% CO_2 for 14 to 16 h. Five colonies were inoculated into 5 mL of BHI and grown to an OD_{620} of 0.08-0.1 (2.2×10^5 CFU/mL). Cultures were then diluted 100-fold with BHI. Probe stocks were serially diluted 2-fold in BHI. In 96-well plates, 100 µL diluted culture was added to 100 µL of serially diluted probes in each well. Each compound was run in duplicate. After incubation at 37°C in an atmosphere of 5% CO_2 for 18 to 20 h, plates were examined by eye. The lowest concentration that inhibited cell growth was noted as the MIC.

4.10.9. 3D-SIM Microscopy of Lactone- and FDAA-Labeled Cells

Cells from an overnight culture were diluted to OD_{620} 0.02 in 2 mL of fresh BHI prewarmed to 37 °C and incubated at 37 °C in an atmosphere of 5% CO_2. At OD_{620} 0.2, 1.5 mL of culture was added to a microfuge tube and centrifuged at room temperature for 5 min at 16000 x g. The supernatant was discarded, the pellet was resuspended in 1 mL room temperature PBS, and the culture was centrifuged a second time. The supernatant was discarded, and the pellet was resuspended in either 50 µL of PBS with 5 µg/mL **7FL** or 100 µL PBS with 5 µg/mL **8T**. The cells were incubated for 20 min at room temperature in the dark. After incubation the cells were spun and washed with 1 mL of PBS (**7FL**) or 1 mL of PBS containing 50 mM glucose (**8T**). The cells were spun a second time and washed with 200 µL of PBS (**7FL**) or 200 µL of PBS with 50 mM glucose (**8T**), and finally spun a third time and resuspended in 100 µL of cold (4 °C) GTE buffer (50 mM glucose, 20 mM Tris pH 7.5, 1 mM EDTA). The cells were spun down at 4 °C, the supernatant was discarded, and the pellet was resuspended in 15 µL of Vectashield Hardest Antifade (Vector Labs) and kept on ice. Cells in antifade (1.2 µL) were pipetted onto a clean coverslip, applied to a slide, and imaged via 3D-SIM. 3D-SIM was performed using the OMX 3D-SIM super-resolution system located in the Indiana University Bloomington Light Microscopy Imaging Center (http:// www.indiana.edu/~lmic/microscopes/index.html#OMX). The system used is equipped with four Photometrics Cascade II EMCCD cameras that allow simultaneous imaging of up to four colors, and is controlled by DV-OMX software, with image processing by Applied Precision softWoRx 6.0.0 software. Exposure times and %T settings for DAPI, Alexa 488, and Alexa 568 images were 5 ms and 100% for all three channels.

For pre-treatment with methicillin followed by lactone probe labeling, duplicate 2 mL cultures of each strain were created and incubated as described above. At OD_{620} 0.12, methicillin was added to a final concentration of 0.1 µg mL^{-1} to one culture for each strain,

and the strains were placed back in the incubator. After 20 min, all cultures were harvested, labeled, and imaged as described above.

For labeling of cells with both lactone probes, the following changes were made: After a 20 min incubation with **7FL**, the cells were spun down and washed once in 1 mL of PBS. The cells were spun again and resuspended in 100 µL of **8T** in PBS at 5 µg/mL. The cells were incubated for 20 min at room temperature in the dark, and then washed and imaged as described above for **8T** labeling.

For labeling of cells with FDAAs and lactone probes, the following changes were made: after diluting cells from an overnight culture to OD_{620} 0.02 in 2 mL of fresh BHI, 0.5 µL of the FDAA HADA (125 µm final, stock is 500 mM in DMSO) was added to the culture and the culture was incubated at 37 °C in an atmosphere of 5% CO_2. At OD_{620} 0.2, 500 µl of culture was added to a microfuge tube and centrifuged at room temperature for 5 min at 16,000 x *g*. The supernatant was discarded, and the pellet was resuspended in 250 µL of prewarmed BHI containing the FDAA TADA (500 µM final, stock is 500 mM in DMSO). The cells were incubated at 37 °C for 5 min, cooled on dry ice for exactly 20 seconds, and spun down in the cold (4 °C) for 2.5 min at 16,000 x *g*. The supernatant was discarded and the pellet was resuspended in 200 µL cold (4 °C) PBS. The cells were spun and washed once more with cold PBS, and then spun down a third time. The pellet was resuspended in 50 µL room temperature PBS with 5 µg/mL **7FL**, and the cells were labeled, washed, and imaged as described above.

4.10.10. Investigation of PBP2x-7FL Complex

4.10.10.1. Recombinant Production of Soluble PBP2x (PBP2x*)

Soluble form of PBP2x*, corresponding to amino acids 49-750 from *S. pneumoniae R6*, was generated as describes in the literature.(190, 206) PBP2x* expression plasmid was a generous donation from Dr. Andrea Dessen at Institut de Biologie Structurale,

France. Briefly, the protein was expressed as a fusion protein to glutathione S-transferase with a thrombin-cleavable linker (pGEX-4T1 plasmid) in the host strain *E. coli* DH5α cells. Transformed cells were grown overnight in LB containing 100 µg/ml ampicillin at 37 °C with shaking at 220 rpm. Ten ml of overnight cultures was inoculated to 1.0 L LB media with 100 µg/ml ampicillin and incubation continued to reach OD_{600} ~0.5. Next, 1 mM isopropyl-β-D-thiogalactoside (IPTG) was added and culture was incubated at 22 °C with shaking at 220 rpm overnight. Cells were harvested from the overnight culture by centrifugation at 8,000 × g, 4 °C for 20 min. Pellets were suspended in 25 ml of buffer A (50 mM Tris.HCl, 100 mM NaCl, 1 mM EDTA, pH = 8.0) to which a protease inhibitor tablet (Roche) was added. Cells were lyzed using a Beanson 250 sonifier (setting 3, 30% cycle, 12 × 15 s on-cycle on ice, with 45 s cooling time in-between cycles). The cell extract was loaded onto a glutathione-Sepharose 4B (SigmaAldrich) affinity column previously equilibrated with buffer A. One hundred units of human thrombin (Sigma) was applied onto the column at room temperature followed by 3 h incubation at room temperature, to elute the water-soluble PBP2x*. SDS PAGE analysis of the collected fractions proved ≥ 95% purity.

4.10.10.2. Titration of PBP2x* with 7FL

Titration was performed as described previously.(207) Briefly, serially diluted solutions of PBP2x* were prepared in duplicate, containing 2, 4, 8, 12, 16, 24, 36, 48 ng of PBP2x*. To 10 µl of each solution was added either 10 µM Boc-FL or **7FL**. All samples were incubated at room temperature for 30 min. The reaction was quenched by the addition of 3.3 µl 4 × SDS loading buffer and heated at 95 °C for 5 min. Samples were loaded on 10% SDS PAGE gel and were run at 180V for 90 min. Gels were scanned and fluorescent bands were integrated as described above. Gel band integrations were plotted against the PBP2x* amount for both probes (**Fig. 4.17**) and showed a linear relationship.

Nest, both gels were stained with Coomassie Brillian Blue R-250 (BioRad) for 30 min while shaking. Gels were destained with water:methanol:acetic acid (5:4:1) to remove background.

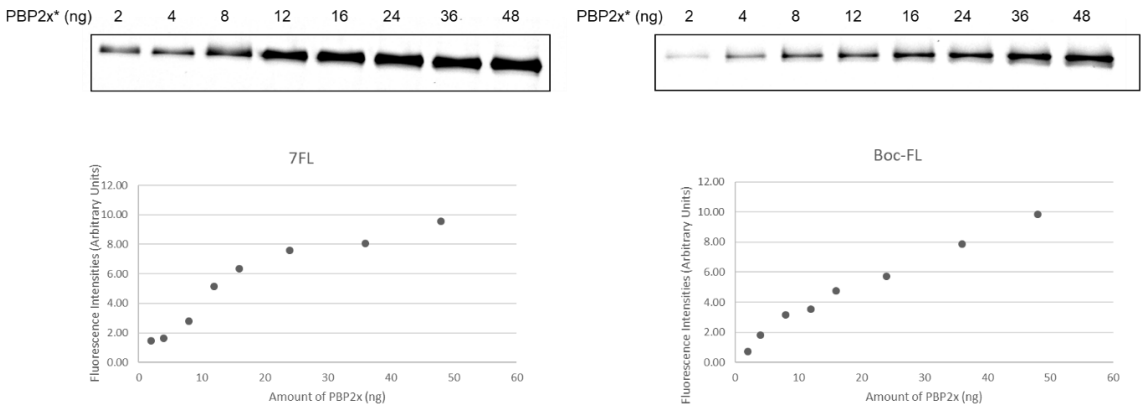

Figure 4.17. Titration of soluble PBP2x with **7FL** probe and comparison with bicillin-FL. Fluorescent signal was measured and plotted against the PBP2x* amount. Both probes showed a linear correlation.

4.10.10.3. In Gel Trypsin Digestion of PBP-Probe Complexes

Gel bands containing 36 and 48 ng PBP2x* were excised by a razor blade and cut into 2 × 2 mm cubes and placed in 1.5 mL snap-cap microcentrifuge tubes. Next, 75 µl 1:1 100mM ammonium bicarbonate:acetonitrile was added to gel pieces. Samples were vortex briefly and incubated for 15 min at room temperature. Solution was removed, and the wash step was repeated 2 more times or until the Coomassie stain was removed. Next, 75 ul of 100% acetonitrile was added. When gel pieces shrank and turned white and semiopaque, acetonitrile was removed (happened in a few min). Reduction and alkylation of proteins was performed next. Gel pieces were rehydrated with 75 µl 10 mM Dithiothreitol (DTT) in 50 mM ammonium bicarbnate solution and incubated for 1 h at 65 °C. Tubes were centrifuged briefly and the solution was removed. Gel pieces were washed with 75 µl 1:1 100mM ammonium bicarbonate:acetonitrile twice. Next, gel pieces were washed with 75 ul of 100% acetonitrile. Acetonitrile was removed when the pieces started to shrink

and turned opaque white. In-gel digestion was performed next, by hydrating gel pieces in ~20 µl of digestion buffer (50 mM NH_4HCO_3, 5 mM $CaCl_2$, 5 ng/µl MS-grade trypsin) at 4 °C for ~15 min. Supernatant was removed and replaced with 70 µl 50 mM NH_4HCO_3, 5 mM $CaCl_2$ and samples were incubated at 37 °C overnight. Tubes were briefly centrifuged the next day and the supernatant was recovered and transferred to a 1.5 mL low-binding Eppendorf tube. Gel pieces were covered with enough amounts of 50% acetonitrile, 0.3% formic aicd and incubated for 15 min at room temperature. The supernatant was recovered and placed in the same Eppendorf tube. Gel pieces were covered with 80& acetonitrile, 0.3% formic acid and incubated for 15 min at room temperature. The supernatant was recovered and added to the same tube. The extracted peptide solutions were lyophilized followed by storage at -80 °C until MS analysis.

4.10.10.4. MS Analysis of Labeled PBP2x*

Ziptip ® C18 pipette tips (Millipore Sigma) were used to remove salts using the protocol from the manufacturer. MS grade water, acetonitrile (ACN) and trifluoroacetic acid (TFA) were used. **T**he dried samples were reconstituted with 13 µL of reconstitution solution (R; 5:95, ACN:water, 0.1% TFA), vortexed and centrifuged (sample pH must be acidic at this point; TFA was added as necessary). ZipTip was placed on a P10 pipettor set to 10 µL. The ZipTip was hydrated by aspirating solution 1 (50:50 ACN:water, 0.1% TFA) followed by solution 2 (0.1% TFA in water). Next, 10 µL of the sample was loaded by pipetting up and down 5-6 times. Next, the salts were removed by aspirating 10 µL of solution 2 (0.1% TFA in water) for a total of 4-5 washes (expel the wash into waste each time). Finally, the peptides were eluted by aspirating and expelling 1.3 µL of elution solution (60:40 ACN:water, 0.1% TFA) on ice 10 times (sample expelled into the same solution each time). Finally, 0.7 µL of saturated matrix solution (CCA; α-cyano-4-hydroxycinnamic acid) was added to the sample and resulting mixture was spotted on a

MALDI target. Analysis of MS raw data and *In silico* tryptic digestion of PBP2x sequence from *S. pneumoniae D39* was performed using mMass software. The m/z for active site tryptic peptide containing the reactive serine residue was identified for the control (no probe sample) and the addition of probe's m/z to that peptide was search in MS spectra of probe-labeled samples.

4.10.11. Synthetic Procedures

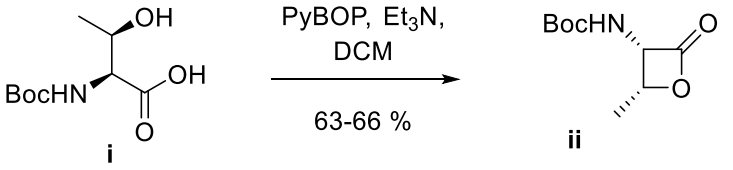

i **ii**

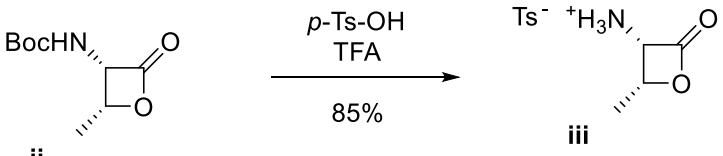

ii **iii**

4.10.11.1. Lactonization

The *para*-toluenesulfonate (PTSA) salt of (2R,3S)-β-lactone was prepared as described previously.(182) Briefly, L-Thr-OH (**i**, 1 eq.), and PyBOP (1.2 eq.) were dissolved in anhydrous DCM at 0 °C and Et_3N (3 eq.) was added dropwise. The reaction mixture was stirred for 30 min at 0 °C and then for 6 h at RT. Solvent was evaporated afterwards and the crude product was purified on silica gel column (ethyl acetate:hexanes 1:6). HRMS (ESI) calcd. for $C_9H_{15}NNaO_4$ [M+Na]+, 224.0893, found 224.0916. Deprotection was performed by adding **ii** (1 eq.) dropwise to a mixture of *p*-toluenesulfonic acid (1.05 eq.) and dichloromethane/TFA (~35 eq.) at 0 °C. The resulting mixture was stirred for 30 min at 0 °C followed by 30 min at RT. TFA/dichloromethane was subsequently removed *in vacuo* and residual TFA was co-evaporated with toluene. Compound **iii** was precipitated by addition of anhydrous THF followed by anhydrous ether

(THF:ether; 1:4), washed with anhydrous ether (2x) and was used in subsequent coupling reactions without further purification. HRMS (ESI) calcd. for $C_{11}H_{16}NO_5S$ [M+H]+, 274.0744, found 274.0747. The S,R isomer was prepared using the same procedures.

4.10.11.2. Fluorophore Coupling to β-Lactones

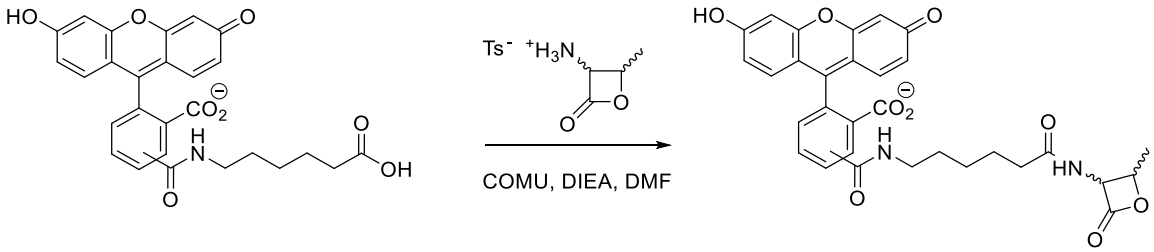

Conditions description

To a solution of 6-[Fluorescein-5(6)-carboxamido]hexanoic acid (0.02 mmol, 10.0 mg) and COMU (0.022 mmol, 9.6 mg) in DMF (0.2 ml) at 0 ^{o}C, DIEA (0.021 mmol, 3.7 µL) was added. After stirring for 15 min., premixed lactone (0.02 mmol, 5.5 mg) and DIEA (0.02 mmol, 3.5 µL) in DMF (0.1 ml) was added in small portions every 15-30 min to the reaction mixture. Once the reaction was completed (hours to days according to HPLC analysis), the solvent was evaporated and residue was purified by HPLC. Fluorescein and TAMRA-containing molecule assignments include both isomers.

2FL: (reaction time : 1 day) Yield = 12%, ^{1}H NMR (CD_3OD, 500 MHz): δ = 1.38 (d, J = 6.3 Hz, 3H), 1.57-1.73 (m, 6H), 2.33 (t, J=6.3 Hz, 2H), 3.45 (t, J = 5.9 Hz, 2H), 4.78-4.83 (m, 1H), 5.56 (d, J = 6.0 Hz, 1H), 6.55 (td, J=8.3, 2.5Hz, 2H), 6.67-6.70 (m, 4H), 7.31 (d, J = 8.0 Hz, 0.5H), 7.61 (s, 0.5H), 8.08-8.13 (m, 1H), 8.16 (dd, J = 8.0, 1.5 Hz, 0.5H), 8.42 (s, 0.5H), 8.50 (s, 0.5H), $[M+H]^+$ = 573.1873, calc for $C_{31}H_{29}N_2O_9^+$ $(M+H)^+$ 573.1868, found 573.1874.

4-FL: (reaction time : 1 day) Yield = 6%, ^{1}H NMR (500 MHz, DMSO-d_6): δ 1.23-1.34 (m, 2H), 1.41-1.47 (m, 2H), 1.50-1.56 (m, 2H), 1.94-2.01 (m, 1H), 2.06-2.16 (m, 2H), 2.32-2.38 (m, 1H), 3.12-3.15 (m, 2H), 4.13-4.20 (m, 1H), 4.26-4.33 (m, 1H), 4.46-4.54 (m, 1H), 5.28-5.31 (m, 1H), 6.49-6.58 (m, 4H), 6.64-6.71 (m, 2H), 7.31-7.36 (m, 1H), 8.17-8.22 (m, 1H), 8.28-8.33 (m, 2H), 8.35-8.44 (m, 1H), 8.78-8.81 (m, 1H); HRMS-ESI: calc for $C_{31}H_{29}N_2O_9^+$ $(M + H)^+$ 573.1873, found 573.1862.

4.10.11.3. Amino Acid Coupling to β-Lactones

The lactones were coupled to various Boc-protected amino acids using ethylchloroformate (ECF; method A) or PyBOP/HOBt (method B) as described previously.(182) In method A, ethyl chloroformate is used as coupling reagent in presence of DIEA in anhydrous dichloromethane (DCM). The activation step was performed at -5 °C for 20 minutes, after which the lactone PTSA salt was added along with two equivalents of pyridine. Reaction mixture is stirred for 30 min, warmed to room temperature and stirred overnight. Solvent was removed and residue dissolved in ethyl acetate, washed with water and dried over Na_2SO_4 or $CaCl_2$. Purification was performed by silica gel chromatography using ethyl acetate/hexane or cyclohexane (1:1) as the eluting solvent. In Method B, the only variation is that PyBOP was used as the coupling reagent in DMF/DCM (1:1) as reaction solvent.

Method A:

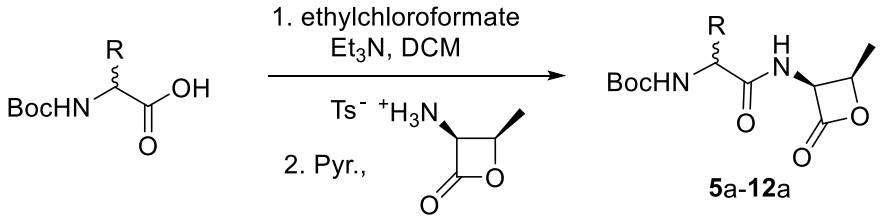

5a-**12**a

Method B:

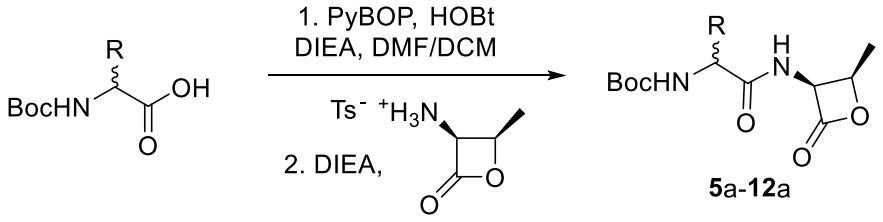

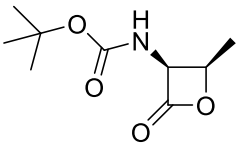

Boc-(2*R*, 3*S*)-β-lactone: Yield = 63%, ^{1}H NMR (300 MHz, $CDCl_3$): δ 1.45 (s, 12H), 4.85 (app. quin, J = 6.2 Hz, 1H), 5.30 (d, *J* = 7.7 Hz, NH), 5.40-5.45 (m, 1H); ^{13}C NMR ($CDCl_3$): □ = 169.3, 154.5, 81.3, 74.9, 60.1, 28.2, 15.0; HRMS-ESI: calc for $C_9H_{15}NNaO_4^+$ $(M + Na)^+$ 224.0893, found 224.0916.

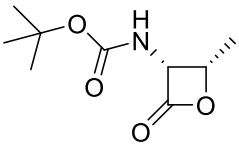

Boc-(2*S*, 3*R*)-β-lactone: Yield = 66%, ^{1}H NMR (300 MHz, $CDCl_3$): δ 1.45 (s, 12H), 4.85 (app. quin, *J*=6.2 Hz, 1H), 5.28 (d, *J*=7.7 Hz, NH), 5.40-5.45 (m, 1H); ^{13}C NMR ($CDCl_3$): □ = 169.3, 154.5, 81.3, 74.9, 60.1, 28.2, 15.0; HRMS-ESI: calc for $C_9H_{15}NNaO_4^+$ $(M + Na)^+$ 224.0893, found 224.0917.

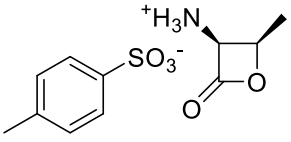

(2*R*, 3*S*)-β-lactone: Yield = 85%, ^{1}H NMR (300 MHz, CD_3CN): δ 1.58 (d, *J* = 6.5 Hz, 3H), 2.36 (s, 3H), 4.94 (app. quin, *J* = 6.5 Hz, 1H), 5.10 (d, J = 6.2 Hz, 1H), 7.23 (m, 2H), 7.65 (m, 2H), 8.35 (Br, 3H, NH); ^{13}C NMR ($(CD_3)_2SO$): □ = 166.0, 145.9, 138.2, 128.6, 125.9, 72.4, 57.7, 21.25, 14.41; HRMS-ESI: calc for $C_{11}H_{16}NO_5S^+$ $(M + H)^+$ 274.0744, found 274.0747.

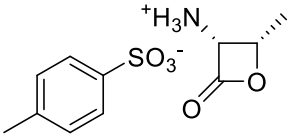

(2*S, 3R*)-β-lactone: Yield = 85%, ^{1}H NMR (300 MHz, CD_3CN): δ 1.57 (d, *J* = 6.5 Hz, 3H), 2.36 (s, 3H), 4.94 (app. quin, *J* = 6.5 Hz, 1H), 5.10 (d, J = 6.2 Hz, 1H), 7.21 (d, J = 8.1 Hz, 2H), 7.65 (d, J = 8.1 Hz, 2H), 8.35 (Br, 3H, NH); ^{13}C NMR ($(CD_3)_2SO$): □ = 166.0, 145.8, 138.3, 128.6, 125.9, 72.4, 57.7, 21.2, 14.4; HRMS-ESI: calc for $C_{11}H_{16}NO_5S^+$ $(M + H)^+$ 274.0744, found 274.0748.

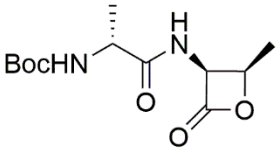

5a: Method A Yield = 75%, ^{1}H NMR (500 MHz, $CDCl_3$): δ 1.29 (d, *J* = 7.0 Hz, 3H), 1.34 (s, 9H), 1.35 (d, *J* = 6.0 Hz, 3H), 4.16-4.22 (m, 1H), 4.82 (app. quin, *J* = 6.0 Hz, 1H), 5.57-5.59 (m, 1H), 8.01 (d, *J* = 8.0 Hz, NH) HRMS-ESI: calc for $C_{12}H_{20}N_2NaO_5^+$ $(M + Na)^+$ 295.1264, found 295.1271.

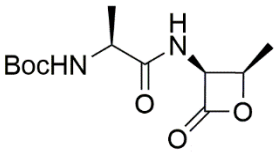

6a: Method A Yield = 80%, ^{1}H NMR (500 MHz, $CDCl_3$): δ 1.36 (d, *J* = 7.0 Hz, 3H), 1.38 (d, *J* = 6.5, 3H), 1.42 (s, 9H), 4.22-4.24 (m, 1H), 4.87 (app. quin, *J* = 6.2 Hz, 1H), 5.27 (d, *J* = 4.5 Hz, NH), 5.58-5.60 (m, 1H), 7.74 (d, *J* = 6.0 Hz, NH); HRMS-ESI: calc for $C_{12}H_{20}N_2NaO_5^+$ $(M + Na)^+$ 295.1264, found 295.1269.

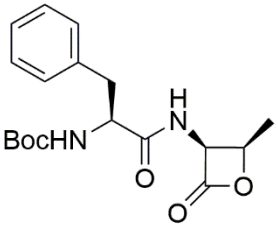

7a: Method B Yield = 60%, ^{1}H NMR (300 MHz, CD_3CN): δ = 1.36 (s, 9H), 1.37 (d, *J* = 6.3 Hz, 3H), 2.83-2.88 (m, 1H), 3.12-3.18 (m, 1H), 4.27-4.30 (m, 1H), 4.84 (app. quin, *J* = 6.2 Hz, 1H), 5.44-5.58 (m, 1H), 5.56 (d, *J* = 7.3 Hz, NH), 7.24-7.36 (m, 5H), 7.40 (d, *J* = 8.1, NH); HRMS-ESI: calc for $C_{18}H_{25}N_2O_5^+$ $(M + H)^+$ 349.1758, found 349.1685.

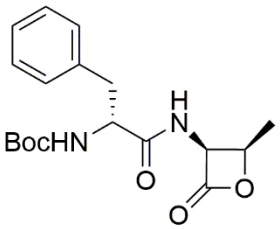

8a: Method B Yield = 55%, ^{1}H NMR (300 MHz, CD_3CN): δ = 1.27 (d, *J* = 6.3 Hz, 3H), 1.36 (s, 9H), 2.82-2.87 (m, 1H), 3.08-3.14 (m, 1H), 4.25-4.33 (m, 1H), 4.81 (app. quin, *J* = 6.3 Hz, 1H), 5.44-5.56 (m, 1H), 5.57 (d, *J* = 7.3 Hz, 1H), 7.26-7.33 (m, 5H), 7.42 (d, *J* = 8.1, NH) ; HRMS-ESI: calc for $C_{18}H_{25}N_2O_5^+$ $(M + H)^+$ 349.1758, found 349.1759.

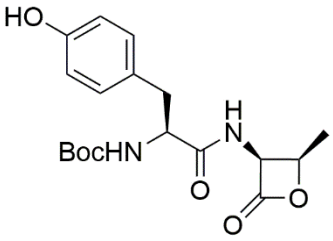

9a: Method A; Compound was obtained by *in situ* deprotection of the benzyl protecting group on the phenolic group after amide bond formation via the following procedure: To a stirred solution of the protected tyrosine derivative (150 mg, 0.33 mmol) in 5 mL of ethanol and 5 mL EtOAc in a round-bottom flask charged with an atmospheric H_2 balloon was added 10 mol % Pd-carbon. The reaction mixture was allowed to stir overnight (18 h). Pd-carbon was removed by filtration and the product was concentrated under reduced pressure. Crude materials were purified using flash column chromatography with 1:1 hexanes:ethyl acetate. Yield = 37% (two steps), ^{1}H NMR (500 MHz, CD_3CN): δ 1.35 (s, 12H), 2.74-2.79 (m, 1H), 3.00-3.04 (m, 1H), 4.20-4.24 (m, 1H), 4.83 (app. quin, *J* = 6.3 Hz, 1H), 5.43 (app. t, *J* = 7.0 Hz, 1H), 5.52 (d, *J* = 7.0 Hz, NH), 6.74 (d, *J* = 8.5 Hz, 2H), 6.89 (s, 1H), 7.06 (d, *J* = 8.0 Hz, 2H), 7.43 (d, *J* = 8.5 Hz, NH); HRMS-ESI: calc for $C_{18}H_{25}N_2O_6^+$ $(M + H)^+$ 365.1707, found 365.1698.

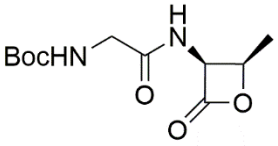

10a: Method B. Semi-purified material taken into next step. Crude ^{1}H NMR (500 MHz, $CDCl_3$): δ 1.42 (s, 9H), 1.44 (d, *J* = 6.5, 3H), 4.08-4.14 (m, 2H), 4.87 (app. quin, *J* = 6.4 Hz, 1H), 5.44-5.46 (m, 6.0 Hz, 1H), 7.70 (d, *J* = 6.3 Hz, 1H); HRMS-ESI: calc for $C_{11}H_{18}N_2NaO_5^+$ $(M + Na)^+$ 281.1108, found 281.1077.

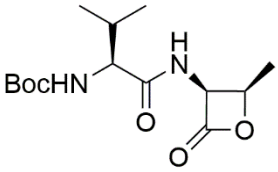

11a: Method B; Yield = 37%, ^{1}H NMR (500 MHz, CD_3CN): δ 0.95 (dd, *J* = 10, 6.5 Hz, 6H), 1.41 (s, 9H), 1.43 (d, *J* = 6.5, 3H), 2.08-2.12 (m, 1H), 4.00 (t, *J* = 7.7 Hz, 1H), 4.91 (app. quin, *J* = 6.2 Hz, 1H), 5.64-5.66 (m, 1H), 6.08 (d, *J* = 8.5 Hz, NH), 8.21 (d, *J* = 7.0 Hz, NH); HRMS-ESI: calc for $C_{14}H_{24}N_2NaO_5^+$ $(M + Na)^+$ 323.1577, found 323.1588.

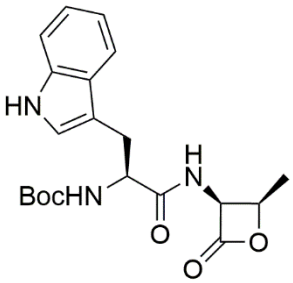

12a: Method B Yield = ~100%, ^{1}H NMR (500 MHz, CD_3CN): δ 1.30 (d, *J* = 6.5 Hz, 3H), 1.37 (s, 9H), 3.09-3.13 (m, 1H), 3.25-3.29 (m, 1H), 4.39-4.44 (m, 1H), 4.79 (app. quin, *J* = 6.3 Hz, 1H), 5.46-5.49 (m, 1H), 5.65 (d, *J* = 7.0 Hz, NH), 7.07 (t, *J* = 7.5 Hz, 1H), 7.13-7.16 (m, 2H), 7.41 (d, *J* = 8.5 Hz, 1H), 7.61 (t, *J* = 7.5 Hz, 2H), 9.30 (s, 1H); HRMS-ESI: calc for $C_{20}H_{25}NaO_5^+$ $(M + Na)^+$ 410.1686, found 410.1645.

4.10.11.4. Deprotection of Boc Group from Amino Acids Coupled to β-Lactone

The β-lactone-amino acid conjugate (0.5 mmol) was dissolved in 0.8 mL of DCM and 0.8 mL of trifluoroacetic acid (9.2 mmol) was added to the solution. After completion of the reaction (usually less than 1 hour), solvent was removed *in vacuo* and the residue co-evaporated with toluene and diethyl ether three times. The crude amine salt was further purified by trituration from EtOAc : Et_2O or pentane.

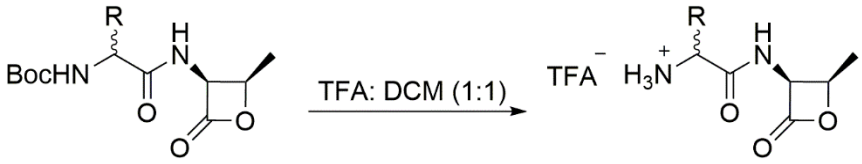

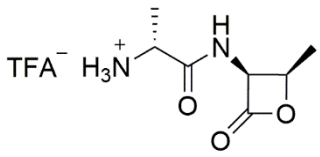

5b: Yield = 32%, ^{1}H NMR (500 MHz, CD_3CN): δ 1.40 (d, *J* = 6.5 Hz, 3H), 1.50 (d, *J* = 7.0 Hz, 3H), 4.16 (q, *J* = 7.0 Hz, 1H), 4.84-4.89 (m, 1H), 5.50-5.53 (m, 1H), 7.83 (br, 3H), 8.24 (s, 1H); HRMS-ESI: calc for $C_7H_{13}N_2O_3$+ $(M + H)^+$ 173.0921, found 173.0941.

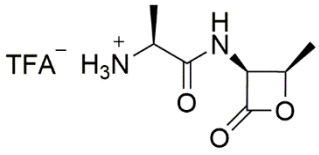

6b: Yield = 35%, ^{1}H NMR (500 MHz, CD_3CN): δ 1.39 (d, *J* = 6.5 Hz, 3H), 1.51 (d, *J* = 7.0, 3H), 4.13 (q, *J* = 7.2 Hz, 1H), 4.85-4.92 (m, 1H), 5.43-5.49 (m, 1H), 7.57 (br, 3H), 7.98 (s, NH); HRMS-ESI: calc for $C_7H_{13}N_2O_3$+ $(M + H)^+$ 173.0921, found 173.0915.

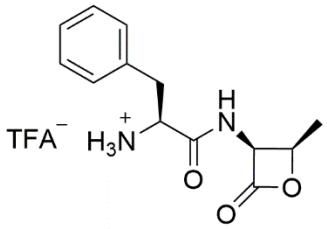

7b: Yield = ~100%, ^{1}H NMR (CD_3CN, 300 MHz): δ = 1.35 (d, *J* = 6.2 Hz, 3H), 3.12-3.23 (m, , 2H), 4.25-4.29 (m, 1H), 4.84 (app. quin, *J* = 6.2 Hz, 1H), 5.44-5.49 (m, 1H), 7.29-7.40 (m, 5H)**,** 8.12 (d, *J* = 7.0, 1H); HRMS-ESI: calc for $C_{13}H_{17}N_2O_3^+$ (M + H)$^+$ 249.1234, found 249.1252.

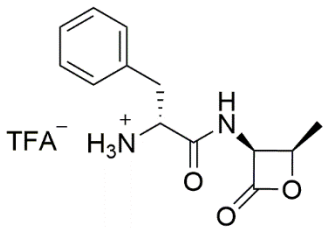

8b: Yield = ~100%, ^{1}H NMR (CD_3CN, 300 MHz): δ = 1.19 (d, *J* = 6.6 Hz, 3H), 3.18-3.21 (m, 2H), 4.26-4.31 (m, 1H), 4.79 (app. quin, *J* = 6.4 Hz, 1H), 5.47-5.52 (m, 1H), 7.30-7.41 (m, 5H), 8.04 (d, *J* = 7.7, 1H); HRMS-ESI: calc for $C_{13}H_{17}N_2O_3^+$ (M + H)$^+$ 249.1234, found 249.1252.

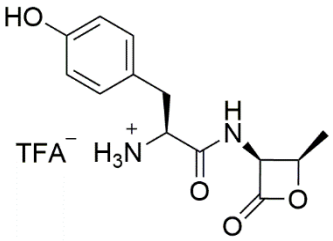

9b: Yield = 48%, ^{1}H NMR (500 MHz, CD_3CN): δ 1.38 (d, *J* = 6.0 Hz, 3H), 2.10 (br, 3H), 3.02-3.08 (m, 1H), 3.14-3.19 (m, 1H), 4.16-4.20 (m, 1H), 4.86 (app. quin, *J* = 6.0 Hz, 1H), 5.46-5.49 (m, 1H), 6.80 (d, J = 8 Hz, 2H), 7.13 (d, *J* = 8.5 Hz, 2H), 7.90-8.05 (br, 1H); HRMS-ESI: calc for $C_{13}H_{17}N_2O_4^+$ $(M + H)^+$ 265.1183, found 265.1179.

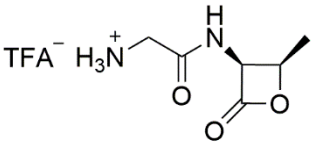

10b: Semi-purified material was carried into the next step. Crude ^{1}H NMR (500 MHz, CD_3CN): δ 1.44 (d, *J* = 6.5 Hz, 3H), 2.10 (s, 2H), 4.93 (app. quin, *J* = 6.5 Hz, 1H), 5.63-5.70 (m, 1H); HRMS-ESI: calc for $C_6H_{11}N_2O_3^+$ $(M + H)^+$ 159.0764, found 159.0758.

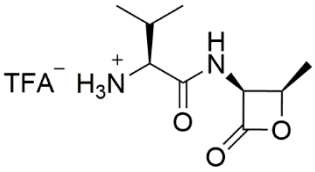

11b: Yield = 96%, ^{1}H NMR (500 MHz, CD_3CN): δ 1.04 (dd, *J* = 8.5, 7.0 Hz, 3H), 1.40 (d, *J* = 6.0 Hz, 3H), 2.23-2.27 (m, 1H), 3.94 (d, *J* = 5.0 Hz, 1H), 4.88 (app. quin, *J* = 6.3 Hz, 1H), 5.43-5.49 (dd, *J* = 8.5, 6.10 Hz, 1H), 7.67 (br, 3H), 8.09 (d, *J* = 8.5 Hz, 1H); HRMS-ESI: calc for $C_9H_{17}N_2O_3^+$ $(M + H)^+$ 201.1234, found 201.1231.

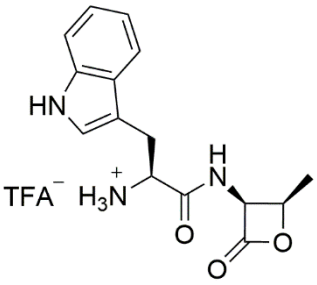

12b: Yield = 49.5%, ^{1}H NMR (500 MHz, CD_3CN): δ 1.36 (d, *J* = 6.5 Hz, 3H), 2.28 (br, 3H), 3.34-3.42 (m, 2H), 4.30-4.32 (m, 1H), 4.85 (app. quin, *J* = 6.2 Hz, 1H), 5.47-5.50 (m, 1H), 7.10 (t, *J* = 7.5 Hz, 1H), 7.18 (t, *J* = 7.5 Hz, 1H), 7.27 (d, *J* = 2.5, 2H), 7.44 (d, *J* = 8.5 Hz, 1H), 7.68 (d, *J* = 8.0 Hz, 1H), 8.19 (d, *J* = 7.5 Hz, NH), 9.37 (s, 1H); HRMS-ESI: calc for $C_{15}H_{18}N_3O_3^+$ $(M + H)^+$ 288.1343, found 288.1324.

4.10.11.5. Coupling of the Amino Acid-β-Lactone-Conjugates to TAMRA or BODIPY

To a solution of the β-lactone amine salt (**5**b-**12**b) (0.008 mmol) in DMF (0.2 mL) at room temperature was added DIEA (0.009 mmol, 1.55 µL, 1.1 equiv) and fluorophore (0.008 mmol, 1 equiv). Once the reaction was completed (hours to days according to HPLC analysis), the solvent was evaporated and residue was purified by HPLC using the above-described conditions.

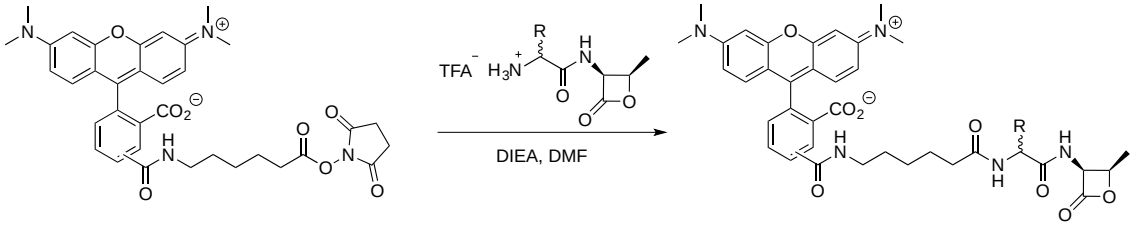

1T-**9**T

2T: Yield = 48%, ^{1}H NMR ($(CD_3)_2CO$, 500 MHz): δ 1.40 (d, *J* = 6.5 Hz, 3H), 1.40-1.52 (m, 2H), 1.61-1.73 (m, 4H), 2.30 (m, 2H), 3.0 (s, 12H), 3.46-3.53 (m, 2H), 4.88 (app. quin, *J* = 6.3 Hz, 1H), 5.66-5.69 (m, 1H), 6.50-6.53 (m, 4H), 6.60 (d, *J* = 8.5 Hz, 2H), 7.11 (d, *J* = 8.0 Hz, 0.5H), 7.31 (d, *J* = 7.5 Hz, 1H), 7.67 (d, *J* = 8.0 Hz, 0.5H), 8.20-8.23 (m, 2H), 8.29 (dt, *J* = 8.0, 1.7 Hz, 1H), 8.42 (d, *J* = 4.5 Hz, 1H), HRMS-ESI: calc for $C_{35}H_{39}N_4O_7^+$ $(M + H)^+$ 627.2813, found 627.2989.

3T: Yield = 5%, ^{1}H NMR (CD_3OD, 500 MHz): δ = 1.39 (d, *J* = 6.5 Hz, 3H), 1.45-1.51 (m, 2H), 1.70-1.74 (m, 4H), 2.34 (t, *J* = 7.3 Hz, 2H), 3.29 (s, 12H), 3.45 (t, *J* = 7.0 Hz, 2H), 4.85 (app. quin, *J* = 6.3 Hz, 1H), 5.55 (d, *J* = 6.0 Hz, 1H), 6.94 (d, *J* = 2.0 Hz, 2H), 7.02 (dd, *J* = 9.5, 2.2 Hz, 2H), 7.24 (d, J = 9.0 Hz, 2H), 7.38 (d, *J* = 7.5 Hz, 1H), 8.06 (dd, *J* = 7.0, 2.0 Hz, 1H), 8.34 (br, 1H), 8.53 (d, *J* =1.5 Hz, 1H). HRMS-ESI: calc for $C_{35}H_{39}N_4O_7^+$ $(M + H)^+$ 627.2813, found 627.2810.

5T: Yield = 14%, ^{1}H NMR (500 MHz, CD_3CN): δ 1.28 (d, *J* = 7.5 Hz, 3H), 1.33 (d, *J* = 6.0 Hz, 3H), 1.38-1.44 (m, 2H), 1.60-1.65 (m, 4H), 2.22 (t, *J* = 7.5 Hz, 2H), 2.99 (s, 12H), 3.38-3.44 (m, 2H), 4.28-4.34 (m, 1H), 4.79 (app. quin, J = 6.3 Hz, 1H), 5.42-5.45 (m, 1H), 6.49-6.54 (m, 4H), 6.61-6.65 (m, 2H), 6.72-6.75 (br, 1H), 7.24 (d, *J* = 8.0 Hz, 1H), 7.38 (br, 1H), 7.48 (d, *J* = 7.5 Hz, 1H), 8.06-8.14 (m, 1H), 8.34-8.37 (m, 1H); HRMS-ESI: calc for $C_{38}H_{44}N_5O_8^+$ $(M + H)^+$ 698.3184, found 698.2365.

6T: Reaction time of 48 h Yield = 16%, ^{1}H NMR (500 MHz, CD_3CN): δ 1.28 (d, *J* = 7.0 Hz, 3H), 1.35 (d, *J* = 6.5 Hz, 3H), 1.38-1.42 (m, 2H), 1.61-1.65 (m, 4H), 2.20-2.23 (m, 2H), 3.08 (s, 12H), 3.38-3.43 (m, 2H), 4.31-4.34 (m, 1H), 4.80-4.83 (m, 1H), 5.38 (d, *J* = 6.0 Hz, 1H), 6.65-6.73 (m, 4H), 6.85 (d, *J* = 9.1 Hz, 2H), 7.25 (d, *J* = 8.0 Hz, 1H), 8.09 (d, *J* = 7.5 Hz, 1H), 8.42 (s, 1H), HRMS-ESI: calc for $C_{38}H_{44}N_5O_8^+$ $(M + H)^+$ 698.3184, found 698.3241.

7T: Yield = 17%, ^{1}H NMR (500 MHz, CD_3CN): δ = 1.34 (d, *J* = 6.0 Hz, 3H), 1.40-1.56 (m, 6H), 2.86-2.88 (m, 1H), 2.99 (s, 12H), 3.14-3.17 (m, 1H), 3.35-3.38 (q, *J* = 6.5 Hz, 2H), 4.63-4.68 (m, 1H), 4.80 (app. quin, *J* = 6.3 Hz, 1H), 5.39-5.43 (m, 1H), 6.49 (d, *J* = 8.5 Hz, 2H), 6.52 (d, *J* = 2.5 Hz, 4H), 6.62 (d, *J* = 9.0 Hz, 2H), 6.72 (d, *J* = 8.5 Hz, NH), 7.22-7.28 (m, 5H), 7.35 (m, 1H), 7.53 (d, *J* = 8.5 Hz, NH), 8.06 (s, 1H), 8.15 (d, *J* = 8.0 Hz, 1H), 8.39 (s, 1H); HRMS-ESI: calc for $C_{44}H_{48}N_5O_8^+$ $(M + H)^+$ 774.3497, found 774.3462.

8T: Yield = 9%, ^{1}H NMR (500 MHz, CD_3OD): δ = 1.14 (d, *J* = 6.5 Hz, 3H), 1.28-1.34 (m, 2H), 1.58-1.64 (m, 4H), 2.15 (s, 12H), 2.23 (t, *J* = 7.5 Hz, 1H), 2.90 (dd, *J* = 13.5, 8.5 Hz, 1H), 3.1 (dd, *J* = 13.5, 7 Hz, 1H), 3.42 (t, *J* = 7.0 Hz, 2H), 4.69-4.75 (m, 2H), 5.47 (d, *J* =

6Hz, 1H), 6.94 (d, *J* = 2.0 Hz, 2H), 7.01-7.03 (m, 2H), 7.24-7.28 (m, 7H), 7.37 (d, J = 8.0 Hz, 1H), 8.06 (d, *J* = 8.0 Hz, 1H), 8.53 (s, 1H); HRMS-ESI: calc for $C_{44}H_{48}N_5O_8^+$ $(M + H)^+$ 774.3497, found 774.6817.

9T: Reaction time of 3 days; Yield = 15%, ^{1}H NMR (500 MHz, CD_3CN): δ 1.35 (d, *J* = 6.5 Hz, 3H), 1.53-1.56 (m, 4H), 1.62-1.65 (m, 2H), 2.99 (s, 12H), 2.73-3.79 (m, 1H), 3.03-3.07 (m, 1H), 3.34-3.38 (m, 2H), 4.57-4.61 (m, 1H), 4.80 (app. quin, *J* = 6.3 Hz, 1H), 5.40-5.43 (m, 1H), 6.48-6.52 (m, 3H), 6.61-6.66 (m, 2H), 6.72 (d, *J* = 8.5 Hz, 2H), 7.05 (d, *J* = 8.0 Hz, 2H), 7.27 (d, *J* = 8.0 Hz, 1H), 7.42 (br, 1H), 7.50-7.53 (m, 1H), 8.11(s, 1H), 8.15-8.18 (m, 2H), 8.39 (s, 1H); HRMS-ESI: calc for $C_{44}H_{48}N_5O_9^+$ $(M + H)^+$ 790.3447, found 790.3478.

10T: Reaction time of 4 days. Yield = 48%, ^{1}H NMR (500 MHz, CD_3CN): δ 1.35 (d, *J* = 6.5 Hz, 3H), 1.41-1.44 (m, 2H), 1.62-1.66 (m, 4H), 2.24-2.26 (m, 2H), 2.99 (s, 12H), 3.39-3.43 (m, 2H), 3.82 (d, *J* = 5.5 Hz, 2H), 4.81 (app. quin, *J* = 6.3 Hz, 1H), 5.44-5.47 (m, 1H), 6.49-6.53 (m, 4H), 6.63 (d, *J* = 8.5 Hz, 2H), 6.80 (br, 1H), 7.25 (d, *J* = 8.0 Hz, 1H), 7.34-7.40 (br, 2H), 8.14 (d, *J* = 8.0 Hz, 1H), 8.36 (s, 1H), HRMS-ESI: calc for $C_{37}H_{42}N_5O_8^+$ $(M + H)^+$ 684.3028, found 684.3051.

11T: Reaction time of 2 days; Yield = 1%, ^{1}H NMR (500 MHz, DMSO-d_6): δ 0.78-0.84 (m, 6H), 1.31 (d, *J* = 6.0 Hz, 3H), 1.51-1.55 (m, 6H), 1.92-1.97 (m, 1H), 2.07-2.20 (m, 2H), 2.92 (s, 12H), 3.35-3.40 (m, 2H), 4.13-4.16 (m, 1H), 4.81-4.84 (m, 1H), 5.49-5.52 (m, 1H), 6.45-6.59 (m, 4H), 6.73 (br, 1H), 7.26 (d, *J* = 8.0 Hz, 1H), 7.92 (d, *J* = 8.5 Hz, 1H), 8.20

(d, *J* = 8.0, 1H), 8.42 (s, 1H), 8.76-8.80 (m, 1H), 8.86 (d, *J* = 8.5 Hz, 1H); 9.31 (br, 1H). HRMS-ESI: calc for $C_{40}H_{48}N_5O_8^+$ $(M + H)^+$ 726.3497, found 726.3449.

12T: Reaction time of 7 days; Yield = 17%, ^{1}H NMR (500 MHz, DMSO-d_6): δ 1.25 (d, *J* = 7.0 Hz, 3H), 1.43-1.46 (m, 2H), 1.57-1.660 (m, 2H), 1.61-1.67 (m, 2H), 1.97-2.01 (m, 2H), 2.06-2.08 (m, 1H), 2.68 (t, *J* = 7.5 Hz, 2H), 2.92 (s, 12H), 3.45 (m, 2H), 4.53-4.56 (m, 1H), 4.80-4.83 (m, 1H), 5.30-5.33 (m, 1H), 5.47-5.51 (m, 1H), 6.29 (m, 1H), 6.45-6.51 (m, 4H), 6.60-6.64 (m, 1H), 7.11-7.19 (m, 2H), 7.28-7.31 (m, 2H), 8.20 (d, *J* = 8.0 Hz, 1H), 8.24 (s, 1H), 8.42 (s, 1H), 8.76-8.81 (m, 1H), 8.95-8.97 (d, *J* = 8.5 Hz, 1H), 10.81 (s, 1H); HRMS-ESI: calc for $C_{46}H_{49}N_6O_8^+$ $(M + H)^+$ 813.3606, found 813.3575.

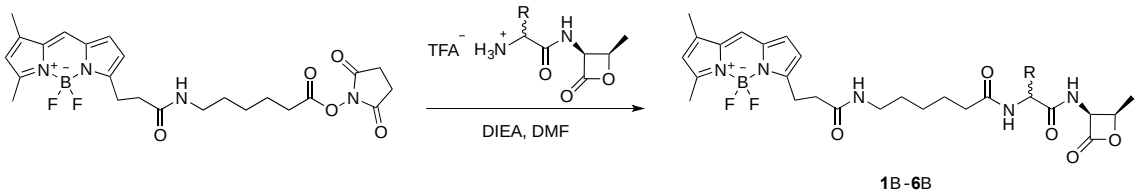

1B-**6B**

2B: Reaction time of 7 days. Yield = 10%, ^{1}H NMR (CD_3CN, 500 MHz): δ 1.28-1.32 (m, 2H), 1.36 (d, *J* = 6.0 Hz, 3H), 1.45 (quin, *J* = 7.3 Hz, 2H), 1.58 (quin, *J* = 7.5 Hz, 2H), 1.97 (t, *J* = 7.5 Hz, 2H), 2.27 (s, 3H), 2.51 (s, 3H), 3.11-3.16 (m, 4H), 4.81 (app. quin, *J* = 6.3 Hz, 1H), 5.45-5.48 (m, 1H), 6.23 (s, 1H), 6.32 (d, *J* = 4.0 Hz, 1H), 6.41 (br, NH), 7.02 (d, *J*=4.0 Hz, 1H), 7.09 (br, NH), 7.33 (br, NH), 7.38 (s 1H). HRMS-ESI: calc for $C_{24}H_{32}BF_2N_4O_4^+$ $(M + H)^+$ 489.2479, found 489.2487.

3B ((S,R)Lactone-BODIPY FL): Reaction time of 44 hrs. Yield = 25%, ^{1}H NMR (CD_2Cl_2, 500 MHz): δ = 1.28-1.34 (m, 2H), 1.43 (d, *J* = 6.0 Hz, 3H), 1.45-1.50 (m, 2H), 1.60-1.70 (m, 2H), 2.24-2.27 (m, 2H), 2.28 (s, 3H), 2.55 (s, 3H), 2.60 (t, *J* = 7.5 Hz, 2H), 3.19-3.25

(m, 4H), 4.87 (app. quin, *J* = 6.3 Hz), 5.54-5.56 (m, 1H), 5.83 (br, 1H), 6.18 (s, 1H), 6.32 (d, *J* = 4.0 Hz, 1H), 6.58 (d, *J* = 8.0 Hz, 1H), 6.95 (d, J = 4.0 Hz, 1H), 7.17 (s, 1H), HRMS-ESI calc for $C_{24}H_{31}BF_2N_4O_4^+$ $(M+H)^+$ 489.2414, found 489.2478.

5B: Reaction time of 5 days Yield = 11%, ^{1}H NMR (500 MHz, CD_3CN): δ 1.30 (d, *J* = 7.5 Hz, 3H), 1.29-1.31 (m, 2H) 1.34 (d, *J* = 6.5 Hz, 3H), 1.45 (quin, *J* = 7.5 Hz, 2H), 1.57 (quin, *J* = 7.5 Hz, 2H), 2.16 (t, *J* = 7.5 Hz, 2H), 2.27 (s, 3H), 2.52 (s, 3H), 2.50-2.53 (m, 2H), 3.12-3.17 (m, 4H), 4.27 (app. quin, *J* = 7.0 Hz, 1H), 4.80 (app. quin., *J* = 6.3 Hz, 1H), 5.42-5.45 (m 1H), 6.23 (s, 1H), 6.32 (d, *J* = 4.0 Hz, 1H), 6.44 (br, NH), 6.67 (d, *J* = 6.5 Hz, NH), 7.02 (d, *J* = 4.0 Hz, 1H), 7.38 (s, 1H), 7.39-7.42 (br, NH); HRMS-ESI: calc for $C_{27}H_{36}BF_2N_5NaO_5^+$ $(M + Na)^+$ 582.2670, found 582.2685.

6-B: Reaction time of 150 h Yield = 22%, ^{1}H NMR (500 MHz, CD_3CN): δ 1.29 (d, *J* = 7.0 Hz, 3H), 1.28-1.32 (m, 2H) 1.36 (d, *J* = 6.0 Hz, 3H), 1.41-1.476 (quin, *J*=7.5 Hz, 2H), 1.53-1.58 (quin, *J* = 7.5 Hz, 2H), 2.17-2.21 (m, 2H), 2.27 (s, 3H), 2.51 (s, 3H), 2.50-2.52 (m, 2H), 3.11-3.17 (m, 4H), 4.29 (app. quin, *J* = 7.0 Hz 1H), 4.80 (app. quin., *J* = 6.5 Hz, 1H), 5.39-5.42 (m, 1H), 6.23 (s, 1H), 6.32 (d, *J* = 3.5 Hz, 1H), 6.45 (br, NH), 6.68 (br, NH), 7.01 (d, *J* = 3.5 Hz, 1H), 7.39 (s, 1H), 7.43 (br, NH); HRMS-ESI: calc for $C_{27}H_{36}BF_2N_5NaO_5^+$ (M + Na)$^+$ 582.2670, found 582.2631.

7-B: Reaction time of 42 hrs. Yield = 32%, ^{1}H NMR (acetone-d_6, 500 MHz): δ = 1.19-1.22 (m, 2H), 1.39 (d, *J* = 6.5 Hz, 3H), 1.42-1.46 (m, 4H), 1.51 (quin, *J* = 7.5 Hz, 2H), 2.30 (s, 3H), 2.52 (s, 3H), 2.57 (t, *J* = 6.5 Hz, 2H), 3.13-3.23 (m, 5H), 4.70-4.72 (m, 1H), 4.87 (app. quin, *J* = 6.3 Hz, 1H), 5.59-5.62(m, 1H), 6.26 (s, 1H), 6.37 (d, *J* = 4.0 Hz, 1H), 7.05 (d, *J* =

4.0 Hz, 1H), 7.09 (br, NH), 7.19-7.28 (m, 6H), 7.53 (s, 1H), 8.23 (d, *J* = 8.0, NH), HRMS-ESI: calc for $C_{33}H_{41}BF_2N_5O_5^+$ $(M + H)^+$ 636.3163, found 636.3029.

8-B: Reaction time of 2 days. Yield = 32%, ^{1}H NMR (acetone-d_6, 500 MHz): δ = 1.25 (d, *J* = 6.5 Hz, 3H), 1.42-1.46 (m, 4H), 1.51 (quin, *J* = 7.5 Hz, 2H), 2.30 (s, 3H), 2.52 (s, 3H), 2.57 (t, *J* = 6.5 Hz, 2H), 2.91 (dd, *J* = 14.0, 9.0 Hz, 2H), 3.12-3.23 (m, 6H), 4.70-4.75 (m, 1H), 4.83 (app. quin, *J* = 6.3 Hz, 1H), 5.62-5.65 (dd, *J* = 8.5, 6.1 Hz, 1H), 6.26 (s, 1H), 6.37 (d, *J* = 4.0 Hz, 1H), 7.05 (d, *J* = 4.0 Hz, 1H), 7.09 (br, NH), 7.19-7.28 (m, 6H), 7.53 (s, 1H), 8.23 (d, *J* = 8.0, NH), HRMS-ESI: calc for $C_{33}H_{41}BF_2N_5O_5^+$ $(M + H)^+$ 636.3163, found 636.3120.

10-B: Reaction time of 5 days. Yield = 12%, ^{1}H NMR (500 MHz, CD_3CN): δ 1.30-1.33 (m, 2H), 1.36 (d, *J* = 6.0 Hz, 3H), 1.45 (quin, *J* = 7.3 Hz, 2H), 1.58 (quin, *J* = 7.5 Hz, 2H), 2.19 (t, *J* = 7.5 Hz, 2H), 2.21 (s, 3H), 2.51-2.55 (m, 6H), 3.16 (m, 4H), 3.80-3.82 (m, 2H), 4.80-4.84 (m, 1H), 5.45-5.50 (m, 1H), 6.24 (d, *J* = 6.5 Hz, 1H), 6.34 (s, 1H), 6.44 (br, NH), 6.72 (br, NH), 7.02 (s, 1H), 7.33(br, NH), 7.39 (d, *J* = 7.5 Hz, 1H), HRMS-ESI: calc for $C_{26}H_{34}BF_2N_5NaO_5^+$ $(M + Na)^+$ 568.2513, found 568.2497.

4.10.11.6. Coupling of Amino Acid-β-Lactone-Conjugates to Fluorescein (2FL, 5FL-7FL, 9FL)

To a solution of 6-[fluorescein-5(6)-carboxamido]hexanoic acid (0.008 mmol, 3.9 mg, 1 equiv), COMU (0.009 mmol, 3.8 mg, 1.1 equiv) in DMF (0.2 mL) at 0 °C, DIEA (0.009, 1.55 µL, 1.1 equiv) was added in a dry 1 dram vial. After stirring for 15 min, a pre-mixture of lactone (0.008 mmol, 1 equiv) and DIEA (0.009, 1.55 µL, 1.1 equiv) in DMF (0.1 mL) was added through syringe to the reaction vial. Once the reaction was completed

(hours to days according to HPLC analysis), the solvent was evaporated and residue purified by HPLC.

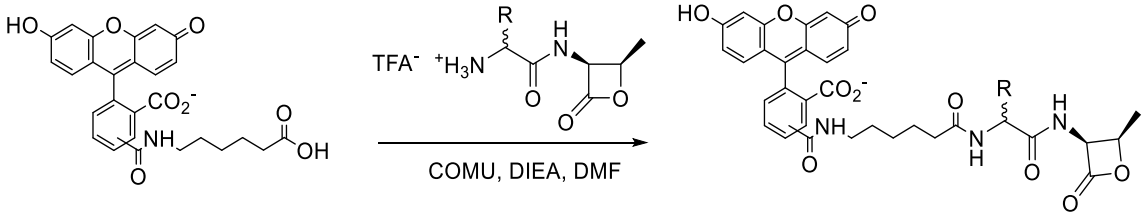

5-FL: Reaction time of 3 days. Yield = 10%, ^{1}H NMR (500 MHz, CD_3CN): δ 1.29 (d, *J* = 6.7 Hz, 3H), 1.33 (d, *J* = 6.4 Hz, 3H), 1.38-1.45 (m, 2H), 1.50-1.59 (m, 2H), 1.60-1.66 (m, 2H), 2.30 (t, *J* = 7.4 Hz, 2H), 3.39-3.42 (m, 2H), 4.28-4.32 (m, 1H), 4.79 (app. quin, *J* = 6.0 Hz, 1H), 5.40-5.45 (m, 1H), 6.57 (dt, *J* = 8.6, 3.0 Hz, 2H), 6.65-6.68 (m, 2H), 6.72 (t, *J* = 2.3 Hz, 2H), 7.28 (d, *J* =8.1 Hz, 1H), 7.38-7.42 (m, 1H), 7.53 (s, 1H), 8.01-8.05 (m, 1H), 8.14 (t, J= 1H), 8.35 (d, *J* =13.0Hz, 1H); HRMS-ESI: calc for $C_{34}H_{34}N_3O_{10}^+$ $(M + H)^+$ 644.2239, found 644.2231.

6-FL: Reaction time of 64 hrs. Yield = 10%, ^{1}H NMR (500 MHz, DMSO-d_6): δ 1.16-1.20 (m, 2H), 1.27 (d, *J* = 7.5 Hz, 3H), 1.30 (d, *J* = 6.5 Hz, 3H), 1.42-1.45 (m, 2H), 1.51-1.54 (m, 2H), 2.21 (t, *J* = 7.3 Hz, 2H), 3.15-3.16 (m, 2H), 4.21-4.26 (m, 1H), 4.82 (app. quin, *J* =6.0 Hz, 1H), 5.46-5.54 (m, 1H), 6.54-6.58 (m, 4H), 6.65-6.79 (m, 2H), 7.35 (d, *J* = 8.0, 1H), 7.65 (s, 1H), 8.06 (d, *J* = 7.5 Hz, 1H), 8.15 (d, *J* = 8.0 Hz, 1H), 8.22 (d, *J* = 8.0, 1H), 8.44 (s, 1H), 8.65-8.67 (m, 1H), 8.79-8.83 (m, 1H), 10.18 (br, 2H); HRMS-ESI: calc for $C_{34}H_{34}N_3O_{10}^+$ $(M + H)^+$ 644.2239, found 644.2196.

7-FL: Reaction time of 22hrs. Yield = 15%, ^{1}H NMR (CD_3OD, 500 MHz): δ = 1.36 (d, J = 6.3 Hz, 3H), 1.46-1.51(m, 2H), 1.54-1.62 (m, 4H), 2.12-2.25 (m, 2H), 2.86-2.92 (m, 1H),

3.11-3.17 (m, 2H), 3.39 (t, *J* =7.0 Hz, 2H), 4.61-4.66 (m, 1H), 5.45 (dd, *J* =12.7, 5.9Hz, 1H), 6.54-6.59 (m, 2H), 6.69-6.72 (m, 4H), 7.16-7.32 (m, 5H), 7.62 (s, 1H), 8.08-8.16 (m, 2H), 8.43 (s, 1H), 8.51 (s, 1H) . HRMS-ESI: calc for $C_{40}H_{38}N_3O_{10}^+$ $(M + Na)^+$ 720.2566, found 720.2552.

8-FL: Reaction time of 1 day. Yield = 15%, ^{1}H NMR (CD_3OD, 500 MHz): δ = 1.36 (d, *J* = 6.3 Hz, 3H), 1.46-1.51 (m, 2H), 1.54-1.61 (m, 4H), 2.13 (t, *J* =7.2 Hz, 1H), 2.20 (t, *J*=7.2 Hz, 1H), 2.86-2.89 (m, 1H), 3.09-3.13 (m, 2H), 3.39 (t, *J* =7.0 Hz, 2H), 5.42-5.46 (m, 1H), 6.61 (t, *J* =9.5 Hz, 2H), 6.70 (s, 2H), 6.82-6.90(m, 2H), 7.18-7.32 (m, 5H), 7.64 (s, 1H), 8.09-8.12 (m, 1H), 8.44 (s, 1H), 8.53 (s, 1H). HRMS-ESI: calc for $C_{40}H_{38}N_3O_{10}^+$ $(M + Na)^+$ 720.2566, found 720.2559.

9-FL: Reaction time of 1 day; Yield = 6%, ^{1}H NMR (500 MHz, DMSO-d_6): δ 1.20 -1.30 (m, 9H), 1.97 -2.05 (m, 2H), 2.14-2.19 (m, 2H), 3.03-3.13 (m, 2H), 3.53-3.61 (m, 2H) 4.20-4.27 (m, 1H), 4.80 (app. q, *J* = 7.0 Hz, 1H), 5.43-5.48 (m, 1H) 6.50-6.68 (m, 8H), 6.98-7.02 (m, 2H), 7.34 (d, *J* = 8.5 Hz, 0.5H), 7.65 (s, 0.5H), 8.01-8.22 (m, 3H), 8.64 (br, 1H), 8.70-8.79 (m, 1H), 8.86-8.91(m, 1H), 9.4-8.16(m, 1H), 10.15 (br, 2H); HRMS-ESI: calc for $C_{42}H_{39}N_4O_{10}^+$ $(M + H)^+$ 759.2661, found 759.2631.

CHAPTER 5

ENRICHMENT OF PBP-PROTEIN COMPLEXES

5. Enrichment of PBP-Protein Complexes

Chemical probes are small molecules with physiologically favorable physicochemical properties and well-defined activity in the biological systems. As such, chemical probes have become an invaluable tool for probing fundamental biological and physiological phenomena and are complementary to genetic manipulation approaches.(31, 189, 208) Chemical proteomics refers to a methodology in which the use of chemical probes is coupled to mass spectrometry, also known as MS-based proteomics, which can provide functional information about the proteome such as profiling the activity of single proteins or protein families, as well as posttranslational modifications (PTMs).(31, 58, 209) Chemical reporters can be incorporated into the proteome through metabolism, or by reacting the proteome with small molecule probes. In the latter approach, the small molecule probe can be applied to cell lysates, whole cells or an organism, followed by proteome analysis to assess the system perturbations. However, the large dynamic range and complexity of an entire cellular proteome limits the detection of low abundance proteins.

Enrichment is a technique by which proteins of a particular type in a biological sample are concentrated for further analysis and identification. Enrichment is used to help concentrate low-abundance proteins to improve their downstream analysis.(210) As such, affinity chromatography methods where tagged proteins are immobilized on beads through specific groups installed on the probe, have been developed to improve in-depth analysis. Activity-Based Protein Profiling (ABPP) exploits small molecule electrophilic probes that can covalently react with the active site of an enzyme, enabling installation of different reporter and affinity groups.(31)

Given the established potency of our chemical probes in selective targeting of the PBPs, we applied them to enrich PBPs from bacterial cells. We are specifically interested

in studying PBP2x, an essential transpeptidase in *Streptococcus pneumoniae*. The Click-MEM probe, which was initially developed to profile the activity of PBP3 in *Bacillus subtilis*, showed a remarkable ability to label PBP2x. Therefore, we developed a strategy to investigate PBP2x and its protein interactors using click-MEM. Probe validation was performed by enrichment of pure PBP2x protein, and then whole cell pulldown assays were performed.

5.1. Bacterial Cell Division Complex

Bacteria come in a range of shapes and volumes, properties that remain conserved in any given species. The shape, size and chaining of bacterial cells, which are fundamental characteristics that enable bacteria to survive and compete in their ecological niches, are largely determined by the resilient murein (peptidoglycan) sacculus that surrounds bacterial cells.(6, 211-213) This mesh-like structure is placed outside the plasma membrane and is composed of a polymeric glycan backbone crosslinked by short peptide groups. Biosynthesis of the PG is a highly dynamic process, requiring the concerted action of synthases to produce new PG material, and hydrolases to cleave the sacculus and insert new material. As such, the spatiotemporal regulation of the cell wall biosynthesis machinery is crucial to maintain healthy cells.(5, 213-215) Comprehensive research on bacterial cell division would not only shed light on this fundamental biological process, but also enable exploitation of cell division proteins as novel antibacterial targets. Thanks to advances in microscopy techniques as well as genetic manipulation methods, the field of bacterial physiology, and the cell division process in particular, has seen remarkable progress over the past few decades (For recent reviews see: (214-218)).

Bacterial cell division and peptidoglycan (PG) synthesis are coordinated by the synchronized dynamic movement of numerous proteins. Peptidoglycan biosynthesis starts in the cytoplasm, where soluble UDP-*N*-acetylglucosamine and UDP-*N*-

acetylmuramyl pentapeptide are synthesized, and subsequently anchored with undecaprenyl phosphate to form lipid II subunits, which are then flipped across the membrane. Once in the periplasmic space, the penicillin-binding proteins (PBPs) polymerize and crosslink the lipid II subunits to form PG chains (CHAPTER 1, **Fig. 1.2**).

Streptococcus pneumoniae (pneumococcus) is an ovoid Gram-positive bacteria that inhabits the human body, mainly the upper respiratory tract, both as a commensal organism and pathogen.(214, 219) Pneumococcus is a leading cause of both common mucosal infections, including otitis media and pneumonia, as well as systemic and more invasive diseases, such as sepsis and meningitis. *S. pneumoniae* continues to be a major cause of morbidity and mortality worldwide, especially in children under 5 years of age.(220, 221) Once curable by penicillins, pneumococcus has evolved resistance against these antibiotics, mediated by expression of mosaic PBP variants.(146, 222) The clinical significance of pneumococcal infections and the rise of moderate to high resistance to β-lactam antibiotics necessitates a deeper understanding of its physiology, and the cell wall biosynthesis machinery in particular, in order to develop effective antimicrobial drugs.

The PG synthesis machines of *S. pneumoniae* contain three class A bifunctional transglycosylase (TG) – transpeptidase (TP) PBPs (PPB1a, PPB1b and PBP2a), two class B monofunctional transpeptidases (TPs) (PBP2x and PBP2b), and one low-molecular-weight D,D-carboxypeptidase PBP (PBP3, also known as DacA).(10, 146, 214, 223, 224) Pneumococcal PBP2x and PBP2b are individually essential and are the homologues of essential PBP3 and PBP2 in *Escherichia coli*, which are involved in septal and lateral PG synthesis, respectively.(10, 191) Unlike the class B PBPs, class A PBPs are non-essential in *S. pneumoniae*. However, Δ*pbp1a* Δ*pbp2a* is synthetically lethal.(196, 223, 224) Evidence that PBP2x functions in septal PG synthesis was provided by multiple studies. Depletion of PBP2x in the *S. pneumoniae* laboratory strain R6 was reported to lead to the formation of enlarged, sometimes elongated, cells with oddly pointed

ends.(191) PBP2x has been shown to localize to septa of dividing *S. pneumoniae* cells using epitope tags or optimized GFP fusion constructs.(22, 23, 195) In addition, inhibition of PBP2x TP activity by methicillin or depletion of PBP2x also indicated that PBP2x migrates to the centers of the septa in mid-to-late divisional cells.(22) Lastly, as was described in CHAPTER 4, we developed a PBP2x-selective activity-based probe, **7FL**, which revealed that the activity of PBP2x concentrates to the division site (CHAPTER 4; **Fig. 4.11**), directly corroborating the findings from these previous experiments.(90)

Homolog-specific probes can aid in studying genetically essential proteins, such as PBP2x and PBP2b in *S. pneumoniae*.(90) Given the important role that PBP2x plays in septal PG synthesis and cell division, we sought to establish a chemical proteomic methodology to investigate its interactors in the cell division machinery. We envisioned that our probe toolkit comprised of β-lactone and β-lactam probes, as described in Chapter 3 and 4, positions us to do so. Indeed, β-lactams have previously been employed in affinity chromatography methods to enrich PBPs in different organisms.(112, 225, 226) Inspired by the strong and specific affinity of β-lactams for the PBPs, Dac-tag was designed based on the interaction between ampicillin, a penicillin, and PBP5, encoded by *dacA* gene in *E. coli*. Given the unique expression of PBPs in bacteria, Dac-tag is claimed to overcome the common limitations of conventional protein and peptide tag, yielding high protein purity at low expression levels in particular.(227) Although the latter example falls beyond the scope of this thesis research, it further demonstrates the unique potential of β-lactams in selective targeting of the PBPs.

To maintain its ovoid shape, *S. pneumoniae* uses peripheral and septal PG synthesis machinery to elongate and separate cells, known as the divisome and elangosome complexes, respectively. The composition, assembly, coordination and regulation of these two systems has been investigated by localization studies.(23, 196,

214, 228) As mentioned previously, we are interested in exploring the specific roles of individual PBPs in these processes, beyond the biochemical role that they play in the synthesis of PG. Historically, bacterial cell division machinery has been studied by genetic manipulations such as deletion and depletion strains, as well as conjugation of the protein of interest to peptide or protein tags.(23, 196, 215, 217, 218) The proposed chemical proteomic approach in this chapter will elaborate on the features of this system that cannot be directly understood via the existing methods, such as protein-protein interactions and the functional state of the PBPs.

5.2. Enrichment of Pneumococcal PBP2x as Proof-of-Concept

5.2.1. Probe Design and Validation

PBP2x is a HMW PBP that acts as a transpeptidase in *S. pneumoniae*. PBP2x is an essential PBP in *S. pneumoniae* with an established role in septal PG synthesis.(22, 23, 191) Mutations in the conserved motifs of PBP2x have been associated with β-lactam resistance; therefore, it is an important target for antibacterial agents.(192-194) In addition, PBP2x contains a C-terminal extension consisting of two PASTA (PBP And Serine/Threonine kinase Associated) domains, each of which possess one α-helix and three β-strands (**Fig. 5.1**).(192, 194, 229)

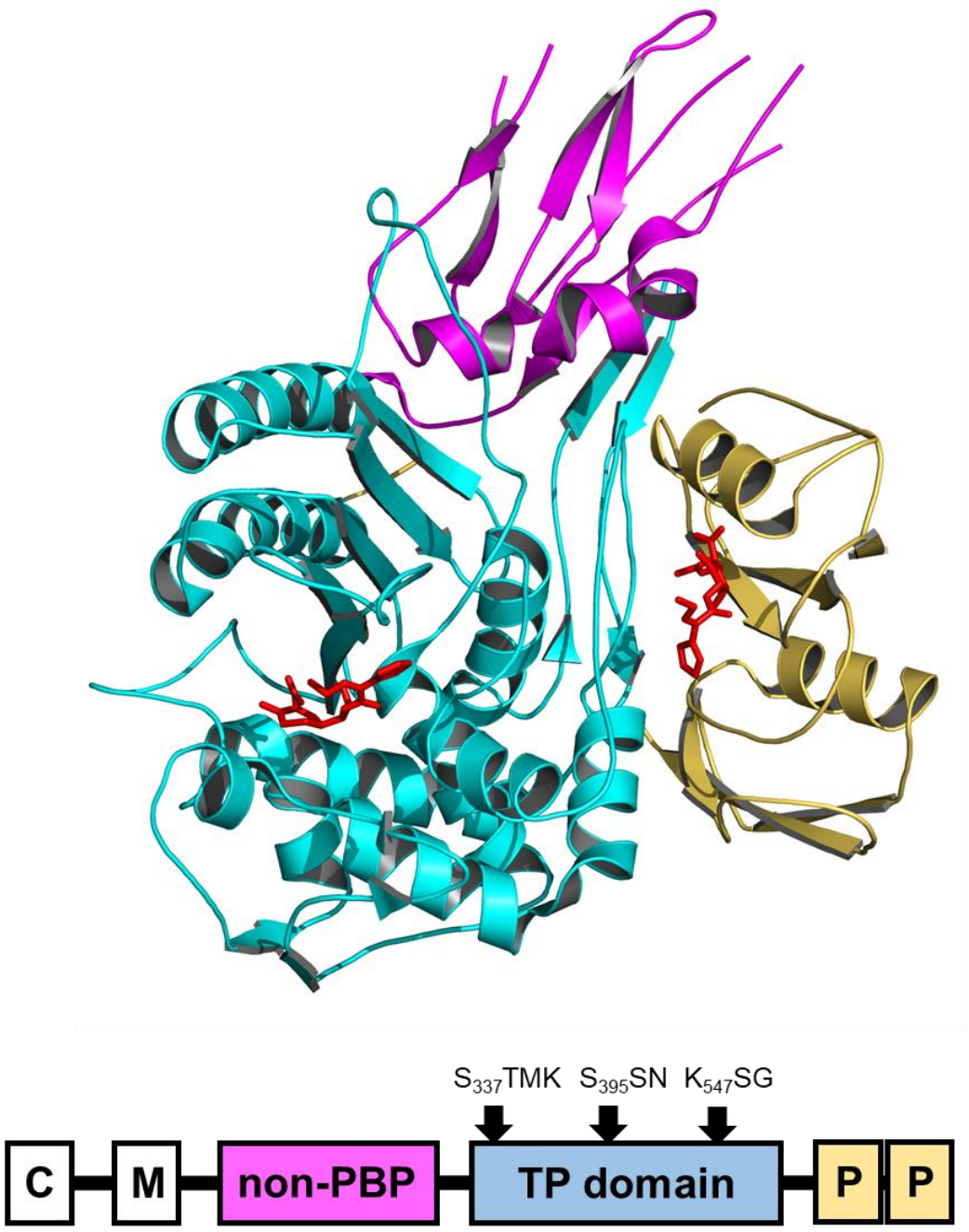

Figure 5.1. Sequence and 3D structure of PBP2x from *S. pneumoniae* strain R6. PBP2x consists of a cytoplasmic tail (C), a transmembrane anchor (M), an extracellular non-PBP binding N-terminal domain (non-PBP) that is implicated in PBP polymerization, a TP domain (TP) and a C-terminal extension consisting of two Penicillin-binding protein And Serine/Threonine kinase Associated (PASTA, P) domains.(190, 230) The crystal structure of a soluble form of PBP2x in complex with two cefuroxime molecules (shown in red), one bound to the active site and the other interacting with the PASTA domain (PDB code = 1QMF)(230). N-terminal, TP and C-terminal PASTA domains are shown in pink, blue and yellow, respectively.

Carbapenems are a subclass of β-lactam antibiotics that were derived from the natural product thienamycin.(231) Titration of *S. pneumoniae* D39 cells with a variety of β-lactams revealed that meropenem has a moderate affinity for PBP2x.(146) Although PBP2x was not the only target of meropenem, we sought to use our click-MEM probe for the enrichment of this essential protein in our proof-of-concept studies. Indeed, treatment of pneumococcal cells by the click-MEM probe revealed PBP2x as the main protein tagged by the probe, along with PBP1a and 3 to a lesser extent (**Fig. 5.2**). The observed labeling result was consistent with the PBP inhibition profile reported previously by our group.(146)

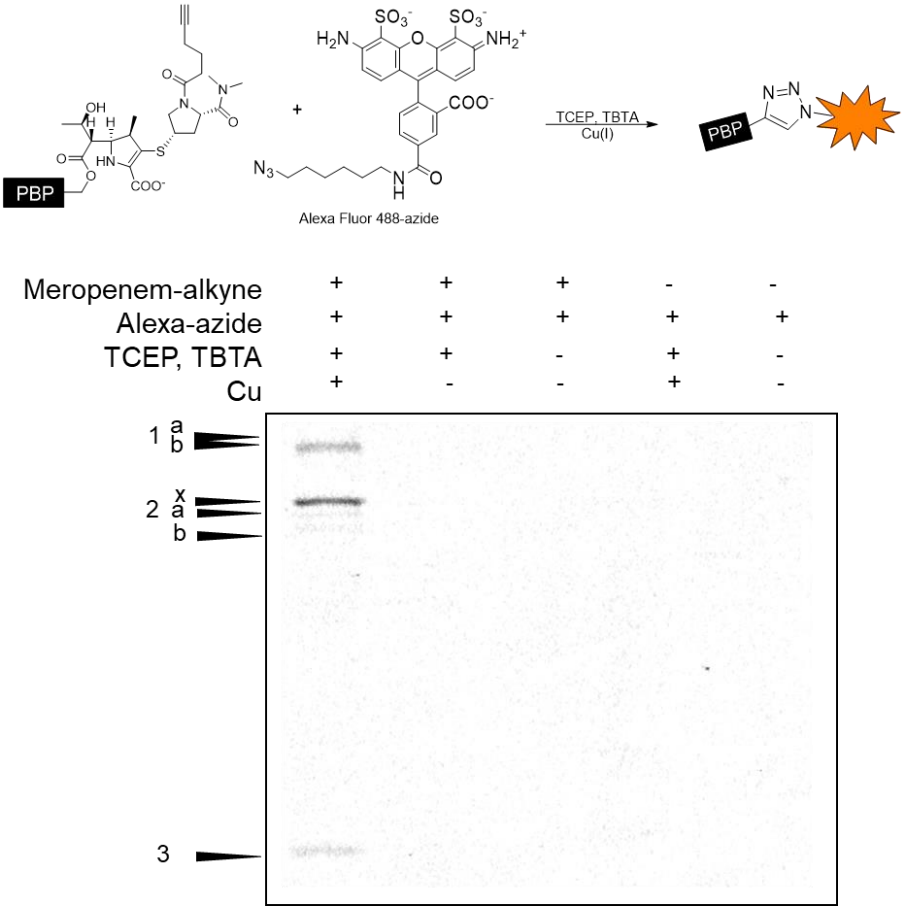

Figure 5.2. PBP labeling profile of click-MEM probe in *S. pneumoniae* D39 cells. Whole cells were treated with 10 μg/mL click-MEM for 30 mins. Click reaction with AlexaFluor488-azide was performed on membrane lysates for 1h. Labeling of PBP2x, along with PBP1a and 3 to a lesser extent, was observed only in the presence of all click reagents.

5.2.2. Enrichment of PBP2x* by Click-MEM

Upon the successful tagging of PBP2x and biorthogonal conjugation of the reporter group, we moved to the optimization of enrichment conditions starting with pure protein. A soluble recombinant PBP2x isoform, PBP2x*, as described in Chapter 4, was produced and utilized in our enrichment assays. Biotin is one of the most frequently used labels for affinity-based protein isolation. The extremely strong interaction between biotin and avidin is used for selective capture of biotinylated molecules. Our initial attempt to capture and release alkynylated PBP2x* through installation of a biotin group using Pierce avidin agarose beads was successful (**Figure 5.3**). However, when the same conditions were applied to the pneumococcal membrane proteome, PBP2x could not be enriched (**Figure 5.3**).

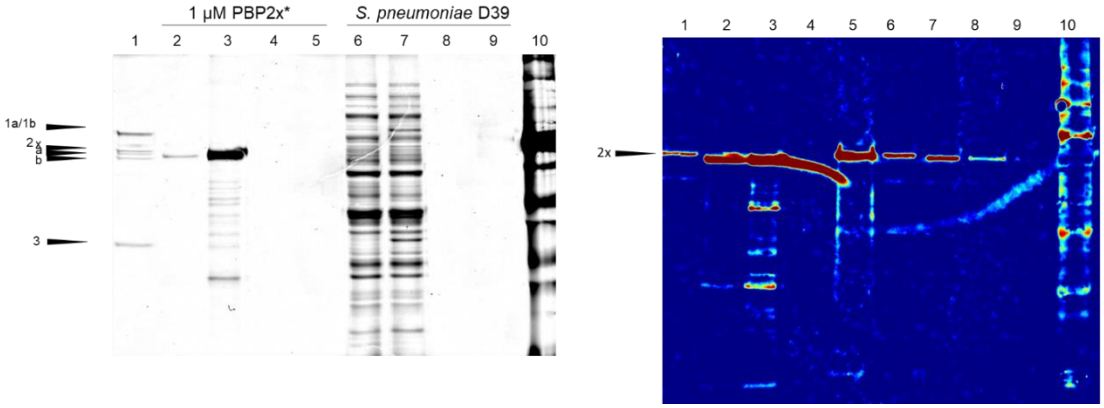

Figure 5.3. Click chemistry-enabled fluorescent detection and enrichment of PBP2x. Soluble PBP2x or whole cells were treated with click-MEM and conjugated with fluorescent or biotin tags and enriched by affinity chromatography. The enrichment results were assessed by western blot on PVDF membranes, using an anti-PBP2x antibody for detection (*right*). 1: Cells labeled by 5 µg/ml Boc-FL (control). 2: 1 µM PBP2x* reacted with Alexa Fluor 488 azide; 3: 1 µM PBP2x* tagged by 5 µM click-MEM then reacted with Alexa Fluor 488 azide. 4: 1 µM PBP2x* reacted biotin-azide and enriched by avidin agarose beads; (released protein) 5: 1 µM PBP2x* tagged by 5 µM click-mem then reacted with biotin-azide and enriched by avidin agarose beads. (released protein) 6: Pneumococcal cells reacted with 250 µM Alexa Fluor 488 azide; 7: Pneumococcal cells tagged by 5 µM click-mem then reacted with 250 µM Alexa Fluor 488 azide. 8: Pneumococcal cells reacted with biotin-azide and enriched by avidin agarose beads; (released proteome) 9: Pneumococcal cells tagged by 5 µM click-mem then reacted with biotin-azide and enriched by avidin agarose beads. (released proteome) 10: protein ladder. The gel on the left shows the fluorescent signal. The presence of several non-PBP bands in lanes 6 and 7 is due to non-specific binding of the fluorophore to proteome.

5.3. Optimization of Cellular Proteome Experiments

5.3.1. Click Chemistry

In order to identify the optimal probe:protein ratio for protein enrichment, 1 μM PBP2x* was incubated with 1, 2, 5 or 10 μM click-MEM, followed by conjugation with Dde-TAMRA Biotin Azide under click reaction conditions. Dde-TAMRA Biotin Azide is a trifunctional, cleavable reagent that is designed to enable efficient and facile recovery of avidin-bound proteins and protein complexes in affinity-based assays.(71, 232) The fluorescent (TAMRA) and affinity (biotin) moieties are linked to azide group through a spacer arm containing the Dde group, which can be cleaved by hydrazine (**Figure 5.4; B**). The trifunctional biotin reagent was chosen so that both a fluorescent and an affinity tag could be installed on the tagged proteins to facilitate downstream enrichment and analysis of captured proteins. Saturation of florescent signal was observed at 2 μM click-mem and 2:1 ratio was found to be the optimal ratio, the lowest concentration that yields saturation of PBP2x, in the following experiments (**Fig. 5.5**).

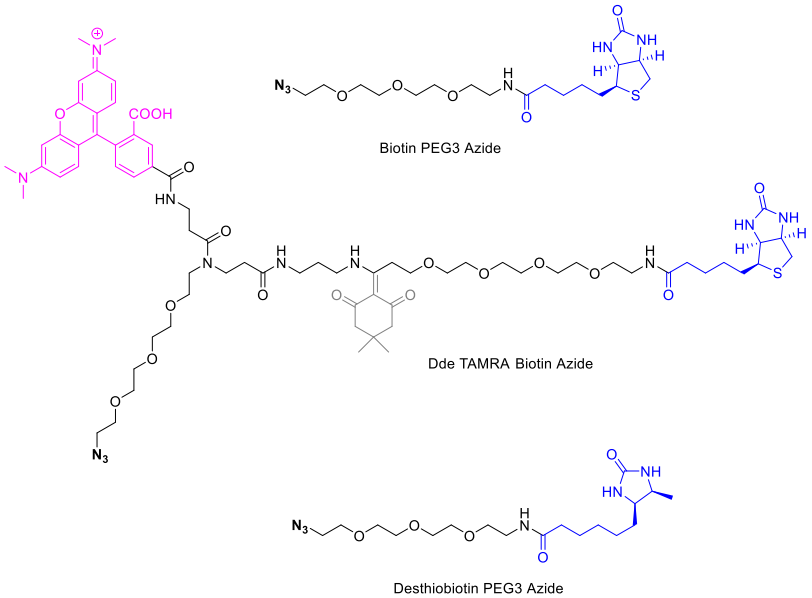

Figure 5.4. Biotin analogs used in this thesis: Biotin-PEG3-Azide, Dde TAMRA Biotin Azide and Desthiobiotin-PEG3-Azide. TAMRA (magenta) and biotin (blue) moieties are connected through a linker arm containing the cleavable Dde linker (gray).

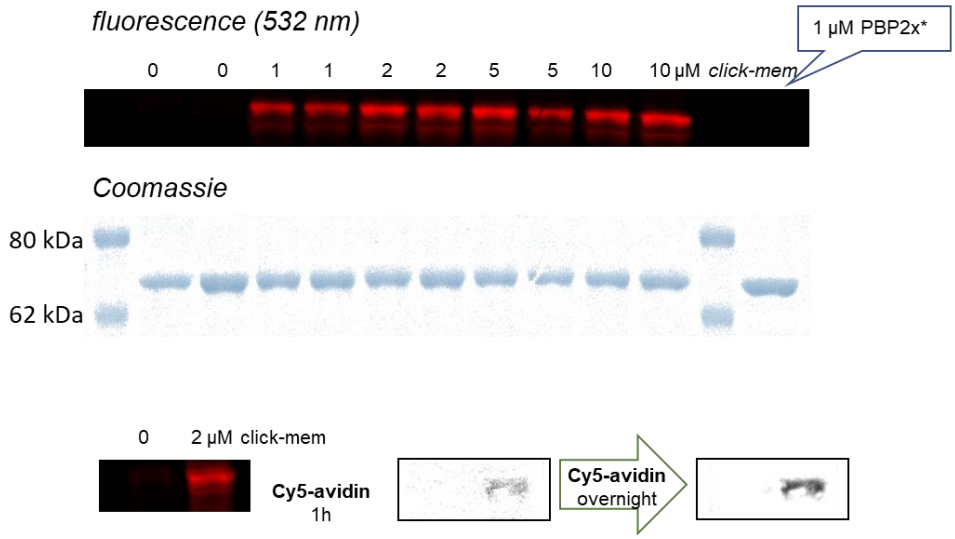

Figure 5.5. Dual labeling of alkynylated PBP2x* by Dde-TAMTA-Biotin-azide. 1 µM PBP2x* was treated with 1, 2, 5 and 10 µM click-MEM for 30 min at RT. Alkynylated protein then underwent click reaction with Dde-TAMRA-Biotin-azide in the presence of sodium ascorbate, aminoguanidine hydrochloride, THPTA and copper (II) sulfate. Fluorescent signal, detected at 532 nm, was saturated at ≥ 2 µM of the probe (*top*). SDS PAGE gels were transferred to a PVDF membrane. Biotinylated protein was visualized upon incubation with Cy5-avidin (*bottom.)* Experimental procedure is described in more detail at the end of this chapter.

Although the dual fluorescent-affinity reagent successfully tagged and visualized the alkynylated PBP2x*, attempts to enrich the tagged PBP2x* by Neutravidin agarose beads were unsuccessful. Literature research revealed the liability of Dde group to hydrolysis by SDS, which must be used as a detergent to solubilize the proteins, particularly in complex mixtures and proteomes.(71) Thus, this commercially available reagent is not viable for use with SDS-PAGE assays.

5.3.2. Release of Bound Biotinylated Proteome

One of the major challenges in biotin-assisted enrichment is the nearly "irreversible" binding event that occurs between biotin and avidin. The affinity of the biotin-streptavidin interaction is extremely strong, dissociation constant (K_d) of 10^{-15}, the highest known non-covalent biochemical interaction, which is stable under a broad range of pH

values and temperature.(233) Therefore, the conditions required to release bitinylated proteins may negatively affect the overall efficiency of this process and potentially affect downstream analysis. The strong biotin-(strept)avidin interaction is attributed to the fact that biotin fits into a pocket in the streptavidin protein, which creates an “enveloping effect”, further supporting the binding interaction.(234-236) There are two main biotin modifications that can enhance the release of biotinylated molecules: biotin analogs containing cleavable groups such as photocleavable (PC) linkers or desthiobiotin. PC biotin carries a photocleavable linker group that cleaves upon irradiation by UV light.(237) Desthiobiotin is a biotin analog missing the sulfur atom (**Fig. 5.4**). This analog still binds to streptavidin with high affinity, $K_d \sim 10^{-11}$, but more weakly compared to biotin molecule. Because of this, streptavidin-bound desthiobiotinylated molecules can be released by rinsing with free biotin.

We decided to move forward with desthiobiotin in our pulldown assays. Application of this new affinity tag to PBP2x* solution provided promising preliminary results (**Fig. 5.6**). Enrichment of PBPs from Pneumococcal cells is currently underway.

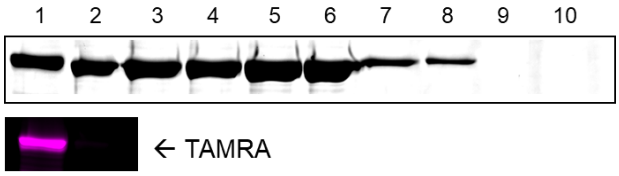

Figure 5.6. Enrichment of soluble PBP2x by Click-MEM probe using desthiobiotin-PEG3-azide as the affinity handle. One μM soluble PBP2x (PBP2x*) was treated with 5 μM click-MEM and conjugated with TAMRA-PEG3-azide (as control for the efficiency and selectivity of click chemistry, 1: 5 μM Click-MEM or 2: no probe treatment, followed by click reaction with TAMRA-PEG3-azide.) or desthiobiotin-PEG3-azide and enriched by Neutravidin agarose beads. Lanes 3-6 are supernatant after loading on neutravidin agarose beads. PBP2x content is reduced in probe-treated samples (3, 4) compared with controls (5, 6), which is released from the beads after biotin treatment (Lane 7 and 8, compared with no PBP2x* was captured in control samples, 9, 10).
The experiment was performed in duplicate.The enrichment results were assessed using SYPRO red as a general protein stain. Experimental details are discussed in further details at the end of the chapter.

5.4. Summary and Future Directions

In Chapter 3, we developed a meropenem-based probe with an alkyne functionality (Click-MEM) to target PBP3 and PBP5 in *B. subtilis* cells. Besides fluorescent imaging to localize the activity of these PBPs, we could show that targeted proteins could be enriched using a streptavidin-functionalized matrix and analyzed by LC-MS/MS. In this chapter, we applied the Click-MEM probe to enrich Pneumococcal PBP2x. In the proof-of-concept studies, our probe successfully captured and released a soluble form of PBP2x in solution. Efforts are currently underway to enrich PBP2x in *S. pneumoniae.* Additionally, our methodology will facilitate the detection of proteins directly associated with PBPs within the cell using pull-down assays. We plan to utilize our PBP-selective probes in conjunction with chemical crosslinking reagents to enrich the protein complexes involved with PG synthesis and cell division. PBPs of interest will first be tagged, followed by chemical crosslinking to preserve interactions between PBPs and their partner proteins. Finally, the enrichment will pe performed followed by LC-MS/MS assessment of the captured proteome to identify the proteins, as described above.

5.5. Methods and Characterization Data

5.5.1. Alkynylation of PBP2x

Expression of PBP2x* was explained in detail previously (see section 4.10.10.1). 50 µL PBP2x* solution in PBS was treated with 1-10 µM click-mem for 30 mins at room temperature.

5.5.2. Click Chemistry Visualization of tagged proteins:

Proteomes were treated with click reagents in the following order: AlexaFluor488 azide 50 µM, TCEP 1 mM, TBTA 0.5 mM, CuSO4 1mM. Incubation at room temperature continued

for 1 hour, with gentle head-over-end shaking. Protein was then precipitated to remove excess reagents using ProteoExtract ® kit. Pellets were then suspended in 60 µl PBS. 20 µl 4x SDS loading was added and samples were vortexed briefly. 12 µl of each sample was loaded on 10% SDS PAGE gel. Gels were run at 180 V, for 90 minutes.

5.5.3. PBP2x* enrichment using Biotin-PEG3-azide conjugate:

Samples were treated with click reagents in the following order: Biotin azied 50 µM, TCEP 1 mM, TBTA 0.5 mM, CuSO4 1mM. Incubation at room temperature continued for 1 hour, with gentle head-over-end shaking. Protein was then precipitated to remove excess reagents using ProteoExtract ® kit, according to the manufacturer's protocol. Briefly, samples were mixed with 200 µl cold Precipitation Agent (-20 °C, vortexed briefly and incubated for 20-60 mins at -20 °C. Samples were centrifuged at 10,000 ×g, for 10 mins at R.T. to pellet the protein. The supernatant was carefully aspirated. The pellet was washed by ~150 µl cold Wash Solution (-20 °C) and vortexed briefly. Samples were centrifuged at 10,000 ×g, for 2 mins at R.T. to pellet the protein. The supernatant was carefully aspirated without disturbing the pellet. The wash step was repeated one more time. Next, samples were dried for 5 min to 1h at R.T. by leaving the open tube in the hood. Fluorescent samples were suspended in 60 µl PBS, to which 20 µl 4x SDS loading buffer was added. Samples were stored at -20 °C before SDS PAGE analysis. For biotinylated samples, dry pellets were suspended in 100 µl binding buffer (1% NP-40, 0.1% SDS in PBS), to which 25 µl equilibtared Pierce Avidin Agarose beads were added. Equilibration of beads was done by 3 × wash with 200 µl PBS. Incubation with beads continued at 4 °C for 48 hours. Beads were then transferred to mini-spin columns and centrifuged at 600 ×g for 30 s. Supernatant was concentrated to ~ 60µl, to which 20 µl 4X SDS loading buffer was added, and stored at -20 °C, to be analyzed by SDS PAGE gel.

Beads were washed 3× with 200 µl lysis buffer to remove loose binders. The beads were then transferred to an epitube. 60 µl of 2X SDS loading buffer was then added to the beads and samples were boiled for 30 min. Solution was then tested on 10% SDS PAGE gel.

5.5.4. Western Blot

SDS PAGE gels were transferred to PVDF membranes at 100 V for 1h on ice. Membranes were washed 3 × with TBS-T (Tris 25 Mm, NaCl 500 mM, Tween 0.01%; pH 7.5). Next, membranes were blocked with 10 ml 1% BSA in TBS at 4 °C overnight with gentle shaking. anti-PBP2x was added at 1:10,000 and incubation happened at room temperature for 1h. Next, membrane was washed 3× with TBS-T. Secondary antibody, goat anti-rabbit IgG-AP was added at 1:10,000 in 10 ml blocking solution and incubation happened at room temperature for 30-60 min. Membrane was washed 3× with TBS-T. Detection of PBP2x was done using AP Conjugate Substrate kit (Bio-rad).

5.5.5. PBP2x enrichment from proteome

Strain 1824, an unencapsulated derivative of *S. pneumoniae* strain D39, was grown statically in brain heart infusion (BHI) medium in 100 x 17 mm tubes by incubation in an atmosphere of 5% CO_2 at 37 °C to an OD_{620} of ~ 0.2. Cell pellets from 20 ml of *S. pneumoniae* cultures were harvested by centrifugation (10,000 × *g* for 10 min at 4 °C) and washed with 1 ml phosphate buffered saline (PBS x 1; pH 7.4). Cell pellets were resuspended in 50 µl of PBS containing 5 µM of Click-MEM and incubated at room temperature (RT) for 30 min. A reference sample was suspended in 50 µl of PBS and incubated for 30 min at RT. The cells were washed and resuspended in 500 µL of PBS containing 1 mg/mL of lysozyme and were incubated for 30 min at 37 °C. The cells were lysed by a Hielscher vial tweeter UP200St (70% C, 95% A, 5% adjustment snap and 1s SD Interval / 10s for 6 x 1 min intervals with 1 min cooling time in between), and membrane

proteome was isolated by at 21,000 × *g* for 15 min at 4 °C. Membrane proteome was resuspended in 220 µL PBS, and the samples were homogenized by sonication. Click reagents were added in the following order: Biotin-PEG3-azied 50 µM, TCEP 1 mM, TBTA 0.5 mM, CuSO4 1mM. Samples were incubated for 1 h at room temperature. Membrane proteome was isolated by centrifugation at 21,000 × *g* for 15 min at 4 °C. Pellets were suspended in 100 µl binding buffer (1% NP-40, 0.1% SDS in PBS), to which 100 µl pre-equilibtared Pierce Avidin Agarose beads were added. Incubation with beads continued at 4 °C overnight. Beads were then transferred to mini-spin columns and centrifuged at 600 ×g for 30 s. Supernatant was concentrated to ~ 60µl, to which 20 µl 4X SDS loading buffer was added, and stored at -20 °C, to be analyzed by SDS PAGE gel. Beads were washed 3× with 200 µl lysis buffer to remove loose binders. The beads were then transferred to an epitube. 60 µl of 2X SDS loading buffer was then added to the beads and samples were boiled for 30 min. Solution was then tested on 10% SDS PAGE gel.

5.5.6. Enrichment using Desthiobiotin-PEG3-azide conjugate

Proteome samples were suspended in 50 µl of PBS (0.1 M sodium phosphate buffer, 0.15 M NaCl, pH = 7.4) containing click reagents: desthiobiotin-PEG3-azide 250 µM, TCEP 1 mM, TBTA 0.5 mM, $CuSO_4$ 1mM. Incubation at room temperature continued for 1 hour, with gentle head-over-end shaking. Protein was then precipitated to remove excess reagents by adding 400 µl cold acetone, vortexed briefly and incubated for 60 mins at -20 °C. Samples were centrifuged at 21,000 × g, for 10 mins at R.T. to pellet the protein. The supernatant was carefully aspirated. The pellet was washed by ~100 µl cold methanol and vortexed briefly. Samples were centrifuged at 21,000 × g, for 2 mins at R.T. to pellet the protein. The supernatant was carefully aspirated without disturbing the pellet. The wash step was repeated one more time. Next, samples were dried for 5 min to 1h at R.T. by leaving the open tube in the hood. (Fluorescent samples were suspended in 60 µl PBS,

to which 20 µl 4x SDS loading buffer was added. Samples were stored at -20 °C before SDS PAGE analysis.) Next, dry pellets were suspended in 50 µl solution of 8M urea in PBS and then diluted 4-fold by adding 150 µl PBS. To each proteome sample, was added 25-50 µl Pierce high capacity Neutravidin agarose bead in ~ 200 µl PBS containing 0.2% NP-40 (loading buffer), pre-equilibrated with PBS + 0.2% NP-40. Incubation with beads continued at room temperature for 1 h while shaking head-over-end. Beads were then transferred to Pierce mini-spin columns and centrifuged at 1,200 ×g for 3 min. Beads were washed 2 × with 200 µl loading buffer, 3 × with PBS and 3 × with miliQ water to remove loose binders. (Supernatant and wash fractions were concentrated to ~ 45 µl, to which 15 µl 4X SDS loading buffer was added, and stored at -20 °C, to be analyzed by SDS PAGE gel.) The beads were then transferred to an Eppendorf tube. To release the captured proteins, beads were suspended in 0.5 ml of 2 mM Biotin (Pierce; ThermoFisher Scientific) followed by 30 min incubation at room temperature with shaking head-over-end. Next, beads were transferred to Pierce mini-spin columns and centrifuged at 1,200 ×g for 3 min. Beads were washed 2 × with 200 µl loading buffer and 3 × with PBS. Collected fractions were mixed and concentrated under vacuum. The residues were suspended in 45 µl PBS, to which 15 µl 4X SDS loading buffer was added. All the samples were heated at 95 °C for 5 min and were run on 10% SDS PAGE gel.

CHAPTER 6

SUMMARY, PERSPECTIVES AND FUTURE WORK

Portions of this work will be published in:

Sharifzadeh S, Carlson EE. 2019. Reviving the “Golden Age”: Incentivizing Innovation in Antibiotic Discovery and Development. *Manuscript in Preparation.*

6. Summary, Perspectives and Future Work

6.1. Summary

Bacterial cells are surrounded by an external layer called the cell wall that protects them from osmolysis, rupture due to the accumulation of fluids. A major component of this protective coating, which is unique to prokaryotes, is the peptidoglycan (PG), a heteropolymeric structure composed of saccharide backbones that are cross-linked by peptide subunits.(6, 14, 213) This exclusive presence in bacteria makes the cell wall an ideal antimicrobial target as it minimizes side effects in humans and other eukaryotes. Penicillin-binding proteins (PBPs) are membrane-associated proteins that are involved in the final stages of PG biosynthesis. PBPs were discovered and named so for their affinity to bind to β-lactam antibiotic penicillin, which comprise the largest class of clinically-utilized antibiotics today. Different bacteria can possess a suite of ~ 4-16 PBPs.(6, 8, 10, 117) Although the importance of the PBPs as antibacterial targets has long been appreciated, the specific roles of individual PBPs, beyond their catalytic function, has remained elusive due to the lack of appropriate chemical and biological tools.(89, 90)

In this dissertation, our efforts to generate such chemical tools were described. Due to the β-lactams' covalent mode of inhibition of the PBPs, β-lactam analogs functionalized with different reporting groups could be generated and utilized to monitor PBP activity. Such fluorescent analogs of penicillin V are commercially available and have been utilized as a global probe for PBPs.(29, 30) Inspired by that, our group previously generated cephalosporin C-based probes with selectivity for a subset of PBPs in different microorganisms.(89, 102) In this work, we expanded our PBP probe toolbox by generating additional chemical probes based on β-lactam antibiotics, and a β-lactone scaffold that we designed and demonstrated to selectively target the PBPs.(90)[CHAPTER 3] We envisioned that β-lactams with cognate selectivity toward certain PBPs of interest could

be utilized to generate probes for those PBPs. To facilitate the development of such probes, we evaluated the PBP binding profile of a library of 21 commercially available β-lactam antibiotics in *Bacillus subtilis*, using a fluorescent cell-based assay previously tested in *Streptococcus pneumoniae* and *Escherichia coli*. (116, 145) As expected, several distinct selectivity profiles were obtained. [CHAPTER 3] Among the examined compounds, the carbapenems doripenem and meropenem stood out with specifically high affinity for PBP3 and 5. Accordingly, we generated meropenem-based probes to visualize the activity of PBP3 in *B. subtilis DK654*, a knockout strain in which PBP5 is removed (CHAPTER 3). Using high resolution fluorescent microscopy, meropenem probes enabled selective visualization of active PBP3, revealing the concentration of its activity at the septal and the division site.[CHAPTER 3] Moreover, probes based on mecillinam (amdinocillin), which we found to be a selective inhibitor of PBP2a and PBP2b in *B. subtilis*, were designed and synthesized (Click-MEC). Importantly, we showed that our Click-MEC probe retained its selectivity for these two PBPs. The click condition for insertion of fluorescent reporter groups are currently under investigation.

Since the β-lactams targeted a limited number of PBPs in each given microorganism, we designed and generated a library of 21 probes based on a β-lactone scaffold carrying various fluorophore groups. We introduced diversity through insertion of different amino acid residues in order to achieve selective labeling of individual PBPs. Our results indicated that all the β-lactone probes specifically targeted PBPs and some showed concentration-dependent selectivity for one or a small number of PBPs in the examined microorganisms. We utilized two of the probes, **7FL** (containing L-Phe amino acid and a fluorescein group) and **8T** (containing D-Phe and a TAMRA group) in the *S. pneumoniae E193* strain, in which the gene encoding PBP1b is knocked out, to simultaneously visualize the activity of PBP2x and PBP2b, respectively. We discovered that the activity

of PBP2x concentrates to the division site at the end of the cell cycle, a finding that is consistent with the fact that PBP2x is essential for the cell division process. Importantly, we could visualize the activity of single PBPs in live cells for the first time.(90)

Given the high affinity of meropenem for PBP2x in *S. pneumoniae*, we employed the meropenem probe containing a click functional group (Click-MEM) to enrich pneumococcal PBP2x using biotin-mediated capture and release method (CHAPTER 5). In our proof-of-concept study using a recombinant soluble PBP2x, we showed that treatment with Click-MEM enables efficient capture and release of this protein. This strategy could be applied to pneumococcal cells to enrich specific PBPs and proteins associate with them.

The rest of this chapter will elaborate on our ongoing efforts to expand our understanding of bacterial cell wall biosynthesis using our ever-growing chemical toolbox. We believe that such deep knowledge of bacterial physiology is critically needed and will open up new horizons in different platforms of antimicrobial discovery campaigns.

6.2. Application of LC-MS to Peptidoglycan Analysis

High performance liquid chromatography (HPLC) has been used for many decades to separate, isolate, identify and quantify biomolecules. HPLC techniques have been tailored to analyze bacterial biomolecules derived from the cell wall digests, including muropeptides, stem peptides, glycan strands and D-amino acid incorporation.(197, 238-240) PG consists of a network of glycan chains of alternating N-acetylmuramic acid (MurNAc) and N-acetylglucosamine (GlcNAc) residues that are connected by short peptide chains containing L- and D-amino acids (**Fig. 6.1**). Structural analysis of PG usually involves enzymatic digestion of the glycan strands and separation of the disaccharide peptides by reversed phase HPLC, followed by collection of individual peaks for mass spectrometry (MS) and or tandem LC-MS analysis. The quantitative nature of this method

enables the measurement of changes to PG composition between different species of bacteria, different strains such as wild-type *vs* drug-resistant, growth conditions or mutation. Detailed PG content such as glycan chain length, muropeptide composition and architecture can be determined in such studies. (239) (238)

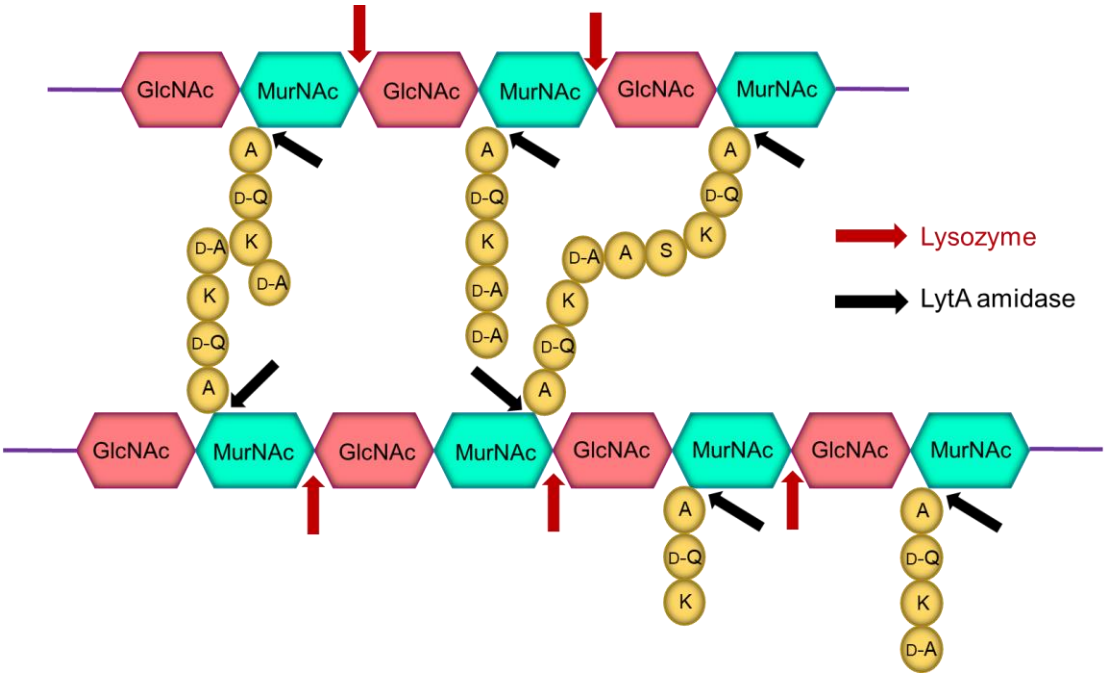

Figure 6.1. Scheme of pneumococcal PG and the cleavage sites of lysozyme and LytA enzymes. The pneumococcal PG consists of glycan chains of alternating N-acetylmuramic acid (MurNAc) and N-acetylglucosamine (GlcNAc) residues interconnected by stem peptide chains. The peptides are designated in single letter code (A = Alanine; D-Q = D-Glutamine; K = Lysine; D-A = D-Alanine; S = Serine).

6.2.1. Characterization of Pneumococcal Peptidoglycan Structure

Relying on the preceding established methodologies, we aimed to further evaluate the disparate roles of the PBPs in PG construction by performing a systematic comparison among different PBP knockout strains of *Streptococcus pneumoniae*. We were specifically interested in identifying how the loss of the transpeptidation function of each PBP would affect PG composition in *S. pneumoniae*. Experiments were designed to be performed in wild-type and PBP knockout strains, as available for non-essential PBPs. Additionally, selective inhibition of individual PBPs can be achieved using the selective inhibitors that

were identified in our PBP profiling assays, such as cefuroxime and aztreonam to inhibit PBP2x and PBP3, respectively.(116) The use of chemical inhibition strategies is highly complementary to genetic deletion as this would enable us to differentiate between PG changes due to the loss of transpeptidase activity versus those caused by the loss of the entire PBP, which may have additional functions.

Cell wall material from *S. pneumoniae* IU1945 was prepared as described previously and the PG isolated.(240, 241) LytA amidase (produced in house) and muramidase (hen egg white lysozyme; commercial source) were used to digest PG into its components. LytA, the major autolysin enzyme in *S. pneumoniae*, is a cytosolic cell wall hydrolase enzyme that also functions as a virulence factor through facilitating the spread of toxins and other factors involved in immune evasion. LytA causes cell lysis by cleaving the lactyl-amide bond that links the stem peptides and the glycan strands of the PG, resulting in hydrolysis of the cell wall.(242, 243) Lysozymes, also known as 1,4-β-N-acetylmuramidases, cleave the 1,4-β-glycosodic bond between MurNAc and GlcNAc residues in the glycan backbone. Used as a natural defense mechanism against bacterial pathogens by plants and animals, lysozymes are widespread in nature (**Fig. 6.1**).(243, 244)

HPLC analysis of the muropeptide mixtures failed to reproduce the chromatogram reported for pneumococcus strains in literature. (197, 241) Indeed, no major peak could be detected at 210 nm or 254 nm wavelength, even after scaling up the sample size (data not shown). Therefore, muropeptide and peptide samples were prepared for mass spectrometry analysis as this instrumentation is much more sensitive than simple absorbance measurements. On a Quadrupole Time-of-Flight (Q-TOF) LC/MS instrument, only the top 4 most abundant peptide species could be observed (**Fig. 6.2**). Due to the

low abundance of the detected ions, it was not possible to accurately quantify these species.

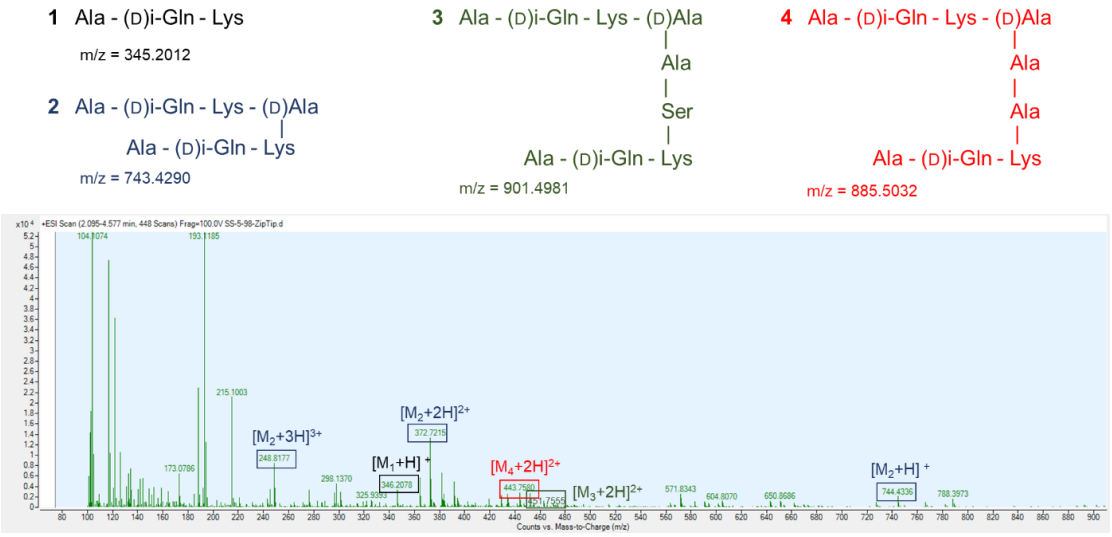

Figure 6.2. LC/MS chromatogram of pneumococcal peptides detected on Q-TOF MS instrument. Structures and the calculated *m/z* values for the neutral form of the peptide species identified in PG digests from *S. pneumoniae* IU1945 are presented.

We postulated that the low recovery of peptides might be due to low efficiency of the enzymatic digestions, which we attributed to either enzyme efficiency or the presence of impurities such as SDS in the isolated cell wall material, which could impede the proper function of enzymes. To address these issues, we generated recombinant LytA in house and purchased mutanolysin (from *Streptomyces globisporous* ATCC21553; Sigma). It is known that different lysozymes exhibit a wide range of substrate selectivity for the cell wall of various bacterial species.(244) Mutanolysin from *S. globisporus* is among the few muramidases that retains its activity against O-acetylated PG (245), which is a resistance mechanism used by many pathogenic bacteria, including *S. pneumoniae*, to evade the lytic action of innate immunity response through blocking the activity of host lysozymes.(244) We also purchased PG from *Bacillus subtilis* from commercial sources (Sigma) to rule out the introduction of impurities during in house production of the cell wall material. Digestion of the *B. subtilis* PG was conducted as described previously and

soluble muropeptides were collected and prepared for MS analysis.(105, 246) We did not detect any known muropeptide species on a MALDI-TOF instrument. Assessment of the sample on a Q-TOF LC/MS instrument was carried out next. This time, one mass corresponding to a small muropeptide species from *B. subtilis* could be detected (**Fig. 6.3**).[For a complete list of expected muropeptide species see reference(105)]

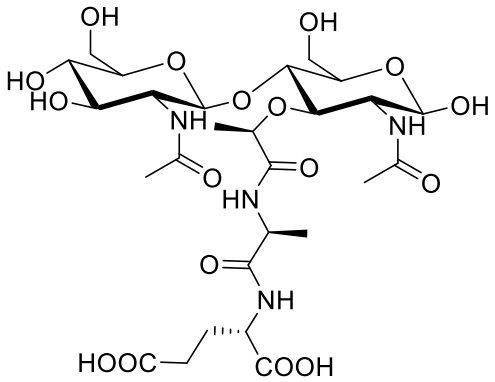

Figure 6.3. Structure of the muropeptide from *B. subtilis* PG that could be detected by LC/MS.

6.2.2. Perspectives on Incomplete Characterization of Pneumococcal PG

Attempts to characterize pneumococcal PG components, either muropeptides or stem peptides, were unsuccessful. Given the finding that only the top 4 most abundant peptide species could be observed by ESI-TOF, it is postulated that peptide content and/or recovery was not sufficient. Some potential explanations for these results include the following:

- The enzymatic digestion is inefficient. Two types of lysozyme and two separate batches of LytA amidase enzyme were tested for the PG digestion. The next step would be to optimize additional conditions such as duration, temperature and dissolution of the PG material. The reported common practice in PG digestion is to add the lytic enzyme in several intervals. Therefore, either higher amounts of enzyme or additional aliquots could be used.

- Peptides and muropeptides could be lost during the preparation of samples for MS analysis. Initially, centrifugal filters with a 3 kDa cut-off (Amico Ultra-0.5 mL Centrifugal Filter; Millipore Sigma) were used to separate the peptides species from undigested PG material. The main issue with these filters was the introduction of impurities such as polyethyleneglycol polymers into the sample, which tend to saturate the MS detector and interfere with the detection of peptide species. Alternatively, PD MidiTrap G-10 columns (GE Healthcare Life Sciences) were used to trap the digested material, which were then eluted by a 1:1 methanol:water solution containing 0.1% formic acid. Although this method solved the issue caused by the presence of polymeric species from the spin filters, only a few relevant ion species could be detected by LC/MS, as described above. The elution conditions could be further optimized, for example by using a methanol gradient so that more material and different types of peptides/muropeptides are recovered. The finding that only the smallest muropeptide from *B. subtilis* could be detected (**Fig. 6.3**) suggests that higher molecular weight species might have been retained/lost during the preparation.

6.3. Mycobacterial Cell Wall

Tuberculosis (TB), caused by *Mycobacterium tuberculosis* (*Mtb*), is one of the top 10 causes of death and the leading cause from a single infectious agent (above HIV/AIDS). Millions of people continue to fall sick with TB each year. In 2017, an estimated 1.3 million deaths were caused by TB among HIV-negative people and there were an additional 300,000 deaths from TB among HIV-positive patients.(247) This death toll is largely due to intrinsic and acquired resistance mechanisms to antimicrobial agents. For example, *Mtb* produces β-lactamases that confer resistance to β-lactam antibiotics

through hydrolysis of these molecules and hence, β-lactams are not extensively utilized as antitubercular agents.

The mycobacterial cell wall acts as a protective barrier and contributes both to *Mtb* survival inside the host and resistance to most antibiotics. Although much is understood about cell wall construction in model microorganisms, it remains poorly characterized in *Mtb*. Further understanding of cell wall synthesis in *Mtb* will aid in discovering new drugs to cripple this critical process and take us one step closer to the eradication of TB.

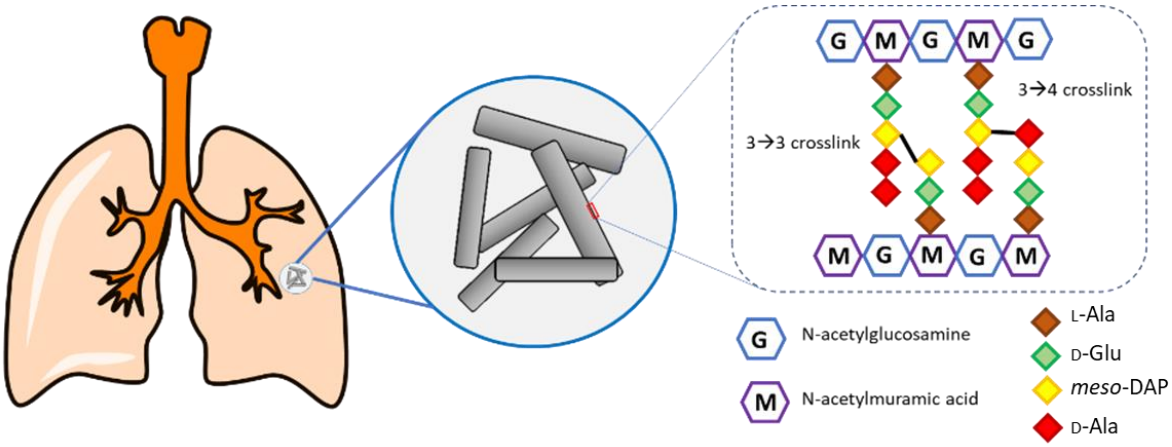

Figure 6.4. Mycobacteria *bacilli* (rod shaped bacteria) infect alveolar units of the host lung. *Mtb* cells are surrounded by a thick supporting layer (cell wall, peptidoglycan = PG). The PG backbone is comprised of alternating *N*-acetylglucosamine and *N*-acetylmuramic acid sugars. The latter contains pentapeptide units, which crosslink adjacent PG chains through formation of amide bonds. Mycobacterial PG possesses both 3→3 and 3→4 crosslinks (where 3 and 4 refer to the order of amino acids in the stem peptide). *meso*-DAP = *meso*-diaminopimelic acid.

Mtb possesses a thick cell wall composed of several layers, which is structurally different from other bacterial species and its PG layer has many unique features. For example, the predominant peptide cross-link in mycobacteria is 3→3, as opposed to classic 3→4 cross-links (**Fig. 6.4**).(248) While the latter is catalyzed by PBPs, the former was more recently discovered to be facilitated by a different class of enzymes known as the L,D-transpeptidases (Ldts). PBPs and Ldts are structurally unrelated and catalyze crosslinks through the actions of serine and cysteine residues, respectively. *Mtb* encodes

five Ldts(249), among which Ldt type 2 (Ldt_{Mt2}) is essential for virulence, resistance to β-lactam antibiotics and normal cell morphology.(250, 251) Carbapenems, such as meropenem, are the only subclass of β-lactam antibiotics that in combination with clavulanic acid, a β-lactamase inhibitor, have shown efficacy against extensively drug-resistant (XDR) *Mtb* strains,(252) which is attributed to inhibition of the formation of both 3→3 and 3→4 crosslinks.(253, 254) Importantly, it is known that the PG structure changes significantly throughout the mycobacterial life cycle and different stages of infection. Consequently, it is crucial to develop tools to study Ldts and PBPs in this pathogen.

6.3.1. Activity-Based Profiling of Mycobacterial Transpeptidases

With the established potency of our probe toolbox, we intend to gain basic knowledge in other life-threatening pathogens, including *Mtb*. Given the previously proven covalent modification of cysteine residues by meropenem(255) and β-lactones,(256) we expect that our probe toolkit possesses the potential to target Mycobacterial Ldts, as well as PBPs. This will enable tracking of these essential transpeptidases, individually and in relation to other proteins. As a proof-of-concept, we chose three Mycobacterial species: *M. tuberculosis H37Ra*, *M. tuberculosis* mc^2*7000* and *M. bovis BCG*.(257) Initial attempts to tag the PBPs by bocillin-FL probe failed to yield detectable labeling of any PBP, which could be explained by the complex structure of the Mycobacterial cell envelope limiting the permeability of exogenous molecules. Most of the previous bocillin-FL binding assays in *Mycobacterium spp.* were either performed on pure PBPs or isolated membrane lysates.(258) Therefore, we isolated the membrane lysates from these three Mycobacterial strains and repeated labeling assays with bocillin-FL and our MEM-BODIPY probe. We detected several bands that were illuminated in each strain (**Fig. 6.5**).

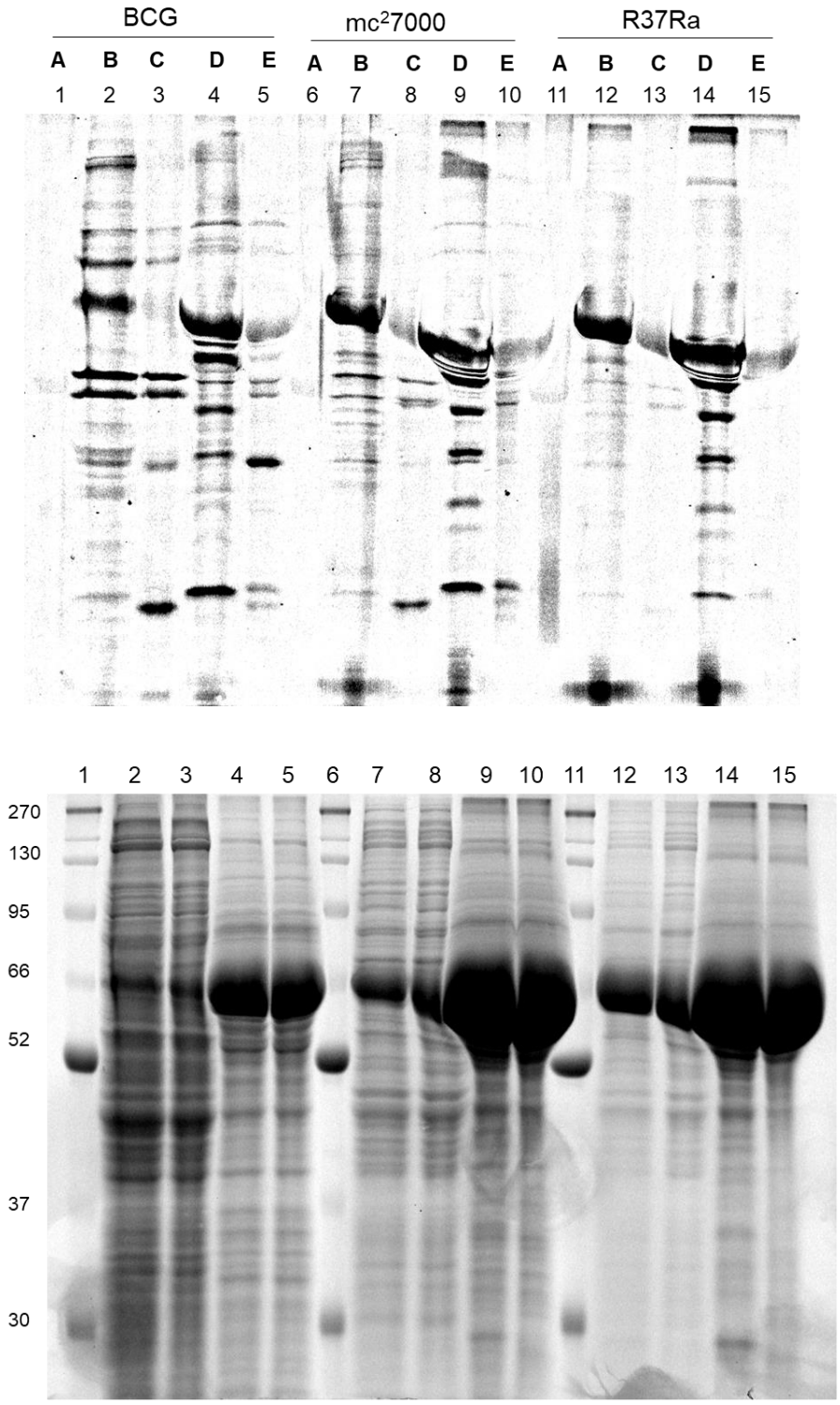

Figure 6.5. Labeling mycobacterial cell lysates by bocillin-FL and MEM-BODIPY probe. Cell lysates from different mycobacterial strains, *M. bovis BCG, M. tuberculosis mc²7000* and *M. tuberculosis H37Ra*, were lyzed, centrifuged, soluble (D, E) and insoluble (B, C) fractions were collected and labeled by 10 μM Boc-FL (B, D) or 5 μM MEM-BODIPY for 30 min. Experimental details are described in detail at the end of the chapter.

6.4. Ideal Antibacterial Targets

The alarming rise of antimicrobial resistance (AMR) is becoming a global health crisis. According to reports by the Centers for Disease Control and Prevention, each year in the U.S. at least 2 million people become infected with bacteria that are resistant to antibiotics and 23,000 people die each year as a direct result of these infections.(259) Today, infectious diseases are the leading cause of death in low-income countries and annual loss of life is expected to reach 10 million deaths by 2050 with an estimated economic cost of $100 trillion.{O'Neill, 2014 #2} On the other hand, robust diagnostic tests for characterization of antibiotic-resistant infections are missing and empirical use of antibiotics has been the common protocol before a diagnosis is made, giving rise to increasing rate of antibiotic resistance and persistent infections.{Fournier, 2014 #10;Hammes, 2011 #9;Ventola, 2015 #11} Widespread use of antibiotics to promote the growth of livestock is another major contributor to AMR.{Landers, 2012 #12;Martin, 2015 #13} The major complication is that resistance to antibiotics increases with their use – an inevitable natural process whereby bacteria evolve mechanisms that render the antibiotic ineffective. However, the development of resistance is accelerated by the inappropriate use and overuse of antibiotics in healthcare, food production, and through pollution of the environment as a result of the release of antibiotic manufacturing waste. Antibiotic resistance becomes an even more serious problem when bacteria become resistant to many antibiotics so that there are few or even no effective antibiotics to treat an infection [i.e., multidrug-resistant (MDR) or extensively drug-resistant (XDR); pandrug-resistant (PDR), respectively].(260) For example, Gonorrhea infection, once an easily treatable infection by sulfonamides in 1930s and penicillin a few years afterwards, has become resistant to all the known antibiotic classes. As the second most prevalent sexually transmitted bacterial disease globally, affecting more than 87 million cases every year, untreated *N. gonorrhea* leads to severe complications such as ectopic pregnancy,

infertility and increased chance of HIV transmission.(259, 261) As such, *N. gonorrhea* is listed as an urgent public health threat by the CDC and the WHO has placed it among the six high priority pathogens.

Although a more judicious use of antibiotics could slow down the rate of evolution of resistance, effective eradication of AMR requires a multifaceted approach that facilitates sustainable and impartial use of antimicrobials on one hand and fosters innovation of new therapies and diagnostic tools on the other hand. A critical component of such an approach includes the development of truly novel antibiotics, that act on clinically unexplored antibacterial targets to ensure effectiveness against resistant pathogens and complement the diminishing effectiveness of existing antibiotics.

The hanging fruits of classic screening methods were harvested by the 1960s and we are now limited in part by the fact that uncultured bacteria comprise more than 99% of all species in external environments, as microbes have traditionally provided the most important leads for antibiotic development. An additional factor that has stalled the discovery of truly innovative antibiotics is the lack of basic knowledge about complex bacterial physiology. A deeper understanding of pathogenesis and resistance mechanisms enables novel therapeutic strategies and/or the revitalization of old antibiotics. The most prominent example is development of β-lactamase inhibitors such as clavulanic acids and sulbactam to reverse the resistance evolved against β-lactam antibiotics. Along these lines, current efforts have focused on the discovery of more effective antibacterial therapy mechanisms that can withstand attempts by bacteria to evolve resistance or alternative approaches to use the bacterium's immune system against itself or block pathogenesis.

Choosing essential bacterial targets, against which the bacterium cannot evolve resistance, is another effective strategy. Bacterial cell wall biosynthesis is a well-recognized antibacterial target as demonstrated by the clinical success of β-lactams and

glycopeptide (e.g., vancomycin) classes of antibiotics, which block PG assembly through the inhibition of PBPs and binding to the terminal D-Ala-D-Ala of PG, respectively. Although studied in some detail, the PG biosynthetic pathway has much potential to be exploited for novel antimicrobial therapies. Moreover, the recent advances in the production and isolation of PG intermediates (13, 35, 37, 39, 262) has generated interest in manipulating the earlier steps of PG synthesis as an antimicrobial strategy (For a detailed description of PG biosynthesis see SECTIONS 1.1 and 1.2). MraY (phospho-N-acetylmuramoyl-pentapeptide transferase) catalyzes the first membrane step of PG biosynthesis by transferring the phospho-N-acetylmuramoyl-pentapeptide motif onto the undecaprenyl phosphate carrier lipid forming the lipid I intermediate. The catalytic activity of MraY is essential for the transfer of PG intermediates to the periplasmic space and there are no counterparts in mammalian cells. As such, MraY is regarded as an ideal novel antibacterial target.(263, 264) Uridyl peptide antibiotics (UPAs) such as muraymycin, tunicamycin, mureidomycin, capuramycin and liposidomycin, are the best known small molecule inhibitors of MraY. Despite their promising antibacterial activity *in vitro*, applying these compounds *in vivo*, especially against Gram-negative bacteria, remains challenging.(265) More recently, caprazamycins, which are naturally-occurring nucleoside antibiotics isolated from *Streptomyces sp.* where shown to inhibit the MraY enzyme. The natural and synthetic caprazamycin antibiotics exhibit potent antibacterial activity against various bacterial species, including XDR *M. tuberculosis*, highlighting the significance of MraY as a promising, novel antibacterial target.(266-268)

MurG is a glycosyltransferase that catalyzes the reaction between UDP-GlcNAc and the lipid I molecule forming the lipid II intermediate. An essential enzyme conserved across almost all bacterial species, MurG is considered another antibacterial target with great potential.(269) Murgocil is a MurG inhibitor that acts as a narrow-spectrum antibiotic with activity against MRSA.(270) Compared with MraY inhibitors, the potential toxicity of

MurG inhibitors *in vivo* due to competition with UDP-GlcNAc in mammalian systems, remains a big concern.(265)

In conclusion, AMR is a major scientific challenge, resulting from how we have developed and used antibiotics to date. Resolving such a crisis requires a multifaceted international solution with coordinated global commitment. Moving forward, we need to focus on developing high-quality antibiotics that demonstrate clinical superiority over existing drugs and can cure multi-drug resistant infections. Such a demanding task requires simultaneous attention and action of multiple stakeholders such as governments, drug companies, regulatory institutes, investors, academia and perhaps patient groups. A broad range of innovative ideas ongoing in industrial and academic institutions together would assure that the research is moving in the right direction.

6.6. Materials, Methods, and Characterization Data

Q-TOF (Agilent, 6540) and MALDI/TOF (AB-Sciex 5800) MS instrumentation were used to obtain accurate mass spectral data. HPLC purification was performed using an Agilent 1200 HPLC using a reverse phase column (Vydac218TP54 C18, 5 µm, 250 × 4.6 mm) detected by diode array detector (200–600 nm). Gradients consisted of 1–95% B (A: H_2O, 0.1% formic acid (FA); B: CH_3OH, 0.1% FA) over 20-60 minutes.

All chemicals were purchased from Sigma-Aldrich, unless mentioned otherwise.

6.6.1. Bacterial Strains, Growth Conditions and Chemicals

6.6.1.1. *S. pneumoniae* Culturing:

Strain IU1945, an unencapsulated derivative of serotype 2 *S. pneumoniae* strain D39, was grown statically in brain heart infusion (BHI) medium in 100 x 17 mm tubes by incubation in an atmosphere of 5% CO_2 at 37 °C.

6.6.1.2. *Mycobacterium spp*. Culturing:

M. tuberculosis H37Ra (a highly attenuated strain of H37Rv clinical isolate), *M. tuberculosis mc²7000 (*a Δ*panCD* Δ*RD1* deletion mutant of H37Rv and *M. bovis BCG* were received from Dr. Anthony Baughn laboratory at Department of Microbiology and Immunology, University of Minnesota). The strains were grown in Middlebrook 7H9 medium (Difco; 2.35 g dissolved in 450 mL MilliQ water) supplemented with 10% (vol/vol) oleic acid-albumin-dextrose-catalase (OADC; Difco; 50 mL), 0.2% (vol/vol) glycerol, and 0.05% (vol/vol) tyloxapol. D,L-pantothenate (50 µg/mL) was added for growth of *M. tuberculosis* strain mc^2 7000. The resulting solution was sterilized using a 0.22 µm filter. To prepare cultures, 50 µL of a glycerol stock of spores was inoculated into 5 mL of media in 25 mL plastic bottles. Cells were grown at 37 °C with shaking (100 rpm) to reach the desired OD.

6.6.1.3. Recombinant Production of LytA

E. coli IU1697, which overexpresses LytA, was a generous donation from Prof. Malcolm Winkler at Indiana University, Bloomington. Cells was grown in 1L LB Amp (50ug/ml) until OD600≈0.5 at 37 °C with shaking. Culture was cooled down at room temperature for 15min. Isopropyl β-D-1-thiogalactopyranoside (IPTG) was then added to a final concentration of 1mM and induction was allowed to happen doe 2 h at 30 °C while shaking. Cells were collected by centrifugation at 4,000 × g for 10min at 4 °C. Pellets were suspended in 25ml of buffer A (20 mM Tris-HC, 500 mM NaCl, pH = 8.0, 10% glycerol) to which a protease inhibitor tablet (Roche) was added. Cells were lyzed using a Beanson 250 sonifier (setting 3, 30% cycle, 12 × 15 s on-cycle on ice, with 45 s cooling time in-between cycles). Cell lysates were centrifuged at 16,000 × g for 10 min at 4 °C. Supernatant was collected and filtered with 0.22 µm filter (Millipore). The cell extract was loaded onto a diethylaminoethyl(DEAE)-cephadex (Sigma) affinity column previously

regenerated according to literature.(271) . Filtered cell lysates were loaded on the equilibrated column and the flow through was collected. Column was washed with at least 3 volumes of buffer X (20 mM sodium phosphate, 1.5 M NaCl buffer, pH = 7.0). Lyt A was subsequently eluted with one column volume buffer X + 0.14 M choline chloride. SDS PAGE analysis of the collected fractions proved ≥ 95% purity.

6.6.2. Isolation of Pneumococcal Cell Wall

Cells from overnight cultures (5 mL) were diluted into 1 L of BHI broth ($OD_{620} <$ 0.01) and incubated at 37 °C, 5% CO_2 to reach an OD_{620} of 0.5. Cells were centrifuged at 16,000 × *g* for 10 min at 4 °C. Pellets were resuspended in 10 mL of cold 1x PBS, centrifuged using the same setting and washed twice more. Next, cells were resuspended in 1 mL of cold 50 mM Tris-HCl (pH 7.0) and cell suspensions were added dropwise to 5 mL of boiling 5% (wt/vol) SDS and boiled for 30 min to 1 h with stirring (final SDS concentration ~ 1%). The mixture, more clear now, was cooled at room temperature for 5 mins, then on ice. Sacculi were collected by centrifugation at 18,500 × *g* for 30 min at room temperature. The pellet was washed twice with 30 mL of 1M NaCl (18,500 × *g*, 30 min, 25 °C). Pellets were then washed three more times with 30 mL cold water, or until no more bubbles were observed (indicates no remaining SDS). Next, pellets were resuspended in 6 mL of H_2O. Sacculi were further disrupted in a Branson sonifier, power setting 4, 30% duty cycle, 4 × 40 s cycles on ice, with ~ 1 min cooling time between cycles. The lysates were centrifuged at 4000 x *g* for 5 min at 4 °C. The supernatant was collected and centrifuged at 130,000 × *g*, 45 min, 4 °C (these conditions were used for all subsequent spins in this procedure). The resulting pellets were resuspended in 100 mM Tris-HCl, pH 7.5 with 20 mM $MgSO_4$. DNase A was added to 10 µg/mL and RNase A was added to 50 µg/mL, and samples were incubated at 37 °C for 2 h with shaking at 400 rpm. $CaCl_2$ and trypsin were added to 10 mM and 100 µg/mL, respectively, and samples were incubated

at 37 °C with shaking at 400 rpm overnight, for approximately 18 h. The next day, SDS was added to a concentration of 1% (wt/vol) to quench the digestion, and samples were incubated at 80 °C for 15 min. Following centrifugation, sacculus pellets were resuspended in 1 mL of 8 M LiCl and incubated at 37 °C for 15 min. Following centrifugation, sacculus pellets were resuspended in 10 mM EDTA (pH=7.0) for 15 min at 37 °C. Samples were centrifuged and washed 3x with water, or until no bubbles were formed, before resuspending in 2 to 4 mL of MilliQ water prior to lyophilization. Cell wall samples (~ 23 mg) were stored at -20 °C until further processing.

6.6.2.1. Preparation of Pneumococcal PG

Cell wall material (5 mg) was stirred with 2 mL of 48% hydrofluoric acid (HF; 55 mmol, 1.0 equiv.) for 48-72 h at 4 °C with shaking in an ultracentrifuge tube made of polyallomer, tightly closed by parafilm. HF was quenched by adding 11.4 mL of methoxytrimethylsilane (83 mmol, 1.5 equiv.). The PG was recovered by centrifugation at 130,000 × *g*, 45 min, 4 °C. The pellet was washed with ice-cold MilliQ water, 100 mM Tris-HCl (pH = 7.0) and then twice more with ice-cold water. The resulting PG material was taken to the digestion step immediately.

6.6.2.2. Preparation of Pneumococcal Muropeptides

About 1-2 mg of PG material produced in the previous step was suspended in 100 µL of 20 mM sodium phosphate (pH = 4.8). Lysozyme (from chicken egg white; Sigma) to a final concentration of 1.0 mg/ml or ~15 µg mutanolysin (Sigma) was added and the mixture was incubated at 37 °C for 24 h with shaking. Subsequently, the sample was heated for 10 min at 100 °C to stop the reaction. The sample was centrifuged at 21,000 × *g*, 10 min, 4 °C to collect the soluble fraction, which was transferred to a 1.5 mL epitube. For reduction, the sample was mixed with equal volume of 500 mM sodium borate (pH = 9.0) and a few crystals of $NaBH_4$. Mixture was incubated at 25 °C for 30 min. Next,

phosphoric acid 98% was added dropwise to adjust the pH at 2-3 (tested by pH paper). The resulting solution was centrifuged, supernatant collected, lyophilized and stored at -20 °C until further analysis.

6.6.2.3. Preparation of Pneumococcal Stem Peptides

Pneumococcal PG (~2 mg) was suspended in 200 µL of 25 mM sodium phosphate buffer (pH = 7.4). A total of 15 µg LytA was added in 5 µg portions at 0, 3 and 24 h time points, while the mixture was shaking at 37 °C. After 48 h, the sample was lyophilized and stored at -20 °C until further use.

6.6.2.4. HPLC Analysis of Muropeptides

Lyophilized muropeptide mixture was dissolved in 50 -20 µL 0.1% formic acid in water solution, vortexed and centrifuged at 3,000 × *g*, 3 min, room temperature to remove insoluble material. Twenty µL of the solution was run on a reverse phase HPLC system using a linear gradient of methanol as described in the general methods section.

6.6.2.5. Preparation of *B. subtilis* Muropeptides

B. subtilis peptidoglycan (1.4 mg; Sigma) was suspended in 500 µL of 20 mM sodium phosphate buffer (pH = 6.0), to which 2 × 100 U mutanolysin (Sigma) was added at 0 and 24 h time points. The mixture was incubated at 37 °C with shaking for a total of 48 h. Next, the muropeptide mixture was mixed with an equal volume of a freshly prepared solution of 0.5 M Borax containing 10 mg/mL $NaBH_4$ (pH = 8.0). After 20 min, 98% phosphoric acid solution was added to quench the reaction until the pH was acidic (tested by pH paper). The mixture was centrifuged at 21,000 × *g*, 10 min, 4 °C to pellet undigested material. The supernatant was collected and lyophilized. The sample was desalted using PD MidiTrap G-10 columns (GE Healthcare Life Sciences) according to the manufacturers

protocol. Briefly, the column was equilibrated with 16 mL MilliQ water. Sample, ~ 1.0 ml in volume, was loaded and allowed to absorb into the matrix, followed by addition of 0.7 ml MilliQ water to reach a total volume of 1.7 mL. The flow-through was collected and saved. The muropeptides were eluted by 1.2 mL of 1:1 methanol:water solution containing 0.1% formic acid. The flow-through from this step and the previous step were lyophilized to remove solvent and the dried samples were stored at -20 °C until further analysis.

6.6.2.6. Preparation of Samples for Mass Spectrometry Analysis

Ziptip ® C18 pipette tips (Millipore Sigma) were used to remove salts using the protocol from the manufacturer. MS grade water, acetonitrile (ACN) and trifluoroacetic acid (TFA) were used. Briefly, the dried samples were reconstituted with 13 µL of reconstitution solution (R; 5:95, ACN:water, 0.1% TFA), vortexed and centrifuged (sample pH must be acidic at this point; TFA was added as necessary). ZipTip was placed on a P10 pipettor set to 10 µL. The ZipTip was hydrated by aspirating solution 1 (50:50 ACN:water, 0.1% TFA) followed by solution 2 (0.1% TFA in water). Next, 10 µL of the sample was loaded by pipetting up and down 5-6 times. Next, the salts were removed by aspirating 10 µL of solution 2 (0.1% TFA in water) for a total of 4-5 washes (expel the wash into waste each time). Finally, the peptides were eluted by aspirating and expelling 1.3-20 µL of elution solution (60:40 ACN:water, 0.1% TFA) on ice 10 times (sample expelled into the same solution each time). For MALDI-TOF analysis, 1.3 µL of the elution solution and for ESI-TOF analysis, 10-20 µL was used.

6.6.2.7. MALDI-TOF Analysis of *B. subtilis* Muropeptides

To 1.3 µL of sample from the last step, 0.7 µL of saturated matrix solution (CCA; α-cyano-4-hydroxycinnamic acid) was added. The resulting mixture was spotted on a MALDI target.

6.6.3. Fluorescent Labeling of Mycobacterial PBPs

6.6.3.1. *In vivo* Bocillin-FL Labeling of Mycobacterial PBPs

Cells from 1.5 mL culture (*M. tuberculosis BCG* and *H37Ra* at OD_{600} ~0.5 and *mc*^{2}*7000* at OD_{600} ~1.5) were harvested by centrifugation at 3,500 × *g*, 15 min, 4 °C. Pellets were washed with 1 mL PBS (8.0 g NaCl, 200.0 mg KCl, 1.44 mg Na_2HPO4, 240.0 mg KH_2PO4; pH = 7.4) and pelleted again. The wash step was repeated one more time. Pellets were suspended in 100 µL PBS, half of which was stored at -80 °C. To the other half, Boc-FL was added at a final concentration of 5.0 µg/mL followed by 30 min incubation at room temperature. Samples were pelleted and washed with 1 mL PBS. Pellets were then suspended in 500 µL cold PBS, and 250 µl silicone beads was added. Cell wall disruption happened using a Vortex Disruptor Genie on maximum speed for 4 cycles of one min each on ice, with 2 min cooling time in between cycles. Next, the samples were centrifuged at 600 × *g*, 5 min, 4 °C. The supernatant, containing the cell lysates was collected and stored at -80 °C until further processing (Proteome concentration of samples were in 0.1 -0.7 mg/mL range).

6.6.3.2. Isolation of Mycobacterial Membrane

The membrane fraction from the cell pellets saved from the previous section were extracted as follows. Cell pellets were suspended in 1 mL PBS and transferred to 1 or 2 O-ring tubes, depending on the sample volume. Silicone beads (~100 µL) were added to each tube, and cells were disrupted as described previously. Next, samples were centrifuged at 600 × *g*, 5 min, 4 °C to separate the beads. The supernatant was transferred to clean tubes and centrifuged at 3,000 × *g*, 10 min, 4 °C to remove whole cells. The supernatant, containing cell lysates, was transferred to clean tubes and stored at -20 °C until further processing.

6.6.3.4. SDS PAGE Analysis of Fluorescent Labeled Samples

Polyacrylamide mini-gels were composed of 10% resolving gel (10.5 mL of 1.5 M Tris-HCl buffer pH 8.8, 10.5 mL of acrylamide:bis-acrylamide 29:1 (40% solution), 21 mL of H_2O, 140 µL of 10% ammonium persulfate (APS), 15 µL of tetramethylethylenediamine (TEMED)) and 4.5% stacking gel (2.5 mL of 0.5 M Tris-HCl buffer pH 6.8, 1.125 mL of acrylamide:bis-acrylamide 29:1 (40% solution), 6.375 mL of H_2O, 30 µL of 10% APS, 10 µL of TEMED). Samples were mixed with 4× SDS-PAGE loading buffer, heated at 95 °C for 5 min and then loaded onto the gel (10-12 µl). Running parameters were 180 V, 400 mA, and 60 W for 1.5 h. After SDS-PAGE, labeled proteins were visualized at 50-µm resolution in gels using a Typhoon 9210 gel scanner (Amersham Biosciences) with 580-nm bandpass filter for TAMRA and 670-nm bandpass filter for BODIPY 650/665. All gel images were analyzed using ImageJ software (National Institutes of Health). The background signal of the gel images was subtracted, and the brightness and contrast were adjusted to optimize the signal-to-noise ratio (all operations were performed over the entire gel uniformly).

REFERENCES

1. **Churchman JW.** 1927. The Structure of B. Anthracis and Reversal of the Gram Reaction. J Exp Med **46:**1007-1029.
2. **Knaysi G.** 1941. Observations on the Cell Division of Some Yeasts and Bacteria. J Bacteriol **41:**141-153.
3. **Salton MR, Horne RW.** 1951. Studies of the bacterial cell wall. I. Electron microscopical observations on heated bacteria. Biochim Biophys Acta **7:**19-42.
4. **Salton MR, Horne RW.** 1951. Studies of the bacterial cell wall. II. Methods of preparation and some properties of cell walls. Biochim Biophys Acta **7:**177-197.
5. **Errington J, Wu LJ.** 2017. Cell Cycle Machinery in Bacillus subtilis. Subcell Biochem **84:**67-101.
6. **Vollmer W, Blanot D, de Pedro MA.** 2008. Peptidoglycan structure and architecture. FEMS Microbiol Rev **32:**149-167.
7. **de Pedro MA, Cava F.** 2015. Structural constraints and dynamics of bacterial cell wall architecture. Front Microbiol **6:**449.
8. **Sauvage E, Kerff F, Terrak M, Ayala JA, Charlier P.** 2008. The penicillin-binding proteins: structure and role in peptidoglycan biosynthesis. FEMS Microbiol Rev **32:**234-258.
9. **Taguchi A, Kahne D, Walker S.** 2019. Chemical tools to characterize peptidoglycan synthases. Curr Opin Chem Biol **53:**44-50.
10. **Zapun A, Contreras-Martel C, Vernet T.** 2008. Penicillin-binding proteins and beta-lactam resistance. FEMS Microbiol Rev **32:**361-385.
11. **Porfirio S, Carlson RW, Azadi P.** 2019. Elucidating Peptidoglycan Structure: An Analytical Toolset: (Trends in Microbiology 27, 607-622; 2019). Trends Microbiol **27:**653-654.
12. **Sarkar P, Yarlagadda V, Ghosh C, Haldar J.** 2017. A review on cell wall synthesis inhibitors with an emphasis on glycopeptide antibiotics. Medchemcomm **8:**516-533.
13. **Schwartz B, Markwalder JA, Wang Y.** 2001. Lipid II: total synthesis of the bacterial cell wall precursor and utilization as a substrate for glycosyltransfer and transpeptidation by penicillin binding protein (PBP) 1b of Escherichia coli. J Am Chem Soc **123:**11638-11643.
14. **Silhavy TJ, Kahne D, Walker S.** 2010. The bacterial cell envelope. Cold Spring Harb Perspect Biol **2:**a000414.
15. **Macheboeuf P, Contreras-Martel C, Job V, Dideberg O, Dessen A.** 2006. Penicillin binding proteins: key players in bacterial cell cycle and drug resistance processes. FEMS Microbiol Rev **30:**673-691.
16. **Meeske AJ, Riley EP, Robins WP, Uehara T, Mekalanos JJ, Kahne D, Walker S, Kruse AC, Bernhardt TG, Rudner DZ.** 2016. SEDS proteins are a widespread family of bacterial cell wall polymerases. Nature **537:**634-638.
17. **Chambers HF, Sachdeva MJ, Hackbarth CJ.** 1994. Kinetics of penicillin binding to penicillin-binding proteins of Staphylococcus aureus. Biochem J **301 (Pt 1):**139-144.
18. **Williamson R, Hakenbeck R, Tomasz A.** 1980. In vivo interaction of beta-lactam antibiotics with the penicillin-binding proteins of Streptococcus pneumoniae. Antimicrob Agents Chemother **18:**629-637.
19. **Curtis NA, Orr D, Ross GW, Boulton MG.** 1979. Affinities of penicillins and cephalosporins for the penicillin-binding proteins of Escherichia coli K-12 and their antibacterial activity. Antimicrob Agents Chemother **16:**533-539.

20. **Scheffers DJ, Jones LJ, Errington J.** 2004. Several distinct localization patterns for penicillin-binding proteins in Bacillus subtilis. Mol Microbiol **51:**749-764.
21. **Sassine J, Xu M, Sidiq KR, Emmins R, Errington J, Daniel RA.** 2017. Functional redundancy of division specific penicillin-binding proteins in Bacillus subtilis. Mol Microbiol **106:**304-318.
22. **Tsui HC, Boersma MJ, Vella SA, Kocaoglu O, Kuru E, Peceny JK, Carlson EE, VanNieuwenhze MS, Brun YV, Shaw SL, Winkler ME.** 2014. Pbp2x localizes separately from Pbp2b and other peptidoglycan synthesis proteins during later stages of cell division of Streptococcus pneumoniae D39. Mol Microbiol **94:**21-40.
23. **Land AD, Tsui HC, Kocaoglu O, Vella SA, Shaw SL, Keen SK, Sham LT, Carlson EE, Winkler ME.** 2013. Requirement of essential Pbp2x and GpsB for septal ring closure in *Streptococcus pneumoniae* D39. Mol Microbiol **90:**939-955.
24. **Margolin W.** 2012. The price of tags in protein localization studies. J Bacteriol **194:**6369-6371.
25. **Landgraf D, Okumus B, Chien P, Baker TA, Paulsson J.** 2012. Segregation of molecules at cell division reveals native protein localization. Nat Methods **9:**480-482.
26. **Vandemoortele G, Eyckerman S, Gevaert K.** 2019. Pick a Tag and Explore the Functions of Your Pet Protein. Trends Biotechnol **37:**1078-1090.
27. **Schnell U, Dijk F, Sjollema KA, Giepmans BN.** 2012. Immunolabeling artifacts and the need for live-cell imaging. Nat Methods **9:**152-158.
28. **Jost AP, Waters JC.** 2019. Designing a rigorous microscopy experiment: Validating methods and avoiding bias. J Cell Biol **218:**1452-1466.
29. **Zhao G, Meier TI, Kahl SD, Gee KR, Blaszczak LC.** 1999. BOCILLIN FL, a sensitive and commercially available reagent for detection of penicillin-binding proteins. Antimicrob Agents Chemother **43:**1124-1128.
30. **Gee KR, Kang HC, Meier TI, Zhao G, Blaszcak LC.** 2001. Fluorescent Bocillins: synthesis and application in the detection of penicillin-binding proteins. Electrophoresis **22:**960-965.
31. **Anonymous.** 2019. Activity-Based Protein Profiling doi:10.1007/978-3-030-11143-4. Springer International Publishing.
32. **Daniel RA, Errington J.** 2003. Control of cell morphogenesis in bacteria: two distinct ways to make a rod-shaped cell. Cell **113:**767-776.
33. **Tiyanont K, Doan T, Lazarus MB, Fang X, Rudner DZ, Walker S.** 2006. Imaging peptidoglycan biosynthesis in *Bacillus subtilis* with fluorescent antibiotics. Proc Natl Acad Sci USA **103:**11033-11038.
34. **Pinho MG, Errington J.** 2003. Dispersed mode of Staphylococcus aureus cell wall synthesis in the absence of the division machinery. Mol Microbiol **50:**871-881.
35. **Ye XY, Lo MC, Brunner L, Walker D, Kahne D, Walker S.** 2001. Better substrates for bacterial transglycosylases. J Am Chem Soc **123:**3155-3156.
36. **VanNieuwenhze MS, Mauldin SC, Zia-Ebrahimi M, Aikins JA, Blaszczak LC.** 2001. The total synthesis of lipid I. J Am Chem Soc **123:**6983-6988.
37. **VanNieuwenhze MS, Mauldin SC, Zia-Ebrahimi M, Winger BE, Hornback WJ, Saha SL, Aikins JA, Blaszczak LC.** 2002. The first total synthesis of lipid II: the final monomeric intermediate in bacterial cell wall biosynthesis. J Am Chem Soc **124:**3656-3660.

38. **Qiao Y, Lebar MD, Schirner K, Schaefer K, Tsukamoto H, Kahne D, Walker S.** 2014. Detection of lipid-linked peptidoglycan precursors by exploiting an unexpected transpeptidase reaction. J Am Chem Soc **136:**14678-14681.
39. **Qiao Y, Srisuknimit V, Rubino F, Schaefer K, Ruiz N, Walker S, Kahne D.** 2017. Lipid II overproduction allows direct assay of transpeptidase inhibition by beta-lactams. Nat Chem Biol **13:**793-798.
40. **Welsh MA, Taguchi A, Schaefer K, Van Tyne D, Lebreton F, Gilmore MS, Kahne D, Walker S.** 2017. Identification of a Functionally Unique Family of Penicillin-Binding Proteins. J Am Chem Soc **139:**17727-17730.
41. **Rubino FA, Kumar S, Ruiz N, Walker S, Kahne DE.** 2018. Membrane Potential Is Required for MurJ Function. J Am Chem Soc **140:**4481-4484.
42. **Rohs PDA, Buss J, Sim SI, Squyres GR, Srisuknimit V, Smith M, Cho H, Sjodt M, Kruse AC, Garner EC, Walker S, Kahne DE, Bernhardt TG.** 2018. A central role for PBP2 in the activation of peptidoglycan polymerization by the bacterial cell elongation machinery. PLoS Genet **14:**e1007726.
43. **Taguchi A, Welsh MA, Marmont LS, Lee W, Sjodt M, Kruse AC, Kahne D, Bernhardt TG, Walker S.** 2019. FtsW is a peptidoglycan polymerase that is functional only in complex with its cognate penicillin-binding protein. Nat Microbiol **4:**587-594.
44. **Caparros M, Pisabarro AG, de Pedro MA.** 1992. Effect of D-amino acids on structure and synthesis of peptidoglycan in Escherichia coli. J Bacteriol **174:**5549-5559.
45. **Cava F, de Pedro MA, Lam H, Davis BM, Waldor MK.** 2011. Distinct pathways for modification of the bacterial cell wall by non-canonical D-amino acids. EMBO J **30:**3442-3453.
46. **Lupoli TJ, Tsukamoto H, Doud EH, Wang TS, Walker S, Kahne D.** 2011. Transpeptidase-mediated incorporation of D-amino acids into bacterial peptidoglycan. J Am Chem Soc **133:**10748-10751.
47. **Gautam S, Kim T, Spiegel DA.** 2015. Chemical probes reveal an extraseptal mode of cross-linking in Staphylococcus aureus. J Am Chem Soc **137:**7441-7447.
48. **Siegrist MS, Whiteside S, Jewett JC, Aditham A, Cava F, Bertozzi CR.** 2013. D-amino acid chemical reporters reveal peptidoglycan dynamics of an intracellular pathogen. ACS Chem Biol **8:**500-503.
49. **Liechti GW, Kuru E, Hall E, Kalinda A, Brun YV, VanNieuwenhze M, Maurelli AT.** 2014. A new metabolic cell-wall labelling method reveals peptidoglycan in Chlamydia trachomatis. Nature **506:**507-510.
50. **Liechti G, Kuru E, Packiam M, Hsu YP, Tekkam S, Hall E, Rittichier JT, VanNieuwenhze M, Brun YV, Maurelli AT.** 2016. Pathogenic Chlamydia Lack a Classical Sacculus but Synthesize a Narrow, Mid-cell Peptidoglycan Ring, Regulated by MreB, for Cell Division. PLoS Pathog **12:**e1005590.
51. **Kuru E, Hughes HV, Brown PJ, Hall E, Tekkam S, Cava F, de Pedro MA, Brun YV, VanNieuwenhze MS.** 2012. In Situ probing of newly synthesized peptidoglycan in live bacteria with fluorescent D-amino acids. Angew Chem Int Ed Engl **51:**12519-12523.
52. **Fura JM, Kearns D, Pires MM.** 2015. D-Amino Acid Probes for Penicillin Binding Protein-based Bacterial Surface Labeling. J Biol Chem **290:**30540-30550.
53. **Hsu YP, Rittichier J, Kuru E, Yablonowski J, Pasciak E, Tekkam S, Hall E, Murphy B, Lee TK, Garner EC, Huang KC, Brun YV, VanNieuwenhze MS.** 2017. Full color palette of fluorescent d-amino acids for in situ labeling of bacterial cell walls. Chem Sci **8:**6313-6321.

54. **Kuru E, Hughes HV, Brown PJ, Hall E, Tekkam S, Cava F, de Pedro MA, Brun YV, VanNieuwenhze MS.** 2012. In situ probing of newly synthesized peptidoglycan in live bacteria with fluorescent D-amino acids. Angew Chem Int Ed Engl **51:**12519-12523.
55. **Hsu YP, Hall E, Booher G, Murphy B, Radkov AD, Yablonowski J, Mulcahey C, Alvarez L, Cava F, Brun YV, Kuru E, VanNieuwenhze MS.** 2019. Fluorogenic D-amino acids enable real-time monitoring of peptidoglycan biosynthesis and high-throughput transpeptidation assays. Nat Chem **11:**335-341.
56. **Liang H, DeMeester KE, Hou CW, Parent MA, Caplan JL, Grimes CL.** 2017. Metabolic labelling of the carbohydrate core in bacterial peptidoglycan and its applications. Nat Commun **8:**15015.
57. **Wang Y, Lazor KM, DeMeester KE, Liang H, Heiss TK, Grimes CL.** 2017. Postsynthetic Modification of Bacterial Peptidoglycan Using Bioorthogonal N-Acetylcysteamine Analogs and Peptidoglycan O-Acetyltransferase B. J Am Chem Soc **139:**13596-13599.
58. **Vogel C, Marcotte EM.** 2012. Insights into the regulation of protein abundance from proteomic and transcriptomic analyses. Nat Rev Genet **13:**227-232.
59. **Sadler NC, Wright AT.** 2015. Activity-based protein profiling of microbes. Curr Opin Chem Biol **24:**139-144.
60. **Böttcher T, Sieber SA.** 2008. Beta-lactones as privileged structures for the active-site labeling of versatile bacterial enzyme classes. Angew Chem Int Ed Engl **47:**4600-4603.
61. **Edgington LE, Verdoes M, Bogyo M.** 2011. Functional imaging of proteases: recent advances in the design and application of substrate-based and activity-based probes. Curr Opin Chem Biol **15:**798-805.
62. **Withana NP, Garland M, Verdoes M, Ofori LO, Segal E, Bogyo M.** 2016. Labeling of active proteases in fresh-frozen tissues by topical application of quenched activity-based probes. Nat Protoc **11:**184-191.
63. **Weerapana E, Simon GM, Cravatt BF.** 2008. Disparate proteome reactivity profiles of carbon electrophiles. Nat Chem Biol **4:**405-407.
64. **Eirich J, Orth R, Sieber SA.** 2011. Unraveling the protein targets of vancomycin in living S. aureus and E. faecalis cells. J Am Chem Soc **133:**12144-12153.
65. **Pearson RG.** 1990. Hard and Soft Acids and Bases - the Evolution of a Chemical Concept. Coordination Chemistry Reviews **100:**403-425.
66. **Narayanan A, Jones LH.** 2015. Sulfonyl fluorides as privileged warheads in chemical biology. Chem Sci **6:**2650-2659.
67. **Leriche G, Chisholm L, Wagner A.** 2012. Cleavable linkers in chemical biology. Bioorg Med Chem **20:**571-582.
68. **Rudolf GC, Heydenreuter W, Sieber SA.** 2013. Chemical proteomics: ligation and cleavage of protein modifications. Curr Opin Chem Biol **17:**110-117.
69. **Kim HY, Tallman KA, Liebler DC, Porter NA.** 2009. An azido-biotin reagent for use in the isolation of protein adducts of lipid-derived electrophiles by streptavidin catch and photorelease. Mol Cell Proteomics **8:**2080-2089.
70. **Orth R, Sieber SA.** 2009. A photolabile linker for the mild and selective cleavage of enriched biomolecules from solid support. J Org Chem **74:**8476-8479.
71. **Yang Y, Verhelst SH.** 2013. Cleavable trifunctional biotin reagents for protein labelling, capture and release. Chem Commun (Camb) **49:**5366-5368.
72. **Sadaghiani AM, Verhelst SH, Bogyo M.** 2007. Tagging and detection strategies for activity-based proteomics. Curr Opin Chem Biol **11:**20-28.

73. **Bogyo M, Verhelst S, Bellingard-Dubouchaud V, Toba S, Greenbaum D.** 2000. Selective targeting of lysosomal cysteine proteases with radiolabeled electrophilic substrate analogs. Chem Biol **7:**27-38.
74. **Patricelli MP, Giang DK, Stamp LM, Burbaum JJ.** 2001. Direct visualization of serine hydrolase activities in complex proteomes using fluorescent active site-directed probes. Proteomics **1:**1067-1071.
75. **McKay CS, Finn MG.** 2014. Click chemistry in complex mixtures: bioorthogonal bioconjugation. Chem Biol **21:**1075-1101.
76. **Hang HC, Yu C, Kato DL, Bertozzi CR.** 2003. A metabolic labeling approach toward proteomic analysis of mucin-type O-linked glycosylation. Proc Natl Acad Sci U S A **100:**14846-14851.
77. **Sletten EM, Bertozzi CR.** 2011. From mechanism to mouse: a tale of two bioorthogonal reactions. Acc Chem Res **44:**666-676.
78. **Lang K, Chin JW.** 2014. Bioorthogonal reactions for labeling proteins. ACS Chem Biol **9:**16-20.
79. **Kolb HC, Finn MG, Sharpless KB.** 2001. Click Chemistry: Diverse Chemical Function from a Few Good Reactions. Angew Chem Int Ed Engl **40:**2004-2021.
80. **Kolb HC, Sharpless KB.** 2003. The growing impact of click chemistry on drug discovery. Drug Discov Today **8:**1128-1137.
81. **Rostovtsev VV, Green LG, Fokin VV, Sharpless KB.** 2002. A stepwise huisgen cycloaddition process: copper(I)-catalyzed regioselective "ligation" of azides and terminal alkynes. Angew Chem Int Ed Engl **41:**2596-2599.
82. **Speers AE, Cravatt BF.** 2004. Profiling enzyme activities in vivo using click chemistry methods. Chem Biol **11:**535-546.
83. **Agard NJ, Baskin JM, Prescher JA, Lo A, Bertozzi CR.** 2006. A comparative study of bioorthogonal reactions with azides. ACS Chem Biol **1:**644-648.
84. **Agard NJ, Prescher JA, Bertozzi CR.** 2004. A strain-promoted [3 + 2] azide-alkyne cycloaddition for covalent modification of biomolecules in living systems. J Am Chem Soc **126:**15046-15047.
85. **Beatty KE, Fisk JD, Smart BP, Lu YY, Szychowski J, Hangauer MJ, Baskin JM, Bertozzi CR, Tirrell DA.** 2010. Live-cell imaging of cellular proteins by a strain-promoted azide-alkyne cycloaddition. Chembiochem **11:**2092-2095.
86. **Chang PV, Prescher JA, Sletten EM, Baskin JM, Miller IA, Agard NJ, Lo A, Bertozzi CR.** 2010. Copper-free click chemistry in living animals. Proc Natl Acad Sci U S A **107:**1821-1826.
87. **Ekkebus R, van Kasteren SI, Kulathu Y, Scholten A, Berlin I, Geurink PP, de Jong A, Goerdayal S, Neefjes J, Heck AJ, Komander D, Ovaa H.** 2013. On terminal alkynes that can react with active-site cysteine nucleophiles in proteases. J Am Chem Soc **135:**2867-2870.
88. **Wu H, Devaraj NK.** 2018. Advances in Tetrazine Bioorthogonal Chemistry Driven by the Synthesis of Novel Tetrazines and Dienophiles. Acc Chem Res doi:10.1021/acs.accounts.8b00062.
89. **Kocaoglu O, Calvo RA, Sham LT, Cozy LM, Lanning BR, Francis S, Winkler ME, Kearns DB, Carlson EE.** 2012. Selective penicillin-binding protein imaging probes reveal substructure in bacterial cell division. ACS Chem Biol **7:**1746-1753.
90. **Sharifzadeh S, Boersma MJ, Kocaoglu O, Shokri A, Brown CL, Shirley JD, Winkler ME, Carlson EE.** 2017. Novel Electrophilic Scaffold for Imaging of Essential Penicillin-Binding Proteins in Streptococcus pneumoniae. ACS Chem Biol **12:**2849-2857.

91. **Jessani N, Niessen S, Wei BQ, Nicolau M, Humphrey M, Ji Y, Han W, Noh DY, Yates JR, 3rd, Jeffrey SS, Cravatt BF.** 2005. A streamlined platform for high-content functional proteomics of primary human specimens. Nat Methods **2:**691-697.
92. **Speers AE, Cravatt BF.** 2009. Activity-Based Protein Profiling (ABPP) and Click Chemistry (CC)-ABPP by MudPIT Mass Spectrometry. Curr Protoc Chem Biol **1:**29-41.
93. **Weerapana E, Speers AE, Cravatt BF.** 2007. Tandem orthogonal proteolysis-activity-based protein profiling (TOP-ABPP)--a general method for mapping sites of probe modification in proteomes. Nat Protoc **2:**1414-1425.
94. **Verheggen K, Raeder H, Berven FS, Martens L, Barsnes H, Vaudel M.** 2017. Anatomy and evolution of database search engines-a central component of mass spectrometry based proteomic workflows. Mass Spectrom Rev doi:10.1002/mas.21543.
95. **Weerapana E, Wang C, Simon GM, Richter F, Khare S, Dillon MB, Bachovchin DA, Mowen K, Baker D, Cravatt BF.** 2010. Quantitative reactivity profiling predicts functional cysteines in proteomes. Nature **468:**790-795.
96. **Cardoza JD, Parikh JR, Ficarro SB, Marto JA.** 2012. Mass spectrometry-based proteomics: qualitative identification to activity-based protein profiling. Wiley Interdiscip Rev Syst Biol Med **4:**141-162.
97. **Chen X, Wong YK, Wang J, Zhang J, Lee YM, Shen HM, Lin Q, Hua ZC.** 2017. Target identification with quantitative activity based protein profiling (ABPP). Proteomics **17**.
98. **Wang S, Tian Y, Wang M, Wang M, Sun GB, Sun XB.** 2018. Advanced Activity-Based Protein Profiling Application Strategies for Drug Development. Front Pharmacol **9:**353.
99. **Wright MH, Sieber SA.** 2016. Chemical proteomics approaches for identifying the cellular targets of natural products. Nat Prod Rep **33:**681-708.
100. **Sharifzadeh S, Shirley JD, Carlson EE.** 2019. Activity-Based Protein Profiling Methods to Study Bacteria: The Power of Small-Molecule Electrophiles. Curr Top Microbiol Immunol **420:**23-48.
101. **Staub I, Sieber SA.** 2008. β-Lactams as selective chemical probes for the in vivo labeling of bacterial enzymes involved in cell wall biosynthesis, antibiotic resistance, and virulence. J Am Chem Soc **130:**13400-13409.
102. **Kocaoglu O, Carlson EE.** 2013. Penicillin-binding protein imaging probes. Curr Protoc Chem Biol **5:**239-250.
103. **Wei Y, Havasy T, McPherson DC, Popham DL.** 2003. Rod shape determination by the Bacillus subtilis class B penicillin-binding proteins encoded by pbpA and pbpH. J Bacteriol **185:**4717-4726.
104. **Foster SJ, Popham DL.** 2002. Structure and synthesis of cell wall, spore cortex, teichoic acids, S-layers, and capsules., p -. *In* Sonenshein L, Losick, R., and Hoch, J.A. (ed), Bacillus subtilis and its close relatives: from genes to cells. American Society for Microbiology, Washington, D. C.
105. **Atrih A, Bacher G, Allmaier G, Williamson MP, Foster SJ.** 1999. Analysis of peptidoglycan structure from vegetative cells of Bacillus subtilis 168 and role of PBP 5 in peptidoglycan maturation. J Bacteriol **181:**3956-3966.
106. **Meador-Parton J, Popham DL.** 2000. Structural analysis of Bacillus subtilis spore peptidoglycan during sporulation. J Bacteriol **182:**4491-4499.
107. **Popham DL.** 2002. Specialized peptidoglycan of the bacterial endospore: the inner wall of the lockbox. Cell Mol Life Sci **59:**426-433.

108. **Reusch VM, Jr., Hale SG, Hurly BJ.** 1982. Levels of cell wall enzymes in endospores and vegetative cells of Bacillus subtilis. J Bacteriol **152:**1147-1153.
109. **McPherson DC, Driks A, Popham DL.** 2001. Two class A high-molecular-weight penicillin-binding proteins of Bacillus subtilis play redundant roles in sporulation. J Bacteriol **183:**6046-6053.
110. **Buchanan CE, Gustafson A.** 1992. Mutagenesis and mapping of the gene for a sporulation-specific penicillin-binding protein in Bacillus subtilis. J Bacteriol **174:**5430-5435.
111. **Blumberg PM, Strominger JL.** 1972. Five penicillin-binding components occur in Bacillus subtilis membranes. J Biol Chem **247:**8107-8113.
112. **Blumberg PM, Strominger JL.** 1972. Isolation by covalent affinity chromatography of the penicillin-binding components from membranes of Bacillus subtilis. Proc Natl Acad Sci U S A **69:**3751-3755.
113. **Buchanan CE, Strominger JL.** 1976. Altered penicillin-binding components in penicillin-resistant mutants of Bacillus subtilis. Proc Natl Acad Sci U S A **73:**1816-1820.
114. **Horikawa S, Ogawara H.** 1980. Penicillin-binding proteins in Bacillus subtilis. The effects on penicillin-binding proteins and the antibacterial activities of beta-lactams. J Antibiot (Tokyo) **33:**614-619.
115. **Kocaoglu O, Carlson EE.** 2015. Profiling of β-Lactam Selectivity for Penicillin-Binding Proteins in *Escherichia coli* DC2. Antimicrob Agents Chemother **59:**2785-2790.
116. **Kocaoglu O, Tsui H-CT, Winkler ME, Carlson EE.** 2015. Profiling of β-Lactam Selectivity for Penicillin-Binding Proteins in *Streptococcus pneumoniae* D39. Antimicrob Agents Chemother **59:**3548-3555.
117. **Waxman DJ, Strominger JL.** 1983. Penicillin-binding proteins and the mechanism of action of beta-lactam antibiotics. Annu Rev Biochem **52:**825-869.
118. **McPherson DC, Popham DL.** 2003. Peptidoglycan synthesis in the absence of class A penicillin-binding proteins in Bacillus subtilis. J Bacteriol **185:**1423-1431.
119. **Popham DL, Setlow P.** 1995. Cloning, nucleotide sequence, and mutagenesis of the Bacillus subtilis ponA operon, which codes for penicillin-binding protein (PBP) 1 and a PBP-related factor. J Bacteriol **177:**326-335.
120. **Popham DL, Setlow P.** 1994. Cloning, nucleotide sequence, mutagenesis, and mapping of the Bacillus subtilis pbpD gene, which codes for penicillin-binding protein 4. J Bacteriol **176:**7197-7205.
121. **Popham DL, Setlow P.** 1996. Phenotypes of Bacillus subtilis mutants lacking multiple class A high-molecular-weight penicillin-binding proteins. J Bacteriol **178:**2079-2085.
122. **Pedersen LB, Angert ER, Setlow P.** 1999. Septal localization of penicillin-binding protein 1 in Bacillus subtilis. J Bacteriol **181:**3201-3211.
123. **Shohayeb M, Chopra I.** 1987. Mutations affecting penicillin-binding proteins 2a, 2b and 3 in Bacillus subtilis alter cell shape and peptidoglycan metabolism. J Gen Microbiol **133:**1733-1742.
124. **Murray T, Popham DL, Pearson CB, Hand AR, Setlow P.** 1998. Analysis of outgrowth of Bacillus subtilis spores lacking penicillin-binding protein 2a. J Bacteriol **180:**6493-6502.
125. **Yanouri A, Daniel RA, Errington J, Buchanan CE.** 1993. Cloning and sequencing of the cell division gene pbpB, which encodes penicillin-binding protein 2B in Bacillus subtilis. J Bacteriol **175:**7604-7616.
126. **Morales Angeles D, Liu Y, Hartman AM, Borisova M, de Sousa Borges A, de Kok N, Beilharz K, Veening JW, Mayer C, Hirsch AK, Scheffers DJ.** 2017.

Pentapeptide-rich peptidoglycan at the Bacillus subtilis cell-division site. Mol Microbiol **104:**319-333.
127. **Murray T, Popham DL, Setlow P.** 1996. Identification and characterization of pbpC, the gene encoding Bacillus subtilis penicillin-binding protein 3. J Bacteriol **178:**6001-6005.
128. **Popham DL, Gilmore ME, Setlow P.** 1999. Roles of low-molecular-weight penicillin-binding proteins in Bacillus subtilis spore peptidoglycan synthesis and spore properties. J Bacteriol **181:**126-132.
129. **Popham DL, Illades-Aguiar B, Setlow P.** 1995. The Bacillus subtilis dacB gene, encoding penicillin-binding protein 5*, is part of a three-gene operon required for proper spore cortex synthesis and spore core dehydration. J Bacteriol **177:**4721-4729.
130. **Spratt BG, Pardee AB.** 1975. Penicillin-binding proteins and cell shape in *E. coli*. Nature **254:**516-517.
131. **Dougherty TJ, Kennedy K, Kessler RE, Pucci MJ.** 1996. Direct quantitation of the number of individual penicillin-binding proteins per cell in Escherichia coli. J Bacteriol **178:**6110-6115.
132. **Schroeder JW, Simmons LA.** 2013. Complete Genome Sequence of Bacillus subtilis Strain PY79. Genome Announc **1**.
133. **Sonenshein AL HJ, Losick R.** 1993. Bacillus subtilis and other GRam-positive bacteria: biochemistry, physiology and molecular genetics. American Society for Microbiology Washington, DC.
134. **Kleppe G, Strominger JL.** 1979. Studies of the high molecular weight penicillin-binding proteins of Bacillus subtilis. J Biol Chem **254:**4856-4862.
135. **Reynolds PE, Shepherd ST, Chase HA.** 1978. Identification of the binding protein which may be the target of penicillin action in Bacillus megaterium. Nature **271:**568-570.
136. **Papp-Wallace KM, Endimiani A, Taracila MA, Bonomo RA.** 2011. Carbapenems: past, present, and future. Antimicrob Agents Chemother **55:**4943-4960.
137. **Queenan AM, Shang W, Flamm R, Bush K.** 2010. Hydrolysis and inhibition profiles of beta-lactamases from molecular classes A to D with doripenem, imipenem, and meropenem. Antimicrob Agents Chemother **54:**565-569.
138. **Jackson JJ, Kropp H.** 1992. beta-Lactam antibiotic-induced release of free endotoxin: in vitro comparison of penicillin-binding protein (PBP) 2-specific imipenem and PBP 3-specific ceftazidime. J Infect Dis **165:**1033-1041.
139. **Horii T, Ichiyama S, Ohta M, Kobayashi M.** 1999. Relationship between morphological changes and endotoxin release induced by carbapenems in Pseudomonas aeruginosa. J Med Microbiol **48:**309-315.
140. **Sumita Y, Fukasawa M.** 1995. Potent activity of meropenem against Escherichia coli arising from its simultaneous binding to penicillin-binding proteins 2 and 3. J Antimicrob Chemother **36:**53-64.
141. **Trautmann M, Heinemann M, Zick R, Moricke A, Seidelmann M, Berger D.** 1998. Antibacterial activity of meropenem against Pseudomonas aeruginosa, including antibiotic-induced morphological changes and endotoxin-liberating effects. Eur J Clin Microbiol Infect Dis **17:**754-760.
142. **Davies TA, Shang W, Bush K, Flamm RK.** 2008. Affinity of doripenem and comparators to penicillin-binding proteins in Escherichia coli and Pseudomonas aeruginosa. Antimicrob Agents Chemother **52:**1510-1512.
143. **Kleppe G, Yu W, Strominger JL.** 1982. Penicillin-binding proteins in Bacillus subtilis mutants. Antimicrob Agents Chemother **21:**979-983.

144. **Neyman SL, Buchanan CE.** 1985. Restoration of vegetative penicillin-binding proteins during germination and outgrowth of Bacillus subtilis spores: relationship of individual proteins to specific cell cycle events. J Bacteriol **161:**164-168.
145. **Kocaoglu O, Carlson EE.** 2015. Profiling of beta-lactam selectivity for penicillin-binding proteins in Escherichia coli strain DC2. Antimicrob Agents Chemother **59:**2785-2790.
146. **Kocaoglu O, Tsui HC, Winkler ME, Carlson EE.** 2015. Profiling of beta-lactam selectivity for penicillin-binding proteins in Streptococcus pneumoniae D39. Antimicrob Agents Chemother **59:**3548-3555.
147. **Hamilton SM, Alexander JAN, Choo EJ, Basuino L, da Costa TM, Severin A, Chung M, Aedo S, Strynadka NCJ, Tomasz A, Chatterjee SS, Chambers HF.** 2017. High-Level Resistance of Staphylococcus aureus to beta-Lactam Antibiotics Mediated by Penicillin-Binding Protein 4 (PBP4). Antimicrob Agents Chemother **61**.
148. **Chatterjee SS, Chen L, Gilbert A, da Costa TM, Nair V, Datta SK, Kreiswirth BN, Chambers HF.** 2017. PBP4 Mediates beta-Lactam Resistance by Altered Function. Antimicrob Agents Chemother **61**.
149. **Park JT, Burman L.** 1973. FL-1060: a new penicillin with a unique mode of action. Biochem Biophys Res Commun **51:**863-868.
150. **Den Blaauwen T, Aarsman ME, Vischer NO, Nanninga N.** 2003. Penicillin-binding protein PBP2 of Escherichia coli localizes preferentially in the lateral wall and at mid-cell in comparison with the old cell pole. Mol Microbiol **47:**539-547.
151. **Spratt BG.** 1975. Distinct penicillin binding proteins involved in the division, elongation, and shape of Escherichia coli K12. Proc Natl Acad Sci U S A **72:**2999-3003.
152. **Daniel RA, Harry EJ, Errington J.** 2000. Role of penicillin-binding protein PBP 2B in assembly and functioning of the division machinery of Bacillus subtilis. Mol Microbiol **35:**299-311.
153. **Penna TC, Ishii M, Junior AP, Cholewa O.** 2004. Thermal stability of recombinant green fluorescent protein (GFPuv) at various pH values. Appl Biochem Biotechnol **113-116:**469-483.
154. **Kimata Y, Iwaki M, Lim CR, Kohno K.** 1997. A novel mutation which enhances the fluorescence of green fluorescent protein at high temperatures. Biochem Biophys Res Commun **232:**69-73.
155. **Frederiksen SM, Grue-Sorensen G.** 2003. Synthesis of tritium labelled mecillinam. Journal of Labelled Compounds & Radiopharmaceuticals **46:**773-779.
156. **Falconer SB, Czarny TL, Brown ED.** 2011. Antibiotics as probes of biological complexity. Nat Chem Biol **7:**415-423.
157. **Böttcher T, Sieber SA.** 2012. β-Lactams and β-lactones as activity-based probes in chemical biology. Med Chem Commun **3:**408-417.
158. **Lakaye B, Damblon C, Jamin M, Galleni M, Lepage S, Joris B, Marchand-Brynaert J, Frydrych C, Frere J-M.** 1994. Synthesis, purification and kinetic properties of fluorescein-labelled penicillins. Biochem J **300:**141-145.
159. **Ghuysen JM.** 1977. The Bacterial DD-Carboxypeptidase-Transpeptidase Enzyme System. Part III. Interactions with Penicillin. University of Tokyo Press, Tokyo, Japan.
160. **Swulius MT, Jensen GJ.** 2012. The helical MreB cytoskeleton in Escherichia coli MC1000/pLE7 is an artifact of the N-Terminal yellow fluorescent protein tag. J Bacteriol **194:**6382-6386.

161. **Lebar MD, May JM, Meeske AJ, Leiman SA, Lupoli TJ, Tsukamoto H, Losick R, Rudner DZ, Walker S, Kahne DE.** 2014. Reconstitution of peptidoglycan cross-linking leads to improved fluorescent probes of cell wall synthesis. J Am Chem Soc **136:**10874-10877.
162. **Pidgeon SE, Fura JM, Leon W, Birabaharan M, Vezenov D, Pires MM.** 2015. Metabolic profiling of bacteria by unnatural C-terminated D-amino acids. Angew Chem Int Ed **54:**6158-6162.
163. **Dargis M, Malouin F.** 1994. Use of biotinylated beta-lactams and chemiluminescence for study and purification of penicillin-binding proteins in bacteria. Antimicrob Agents Chemother **38:**973-980.
164. **Kim DH, Park JI, Chung SJ, Park JD, Park NK, Han JH.** 2002. Cleavage of beta-lactone ring by serine protease. Mechanistic implications. Bioorg Med Chem **10:**2553-2560.
165. **Venukadasula PKM, Chegondi R, Maitra S, Hanson PR.** 2010. A Concise, Phosphate-Mediated Approach to the Total Synthesis of (-)-Tetrahydrolipstatin Org Lett **12:**1556-1559.
166. **Lawasut P, Chauhan D, Laubach J, Hayes C, Fabre C, Maglio M, Mitsiades C, Hideshima T, Anderson KC, Richardson PG.** 2012. New proteasome inhibitors in myeloma. Curr Hematol Malig Rep **7:**258-266.
167. **Basha RH, Sankaranarayanan C.** 2016. beta-Caryophyllene, a natural sesquiterpene lactone attenuates hyperglycemia mediated oxidative and inflammatory stress in experimental diabetic rats. Chem Biol Interact **245:**50-58.
168. **Wells JS, Hunter JC, Astle GL, Sherwood JC, Ricca CM, Trejo WH, Bonner DP, Sykes RB.** 1982. Distribution of beta-lactam and beta-lactone producing bacteria in nature. J Antibiot (Tokyo) **35:**814-821.
169. **Aldridge DC, Giles D, Turner WB.** 1971. Antibiotic 1233A: a fungal beta-lactone. J Chem Soc Perkin 1 **23:**3888-3891.
170. **Tymiak AA, Culver CA, Malley MF, Gougoutas JZ.** 1985. Structure of obafluorin: an antibacterial beta-lactone from pseudomonas fluorescens. J Org Chem **50:**5491-5495.
171. **Parker WL, Rathnum ML, Liu WC.** 1982. SQ 26,517 A beta-lactone produced by a Bacillus species. J Antibiot **35:**900-902.
172. **Ravindran MS, Rao SP, Cheng X, Shukla A, Cazenave-Gassiot A, Yao SQ, Wenk MR.** 2013. Targeting lipid esterases in mycobacteria grown under different physiological conditions using activity-based profiling with tetrahydrolipstatin (THL). Mol Cell Proteomics **13:**435-448.
173. **Christenson JK, Richman JE, Jensen MR, Neufeld JY, Wilmot CM, Wackett LP.** 2017. β-Lactone Synthetase Found in the Olefin Biosynthesis Pathway. Biochemistry **56:**348-351.
174. **Schaffer JE, Reck MR, Prasad NK, Wencewicz TA.** 2017. β-Lactone formation during product release from a nonribosomal peptide synthetase. Nat Chem Bio **13:**737-744.
175. **Wolf F, Bauer JS, Bendel TM, Kulik A, Kalinowski J, Gross H, Kaysser L.** 2017. Biosynthesis of the β-lactone proteasome inhibitors belactosin and cystargolide. Angew Chem Int Ed **56:**6665-6668.
176. **Robinson SL, Christenson JK, Wackett LP.** 2019. Biosynthesis and chemical diversity of beta-lactone natural products. Nat Prod Rep **36:**458-475.
177. **Wells JS, Trejo WH, Principe PA, Sykes RB.** 1984. Obafluorin, a novel beta-lactone produced by Pseudomonas fluorescens. Taxomony, fermentation and biological properties. J Antibiot **37:**802-803.

178. **Böttcher T, Sieber SA.** 2008. Beta-lactones as specific inhibitors of ClpP attenuate the production of extracellular virulence factors of Staphylococcus aureus. J Am Chem Soc **130:**14400-14401.
179. **Zeiler E, Braun N, Bottcher T, Kastenmuller A, Weinkauf S, Sieber SA.** 2011. Vibralactone as a tool to study the activity and structure of the ClpP1P2 complex from Listeria monocytogenes. Angew Chem Int Ed Engl **50:**11001-11004.
180. **Compton CL, Schmitz KR, Sauer RT, Sello JK.** 2013. Antibacterial activity of and resistance to small molecule inhibitors of the ClpP Peptidase. ACS Chem Biol **8:**2669-2677.
181. **Pu Y, Lowe C, Sailer M, Vederas JC.** 1994. Synthesis, Stability and Antimicrobial Activity of (+)-Obafluorin and Related beta-Lactone Antibiotics. J Org Chem **59:**3642-3655.
182. **Wang Z, Gu C, Colby T, Shindo T, Balamurugan R, Waldmann H, Kaiser M, van der Hoorn RA.** 2008. Beta-lactone probes identify a papain-like peptide ligase in Arabidopsis thaliana. Nat Chem Biol **4:**557-563.
183. **Duranti A, Tontini A, Antonietti F, Vacondio F, Fioni A, Silva C, Lodola A, Rivara S, Solorzano C, Piomelli D, Tarzia G, Mor M.** 2012. N-(2-oxo-3-oxetanyl)carbamic acid esters as N-acylethanolamine acid amidase inhibitors: synthesis and structure-activity and structure-property relationships. J Med Chem **55:**4824-4836.
184. **Welsh MA, Blackwell HE.** 2016. Chemical probes of quorum sensing: from compound development to biological discovery. FEMS Microbiol Rev **40:**774-794.
185. **Konaklieva MI.** 2014. Molecular targets of β-lactam-based antibiotics: Beyond the usual suspects. Antibiotics **3:**128-142.
186. **Yamada M, Watanabe T, Baba N, Takeuchi Y, Ohsawa F, Gomi S.** 2008. Crystal Structures of Biapenem and Tebipenem Complexed with Penicillin-Binding Proteins 2X and 1A from *Streptococcus pneumoniae*. Antimicrob Agents Chemother **52:**2053-2060.
187. **Henriques-Normark B, Tuomanen EI.** 2013. The pneumococcus: epidemiology, microbiology, and pathogenesis. Cold Spring Harb Perspect Med **3:**a010215.
188. **Morlot C, Pernot L, Le Gouellec A, Di Guilmi AM, Vernet T, Dideberg O, Dessen A.** 2005. Crystal structure of a peptidoglycan synthesis regulatory factor (PBP3) from Streptococcus pneumoniae. J Biol Chem **280:**15984-15991.
189. **Speers AE, Cravatt BF.** 2005. A tandem orthogonal proteolysis strategy for high-content chemical proteomics. J Am Chem Soc **127:**10018-10019.
190. **Mouz N, Di Guilmi AM, Gordon E, Hakenbeck R, Dideberg O, Vernet T.** 1999. Mutations in the active site of penicillin-binding protein PBP2x from Streptococcus pneumoniae. Role in the specificity for beta-lactam antibiotics. J Biol Chem **274:**19175-19180.
191. **Berg KH, Stamsas GA, Straume D, Havarstein LS.** 2013. Effects of low PBP2b levels on cell morphology and peptidoglycan composition in Streptococcus pneumoniae R6. J Bacteriol **195:**4342-4354.
192. **Hakenbeck R, Bruckner R, Denapaite D, Maurer P.** 2012. Molecular mechanisms of beta-lactam resistance in Streptococcus pneumoniae. Future Microbiol **7:**395-410.
193. **Nagai K, Davies TA, Jacobs MR, Appelbaum PC.** 2002. Effects of amino acid alterations in penicillin-binding proteins (PBPs) 1a, 2b, and 2x on PBP affinities of penicillin, ampicillin, amoxicillin, cefditoren, cefuroxime, cefprozil, and cefaclor in 18 clinical isolates of penicillin-susceptible, -intermediate, and -resistant pneumococci. Antimicrob Agents Chemother **46:**1273-1280.

194. **Maurer P, Todorova K, Sauerbier J, Hakenbeck R.** 2012. Mutations in Streptococcus pneumoniae penicillin-binding protein 2x: importance of the C-terminal penicillin-binding protein and serine/threonine kinase-associated domains for beta-lactam binding. Microb Drug Resist **18:**314-321.
195. **Fleurie A, Manuse S, Zhao C, Campo N, Cluzel C, Lavergne JP, Freton C, Combet C, Guiral S, Soufi B, Macek B, Kuru E, VanNieuwenhze MS, Brun YV, Di Guilmi AM, Claverys JP, Galinier A, Grangeasse C.** 2014. Interplay of the serine/threonine-kinase StkP and the paralogs DivIVA and GpsB in pneumococcal cell elongation and division. PLoS Genet **10:**e1004275.
196. **Land AD, Winkler ME.** 2011. The requirement for pneumococcal MreC and MreD is relieved by inactivation of the gene encoding PBP1a. J Bacteriol **193:**4166-4179.
197. **Boersma MJ, Kuru E, Rittichier JT, VanNieuwenhze MS, Brun YV, Winkler ME.** 2015. Minimal Peptidoglycan (PG) Turnover in Wild-Type and PG Hydrolase and Cell Division Mutants of *Streptococcus pneumoniae* D39 Growing Planktonically and in Host-Relevant Biofilms. J Bacteriol **197:**3472-3485.
198. **Rued BE, Zheng JJ, Mura A, Tsui H-CT, Boersma MJ, Mazny JL, Corona F, Perez AJ, Fadda D, Doubravová L, Buriánkova K, Branny P, Massidda O, Winkler ME.** 2017. Suppression and synthetic-lethal genetic relationships of ΔgpsB mutations indicate that GpsB mediates protein phosphorylation and penicillin-binding protein interactions in Streptococcus pneumoniae D39. Mol Microbiol **103:**931-957.
199. **Tsui H-CT, Land AD, Kocaoglu O, Vella S, Carlson EE, Winkler ME.** 2013. PBP2x and GpsB Are Essential for Septal Formation in *Streptococcus pneumoniae* D39. Mol Microbiol **90:**939-955.
200. **Tsui H-C, Zheng JJ, Magallon AN, Ryan JD, Yunck R, Rued BE, Bernhardt TG, Winkler ME.** 2016. Suppression of a deletion mutation in the gene encoding essential PBP2b reveals a new lytic transglycosylase involved in peripheral peptidoglycan synthesis in Streptococcus pneumoniae D39. Mol Microbiol **100:**1039-1065.
201. **Grebe T, Hakenbeck R.** 1996. Penicillin-binding proteins 2b and 2x of *Streptococcus pneumoniae* are primary resistance determinants for different classes of beta-lactam antibiotics. Antimicrob Agents Chemther **40:**829-834.
202. **Peters K, Schweizer I, Beilharz K, Stahlmann C, Veening JW, Hakenbeck R, Denapaite D.** 2014. Streptococcus pneumoniae PBP2x mid-cell localization requires the C-terminal PASTA domains and is essential for cell shape maintenance. Mol Microbiol **92:**733-755.
203. **Kunst F, Ogasawara N, Moszer I, Albertini AM, Alloni G, Azevedo V, Bertero MG, Bessieres P, Bolotin A, Borchert S, Borriss R, Boursier L, Brans A, Braun M, Brignell SC, Bron S, Brouillet S, Bruschi CV, Caldwell B, Capuano V, Carter NM, Choi SK, Cordani JJ, Connerton IF, Cummings NJ, Daniel RA, Denziot F, Devine KM, Dusterhoft A, Ehrlich SD, Emmerson PT, Entian KD, Errington J, Fabret C, Ferrari E, Foulger D, Fritz C, Fujita M, Fujita Y, Fuma S, Galizzi A, Galleron N, Ghim SY, Glaser P, Goffeau A, Golightly EJ, Grandi G, Guiseppi G, Guy BJ, Haga K, et al.** 1997. The complete genome sequence of the gram-positive bacterium Bacillus subtilis. Nature **390:**249-256.
204. **Pereira SF, Henriques AO, Pinho MG, de Lencastre H, Tomasz A.** 2009. Evidence for a dual role of PBP1 in the cell division and cell separation of Staphylococcus aureus. Mol Microbiol **72:**895-904.
205. **Reed P, Atilano ML, Alves R, Hoiczyk E, Sher X, Reichmann NT, Pereira PM, Roemer T, Filipe SR, Pereira-Leal JB, Ligoxygakis P, Pinho MG.** 2015.

Staphylococcus aureus Survives with a Minimal Peptidoglycan Synthesis Machine but Sacrifices Virulence and Antibiotic Resistance. PLoS Pathog **11:**e1004891.
206. **Mouz N, Gordon E, Di Guilmi AM, Petit I, Petillot Y, Dupont Y, Hakenbeck R, Vernet T, Dideberg O.** 1998. Identification of a structural determinant for resistance to beta-lactam antibiotics in Gram-positive bacteria. Proc Natl Acad Sci U S A **95:**13403-13406.
207. **Zhao G, Meier TI, Kahl SD, Gee KR, Blaszczak LC.** 1999. BOCILLIN FL, a sensitive and commercially available reagent for detection of penicillin-binding proteins. Antimicrob Agents Chemother **43:**1124-1128.
208. **Arrowsmith CH, Audia JE, Austin C, Baell J, Bennett J, Blagg J, Bountra C, Brennan PE, Brown PJ, Bunnage ME, Buser-Doepner C, Campbell RM, Carter AJ, Cohen P, Copeland RA, Cravatt B, Dahlin JL, Dhanak D, Edwards AM, Frederiksen M, Frye SV, Gray N, Grimshaw CE, Hepworth D, Howe T, Huber KV, Jin J, Knapp S, Kotz JD, Kruger RG, Lowe D, Mader MM, Marsden B, Mueller-Fahrnow A, Muller S, O'Hagan RC, Overington JP, Owen DR, Rosenberg SH, Roth B, Ross R, Schapira M, Schreiber SL, Shoichet B, Sundstrom M, Superti-Furga G, Taunton J, Toledo-Sherman L, Walpole C, Walters MA, et al.** 2015. The promise and peril of chemical probes. Nat Chem Biol **11:**536-541.
209. **Shannon DA, Weerapana E.** 2015. Covalent protein modification: the current landscape of residue-specific electrophiles. Curr Opin Chem Biol **24:**18-26.
210. **Azarkan M, Huet J, Baeyens-Volant D, Looze Y, Vandenbussche G.** 2007. Affinity chromatography: a useful tool in proteomics studies. J Chromatogr B Analyt Technol Biomed Life Sci **849:**81-90.
211. **Sun SX, Jiang H.** 2011. Physics of bacterial morphogenesis. Microbiol Mol Biol Rev **75:**543-565.
212. **Lovering AL, Safadi SS, Strynadka NC.** 2012. Structural perspective of peptidoglycan biosynthesis and assembly. Annu Rev Biochem **81:**451-478.
213. **Typas A, Banzhaf M, Gross CA, Vollmer W.** 2011. From the regulation of peptidoglycan synthesis to bacterial growth and morphology. Nat Rev Microbiol **10:**123-136.
214. **Massidda O, Novakova L, Vollmer W.** 2013. From models to pathogens: how much have we learned about Streptococcus pneumoniae cell division? Environ Microbiol **15:**3133-3157.
215. **Egan AJ, Vollmer W.** 2013. The physiology of bacterial cell division. Ann N Y Acad Sci **1277:**8-28.
216. **de Boer PA.** 2010. Advances in understanding E. coli cell fission. Curr Opin Microbiol **13:**730-737.
217. **Eswara PJ, Ramamurthi KS.** 2017. Bacterial Cell Division: Nonmodels Poised to Take the Spotlight. Annu Rev Microbiol **71:**393-411.
218. **Egan AJ, Cleverley RM, Peters K, Lewis RJ, Vollmer W.** 2017. Regulation of bacterial cell wall growth. FEBS J **284:**851-867.
219. **Weiser JN.** 2010. The pneumococcus: why a commensal misbehaves. J Mol Med (Berl) **88:**97-102.
220. **Tan TQ.** 2012. Pediatric invasive pneumococcal disease in the United States in the era of pneumococcal conjugate vaccines. Clin Microbiol Rev **25:**409-419.
221. **O'Brien KL, Wolfson LJ, Watt JP, Henkle E, Deloria-Knoll M, McCall N, Lee E, Mulholland K, Levine OS, Cherian T, Hib, Pneumococcal Global Burden of Disease Study T.** 2009. Burden of disease caused by Streptococcus

pneumoniae in children younger than 5 years: global estimates. Lancet **374:**893-902.
222. **Philippe J, Gallet B, Morlot C, Denapaite D, Hakenbeck R, Chen Y, Vernet T, Zapun A.** 2015. Mechanism of beta-lactam action in Streptococcus pneumoniae: the piperacillin paradox. Antimicrob Agents Chemother **59:**609-621.
223. **Hoskins J, Matsushima P, Mullen DL, Tang J, Zhao G, Meier TI, Nicas TI, Jaskunas SR.** 1999. Gene disruption studies of penicillin-binding proteins 1a, 1b, and 2a in Streptococcus pneumoniae. J Bacteriol **181:**6552-6555.
224. **Paik J, Kern I, Lurz R, Hakenbeck R.** 1999. Mutational analysis of the Streptococcus pneumoniae bimodular class A penicillin-binding proteins. J Bacteriol **181:**3852-3856.
225. **Amanuma H, Strominger JL.** 1980. Purification and properties of penicillin-binding proteins 5 and 6 from Escherichia coli membranes. J Biol Chem **255:**11173-11180.
226. **Pollock JJ, Nguyen-Disteche M, Ghuysen JM, Coyette J, Linder R, Salton MR, Kim KS, Perkins HR, Reynolds P.** 1974. Fractionation of the DD-carboxypeptidase-transpeptidase activities solubilized from membranes of Escherichia coli K12, strain 44. Eur J Biochem **41:**439-446.
227. **Lee DW, Peggie M, Deak M, Toth R, Gage ZO, Wood N, Schilde C, Kurz T, Knebel A.** 2012. The Dac-tag, an affinity tag based on penicillin-binding protein 5. Anal Biochem **428:**64-72.
228. **Xiang Z, Li Z, Zeng J, Li Y, Li J.** 2019. Regulation of Cell Division in Streptococci: Comparing with the Model Rods. Curr Issues Mol Biol **32:**259-326.
229. **Yeats C, Finn RD, Bateman A.** 2002. The PASTA domain: a beta-lactam-binding domain. Trends Biochem Sci **27:**438.
230. **Gordon E, Mouz N, Duee E, Dideberg O.** 2000. The crystal structure of the penicillin-binding protein 2x from Streptococcus pneumoniae and its acyl-enzyme form: implication in drug resistance. J Mol Biol **299:**477-485.
231. **Kahan FM, Kropp H, Sundelof JG, Birnbaum J.** 1983. Thienamycin: development of imipenen-cilastatin. J Antimicrob Chemother **12 Suppl D:**1-35.
232. **Berry AF, Heal WP, Tarafder AK, Tolmachova T, Baron RA, Seabra MC, Tate EW.** 2010. Rapid multilabel detection of geranylgeranylated proteins by using bioorthogonal ligation chemistry. Chembiochem **11:**771-773.
233. **Stayton PS, Freitag S, Klumb LA, Chilkoti A, Chu V, Penzotti JE, To R, Hyre D, Le Trong I, Lybrand TP, Stenkamp RE.** 1999. Streptavidin-biotin binding energetics. Biomol Eng **16:**39-44.
234. **Hendrickson WA, Pahler A, Smith JL, Satow Y, Merritt EA, Phizackerley RP.** 1989. Crystal structure of core streptavidin determined from multiwavelength anomalous diffraction of synchrotron radiation. Proc Natl Acad Sci U S A **86:**2190-2194.
235. **Weber PC, Ohlendorf DH, Wendoloski JJ, Salemme FR.** 1989. Structural origins of high-affinity biotin binding to streptavidin. Science **243:**85-88.
236. **Fan X, Wang J, Zhang X, Yang Z, Zhang JC, Zhao L, Peng HL, Lei J, Wang HW.** 2019. Single particle cryo-EM reconstruction of 52 kDa streptavidin at 3.2 Angstrom resolution. Nat Commun **10:**2386.
237. **Olejnik J, Sonar S, Krzymanska-Olejnik E, Rothschild KJ.** 1995. Photocleavable biotin derivatives: a versatile approach for the isolation of biomolecules. Proc Natl Acad Sci U S A **92:**7590-7594.
238. **Schaub RE, Dillard JP.** 2017. Digestion of Peptidoglycan and Analysis of Soluble Fragments. Bio Protoc **7**.

239. **Desmarais SM, De Pedro MA, Cava F, Huang KC.** 2013. Peptidoglycan at its peaks: how chromatographic analyses can reveal bacterial cell wall structure and assembly. Mol Microbiol **89:**1-13.
240. **Kuhner D, Stahl M, Demircioglu DD, Bertsche U.** 2014. From cells to muropeptide structures in 24 h: peptidoglycan mapping by UPLC-MS. Sci Rep **4:**7494.
241. **Bui NK, Eberhardt A, Vollmer D, Kern T, Bougault C, Tomasz A, Simorre JP, Vollmer W.** 2012. Isolation and analysis of cell wall components from Streptococcus pneumoniae. Anal Biochem **421:**657-666.
242. **Mellroth P, Daniels R, Eberhardt A, Ronnlund D, Blom H, Widengren J, Normark S, Henriques-Normark B.** 2012. LytA, major autolysin of Streptococcus pneumoniae, requires access to nascent peptidoglycan. J Biol Chem **287:**11018-11029.
243. **Vollmer W, Joris B, Charlier P, Foster S.** 2008. Bacterial peptidoglycan (murein) hydrolases. FEMS Microbiol Rev **32:**259-286.
244. **Nakimbugwe D, Masschalck B, Deckers D, Callewaert L, Aertsen A, Michiels CW.** 2006. Cell wall substrate specificity of six different lysozymes and lysozyme inhibitory activity of bacterial extracts. FEMS Microbiol Lett **259:**41-46.
245. **Hamada S, Torii M, Kotani S, Masuda N, Ooshima T, Yokogawa K, Kawata S.** 1978. Lysis of Streptococcus mutans cells with mutanolysin, a lytic enzyme prepared from a culture liquor of Streptomyces globisporus 1829. Arch Oral Biol **23:**543-549.
246. **Mesnage S, Dellarole M, Baxter NJ, Rouget JB, Dimitrov JD, Wang N, Fujimoto Y, Hounslow AM, Lacroix-Desmazes S, Fukase K, Foster SJ, Williamson MP.** 2014. Molecular basis for bacterial peptidoglycan recognition by LysM domains. Nat Commun **5:**4269.
247. **Organization WH.** 2018. Tuberculosis report, Executive summary.
248. **Alderwick LJ, Harrison J, Lloyd GS, Birch HL.** 2015. The Mycobacterial Cell Wall--Peptidoglycan and Arabinogalactan. Cold Spring Harb Perspect Med **5:**a021113.
249. **Sanders AN, Wright LF, Pavelka MS, Jr.** 2014. Genetic characterization of mycobacterial L,D-transpeptidases. Microbiology **160:**1795-1806.
250. **Gupta R, Lavollay M, Mainardi JL, Arthur M, Bishai WR, Lamichhane G.** 2010. The Mycobacterium tuberculosis protein LdtMt2 is a nonclassical transpeptidase required for virulence and resistance to amoxicillin. Nat Med **16:**466-469.
251. **Schoonmaker MK, Bishai WR, Lamichhane G.** 2014. Nonclassical transpeptidases of Mycobacterium tuberculosis alter cell size, morphology, the cytosolic matrix, protein localization, virulence, and resistance to beta-lactams. J Bacteriol **196:**1394-1402.
252. **Hugonnet JE, Tremblay LW, Boshoff HI, Barry CE, 3rd, Blanchard JS.** 2009. Meropenem-clavulanate is effective against extensively drug-resistant Mycobacterium tuberculosis. Science **323:**1215-1218.
253. **Wivagg CN, Bhattacharyya RP, Hung DT.** 2014. Mechanisms of beta-lactam killing and resistance in the context of Mycobacterium tuberculosis. J Antibiot (Tokyo) **67:**645-654.
254. **Kumar P, Arora K, Lloyd JR, Lee IY, Nair V, Fischer E, Boshoff HI, Barry CE, 3rd.** 2012. Meropenem inhibits D,D-carboxypeptidase activity in Mycobacterium tuberculosis. Mol Microbiol **86:**367-381.

255. **Li WJ, Li DF, Hu YL, Zhang XE, Bi LJ, Wang DC.** 2013. Crystal structure of L,D-transpeptidase LdtMt2 in complex with meropenem reveals the mechanism of carbapenem against Mycobacterium tuberculosis. Cell Res **23:**728-731.
256. **Armirotti A, Romeo E, Ponzano S, Mengatto L, Dionisi M, Karacsonyi C, Bertozzi F, Garau G, Tarozzo G, Reggiani A, Bandiera T, Tarzia G, Mor M, Piomelli D.** 2012. beta-Lactones Inhibit N-acylethanolamine Acid Amidase by S-Acylation of the Catalytic N-Terminal Cysteine. ACS Med Chem Lett **3:**422-426.
257. **Dillon NA, Peterson ND, Rosen BC, Baughn AD.** 2014. Pantothenate and pantetheine antagonize the antitubercular activity of pyrazinamide. Antimicrob Agents Chemother **58:**7258-7263.
258. **Patru MM, Pavelka MS, Jr.** 2010. A role for the class A penicillin-binding protein PonA2 in the survival of Mycobacterium smegmatis under conditions of nonreplication. J Bacteriol **192:**3043-3054.
259. **Golparian D, Unemo M.** 2019. Now Is the Time to Implement Whole Genome Sequencing in the Global Antimicrobial Resistance Surveillance for Neisseria gonorrhoeae? EClinicalMedicine **7:**11-12.
260. **Magiorakos AP, Srinivasan A, Carey RB, Carmeli Y, Falagas ME, Giske CG, Harbarth S, Hindler JF, Kahlmeter G, Olsson-Liljequist B, Paterson DL, Rice LB, Stelling J, Struelens MJ, Vatopoulos A, Weber JT, Monnet DL.** 2012. Multidrug-resistant, extensively drug-resistant and pandrug-resistant bacteria: an international expert proposal for interim standard definitions for acquired resistance. Clin Microbiol Infect **18:**268-281.
261. **Unemo M, Shafer WM.** 2014. Antimicrobial resistance in Neisseria gonorrhoeae in the 21st century: past, evolution, and future. Clin Microbiol Rev **27:**587-613.
262. **van Heijenoort J.** 2007. Lipid intermediates in the biosynthesis of bacterial peptidoglycan. Microbiol Mol Biol Rev **71:**620-635.
263. **Bouhss A, Crouvoisier M, Blanot D, Mengin-Lecreulx D.** 2004. Purification and characterization of the bacterial MraY translocase catalyzing the first membrane step of peptidoglycan biosynthesis. J Biol Chem **279:**29974-29980.
264. **Chung BC, Zhao J, Gillespie RA, Kwon DY, Guan Z, Hong J, Zhou P, Lee SY.** 2013. Crystal structure of MraY, an essential membrane enzyme for bacterial cell wall synthesis. Science **341:**1012-1016.
265. **Liu Y, Breukink E.** 2016. The Membrane Steps of Bacterial Cell Wall Synthesis as Antibiotic Targets. Antibiotics (Basel) **5**.
266. **Takahashi Y, Igarashi M, Miyake T, Soutome H, Ishikawa K, Komatsuki Y, Koyama Y, Nakagawa N, Hattori S, Inoue K, Doi N, Akamatsu Y.** 2013. Novel semisynthetic antibiotics from caprazamycins A-G: caprazene derivatives and their antibacterial activity. J Antibiot (Tokyo) **66:**171-178.
267. **Salomon JJ, Galeron P, Schulte N, Morow PR, Severynse-Stevens D, Huwer H, Daum N, Lehr CM, Hickey AJ, Ehrhardt C.** 2013. Biopharmaceutical in vitro characterization of CPZEN-45, a drug candidate for inhalation therapy of tuberculosis. Ther Deliv **4:**915-923.
268. **Patel B, Ryan P, Makwana V, Zunk M, Rudrawar S, Grant G.** 2019. Caprazamycins: Promising lead structures acting on a novel antibacterial target MraY. Eur J Med Chem **171:**462-474.
269. **Hu Y, Chen L, Ha S, Gross B, Falcone B, Walker D, Mokhtarzadeh M, Walker S.** 2003. Crystal structure of the MurG:UDP-GlcNAc complex reveals common structural principles of a superfamily of glycosyltransferases. Proc Natl Acad Sci U S A **100:**845-849.
270. **Mann PA, Muller A, Xiao L, Pereira PM, Yang C, Ho Lee S, Wang H, Trzeciak J, Schneeweis J, Dos Santos MM, Murgolo N, She X, Gill C, Balibar CJ,**

Labroli M, Su J, Flattery A, Sherborne B, Maier R, Tan CM, Black T, Onder K, Kargman S, Monsma FJ, Jr., Pinho MG, Schneider T, Roemer T. 2013. Murgocil is a highly bioactive staphylococcal-specific inhibitor of the peptidoglycan glycosyltransferase enzyme MurG. ACS Chem Biol **8:**2442-2451.

271. **Sanchez-Puelles JM, Sanz JM, Garcia JL, Garcia E.** 1992. Immobilization and single-step purification of fusion proteins using DEAE-cellulose. Eur J Biochem **203:**153-159.

APENDIX

Permission for Publication of Published Manuscripts

9/5/2019 Rightslink® by Copyright Clearance Center

Copyright Clearance Center RightsLink®

Home | Create Account | Help | LIVE CHAT

ACS Publications Most Trusted. Most Cited. Most Read.

Title: Novel Electrophilic Scaffold for Imaging of Essential Penicillin-Binding Proteins in Streptococcus pneumoniae

Author: Shabnam Sharifzadeh, Michael J. Boersma, Ozden Kocaoglu, et al

Publication: ACS Chemical Biology

Publisher: American Chemical Society

Date: Nov 1, 2017

Copyright © 2017, American Chemical Society

LOGIN

If you're a copyright.com user, you can login to RightsLink using your copyright.com credentials.

Already a RightsLink user or want to learn more?

PERMISSION/LICENSE IS GRANTED FOR YOUR ORDER AT NO CHARGE

This type of permission/license, instead of the standard Terms & Conditions, is sent to you because no fee is being charged for your order. Please note the following:

- Permission is granted for your request in both print and electronic formats, and translations.
- If figures and/or tables were requested, they may be adapted or used in part.
- Please print this page for your records and send a copy of it to your publisher/graduate school.
- Appropriate credit for the requested material should be given as follows: "Reprinted (adapted) with permission from (COMPLETE REFERENCE CITATION). Copyright (YEAR) American Chemical Society." Insert appropriate information in place of the capitalized words.
- One-time permission is granted only for the use specified in your request. No additional uses are granted (such as derivative works or other editions). For any other uses, please submit a new request.

BACK | CLOSE WINDOW

Copyright © 2019 Copyright Clearance Center, Inc. All Rights Reserved. Privacy statement. Terms and Conditions.
Comments? We would like to hear from you. E-mail us at customercare@copyright.com

SPRINGER NATURE LICENSE
TERMS AND CONDITIONS

Sep 14, 2019

This Agreement between University of Minnesota -- Shabnam Sharifzadeh ("You") and Springer Nature ("Springer Nature") consists of your license details and the terms and conditions provided by Springer Nature and Copyright Clearance Center.

License Number	4667740285211
License date	Sep 14, 2019
Licensed Content Publisher	Springer Nature
Licensed Content Publication	Springer eBook
Licensed Content Title	Activity-Based Protein Profiling Methods to Study Bacteria: The Power of Small-Molecule Electrophiles
Licensed Content Author	Shabnam Sharifzadeh, Joshua D. Shirley, Erin E. Carlson
Licensed Content Date	Jan 1, 2018
Type of Use	Thesis/Dissertation
Requestor type	academic/university or research institute
Format	print and electronic
Portion	full article/chapter
Will you be translating?	no
Circulation/distribution	1 – 29
Author of this Springer Nature content	yes
Title	Chemical Tools for Selective Activity Profiling of PBP Class of Antibacterial Tergets
Institution name	University of Minnesota
Expected presentation date	Oct 2019
Order reference number	NA
Requestor Location	University of Minnesota 1031 29th Ave SE Apt #F MINNEAPOLIS, MN 55414 United States Attn: Shabnam Sharifzadeh
Total	0.00 USD
Terms and Conditions	